EVALUATION OF INDIRECT TENSILE STRENGTH AS DESIGN CRITERIA FOR SUPERPAVE MIXTURES

by

N. Paul Khosla
and
Nathaniel Harvey

HWY-2008-02

FINAL REPORT
FHWA/NC/2008-02

in Cooperation with

North Carolina Department of Transportation

Department of Civil Engineering
North Carolina State University

July 2009

Technical Report Documentation Page

1. Report No. **FHWA/NC/2008-02**	2. Government Accession No.	3. Recipient's Catalog No.
5. Title and Subtitle **Evaluation of Indirect Tensile Strength as Design Criteria for SuperPave Mixtures**		6. Report Date **July 2009**
		6. Performing Organization Code
7. Author(s) **N. Paul Khosla and Nathaniel Harvey**		8. Performing Organization Report No.
9. Performing Organization Name and Address **Department of Civil Engineering,** **North Carolina State University** **Raleigh, NC, 27695-7908**		10. Work Unit No. (TRAIS)
		11. Contract or Grant No.
12. Sponsoring Agency Name and Address **North Carolina Department of Transportation** **Research and Analysis Group** **1 South Wilmington Street** **Raleigh, North Carolina 27601**		13. Type of Report and Period Covered **Final Report** **August 2007-July 2009**
		14. Sponsoring Agency Code **2008 - 02**
Supplementary Notes:		

16. Abstract

Distresses in asphalt pavements are typically due to traffic loading, resulting in rutting or fatigue cracking. The presence of water (or moisture) often results in premature failure of asphalt pavements in the form of isolated distress caused by debonding of the asphalt film from the aggregate surface or early rutting/fatigue cracking due to reduced mix strength. Tensile strength of asphalt concrete is a function of the amount of asphalt binder in the mix, mixture stiffness, absorption capacity of the aggregates used, asphalt film thickness at the aggregate interface and total voids in the mix. The presence of moisture accelerates pavement deterioration under traffic loading. This study suggests that tensile strength can be used as a design tool in the Superpave mix design stage and a modified mix design procedure is proposed based on individual tensile strength.

This research study shows that reliance on the Tensile Strength Ratio (TSR) values only may be misleading in many cases. The individual values of tensile strength of conditioned and unconditioned specimens in conjunction with TSR values should be employed in assessing the effect of water damage on the performance of pavements. This study found that a minimum tensile strength should be established for a given ESAL range. The fatigue life of mixtures decreases exponentially with decreasing tensile strength. This trend is justified by the loss in stiffness and thereby initiating cracks and stripping. A minimum tensile strength for a given ESALs level can be used as a surrogate criterion for fatigue life estimation. This research study also shows that the mixtures with lower tensile strength have higher rut depths, as the aggregate structure is affected due to moisture damage and subsequent loss in tensile strengths of the mixtures.

17. Key Words Indirect Tensile Strength, Rutting Life, Fatigue Life, Moisture Sensitivity, Dynamic Modulus, SuperPave Shear Tester		18. Distribution Statement	
19. Security Classif. (of this report) Unclassified	20. Security Classif. (of this page) Unclassified	21. No. of Pages 114	22. Price

Form DOT F 1700.7 (8-72) **Reproduction of completed page authorized**

DISCLAMIER

The contents of this report reflect the views of the authors and not necessarily the views of the University. The authors are responsible for the facts and the accuracy of the data presented herein. The contents do not necessarily reflect the official views or policies of either the North Carolina Department of Transportation or the Federal Highway Administration at the time of publication. This report does not constitute a standard, specification, or regulation.

ACKNOWLEDGMENTS

The author expresses his sincere appreciation to the authorities of the North Carolina Department of Transportation for making available the funds needed for this research.

Sincere thanks go to Mr. Jack E. Cowsert, Chairman, Technical Advisory Committee, for his interest and helpful suggestions through the course of this study. Equally, the appreciation is extended to other members of the committee, Mr. Dennis W. Jerrigan, Mr. Todd. W. Whittington, Mr. James Budday, Mr. Hesham M. El-Boulaki, Ms. Tracey C. Pittman, Mr. Wiley W. Jones III, Mr. James Phillips, Ms. Jan Womble, Mr. Steve McAllister, Mr. Cecil L. Jones, Dr. Judith Corley-lay, Mr. Moy Biswas and Mr. Mustan Kadibhai for their continuous support during this study. The author also expresses his thanks to K. I. Harikrishnan for his work in the first part of this study (HWY-2005-14) and his assistance in this project.

EXECUTIVE SUMMARY

Many factors contribute to the degradation of asphalt pavements. When high quality materials are used, distresses are typically due to traffic loading, resulting in rutting or fatigue cracking. The presence of water (or moisture) often results in premature failure of asphalt pavements in the form of isolated distress caused by debonding of the asphalt film from the aggregate surface or early rutting/fatigue cracking due to reduced mix strength. Moisture sensitivity has long been recognized as an important mix design consideration. The tensile strength is primarily a function of the binder properties. The amount of asphalt binder in a mixture and its stiffness influence the tensile strength. Tensile strength also depends on the absorption capacity of the aggregates used. At given asphalt content, the film thickness of asphalt on the surface of aggregates and particle-to-particle contact influences the adhesion or tensile strength of a mixture. Various studies have repeatedly proved that the tensile strength increases with decreasing air voids. The tensile strength of a mixture is also strongly influenced by the consistency of the asphalt cement, which can influence rutting. Thus, tensile strength plays an important role as a design and evaluation tool for Superpave mixtures

Moisture damage of asphalt pavements is a serious problem. The presence of moisture tends to reduce the stiffness of the asphalt mix as well as create the opportunity for stripping of the asphalt from the aggregate. This, in combination with repeated wheel loadings, can accelerate pavement deterioration. Strength loss is now evaluated by comparing indirect tensile strengths of an unconditioned control group to those of the conditioned samples. If the average retained strength of the conditioned group is less than eighty-five percent of the control group strength, the mix is determined to be moisture susceptible. This research study shows that reliance on the Tensile Strength Ratio (TSR) values only may be misleading in many cases. The individual values of tensile strength of conditioned and unconditioned specimens in conjunction with TSR values should be employed in assessing the effect of water damage on the performance of pavements. This study found that a minimum tensile strength should be established for a given ESAL range. The fatigue life of the mixtures decrease exponentially with decreasing tensile strength. This trend is justified by the loss in stiffness and thereby initiating cracks and stripping. There exists a minimum tensile strength for a given ESALs

level that can be used as a surrogate criterion for fatigue life estimation. This research study also shows that the mixtures with lower tensile strength have higher rut depths. Rut depths of mixtures were shown to increase with decreasing tensile strength, which can be attributed to the fact that the aggregate structure is affected due to moisture damage and subsequent loss in tensile strengths of the mixtures. This study suggests that tensile strength can be used as a design tool in the Superpave mix design stage and a modified mix design procedure is proposed based on individual tensile strength.

TABLE OF CONTENTS

LIST OF TABLES

LIST OF FIGURES

NOTATIONS

VMA – Voids in Mineral Aggregate

VFA – Voids Filled With Asphalt

TSR – Tensile Strength Ratio

ESAL - Equivalent Single Axle Load

FHWA- Federal Highway Administration

LVDT - Linear Variable Differential Transducer

CHAPTER 1

1. INTRODUCTION

Many factors contribute to the degradation of asphalt pavements. When high quality materials are used, distresses are typically due to traffic loading, resulting in rutting or fatigue cracking. Environmental conditions such as temperature and water can have a significant effect on the performance of asphalt concrete pavements as well. The presence of water (or moisture) often results in premature failure of asphalt pavements in the form of isolated distress caused by debonding of the asphalt film from the aggregate surface or early rutting/fatigue cracking due to reduced mix strength [1]. Moisture sensitivity has long been recognized as an important mix design consideration.

Probably the most damaging and often hidden effect of moisture damage is reduced pavement strength. Tensile strength plays an important role in the performance of a mixture under fatigue, rutting, and moisture susceptibility. The damage due to moisture is controlled by the specific limits of the tensile strength ratios (TSR) or the percent loss in tensile strength of the mix. The moisture sensitivity of a mixture is evaluated by performing the AASHTO T-283 test [2]. This test has a conditioning phase, where the sample is subjected to saturation and immersion in a heated water bath to simulate field conditions over time. Strength loss is then determined by comparing indirect tensile strengths of an unconditioned control group to those of the conditioned samples. If the average retained strength of the conditioned group strength is less than eighty-five

percent of the control group strength, the mix is determined to be moisture susceptible. This indicates that the combination of asphalt aggregate would fail due to water damage during the early part of the service life of the pavement. However, a total dependency and reliance on the TSR values only may be misleading in many cases. For instance, Table 1.1 shows hypothetical TSR data for two different mixtures (A and B).

Table 1.1Hypothetical TSR Data

Mix	Tensile Strengths (psi)		TSR (%)
	Unconditioned	Conditioned	
A	200	156	78
B	100	84	84

The mixtures A and B have TSR values of 78% and 84%, respectively. Even though both mixes do not meet the criteria of a minimum TSR value of 85%, the conditioned tensile strength of mix A is 56% higher than the unconditioned tensile strength of mix B. Furthermore, the effect of using mix A will not be as detrimental on the pavement performance as compared to the case if mix B were to be used as a surface course in a given pavement structure. It is evident that individual tensile strength of the mixtures after conditioning will also govern the rutting and fatigue life of the mixtures. Thus, a total dependency and reliance on the TSR values will not necessarily be sufficient to mitigate moisture susceptibility. There has been no concerted effort at national or state level towards establishing the quantitative causal effects of failing to meet the minimum

prescribed value of TSR or loss in tensile strength. The individual values of tensile strength of conditioned and unconditioned specimens along with TSR values should be employed in assessing the effect of water damage on the performance of pavements.

The tensile strength is one of the critical parameters to be always taken into consideration for performance evaluation. The evaluation of the fatigue life of a mixture is based on the flexural stiffness measurements. Tensile strain at the bottom of the asphalt concrete layer in a pavement is an important parameter in the measurement of fatigue life of a mixture. The bottom of asphalt concrete layer has the greatest tensile stress and strain. Cracks are initiated at the bottom of this layer and later propagate due to the repeated stressing in tension of asphalt concrete pavements caused by bending beneath the wheel loads. Ultimately, the crack appears on the surface in the wheel paths, which later forms a series of interconnected cracks, called as alligator or bottom-up fatigue cracking.

The tensile strength is primarily a function of the binder properties. The amount of asphalt binder in a mixture and its stiffness influence the tensile strength. Tensile strength also depends on the absorption capacity of the aggregates used. At given asphalt content, the film thickness of asphalt on the surface of aggregates and particle-to-particle contact influences the adhesion or tensile strength of a mixture. Various studies have repeatedly proved that the tensile strength increases with decreasing air voids. The tensile strength of a mixture is strongly influenced by the consistency of the asphalt cement, which can influence rutting. Thus, tensile strength plays an important role as a design and evaluation tool for Superpave mixtures.

In order to reduce pavement damage related to stripping, additives are often used to decrease moisture susceptibility. The use of lime to reduce moisture sensitivity has been promoted by Federal Highway Administration (FHWA) for many years. While reviewing the records of Hot Mix Asphalt (HMA) mixtures produced in the early 1960's and today, a major difference was identified as the lack of mineral fillers in today's mixes. These fillers increase film thickness, improve the cohesion of the binders and increase the stiffness of the mixtures. Research studies indicated that the addition of hydrated lime as mineral filler improved the permanent deformation characteristics and fatigue endurance of the asphalt concrete mixtures. This improvement was particularly more effective at higher testing temperatures with mixtures containing polymer modified asphalt and limestone aggregate. At the same time, lime had a few problems in the field, as there were instances where contractors expressed concern about personnel exposure and problems handling lime. Liquid anti-stripping agents, such as liquid amines and liquid phosphate ester, are also used as anti-stripping agents. The liquid additives can be mixed with large amounts of asphalt and stored for use in many mixes. One disadvantage with the liquid surfactants reported in literatures is possible heat degradation. i.e., if the asphalt mixture is held at high temperature for long periods, the effectiveness may be reduced. In addition, it has to be added uniformly and mixed consistently throughout the mix. However, in the case of lime it is possible to get a uniform coating of lime particles around the aggregate. The performance of lime as an anti-stripping agent should be compared with the performance of a liquid anti-stripping agent. The difference in the performance of these two anti-stripping agents should be studied.

The current Superpave Mix design involves only the calculation of volumetric properties (such as Voids in Mineral Aggregate (VMA), Voids Filled with Asphalt (VFA), %Air Voids etc). At present, the Superpave volumetric design method contains no strength or 'proof' test for quality control and quality assurance of mixtures. Test procedures that are used in the Superpave intermediate and complete procedures require expensive and complex test equipment. For Superpave mixtures, the test for moisture sensitivity is generally conducted along with the level 1 mix design. NCDOT currently uses the Tensile Strength Ratio (TSR) test to evaluate moisture sensitivity and stripping potential of HMA Mixtures. If the ratio is less than 85%, the mixture is determined to be moisture susceptible. Once a mix is accepted for production, it is believed that the mix would perform satisfactorily under in-situ conditions. If the test results upon which such decisions are based are subject to variability, the problems that will arise are obvious. A mix may fail prematurely requiring the expense of removal and replacement of the failed pavement. This may result in major reconstruction cost to the Department of Transportation. In this context, there is a need to develop a procedure that is effective in controlling moisture-related problems and to achieve: (i) to maximize the fatigue life, and (ii) to minimize the potential for rutting. This research study is investigating whether individual tensile strength can be used as a design and evaluation for Superpave mixtures. This research study is aiming to develop a relationship between the indirect tensile strength of a mixture and its estimated fatigue and rutting life.

1.1. Research Objectives

The primary objectives of this research study were to:

1. Evaluate the tensile strengths of conditioned and unconditioned specimens and their tensile strength ratios (TSRs) for mixtures with different aggregates and gradations.
2. Conduct a comparative study on the effects of hydrated lime and a liquid anti-stripping agent on tensile strength and TSR values of the mixtures.
3. Develop the relationship between the tensile strength for mixtures with different aggregates and gradations and their fatigue performance as estimated using the Frequency Sweep Test at Constant Height, Dynamic Modulus Test and Indirect Tensile Test.
4. Conduct a detailed study to investigate the rutting performance of mixtures with different aggregates and gradations using the Repeated Shear Test at Constant Height and develop its relationship with the tensile strengths of the mixtures.
5. Develop a minimum tensile strength criterion along with TSRs for mixtures with different aggregates and gradations.

1.2. Research Methodology

1.2.1. Task 1 – Materials and Superpave Mix Design

Three aggregate types, three gradations and three asphalt grades were used this study. The mixtures were designed to meet the Superpave mix design criterion. Two anti-stripping agents including hydrated lime and a liquid anti-stripping agent were used in this study. The comparative effects of hydrated lime and the liquid anti-stripping agent on the tensile strength and TSR values of the mixtures were evaluated. If any statistically significant difference existed between the performances of these agents, it was planned to conduct further tests for fatigue and rutting with both anti-stripping agents. If there were

no significant difference between the performances of these agents, then the fatigue and rutting tests would be conducted for one of the two anti-stripping agents.

1.2.2. Task 2: Evaluation of Indirect Tensile Strength and Moisture Sensitivity

After the design of mixtures for optimum aggregate gradation and asphalt content, the moisture sensitivity of the mixtures was evaluated. The calculation of the TSR in accordance to AASHTO T-283 is the standard method under the Superpave mix design system to evaluate a mixture's moisture sensitivity. A set of samples were conditioned by saturation and immersion to simulate the moisture damage of a mixture in field. The indirect tensile strengths of the unconditioned and conditioned sets were measured to evaluate the moisture damage induced by conditioning. This loss of cohesion and adhesion manifests itself in the loss of tensile strength of a mix. The indirect tensile strengths of the mixtures in both conditioned and unconditioned states were measured using the indirect tension test (IDT). The IDT test is described as follows:

1.2.2.1. Indirect Tension Test

The indirect tensile test is one of the most popular tests used for HMA mixture characterization in evaluating pavement structures. The indirect tensile test has been extensively used in structural design research for flexible pavements since the 1960s and, to a lesser extent, in HMA mixture design research.

The indirect tensile test is performed by loading a cylindrical specimen with a single or repeated compressive load, which acts parallel to and along the vertical diametral plane. This loading configuration develops a relatively uniform tensile stress perpendicular to the direction of the applied load and along the vertical diametral plane, which ultimately causes the specimen to fail by splitting along the vertical diameter as shown in Figure

1.1. A curved loading strip is used to provide a uniform loading width, which produces a nearly uniform stress distribution. The equations for tensile stress and tensile strain at failure have been developed and simplified. These equations assume the HMA is homogenous, isotropic, and elastic. None of these assumptions is exactly true, but estimates of properties based on these assumptions are standard procedure and are useful in evaluating relative properties of HMA mixtures.

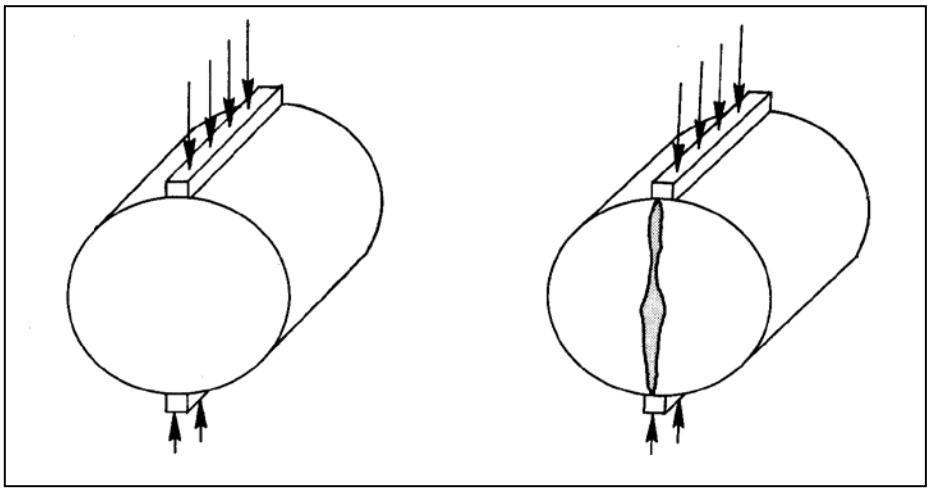

Figure 1.1 Indirect Tensile Test during Loading and at Failure

The equations for the indirect tensile stress and strain at failure are provided below:

$\sigma_x = 2P/\pi tD$

$\varepsilon_f = 0.52x_t$

Where,

σ_x = horizontal tensile stress at center of specimen, psi

σ_y, = vertical compressive stress at center of specimen, psi

ε_f = tensile strain at failure, inches/inch

P =applied load, lbs.

D = diameter of specimen, inches

t = thickness of specimen, inches and

x_t = horizontal deformation across specimen, inches.

The above equation applies for 4-inch diameter samples having a 0.5 inch curved loading strip and for 6-inch diameter samples having a 0.75-inch curved loading strip. The indirect tensile test provides two mixture properties that are useful in characterizing HMA. The first property is tensile strength, which is often used in evaluating water susceptibility of mixtures.

1.2.3. Task 3: Performance Based Testing, Analysis of Service Life of the Pavements and its relation to Indirect Tensile Strength values

The mixtures were evaluated for their resistance to fatigue and rutting performances. Performance evaluation tests were conducted on both conditioned and unconditioned specimens to investigate the effect of moisture damage on fatigue and rutting characteristics of the mixtures. The indirect tensile strength values of the mixtures, measured from the IDT test, were compared with the estimated fatigue and rutting parameters of the mixtures.

1.2.4. Task 3.1 Evaluation of Fatigue Performance

The Frequency Sweep test at Constant Height (FSTCH) and the Dynamic Modulus test were conducted on the mixtures to evaluate their fatigue life. The dynamic modulus values and phase angles measured from the FSCH test were used in the surrogate models of SHRP to estimate the fatigue life of the mixtures. Similarly, the test data from the Dynamic Modulus load test was used in the available models for estimating the fatigue

life of the mixtures. In both cases, the stiffness of the mixtures and the tensile strain would be the governing parameters in the fatigue life estimation.

To simulate different degrees of moisture damage in the laboratory samples, the specimens were subjected to 0, 12 and 24 hours of conditioning that corresponds to 0, 0.5 and 1 cycle of conditioning, respectively. The tensile strengths of the mixtures were then measured at these cycles of conditioning. The shear tests and dynamic modulus tests were conducted on the specimens that are subjected to moisture damage at these different cycles. The fatigue life of the mixtures estimated from these performance evaluation tests were correlated with their corresponding tensile strengths of mixtures. A minimum tensile strength criterion was recommended for different traffic levels.

1.2.5. Task 3.2 Evaluation of Rutting Performance

The repeated shear test at constant height (RSCH) was performed to investigate the rutting potential of asphalt mixtures. The accumulation of plastic shear strain in a mixture under repeated loading gives an indication about the mixture's resistance to rutting. The shear strain measured at the end of 5000 loading cycles was used in SHRP surrogate rutting models to estimate the rut depths.

1.2.6. Task 4: Incorporation of Tensile Strength as a Design and Evaluation Tool for Superpave Mixtures

An experimental plan including the number of replicates for this study is shown in Table 1.2. As mentioned in Table 1.2, the three source aggregates, two nominal sizes, two levels of conditioning, and three asphalt binder grades were used in this research study.

Table 1.2.1 Experimental Plan

Mix Type	Aggregate Source	Conditioning	Without Anti-Stripping Agent				With Anti-Stripping Agent			
			FSCH	RSCH	Dynamic Modulus	ITS	FSCH	RSCH	Dynamic Modulus	ITS
12.5mm, PG 70-22	A	UC	3*	3	2	3	3	3	2	6
		HC	3	3	2	3	3	3	2	6
		FC	3	3	2	3	3	3	2	6
	B	UC	3	3	2	3	3	3	2	6
		HC	3	3	2	3	3	3	2	6
		FC	3	3	2	3	3	3	2	6
	C	UC	3	3	2	3	3	3	2	6
		HC	3	3	2	3	3	3	2	6
		FC	3	3	2	3	3	3	2	6
9.5mm, PG 70-22	A	UC	3	3	2	3	3	3	2	6
		HC	3	3	2	3	3	3	2	6
		FC	3	3	2	3	3	3	2	6
	B	UC	3	3	2	3	3	3	2	6
		HC	3	3	2	3	3	3	2	6
		FC	3	3	2	3	3	3	2	6
	C	UC	3	3	2	3	3	3	2	6
		HC	3	3	2	3	3	3	2	6
		FC	3	3	2	3	3	3	2	6

UC – Unconditioned Specimens
HC – Half Conditioned Specimens (12 hours of Conditioning)
FC- Full Conditioned Specimens (24 hours of Conditioning)
* Number of Replicates

Table 1.3.2 Experimental Plan (continued)

Asphalt PG Grade	Aggregate Source	Conditioning	Without Anti-Stripping Agent				With Anti-Stripping Agent			
			FSCH	RSCH	Dynamic Modulus**	ITS	FSCH	RSCH	Dynamic Modulus**	ITS
12.5mm, PG 64-22	A	UC	3*	3		3	3	3		6
		HC	3	3		3	3	3		6
		FC	3	3		3	3	3		6
	B	UC	3	3		3	3	3		6
		HC	3	3		3	3	3		6
		FC	3	3		3	3	3		6
	C	UC	3	3		3	3	3		6
		HC	3	3		3	3	3		6
		FC	3	3		3	3	3		6
12.5mm, PG 76-22	A	UC	3	3		3	3	3		6
		HC	3	3		3	3	3		6
		FC	3	3		3	3	3		6
	B	UC	3	3		3	3	3		6
		HC	3	3		3	3	3		6
		FC	3	3		3	3	3		6
	C	UC	3	3		3	3	3		6
		HC	3	3		3	3	3		6
		FC	3	3		3	3	3		6

UC – Unconditioned Specimens
HC – Half Conditioned Specimens (12 hours of Conditioning)
FC- Full Conditioned Specimens (24 hours of Conditioning)
* Number of Replicates
** Note: Fatigue Life as predicted by Dynamic Modulus is highly variable and as such no Dynamic Modulus tests were conducted on these mixes

1.3. Organization of the Report

This report contains eight chapters. Chapter 2 discusses the literature pertaining to the research. The mixture information is furnished in Chapter 3. It includes sources of aggregates, gradations and volumetric properties of mixtures as well as the recommended additional indirect tensile testing to confirm that maximum strength is attained at 4% air voids in the mix. Chapters 4, 5 and 6 include the results of performance evaluation tests conducted on different mixtures. The performance evaluation tests include indirect tensile strength test, shear tests and dynamic modulus test. The analysis of performance evaluation tests is furnished in Chapter 7 along with an example design, implementing all suggested changes to the Superpave^{TM} mix design process. The results are summarized and discussed in the last chapter.

CHAPTER 2

2. LITERATURE REVIEW

2.1. Introduction

Moisture damage of asphalt concrete pavement is a problem that most of the State highway agencies are experiencing. This damage is commonly known as stripping. The most serious consequence of stripping is the loss of strength and integrity of the pavement. Stripping of an asphalt concrete mixture takes place when adhesion is lost between the aggregate surface and the asphalt cement. The loss of adhesion is primarily due to the action of moisture. Modes of failure, as a result of stripping, include raveling, rutting, shoving and cracking. The Superpave mix design incorporates a test for moisture sensitivity as part of the mix design process. This chapter reviews the background literature that deals with moisture damage of asphalt concrete pavement, different types of moisture sensitivity testing and current methods to improve moisture susceptibility of aggregates.

2.2. Theories of Moisture Susceptibility

The moisture affects asphalt mixes in three ways: loss of cohesion, loss of adhesion, and aggregate degradation. The loss of cohesion and adhesion are important to the process of stripping. A reduction in cohesion results in a reduction in strength and stiffness. The loss of adhesion is the physical separation of the asphalt cement and aggregate, primarily caused by the action of moisture [3]. The air void system in the asphalt concrete provides the means by which moisture can enter the mix. Once moisture is present through voids or from incomplete drying during the mixing process, it interacts with the asphalt-aggregate interface.

2.2.1. Theory of Adhesion

The loss of adhesion is explained in current literature using one or a combination of four theories. The theories include chemical reaction, mechanical adhesion, surface energy and molecular orientation. Chemical reaction is a possible mechanism for adhesion of the asphalt cement to the aggregate surface. Research [3] indicates that better adhesion may be achieved with basic aggregates than with acidic aggregates but, acceptable asphalt mixes have been made with all types of the aggregate. Recent studies concentrating on the chemical interactions at the asphalt aggregate bond have found adhesion to be unique to individual material combinations [4]. Mechanical adhesion depends primarily on the physical properties of the aggregate such as surface texture, surface area, particle size and porosity. A rough porous surface absorbs asphalt and the greater surface area promotes greater mechanical interlock. The surface energy theory is used to explain the wettability of the aggregate surface by asphalt and water. Water has a lower viscosity and lower surface tension than asphalt cement and thus a better wetting agent. The final theory is regarding the molecular orientation, according to which molecules of asphalt align with aggregate surface charges. Since water is bipolar, a preference for water molecules over asphalt is found for acidic aggregate.

Current literature suggests seven factors that affect adhesion and were used to develop the theories [4]:

1. Surface tension of the asphalt cement and aggregate
2. Chemical composition of the asphalt cement and the aggregate
3. Asphalt viscosity

4. Surface texture of the aggregate
5. Aggregate porosity
6. Aggregates cleanliness
7. Aggregate moisture content and temperature at the time of mixing

2.2.2. Theory of Cohesion

Cohesion is defined as the molecular attraction by which the particles of a body are united throughout the mass. In compacted asphalt concrete, cohesion may be explained as the overall integrity of the material when subjected to load or stress. On a micro scale, in the asphalt film surrounding, the aggregate, cohesion can be considered the resistance to deformation under load that occurs at a distance from the aggregate, beyond the influences of mechanical interlock and molecular orientation [4]. If the adhesion between aggregate and asphalt is adequate, cohesive forces will develop in the asphalt matrix. It may be thought of as the initial resistance since it is independent of applied load. Quantitatively, cohesion is the magnitude of the intercept of the Mohr envelope in a Mohr diagram. A loss of cohesion is typically manifested as softening of the asphalt mixture.

Cohesive forces are influenced by the mix properties such as viscosity of the asphalt-mineral filler system. The cohesive forces in an asphalt concrete mix are inversely proportional to the temperature of the mix. The stability test, resilient modulus test or tensile strength test are typically used to measure cohesive resistance. A mechanical test such as the tensile strength test primarily measures overall effects of moisture-induced damage. As a result, the mechanisms of cohesion and adhesion cannot be distinguished separately in the test results.

2.3. Factors Affecting Moisture Susceptibility

In many cases, the in-place properties and service conditions of HMA pavements induce premature stripping in asphalt pavements. An understanding of these factors is important to investigate and solve the problem of moisture-induced damage. Three indicators of stripping (white spots, fatty areas, and potholes) usually start at the bottom of the HMA layer and continue upward. The surface of the pavement is exposed to high temperatures and long drying periods whereas the bottom of the HMA layer experiences longer exposures to moisture and lower temperatures.

2.3.1. Mixture Considerations

The physio-chemical properties of the aggregate are important to the overall water susceptibility of an asphalt pavement. Aggregates can greatly influence the moisture sensitivity of a mixture. The aggregate surface chemistry and the presence of clay fines are important factors affecting the adhesion between the aggregate and the asphalt binder. Common methods to mitigate moisture sensitivity are using anti-strip agents such as liquids or lime and by the elimination of detrimental clay fines through proper processing or by specifying specification limit on clay content. Chemical and electrochemical properties of the aggregate surface in the presence of water have a significant effect on stripping. Aggregates that impart a high pH value to water are more susceptible to stripping. These aggregates are classified as hydrophilic, or water loving. Hydrophobic aggregates typically exhibit low silica contents and are generally alkaline. Hydrophobic aggregates such as limestone provide better resistance to stripping.

Excessive dust coating on the aggregate can prevent a thorough coating of asphalt cement on the aggregate. Fine clays may also emulsify the asphalt in the presence of water. Both

conditions increase the probability of an asphalt mix to strip prematurely. High moisture contents in the mineral aggregates before mixing with the asphalt cement can also increase the potential for stripping. Most states require temperatures to ensure proper drying of aggregates. The degradation of aggregates in HMA mixes also contributes to stripping. Broken aggregates from compacting and traffic loading expose new surfaces. These uncoated surfaces absorb water and initiate premature stripping.

The asphalt binder can influence its adhesion with aggregate as well as the cohesion of the mastic. Adhesion is influenced by the chemistry of the asphalt as well as by the stiffness of the binder. The cohesive strength of the asphalt matrix in the presence of moisture is also influenced by the chemical nature of the binder and processing techniques. The viscosity of the asphalt plays a significant role in the propensity of the asphalt mix to strip. High viscosity asphalt resists displacement by water better than those that have a low viscosity. High viscosity asphalt provides a better retention of asphalt on the aggregate surface [5]. However, a low viscosity is advantageous during mixing because of increased coatability, providing a uniform film of asphalt over the aggregate particles. Based on the theory of adhesion presented earlier the properties of asphalt cement and aggregate materials directly influence the adhesion developed between the binder and aggregates.

The type of HMA has been related to the water susceptibility of mix. Open graded base courses are more prone to premature stripping because mixes are more permeable to water when compared to dense graded mixes. Surface treatments have been observed to

be particularly susceptible to stripping [5]. A well-compacted, dense graded hot mix provides better moisture resistance. Water susceptibility can be further minimized with full depth asphalt pavement. Dense graded bases found in full depth pavements act as a moisture barrier between the subbase and the surface course.

Moisture-related problems do not occur without the presence of water and traffic, which provides energy to break the adhesive bonds and cause cohesive failures. Repeated freeze–thaw cycles can also accelerate the distress in the pavement. Moisture comes from rain infiltration or from beneath the surface. Once the moisture is in the pavement, it can affect either the adhesive bond or cohesive strength. Test methods, which have historically been used to evaluate mixes for moisture sensitivity, have generally examined the effect of moisture on the mix strength or the coating on the aggregate. They have not included the effect of traffic on accelerating the moisture-related distress.

2.3.2. Pavement Design Considerations

Pavements may have fundamental design flaws that trap water or moisture within the structural layers. There must be good drainage design, both surface and subsurface, since water causes moisture-related distress. The application of surface seals to a moisture-sensitive mix can also be a factor in accelerating moisture damage.

2.3.3. Construction Issues

A number of construction issues can affect the moisture sensitivity of a mix. Weather conditions are important in that they can affect mix compaction or trap mix moisture. Mix handling techniques can influence segregation and affect the permeability of the mix. Joint construction techniques can also affect compaction and permeability. The amount of compaction achieved (relative density) has a major effect on the air void

content, the permeability of the finished pavement, and the mix sensitivity to moisture damage [6]. Control (or lack thereof) of required additives can influence the long-term performance of the mix.

2.4. Moisture-Related Distress

Moisture-related distress is similar in many ways to distress caused by other factors (materials, design, and construction). Moisture tends to accelerate the presence of the distress types. The types of distress that can be related to moisture, or the other factors, are described below:

Bleeding, cracking, and rutting: These distresses are caused by a partial or complete loss of the adhesion bond between the aggregate surface and the asphalt cement. This may be caused by the presence of water in the mix due to poor compaction, inadequately dried or dirty aggregate, poor drainage, and poor aggregate–asphalt chemistry [6]. It is aggravated by the presence of traffic and freeze–thaw cycles and can lead to early bleeding, rutting, or fatigue cracking.

Raveling: Progressive loss of surface material by weathering or traffic abrasion, or both, is another manifestation of moisture-related distress. It may be caused by poor compaction, inferior aggregates, low asphalt content, high fines content, or moisture-related damage, and it is aggravated by traffic.

2.5. Current Test methods for Evaluating Moisture Susceptibility

Several test methods have been developed and used to evaluate the moisture susceptibility of HMA mixes. These tests are used to assess the following:

- Severity of moisture damage in asphalt mixtures

- Evaluating the effectiveness of anti-stripping agents to decrease water susceptibility in asphalt mixes

Typically, the test for evaluation contains a conditioning phase and an evaluation phase. The conditioning phase simulates in service conditions that increases water sensitivity, usually this includes a period of exposure to moisture. The evaluation phase may be qualitative or quantitative. A qualitative test estimates the severity of moisture damage by visual inspection, whereas a quantitative test measures a strength parameter. Often in quantitative testing, one sample is conditioned and another tested dry, then a ratio is computed for conditioned strength versus unconditioned strength. Under the SHRP method of mix design, the Modified Lottman test (AASHTO T-283) was adopted and therefore, this test will be used to assess moisture susceptibility. In addition to this, Dynamic Indirect Tensile Test and Simple Shear Tester can also be used to evaluate the moisture sensitivity of asphalt mixtures.

These moisture related problems stimulated considerable research in the United States in the late 1970s and during the 1980s. NCHRP projects were initiated to develop improved water sensitivity tests for HMA [7, 8, and 9]. The present AASHTO and ASTM test methods were developed based on this research (AASHTO T 283 and ASTM D 4867). Several other test methods have also been developed to determine the water susceptibility of HMA and other types of asphalt aggregate combinations. Most of the tests are intended for use during the mixture design process and but are not suitable for quality control and quality assurance purposes. For the most part, extensive data is not available to correlate laboratory tests and field performance. Laboratory tests for water susceptibility can be grouped into three mixture categories: loose, representative, and

compacted. □Loose mixture tests include soaking and boiling tests (e.g., ASTM D 3625) performed on loose or uncompacted mixtures. Representative Mix tests are performed on a selected portion of the aggregate fraction (for example the fine aggregate). One example is the "pedestal freeze-thaw test." Compacted mix tests comprise most of the testing presently performed in the United States. The immersion compression (ASTM D 1075), Root-Tunnicliff (ASTM D 4867), and Lottman (AASHTO T 283) tests are the most widely used. Important features of a water sensitivity test include: compaction of the HMA to an air void content typical of that which is achieved at the time of construction (six to eight percent), ensuring that the sample is exposed to water (using a vacuum saturation procedure), and exposing the sample to a severe test environment (freeze-thaw cycle or cycles). It is important that the air voids and the degree of saturation be controlled in whatever test method is used. The vacuum level and freeze-thaw cycles to stress the bond at the interface of the asphalt binder and aggregate must also be controlled. The Lottman test (AASHTO T 283) with a single freeze-thaw cycle is the best standardized test presently used in the United States. Multiple freeze-thaw cycles may be used to increase precision.

2.6. Tests on Compacted Mixtures

These tests are conducted on laboratory-compacted specimens or field cores or slabs. Examples include indirect tensile freeze–thaw cyclic with modulus and strength measurement, immersion– compression, abrasion weight loss, and sonic vibration tests. The major advantage of these tests is that the mix physical and mechanical properties, water/traffic action, and pore pressure effects can be taken into account. The results can be measured quantitatively, which minimizes subjective evaluation of test results. The

drawback of these tests is that they require elaborate testing equipment, longer testing times, and more laborious test procedures are needed.

2.6.1. Immersion–Compression Test ASTM D1075 (1949 and 1954) and AASHTO T165-55 (Effect of Water on Compressive Strength of Compacted Bituminous Mixtures):

The immersion–compression procedure was originally published as ASTM D1075-49. Therefore, the test is among the first to be used for evaluation of moisture sensitivity. Revisions were made to the procedure in 1996. Goode (1959) [10] explains the test in detail in *ASTM Special Technical Publication 252*. Two groups of compacted specimens are used in this test method. One group is submerged in a 120° F water bath for 4 days for conditioning, and the other group is maintained dry. An alternative approach to conditioning is to immerse the test specimens in water for 24 h at 140° F. Compressive strength is measured on specimens of both groups at 77° F at a deformation rate of 0.05 inch/min per inch of height. For a 4-inch tall specimen, the rate would be 0.2 inch/min. The average strength of conditioned specimens over that of dry specimens is used as a measure of moisture sensitivity of the mix. Most agencies have used a 70% ratio as the passing criterion for moisture sensitivity.

2.6.2. Marshall Immersion Test

The conditioning phase of this test is identical to the one used for the immersion–compression test. However, the Marshall stability is used as a strength parameter rather than compressive strength.

2.6.3. Moisture Vapor Susceptibility

The moisture vapor susceptibility procedure was developed and has been used by the California Department of Transportation (California Test Method 307). Two specimens

are prepared and compacted using the kneading compactor, as for mix design testing, except that they are prepared in stainless steel molds. The compacted surface of each specimen is covered with an aluminum seal cap, and a silicone sealant is applied around the edges to prevent the escape of moisture vapor. An assembly with a felt pad, seal cap, and strip wick is prepared to make water vapor available to the specimen by placing the free ends of the strip wick in water. After the assembly is left in an oven at 60° C with the assembly suspended over water for 75 h, the specimen is removed and tested immediately in the Hveem stabilometer. A minimum Hveem stabilometer value is required, which is less than that required for the dry specimens used for mix design.

2.6.4. Repeated Pore Water Pressure Stressing and Double-Punch Method

This test procedure was developed by Jimenez at the University of Arizona (1974) [11]. The test falls in the category of those that include measurement of mix mechanical properties and those that consider traffic dynamic loading. To capture the water pore pressure effect, compacted specimens undergo a cyclic stressing under water. The load is not directly in contact with the specimen. This stressing is accomplished through generating cyclic pressure within water at a rate of 580 rpm. The generated water pressure is between 35 and 217 kPa, which, according to Jimenez, is within a range comparable with pressure expected in saturated pavements under traffic. Once cyclic water pressure inducement is complete, the tensile strength of the specimens is determined by using the double-punch equipment. Compacted specimens are tested through steel rods placed at either end of the specimen in a punching configuration. Jimenez demonstrated the severity of this test by comparing predictions on similar mixtures using the immersion–compression test.

2.6.5. Original Lottman Indirect Tension Test

The original Lottman procedure was developed by Lottman at the University of Idaho in the late 1970s (Lottman 1978) [7]. The procedure requires one group of dry specimens and one group of conditioned specimens. The specimens are 4 in. in diameter and about 2.5 in. thick. Conditioning includes vacuum saturation of specimens fewer than 26 in. of mercury vacuum for 30 min followed by 30 min at atmospheric pressure. The partially saturated specimens are frozen at 0° F for 15 h followed by 24 h in a 140° F water bath. This is considered accelerated freeze–thaw conditioning. Lottman proposed thermal cyclic conditioning as an alternative. For each cycle, after 4 h of freeze at 0° F, the temperature is raised to 140^{O} for next 4 hours therefore, a complete thermal cycle lasts 8 h. The specimens go through 18 thermal cycles of this type. Lottman concluded that thermal cycling was somewhat more severe than the accelerated freeze–thaw conditioning with water bath. Conditioned and dry specimens are both tested for tensile resilient modulus and tensile strength using indirect tensile equipment. The loading rate is 0.065 in. /min for testing at 55° F or 0.150 in. /min for testing at 73° F. The severity of moisture sensitivity is judged based on the ratio of test values for conditioned and dry specimens.

2.6.6. AASHTO T283 (Modified Lottman Indirect Tension Test Procedure)

The AASHTO Standard Method of Test T283 [2], “Resistance of Compacted Bituminous Mixture to Moisture Induced Damage,” is one of the most commonly used procedures for determining HMA moisture susceptibility. The test is similar to the original Lottman with a few exceptions. One of the modifications is that the vacuum saturation is continued until a saturation level between 70% and 80% is achieved, compared with the original Lottman procedure that required a set time of 30 min. Another change is in the test

temperature and loading rate for the strength test. The modified procedure requires a rate of 2 in. /min at 77° F rather than 0.065 in. /min at 55° F. A higher rate of loading and a higher temperature were selected to allow testing of specimens with a Marshall Stability tester, available in most asphalt laboratories. The higher temperature also eliminates the need for a cooling system. Briefly, the test includes curing loose mixtures for 16 h at 60° C, followed by a 2-h aging period at 135° C. At least six specimens are prepared and compacted. The compacted specimens should have air void contents between 6.5% and 7.5%. Half of the compacted specimens are conditioned through a freeze (optional) cycle followed by a water bath. First, vacuum is applied to partially saturate specimens to a level between 55% and 80%. Vacuum-saturated samples are kept in a –18° C freezer for 16 h and then placed in a 60° C water bath for 24 h. After this period, the specimens are considered conditioned. The other three samples remain unconditioned. All of the samples are brought to a constant temperature, and the indirect tensile strength is measured on both dry (unconditioned) and conditioned specimens. Several research projects have dealt with the method's shortcomings, resulting in suggested "fixes," but the test remains empirical and liable to give either false positives or false negatives in the prediction of moisture susceptibility. Major concerns with this test are its reproducibility and its ability to predict moisture susceptibility with reasonable confidence (Solaimanian and Kennedy 2000a). AASHTO T283 was adopted by the Superpave system as the required test for determination of moisture damage. Following this adoption, state highway agencies made this test the most widely used procedure for determination of moisture damage potential. Later, Epps et al. (2000) investigated this test extensively under NCHRP Project 9-13. The researchers investigated the effect of a number of

factors on the test results, including different compaction types, diameter of the specimen, degree of saturation, and the freeze–thaw cycle. They used five aggregates, two considered good performers in terms of moisture resistance and the other three considered to have low to moderate resistance to moisture damage. Binders were specific to each mix and included PG 58-28, 64-22, 64-28, and 70-22. In summary, the following conclusions were drawn from that study, as reported by Epps et al. (2000): (i) In general, resilient modulus had no effect on tensile strength of dry specimens, conditioned specimens with no freeze–thaw, or conditioned specimens with freeze–thaw (ii) Dry strength of 100-mm-diameter Superpave gyratory compactor (SGC) specimens and 100-mm Hveem specimens was greater than that of 150-mm SGC specimens (iii) Dry strength increased as the aging time for the loose mix increased and, (iv)The tensile strength ratio of 150-mm SGC specimens was larger than the tensile strength ratio of 100-mm-diameter SGC specimens or 100-mm Hveem specimens.

2.6.7. ASTM D4867 (Tunnicliff–Root Test Procedure)

ASTM D4867, "Standard Test Method for Effect of Moisture on Asphalt Concrete Paving Mixtures," is comparable with AASHTO T283. In both methods, the freeze cycle is optional. However, curing of the loose mixture in a 60°C oven for 16hour is eliminated in the ASTM D4867 procedure.

2.6.8. Texas Freeze–Thaw Pedestal Test

The Texas freeze–thaw pedestal test was proposed by Kennedy et al. (1982) [12] as a modification of the water susceptibility test procedure proposed by Plancher et al. (1980) at the Western Research Institute. The test is in the category of those evaluating the compatibility between asphalt binder and aggregate and the corresponding adhesiveness.

The test is designed to minimize the effect of mechanical properties of the mix by using a Uniform-sized aggregate. It prescribes the preparation of hot mix using a fine fraction of aggregate [passing the No. 20 (0.85-mm) and retained on the No. 35 (0.50-mm) sieve] and asphalt at a temperature of 150° C. The hot mix so prepared is kept in the oven at 150° C for 2 h and stirred for uniformity of temperature every hour. At the end of 2 h, the mix is removed from the oven and cooled to room temperature, reheated to 150° C, and compacted with a load of about 28 kN for 15 min to form a briquette 41 mm in diameter by 19 mm in height (the procedure does not prescribe any tolerance for the dimensions). The briquette is cured for 3 days at room temperature and placed on a pedestal in a covered jar of distilled water. It is then subjected to thermal cycling of 15 h at –12° C, followed by 9 h at 49° C. After each cycle, the briquette surface is checked for cracks. The number of cycles required to induce cracking is a measure of water susceptibility (typically 10 freeze–thaw cycles). Pedestal test specimens are prepared from a narrow range of uniformly sized aggregate particles coated with 5% asphalt. This formulation reduces aggregate particle interactions in the mixture matrix, and the thin asphalt coating between aggregate particles produces a test specimen that is highly permeable and thus allows easy penetration of water into the interstices found between aggregate particles. Therefore, moisture-induced damage in the specimen can easily arise either from bond failure at the asphalt–aggregate interface region (stripping) or from the fracture of the thin asphalt–cement films bonding aggregate particles (cohesive failure) by formation of ice crystals.

2.6.9. Hamburg Wheel-Tracking Device (HWTD)

The HWTD was developed by Esso A.G. in the 1970s in Hamburg, Germany (Romero and Stuart 1998) [13]. This device measures the combined effects of rutting and moisture damage by rolling a steel wheel across the surface of an asphalt concrete specimen that is immersed in hot water. The wheel rolls back and forth on the submerged specimen. Originally, a pair of cubical or beam test specimens were used. Typically, gyratory-compacted specimens are arranged in a series to provide the required path length for the wheels. Each steel wheel passes 20,000 times or until 20 mm of deformation is reached. The measurements are customarily reported versus wheel passes.

The results from the HWTD are the post compaction consolidation, creep slope, stripping Slope and stripping inflection point. The post compaction consolidation is the deformation measured at 1,000 passes, assuming that the wheel is densifying the mixture within the first 1,000 wheel passes. The creep slope is the number of repetitions or wheel passes to create a 1-mm rut depth due to viscous flow. The stripping slope is represented by the inverse of the rate of deformation in the linear region of the deformation curve, after stripping begins and until the end of the test. The stripping slope can be quantified as the number of passes required to create a 1-mm impression from stripping. The stripping inflection point is the number of passes at the intersection of the creep slope and the stripping slope. It represents the moisture damage resistance of the HMA and is assumed to be the initiation of stripping (Aschenbrener and Currier 1993) [14].

2.6.10. Georgia Loaded Wheel Tester

The Georgia Loaded wheel Tester (GLWT) was developed by the Georgia Department of Transportation. Development of the GLWT included comparisons of the creep tests and

the repeated load triaxial test with data obtained from GLWT testing. These comparisons were used to evaluate the GLWT ability to produce results in line with rutting in the field [15]. The GLWT measures the rutting susceptibility of a HMA mix by rolling a steel wheel across the top of a pressurized hose placed on top of an asphalt beam. The hose is made of stiff 29mm diameter rubber. The wheel travels at a rate of 33 cycles or 67 passes per minute. Steel plates confine the beams that are used. The machine has a temperature-controlled compartment.

In 1996 Collins, Shami and Lai [16] developed a gyratory sample mold that could be used in the GLWT. The GLWT that was used had three wheel testers that run simultaneously. The mold that was developed was made of high-density polyethylene. Their results indicated that the GLWT could be used in conjunction with Superpave Level 1 mix design to develop mix designs with low susceptibility to rutting.

The projected use of the GLWT was an inexpensive proof tester. Watson, Johnson, and Jared (1997) [17] found that some HMA mixes that fell outside the Superpave restricted zone performed well in the GLWT. Therefore, in order to prevent economical mixes from being rejected, mixes should be tested even if they fall into the restricted area. In 1997, Shami, Lai and Harmen [18] developed a temperature effect model to be used with the GLWT. With this model, rutting susceptibility can be tested at one temperature for different environments.

2.7. Prevention of Moisture Damage

When subject to moisture, pavements may suffer accelerated damage leading to reduced pavement life. If asphalt pavement does suffer from water sensitivity, serious distresses

may occur. As a result, the asphalt pavement reduces in performance and increases in maintenance costs. To alleviate or to control this problem, various liquid or solid anti-stripping additives have been developed, which can be used to promote adhesion between asphalt and aggregate. Anderson and Dulkatz (1982) [19] reviewed the effects of commercially available anti-stripping additives on the physical properties of asphalt cement. Anderson and Dulkatz's experimental studies of the physical and compositional properties of asphalt cement with anti-stripping additives demonstrated that anti-stripping additives tend to soften the asphalt, reduce the temperature susceptibility, and improve the aging characteristics of asphalt cement.

2.8. Anti-stripping Agents

In order to reduce pavement damage related to stripping, additives are used to decrease moisture susceptibility. Liquid anti-stripping agent and lime additives are among the most commonly used type of anti-stripping agent. However, if an additive is used when it is not needed or if it is used incorrectly, adverse effects may occur. Such adverse effects increase economic cost as well as early maintenance or rehabilitation. (Tunnicliff and root 1984) [9].

2.8.1. Lime additives

The hydrated lime is applied to the aggregates before mixing in several different ways. The lime can be added as a dry powder to wet or dry aggregates or as slurry to the aggregates, which are then dried before mixing. Lime is typically added to the aggregates at 1 to 2 percent of the aggregate weight. Lime increases the adhesion between asphalt and aggregates through different chemical reactions. The increase in adhesion reduces stripping, providing a more durable pavement.

2.8.2. Liquid anti-stripping agent

Liquid surfactants reduce the surface tension of the asphalt, allowing for greater adhesion between the asphalt and aggregate. Liquid amines and liquid phosphate ester are the two types of anti-strip additives used in HMA. They are mixed with the asphalt prior to mixing at a dosage of about 0.5 to 1 percent of the asphalt weight. Unlike the application of the hydrated lime, the liquid additives can be mixed with large amounts of asphalt and stored for use in many mixes. These advantages save time and money by using less material and not affecting the production process greatly. One disadvantage with the liquid surfactants is possible heat degradation [20]. If the asphalt mixture is held at high temperature for long periods, the effectiveness may be reduced. In addition, it has to be added uniformly and mixed consistently throughout the mix.

2.9. Studies of Additive Effectiveness

Previous studies have been conducted on the subject of moisture sensitivity and anti-strip additives. To evaluate the properties of bituminous mixtures containing hydrated lime, Mohammad et al (2000) [21] studied TSR values, rutting and resilient modulus. They found that when hydrated lime was added as mineral filler, the permanent deformation and fatigue endurance improved. In addition, their test results illustrated that adding lime increased the tensile strength of HMA Mixtures. Field and laboratory studies conducted by Kennedy and Anagnos (1984) [22] found that both dry lime and lime slurry improved moisture resistance. However, lime slurry had a better performance than the dry lime. Adding the lime in a drum mix plant was found to be effective because a great deal of the lime was lost before mixing with the asphalt. Birdsall and Khosla performed a study using three different aggregates and three different additives as well as a control set

without additives. The results showed significant increases in the tensile strength and the TSR values with the use of lime, amine, and ester [23].

2.10. Adding Hydrated Lime to Hot Mix Asphalt

There are several proven and effective methods for adding hydrated lime to asphalt. Various states in the USA use different methods of incorporating hydrated lime in mixtures. Different states have formulated a variety of methods that are most effective in their own states based on these three basic methods. However, it may be noted that most states use lime in hydrated form rather than quicklime.

Addition of Dry Hydrated Lime to Dry Aggregates:Addition of lime powder to dry aggregates is the simplest method of incorporating hydrated lime to asphalt mixes. This method was first adopted by the State of Georgia in early 1980's. In this method, hydrated lime and mineral filler is introduced in a drum mixer just after the point at which asphalt is introduced. Hydrated lime thus introduced comes in contact with aggregates and directly results in improved bond between aggregate and asphalt. Some portion of lime that fails to come in contact with aggregate will be mixed with asphalt. This results in lime reacting with highly polar molecules in asphalt to form insoluble salts that no longer attract water thus reducing stripping and oxidation potential [24]. The amount of hydrated lime used in this method is usually 0.9% by the weight of dry aggregates.

Addition of Dry Hydrated Lime to Wet Aggregates: Addition of lime powder to wet aggregates is the most common method of incorporating of hydrated lime in asphalt mixes. In this method, hydrated lime is metered into aggregate that has a moisture content of 2-3% over its saturated-surface-dry (SSD) condition. After hydrated lime is added to

wet aggregates, the lime-aggregate mix is run through a pug mill to ensure thorough mixing. The advantage of adding dry hydrated lime to wet aggregates is to ensure a better coverage and proper application compared to the previous method. This is possible because moisture ionizes lime and helps distribute it on the surface of aggregate. The portion of hydrated lime that does not adhere to the aggregates eventually gets mixed with asphalt and contributes to the improvements that are described in the dry method. The main disadvantage of using this method is the extra effort and fuel required to dry the aggregates before mix production. When using this method of adding hydrated lime, many states require that lime-aggregate mix be marinated for about 48 hours. This marination process has the following advantages: 1) moisture content is reduced over the period of stockpiling; and 2) due to stockpiling lime treatment can be carried out separately from the main HMA production providing some economic advantage. Disadvantages of marination are: 1) additional effort required for handling aggregate load; 2) additional space required for stocking both lime-treated and untreated aggregates; 3) carbonation of aggregates could occur due to chemical reaction.

Addition of Hydrated Lime in the Form of Slurry: In this method of incorporating lime, slurry of lime and water is metered and applied to aggregates to achieve a superior coverage of the stone surfaces. Lime slurries are made from hydrated lime but sometimes quicklime is also used. As indicated in the previous method, the treated aggregates can be marinated or used directly further. Advantages of using this method are as follows: 1) improved resistance of HMA to stripping; 2) as lime slurry is used, lime dispersion due to dusting and blowing is minimized; and 3) this method results in the best coverage of lime

over aggregate. The disadvantages of using lime slurries are: 1) use of lime slurries can substantially increase the water content of aggregate resulting in increased fuel consumption during drying process; and 2) use of this method requires specialized equipment that is costly to purchase and maintain. Table 2.1 shows methods of lime addition used by different states. Based on the information presented in Table 2.1, it can be observed that the most common method used for incorporating lime is the addition of dry lime to wet aggregates. Except for Nevada, most states either do not require marination of aggregate, or it is optional. Several states have conducted studies to evaluate the efficacy of various methods of incorporating lime in asphalt mixes with and without marination process. Other states also use hydrated lime in asphalt, including Florida (injecting hydrated lime into the drum or adding lime slurry to aggregate), Montana (injecting hydrated lime into the drum), Wyoming (adding dry hydrated lime to wet aggregate), New Mexico (adding dry hydrated lime to wet aggregate), and South Dakota (adding dry hydrated lime to wet aggregate).

Table 2.1 Summary of Methods Adopted for Incorporating Lime by Various States [25, 26]

State	Method of adding hydrated lime to asphalt				
	Dry hydrated lime to dry aggregate		Dry hydrated lime to wet aggregate	Lime slurry to aggregate	Marination
	Drum	Batch			
Arizona			*		No
California				*	Yes
Colorado			*	*	Optional
Georgia	*	*			No
Mississippi			*		No
Nevada			*		Yes
Oregon			*		Optional
South Carolina			*		No
Texas	*		*	*	No
Utah			*		Optional
Florida	*			*	-
Montana	*				-
Wyoming			*		-
New Mexico			*		-
South Dakota			*		-

2.11. Advantages of Adding Hydrated Lime

Hydrated Lime Improves Stiffness and Reduces Rutting: Rutting is permanent deformation of the asphalt, caused when elasticity is exceeded. The ability of hydrated lime to make an asphalt mix stiffer, tougher, and resistant to rutting, is a reflection of its superior performance as active mineral filler. Hydrated lime significantly improves the performance of asphalt in this respect. Unlike most mineral fillers, lime is chemically active rather than inert. It reacts with the bitumen, removing undesirable components at the same time that its tiny particles disperse throughout the mix, making it more resistant to rutting and fatigue cracking. The stiffening that results from the addition of hydrated lime can increase the PG rating of asphalt cement [27].

Hydrated Lime Reduces Oxidation and Aging: Oxidation and aging occur over time to generate a brittle pavement, in particular, polar molecules react with the environment, breaking apart and contributing to pavement failure. Another benefit that results from the addition of hydrated lime to many asphalt cements is a reduction in the rate at which the asphalt oxidizes and ages [28]. This is a result of the chemical reactions that occur between the calcium hydroxide and the highly polar molecules in the bitumen. If left undisturbed in the mix, many of those polar molecules will react with the environment, breaking apart and contributing to a brittle pavement over time. Hydrated lime combines with the polar molecules at the time that it is added to the asphalt and thus, they do not react with the environment. Consequently, the asphalt cement remains flexible and protected from brittle cracking for years longer than it would without the contribution of lime [24].

Hydrated Lime Reduces Cracking: Hydrated lime reduces asphalt cracking that can result from causes other than aging, such as fatigue and low temperatures. Although, in general, stiffer asphalt mixes crack more, the addition of lime improves fatigue characteristics and reduces cracking. Progressive cracking is typically due to the formation of microcracks. These microcracks are intercepted and deflected by tiny particles of hydrated lime. Lime reduces cracking more than inactive fillers because of the reaction between the lime and the polar molecules in the asphalt cement, which increases the effective volume of the lime particles by surrounding them with large organic chains [29, 30].

2.12. Summary

Stripping of HMAC mixture is a serious and costly problem for many highway agencies. Over the years, many testing procedures have been developed to predict the moisture

susceptibility of a HMA mixture. Two types of testing have been developed: strength tests and subjective tests. Of the strength tests, The AASHTO Standard Method of Test "Resistance of Compacted Bituminous Mixture to Moisture Induced Damage," is most commonly used procedures for determining HMA moisture susceptibility. The method of adding dry hydrated lime to wet aggregate seems to be the most widely used method.

CHAPTER 3

3. MATERIAL CHARACTERIZATION

This chapter describes the mixtures used in this study. Asphalt concrete is typically composed of aggregates and asphalt cement. The mix designs were performed with the three sources of aggregates and one asphalt binder for two gradation types (12.5 mm and 9.5 mm mixtures).

3.1. Aggregates

Three different aggregates used in this study, each with a different level of moisture sensitivity. Marine Limestone from the Castle Hayne quarry in Castle Hayne, NC, was selected for its low moisture susceptibility. Slate aggregate from the Asheboro quarry, NC, was selected because of its moderate moisture susceptibility. Granitic Gneiss from the Fountain quarry near Rocky Mount, NC, was selected because of its high propensity to strip. The selection was based on providing three different levels of moisture susceptibility without the influence of anti-strip additives.

3.1.1. Aggregate properties

The specific gravity and percent absorption of the coarse and fine fractions were determined in accordance with ASTM C127 (Standard Test Method for Specific Gravity and absorption of Coarse aggregate) and ASTM C128 (Standard Test method for Specific Gravity and Absorption of Fine aggregate). Table 3.1 gives the bulk specific gravity (G_{sb}) of the fractions.

Table 3.1 Aggregate Bulk Specific Gravity

Material Source		Material Property	
Quarry Source	Aggregate Fraction	Bulk Specific gravity	Percent Absorption
Fountain	Coarse aggregate	2.645	0.48
	Fine aggregate	2.612	1.47
Asheboro	Coarse aggregate	2.784	0.30
	Fine aggregate	2.542	3.06
Castle Hayne	Coarse aggregate	2.392	3.73
	Fine aggregate	2.608	1.01

3.2. Asphalt Binder

PG70-22, PG 76-22 and PG 64-22 binders from Citgo Oil Company Savannah, Georgia, was used for all the mixtures in the study.

3.3. Design of Asphalt Concrete Mixtures (12.5mm)

S -12.5C, S – 12.5D and S – 12.5B mixtures (NCDOT designation for 12.5mm mixtures with PG 70-22, PG 76-22 and PG 64-22, respectively) were used for this study. Superpave^{TM} mix designs were performed on three sources of aggregates to be evaluated. In the mix design process, a single aggregate gradation was arrived at for each asphalt binder grade that was acceptable for all three aggregates. Using these trial gradations, samples were made at variable asphalt contents and the volumetric properties were determined. From the volumetric data, optimum asphalt content was selected for each

gradation and each aggregate source. The Superpave^{TM} compaction criteria for a mix design are based on three points throughout the compactive effort: an initial (N_{ini}), design (N_{des}), and maximum (N_{max}) number of gyrations. These various levels of gyrations were established from in-service pavements with different traffic levels and design temperatures. The N_{ini}, N_{des} and N_{max} for the S – 12.5C mixture were 8, 100 and 160 respectively. The N_{ini}, N_{des} and N_{max} for the S – 12.5D mixture were 9, 125 and 205 respectively. The N_{ini}, N_{des} and N_{max} for the S – 12.5B mixture were 7, 75 and 115 respectively.

The first step in the design of asphalt concrete mixtures is to select the design aggregate structure. To select the design aggregate structure, three trial blends were established. Any number of trial blends can be attempted, but at least three are recommended. The next step was to evaluate the trial blends through compaction of specimens and determine the volumetric properties of each trial blend. This was done at the trial asphalt binder content for each trial gradation. The trial asphalt binder content is based on the estimated effective specific gravity of the blend and an assumption for asphalt absorption.

Two specimens were compacted to the maximum number of gyrations with the specimen height recorded during the compaction process. After compaction of the trial blends, the volumetric properties were determined. The aggregate structure, which satisfied the Superpave^{TM} mix design criteria (Table 3.2), was selected as the design aggregate structure.

Table 3.2 Superpave Mix Design Criteria

Mix Type	VMA %	VFA %	$\%G_{mm}$ @ N_{ini}	%Gmm@ N_{max}	Dust Proportion
S – 12.5C	14.0 (Min)	65-75	≤90.0	≤98.0	0.6-1.4
S – 12.5D	14 (Min)	65-75	≤90.0	≤98.0	0.6-1.4
S – 12.5 B	14 (Min)	65-80	≤90.5	≤98.0	0.6-1.4

The next step was to find the design asphalt content. Once the design aggregate was selected, specimens were compacted at varying asphalt binder contents. Two specimens were compacted at the selected blend's estimated asphalt content, at $\pm$ 0.5% and +1.0% of the estimated binder content. Two specimens were also prepared at the estimated asphalt content for the determination of maximum theoretical specific gravity. The mixture properties were then evaluated to determine the design asphalt binder content. Using the densification data at N_{ini}, N_{des} and N_{max}, the volumetric properties were calculated for all asphalt contents. The volumetric properties were plotted against asphalt binder content. The design asphalt binder content was established as 4.0% air voids at N_{des} gyrations for each mixture. All other mixture properties were checked at the design asphalt binder content to ensure that they met the criteria. The design of asphalt concrete mixtures for the three different aggregates and the three different asphalt binder grades is presented in the following sections.

3.3.1. Design of Asphalt Concrete Mixtures (Castle Hayne, S – 12.5 C)

Selection of Aggregate Structure – Castle Hayne Aggregate

A trial gradation was selected based on Superpave™ 12.5mm nominal maximum size to yield approximately 4% air voids at $N_{des.}$ Table 3.3 lists the selected aggregate gradation and the Superpave™ control points. Superpave™ uses a gradation plot based on a 0.45 power chart. Figure 3.1 shows the percent passing for the selected aggregate gradation as well as the Superpave™ restrictions for all the three sources of aggregate for 12.5mm nominal maximum size. It is appropriate to note that Superpave™ defines the nominal maximum size of the aggregate as one sieve size larger than the first sieve to retain more than ten-percent cumulative weight. It defines the maximum aggregate size as one sieve size larger than the nominal maximum size. In view of this definition, the trial gradation had a nominal maximum size of 12.5 mm and a maximum size of 19.0mm.

Table 3.3 Percent passing (12.5 mm Nominal Size)

Sieve Size, mm	**Percent Passing**	
	Mix Gradation	Superpave™ restrictions
19.0	100	100
12.5	92	90-100
9.5	76	
4.75	50	
2.36	30	28-58
1.18	16	
0.6	10	
0.3	7	
0.15	5	
0.075	4	2-10
Pan	0	

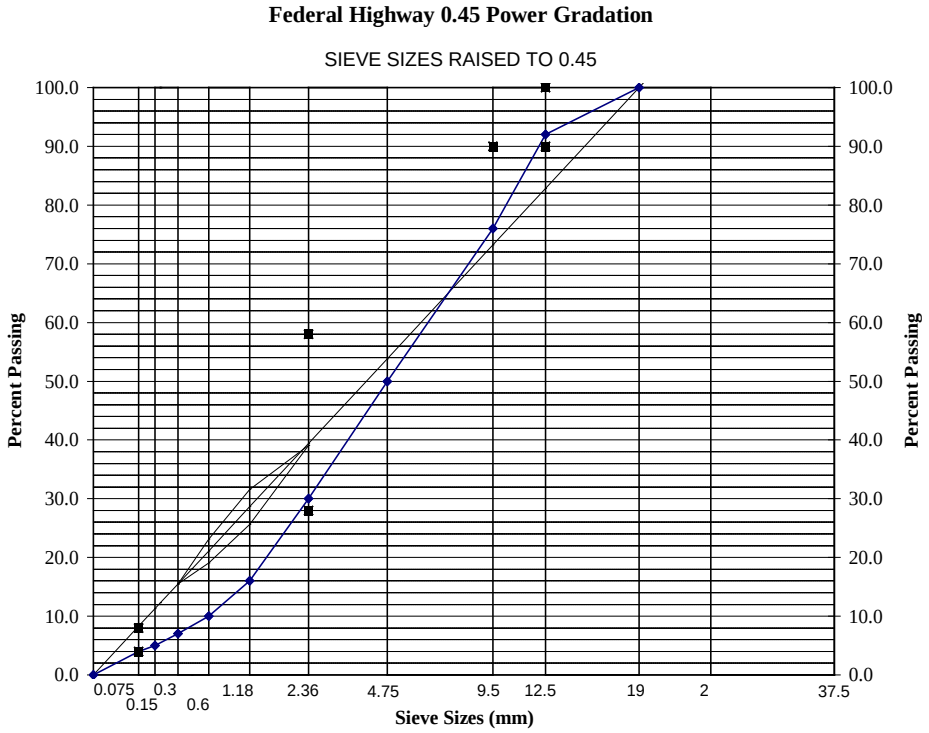

Figure 3.1 Selected Aggregate Gradation

Once the design aggregate structure of Castle Hayne aggregate was selected, specimens were compacted at varying asphalt binder contents. The mixture properties were then evaluated to determine design asphalt binder content. Using the densification data at N_{ini}, N_{des} and N_{max} the volumetric properties were calculated at N_{des} for all asphalt contents. The volumetric properties were plotted against asphalt binder content. The design asphalt binder content is established at 4.0% air voids and at N_{des} of 100 gyrations. The plot of air voids versus asphalt content for the Castle Hayne mixture is shown in Figure 3.2. From this plot, a trial design asphalt content of 5.2 percent is obtained at an air void content of 4%.

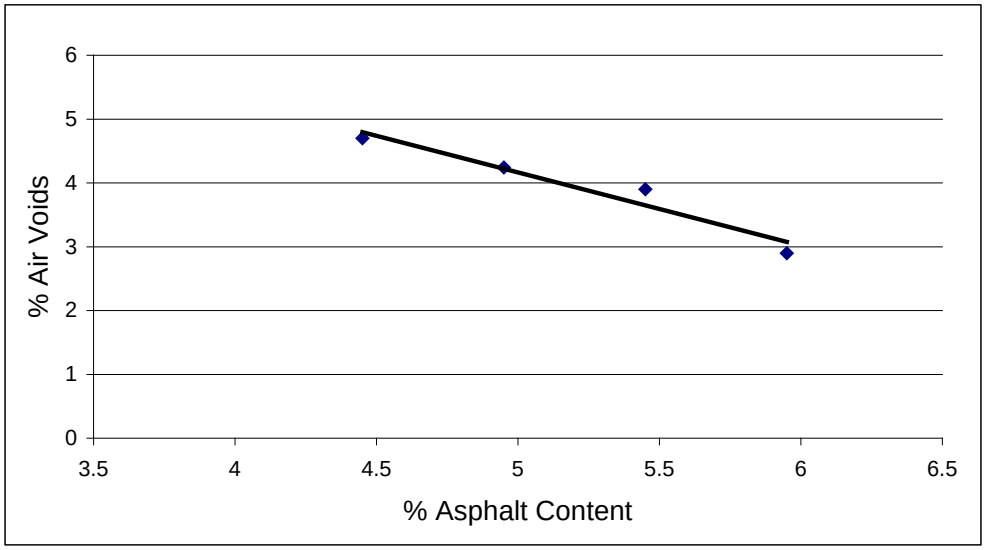

Figure 3.2 Air voids versus Asphalt Content for Castle Hayne, S – 12.5 C Mixture

The mixture properties were checked at the design asphalt binder content to ensure that they met the criteria. The observed mixture properties and the Superpave Mix Design criteria are in the Table 3.4. It is shown that the mixture properties satisfy the SuperPave mix design criteria.

Table 3.4 Summary of Mixture Properties (Castle Hayne, S – 12.5 C)

Properties	Mixture Properties	SuperPave Criteria
VMA	14.51	>14%
VFA	71.24	65 - 75
%Gmm@Nini	87.44	$\leq$ 90
%Gmm@Nmax	96.97	$\leq$ 98

3.3.2. Design of Asphalt Concrete Mixtures (Fountain, S – 12.5 C)

As discussed in section 3.3, a single aggregate gradation was arrived at and that was acceptable for all three aggregates when using PG 70-22 asphalt binder. The aggregate structure is the same as that used for the Castle Hayne aggregate. A trial design asphalt content of 4.9 percent is obtained at an air void content of 4%. The mixture properties were checked at the design asphalt binder content to ensure that they met the criteria. The observed mixture properties and the Superpave Mix Design criteria are in the Table 3.5. It is shown that the mixture properties satisfy the SuperPave mix design criteria.

Table 3.5 Summary of Mixture Properties (Fountain, S – 12.5 C)

Properties	Mixture Properties	SuperPave Criteria
VMA	14.34	>14%
VFA	72.19	65 – 75
%Gmm@Nini	87.40	$\leq$ 90
%Gmm@Nmax	97.63	$\leq$ 98

3.3.3. Design of Asphalt Concrete Mixtures (Asheboro, S – 12.5 C)

The aggregate structure is the same as that used for the Castle Hayne, S – 12.5 C Mixture. A trial design asphalt content of 5.7 percent is obtained at an air void content of 4%. The mixture properties were checked at the design asphalt binder content to ensure that they met the criteria. The observed mixture properties and the Superpave Mix Design criteria are in the Table 3.6.

Table 3.6 Summary of Mixture Properties (Asheboro, S – 12.5 C)

Properties	Mixture Properties	SuperPave Criteria
VMA	14.16	>14%
VFA	71.85	65 - 75
%Gmm@Nini	85.68	$\leq$ 90
%Gmm@Nmax	96.11	$\leq$ 98

3.3.4. Design of Asphalt Concrete Mixtures (Fountain, PG 76-22)

As discussed in section 3.3, a single aggregate gradation was arrived at and that was acceptable for all three aggregates when using PG 76-22 asphalt binder. To avoid confusion and to provide better comparison between results, a single gradation was found that satisfied SuperPave™ volumetric requirements for all three aggregate sources using both PG 76-22 and PG 64-22 asphalt binder grades.

Table 3.7 Percent passing (12.5 mm Nominal Size)

Sieve Size, mm	**Percent Passing**	
	Mix Gradation	Superpave™ restrictions
19.0	100	100
12.5	95	90-100
9.5	88	
4.75	62	
2.36	44	28-58
1.18	33	
0.6	25	
0.3	17	
0.15	8	
0.075	4.5	2-10
Pan	0	

A trial design asphalt content of 4.9 percent is obtained at an air void content of 4%. The mixture properties were checked at the design asphalt binder content to ensure that they met the criteria. The observed mixture properties and the Superpave Mix Design criteria are in the Table 3.8. It is shown that the mixture properties satisfy the SuperPave mix design criteria.

Table 3.8 Summary of Mixture Properties (Fountain, S – 12.5 D)

Properties	Mixture Properties	SuperPave Criteria
VMA	15.12	>14%
VFA	72.56	65 – 75
%Gmm@Nini	88.30	≤90
%Gmm@Nmax	95.90	≤98

3.3.5. Design of Asphalt Concrete Mixtures (Asheboro, S – 12.5 D)

The aggregate structure is the same as that used for the Fountain, S – 12.5 D Mixture. A trial design asphalt content of 4.9 percent is obtained at an air void content of 4%. The mixture properties were checked at the design asphalt binder content to ensure that they met the criteria. The observed mixture properties and the Superpave Mix Design criteria are in the Table 3.9.

Table 3.9 Summary of Mixture Properties (Asheboro, S – 12.5 D)

Properties	Mixture Properties	SuperPave Criteria
VMA	14.14	>14%
VFA	70.67	65 - 75
%Gmm@Nini	89.92	≤90
%Gmm@Nmax	98.00	≤98

3.3.6. Design of Asphalt Concrete Mixtures (Castle Hayne, S – 12.5 D)

The aggregate structure is the same as that used for the Fountain, S – 12.5 D Mixture. A trial design asphalt content of 5.4 percent is obtained at an air void content of 4%. The mixture properties were checked at the design asphalt binder content to ensure that they met the criteria. The observed mixture properties and the Superpave Mix Design criteria are in the Table 3.10.

Table 3.10 Summary of Mixture Properties (Castle Hayne, S – 12.5 D)

Properties	Mixture Properties	SuperPave Criteria
VMA	14.71	>14%
VFA	72.08	65 - 75
%Gmm@Nini	87.86	≤90
%Gmm@Nmax	95.87	≤98

3.3.7. Design of Asphalt Concrete Mixtures (Fountain, S – 12.5 B)

As discussed in Section 3.3.4, the aggregate structure for all S – 12.5 B mixtures is the same as that used for the S – 12.5D mixtures. A trial design asphalt content of 4.9 percent is obtained at an air void content of 4%. The mixture properties were checked at the design asphalt binder content to ensure that they met the criteria. The observed mixture properties and the Superpave Mix Design criteria are in the Table 3.11.

Table 3.11 Summary of Mixture Properties (Fountain, S – 12.5 B)

Properties	Mixture Properties	SuperPave Criteria
VMA	15.60	>14%
VFA	74.01	65 – 80
%Gmm@Nini	88.22	≤90.5
%Gmm@Nmax	96.18	≤98

3.3.8. Design of Asphalt Concrete Mixtures (Asheboro, S – 12.5 B)

The aggregate structure is the same as that used for the Fountain, S – 12.5 B mixture. A trial design asphalt content of 4.5 percent is obtained at an air void content of 4%. The mixture properties were checked at the design asphalt binder content to ensure that they met the criteria. The observed mixture properties and the Superpave Mix Design criteria are in the Table 3.12.

Table 3.12 Summary of Mixture Properties (Asheboro, S – 12.5 B)

Properties	Mixture Properties	SuperPave Criteria
VMA	14.51	>14%
VFA	73.11	65 – 80
%Gmm@Nini	86.83	≤90.5
%Gmm@Nmax	96.08	≤98

3.3.9. Design of Asphalt Concrete Mixtures (Castle Hayne, S – 12.5 B)

The aggregate structure is the same as that used for the Fountain, S – 12.5 B mixture. A trial design asphalt content of 6.0 percent is obtained at an air void content of 4%. The mixture properties were checked at the design asphalt binder content to ensure that they met the criteria. The observed mixture properties and the Superpave Mix Design criteria are in the Table 3.13.

Table 3.13 Summary of Mixture Properties (Castle Hayne, S – 12.5 B)

Properties	Mixture Properties	SuperPave Criteria
VMA	16.48	>14%
VFA	75.68	65 – 80
%Gmm@Nini	88.03	≤90.5
%Gmm@Nmax	95.99	≤98

3.4. Design of Asphalt Concrete Mixtures (S – 9.5)

S -9.5C mixtures (NCDOT designation for 9.5mm mixtures with PG 70-22) were used for this study. The aggregate structure as shown in Table 3.8, which satisfied the Superpave^{TM} mix design criteria (Table 3.7), was selected as the design aggregate structure for all the three aggregates.

Table 3.14 Superpave Mix Design Criteria

VMA %	VFA %	$\%G_{mm}$ @ N_{ini}	%Gmm@ N_{max}	Dust Proportion
15.0 (Min)	65-75	<90	<98.0	0.6-1.4

Table 3.15 Percent passing (S – 9.5)

Sieve Size, mm	Percent Passing Mix Gradation	Percent Passing Superpave™ restrictions
12.5	100	100
9.5	93	90-100
4.75	58	
2.36	41	32-67
1.18	27	
0.6	18	
0.3	13	
0.15	8	
0.075	4	2-10

Figure 3.3 shows the percent passing for the selected gradation as well as the Superpave™ restrictions for all three aggregate types. Superpave™ defines the nominal maximum size of the aggregate as one sieve size larger than the first sieve to retain more than ten-percent cumulative weight. It defines the maximum aggregate size as one sieve size larger than the nominal maximum size. In view of this definition, the trial gradation had a nominal maximum size of 9.5 mm and a maximum size of 12.5mm.

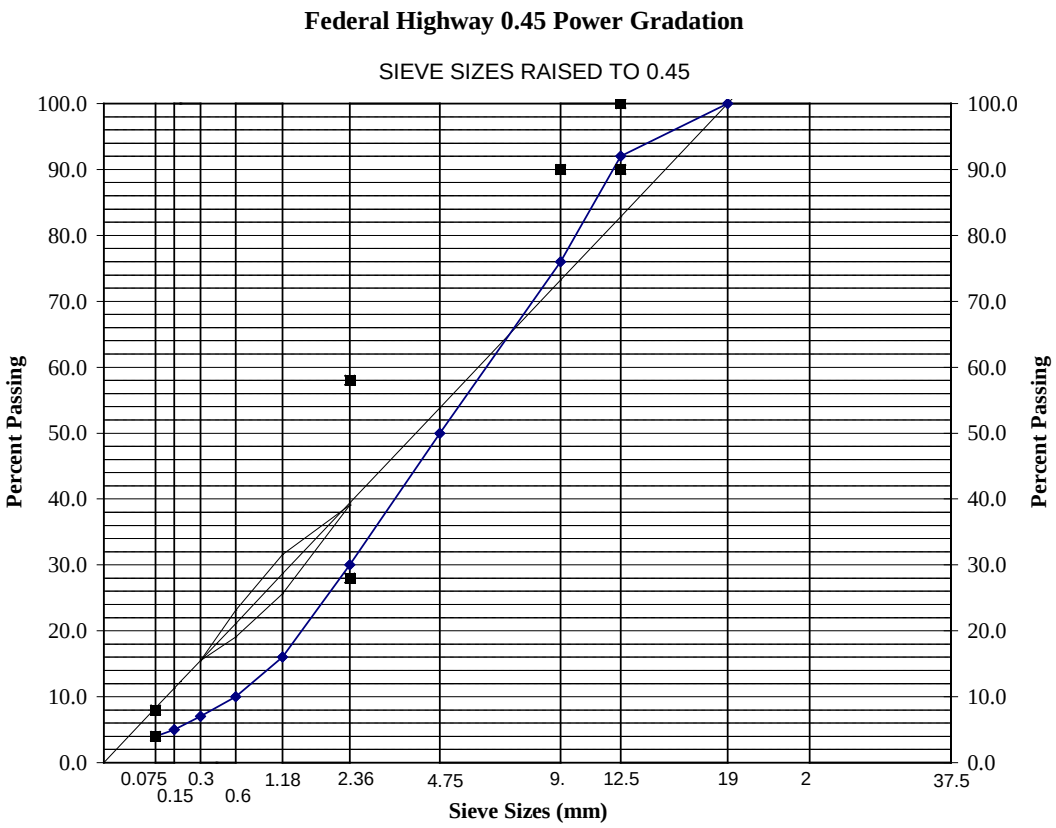

Figure 3.3 Aggregate Gradation (S – 9.5 C)

All mixture properties are checked at the design asphalt binder content to ensure that they met the criteria. The mixture properties obtained with a design asphalt content of 4.5% (Asheboro Mix) and the Superpave Mix Design criteria are in the Table 3.16.

Table 3.16 Observed Mix Properties (Asheboro Mix) and the Superpave Mix Design Criteria

Properties	Mixture Properties	SuperPave Criteria
VMA	15.3	>15%
VFA	72.4	65 – 76
%Gmm@Nini	85.3	$\leq$ 90
%Gmm@Nmax	97.1	$\leq$ 98

The mixture properties obtained with a design asphalt content of 4.9% (Castle Hayne Mix) and the Superpave Mix Design criteria are in the Table 3.17.

Table 3.17 Observed Mix Properties (CastleHayne Mix) and the Superpave Mix Design Criteria

Properties	Mixture Properties	SuperPave Criteria
VMA	15.9	>15%
VFA	73.5	65 - 76
%Gmm@Nini	85.9	$\leq$ 89
%Gmm@Nmax	96.8	$\leq$ 98

The mixture properties obtained with a design asphalt content of 5.1 % (Fountain Mix) and the Superpave Mix Design criteria are in the Table 3.18.

Table 3.18 Observed Mix Properties (Fountain Mix) and the Superpave Mix Design Criteria

Properties	Mixture Properties	SuperPave Criteria
VMA	15.6	>15%
VFA	72.1	65 - 76
%Gmm@Nini	86.8	$\leq$ 89
%Gmm@Nmax	96.9	$\leq$ 98

3.5. Anti-stripping Additives

The mixtures that contain moisture susceptible aggregates may be treated with a number of anti-stripping additives. There are several additives available on the market today. For this study, two additives were used- Hydrated lime and LOF 6500 (liquid anti-stripping agent). The following sections provide specific information for each additive utilized in this research.

3.5.1. Hydrated Lime

Hydrated lime ($Ca(OH)_2$) was used in this study as anti-strip additive, which is referred as lime throughout this report. This should not be confused with quicklime (CaO). The difference between lime and quicklime is in the amount of chemically combined water. Both lime and quicklime are available in fine powder form. Quicklime is highly receptive of water. The amount of hydrated lime added was one percent by weight of the aggregate in all cases. This is typical treatment level for hydrated lime in today's hot mix

production. Based on the information obtained from literature, it is observed that the most common method used for incorporating lime is the addition of dry lime to wet aggregates. Based on these findings and upon recommendation from NCDOT personnel, the method of adding dry lime to wet aggregates without marination was adopted for this study.

3.5.2. Liquid anti-stripping agent

LOF 6500 was used as liquid anti-strip additive. LOF 6500 was added to the asphalt cement at 0.5 percent by weight of the asphalt.

3.6. Mixture design Using Additives

Mix Design checking of Asphalt Mixtures Using hydrated lime and Liquid anti-stripping agent were conducted. To accommodate 1% hydrated lime in the original gradation, a slight modification in the mineral portion of the gradation (#200) was done. Mix checking was done using the same optimum asphalt content as obtained during mixture design without additive for all mixtures. Volumetric properties were measured and for all mixtures. It was found that for all mixtures, air voids were with in the range of 3.8 to 4.2. Based on the results no modification to design asphalt content was made for mixtures with hydrated lime and liquid anti-stripping agent.

3.7. Indirect Tensile Strength in Mixture Design

Although the volumetric Superpave mixture and analysis system has been very successful in developing durable mix designs, many engineers and technicians feel that a simple performance, or “proof” test is needed to ensure adequate performance for asphalt concrete mixtures. Of special concern is resistance to permanent deformation or rutting. Accurate prediction of pavement response and performance requires the use of theoretical

models, which closely represent both the pavement structure, and the behavior of the individual materials within the structure. The Strategic Highway Research Program (SHRP) concluded with the introduction of the Superpave mix design and analysis system. As part of Superpave, a series of mechanical testing procedures were developed by SHRP researchers for advanced mixture analysis. Unfortunately, the cost of the test equipment was prohibitive for routine use by hot mix asphalt contractors and state highway agencies. The high cost of the performance testing equipment was only one part of the problem faced by users. Of equal importance, execution of the testing and proper analysis of the results required well-trained, experienced personnel. As a result, most state highway agencies moved towards implementation of the Superpave mix design process relying only on analysis of volumetric and densification properties of the mixture. Unlike the Marshall or Hveem mix design procedures there was no final "strength" test included in the Superpave level 1 mix design. Many in the asphalt industry believed that a simple strength test should be included in the Superpave mix design procedure. This would include measurement and determination of properties related to performance. In Chapter 7, it has been shown that the Indirect Tensile Strength (ITS) test can be used to estimate both fatigue life and rutting for a typical pavement structure. This chapter will discuss the usefulness of ITS testing for the purpose of confirming the design asphalt content selected by using the SuperPave™ volumetric mix design.

3.7.1. Specimen Fabrication for Indirect Tensile Testing

Specimens were fabricated for each of the mixtures immediately after the mix design process by mixing at the SuperPave™ design asphalt content, ±0.5% asphalt content and ±1.0% asphalt content. Three specimens were created at each asphalt content for all

mixes. A fixed weight was then selected for all specimens (4000 grams for this study) and specimens were compacted to Ndes in a gyratory compactor. A 4000 gram compaction weight was selected in order to insure that fabricated specimens would fit into the indirect tensile strength test machine. For each specimen, the height at Ndes was recorded and used to calculate ITS. Below is a table detailing the specimens fabricated.

Table 3.19 Indirect Tensile Strength Test Specimens for Mix Design

Aggregate	Mix Type	Design Asphalt Content	-1.0%	-0.5%	Design Content	+0.5%	+1.0%
Fountain	S – 12.5 B	4.9%	3*	3	3	3	3
Fountain	S – 12.5 C	4.9%	3	3	3	3	3
Fountain	S – 9.5 C	5.1%	3	3	3	3	3
Fountain	S – 12.5 D	4.9%	3	3	3	3	3
Asheboro	S – 12.5 B	4.5%	3	3	3	3	3
Asheboro	S – 12.5 C	5.7%	3	3	3	3	3
Asheboro	S – 9.5 C	4.5%	3	3	3	3	3
Asheboro	S – 12.5 D	4.9%	3	3	3	3	3
Castle Hayne	S – 12.5 B	6.0%	3	3	3	3	3
Castle Hayne	S – 12.5 C	5.2%	3	3	3	3	3
Castle Hayne	S – 9.5 C	4.9%	3	3	3	3	3
Castle Hayne	S – 12.5 D	5.4%	3	3	3	3	3
Total Specimens Fabricated							**180**

*Number denotes number of specimens fabricated for testing

3.7.2. Indirect Tensile Test

The indirect tensile strength test involves measuring a strength parameter, known as indirect tensile strength (ITS) of conditioned and unconditioned samples. The samples are conditioned as described earlier. The indirect tensile strength (ITS) for each specimen was computed as follows:

$$S_t = 2*P/\pi tD$$

Where

S_t = Indirect tensile strength (psi)

P = maximum load (lb)

t = specimen height (in)

D= specimen diameter (in)

The maximum load, P was obtained using a Geotest loading frame as shown in Figure 4.1, which is equipped with a chart recorder. From the measured tensile strengths a tensile strength ratio (TSR) was calculated as follows:

$$TSR = S_{tm}/S_{td} *100$$

Where

S_{tm} = average indirect tensile strength of the moisture-conditioned subset (fully conditioned) (psi)

S_{td} = average indirect tensile strength of the unconditioned subset (psi)

Figure 3.4 Loading frame used for measuring Indirect Tensile strength

3.7.3. Indirect Tensile Testing and Data Acquisition

ITS testing was conducted as described in Section 1.2.2.1 on all samples. The average of the three specimens tested at each asphalt content for each mix type is tabulated in Table 3.20.

Table 3.20 Indirect Tensile Strength Test Results

Aggregate	Mix Type	Design Asphalt Content	Indirect Tensile Strength (psi)				
			-1.0%	-0.5%	Design Content	+0.5%	+1.0%
Fountain	S – 12.5 B	4.9%	161	215	226	201	158
Fountain	S – 12.5 C	4.9%	189	220	236	225	180
Fountain	S – 9.5 C	5.1%	273	313	315	307	266
Fountain	S – 12.5 D	4.9%	200	289	311	274	163
Asheboro	S – 12.5 B	4.5%	107	164	201	182	111
Asheboro	S – 12.5 C	5.7%	193	226	236	231	200
Asheboro	S – 9.5 C	4.5%	273	314	317	305	269
Asheboro	S – 12.5 D	4.9%	161	213	238	218	171
Castle Hayne	S – 12.5 B	6.0%	105	164	183	155	119
Castle Hayne	S – 12.5 C	5.2%	204	242	250	233	183
Castle Hayne	S – 9.5 C	4.9%	300	318	325	313	302
Castle Hayne	S – 12.5 D	5.4%	187	271	294	260	202

As seen in Table 3.20, ITS reaches a maximum very near the design asphalt content from the SuperPave™ volumetric mix design procedure. This phenomenon occurs because as asphalt content increases from zero, it acts as a lubricant during compaction, bringing aggregate particles closer together than they would have been without the presence of asphalt. This effect increases with increased asphalt content until it reaches a specific point at which the asphalt has saturated all useful voids and begins to interfere with aggregate interlock. It is generally accepted that this critical point lies somewhere

between 3% and 6% air voids in the compacted mix. This study shows through ITS testing that the SuperPave^{TM} volumetric mix design using 4% air voids as a target is very accurate for all of the mixes used herein.

3.7.4. Indirect Tensile Strength Data Analysis

Figures 3.4 to 3.15 show a parabolic regression, fitted to the ITS data. From these figures, it can be seen that the peak of ITS falls very near to the SuperPave^{TM} design asphalt content. This indicates that ITS can be used as the simple strength test to confirm mix designs.

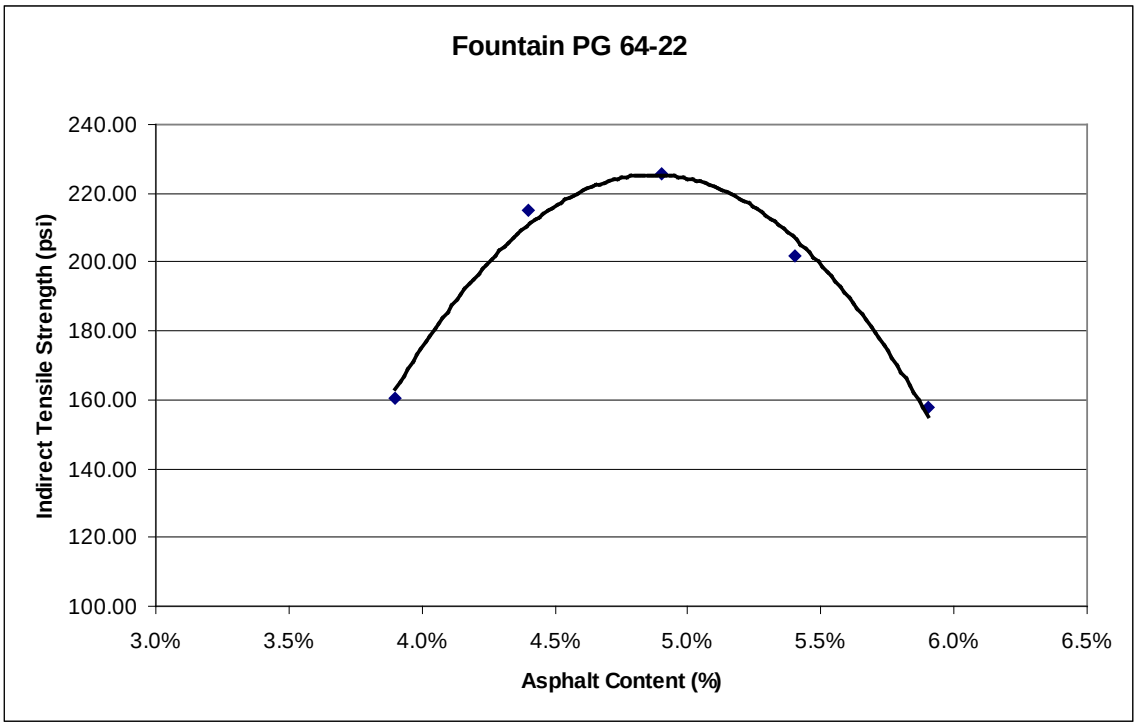

Figure 3.5 Parabolic Relation of ITS and Asphalt Content for Fountain S – 12.5 B Mix.

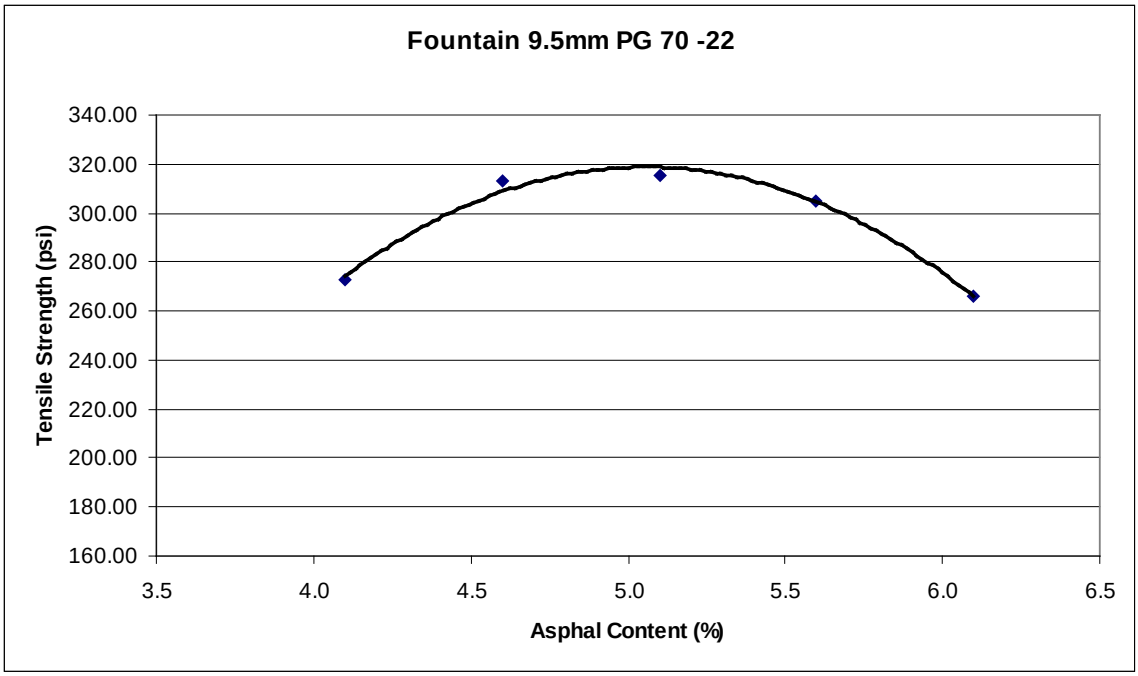

Figure 3.6 Parabolic Relation of ITS and Asphalt Content for Fountain S – 9.5 C Mix.

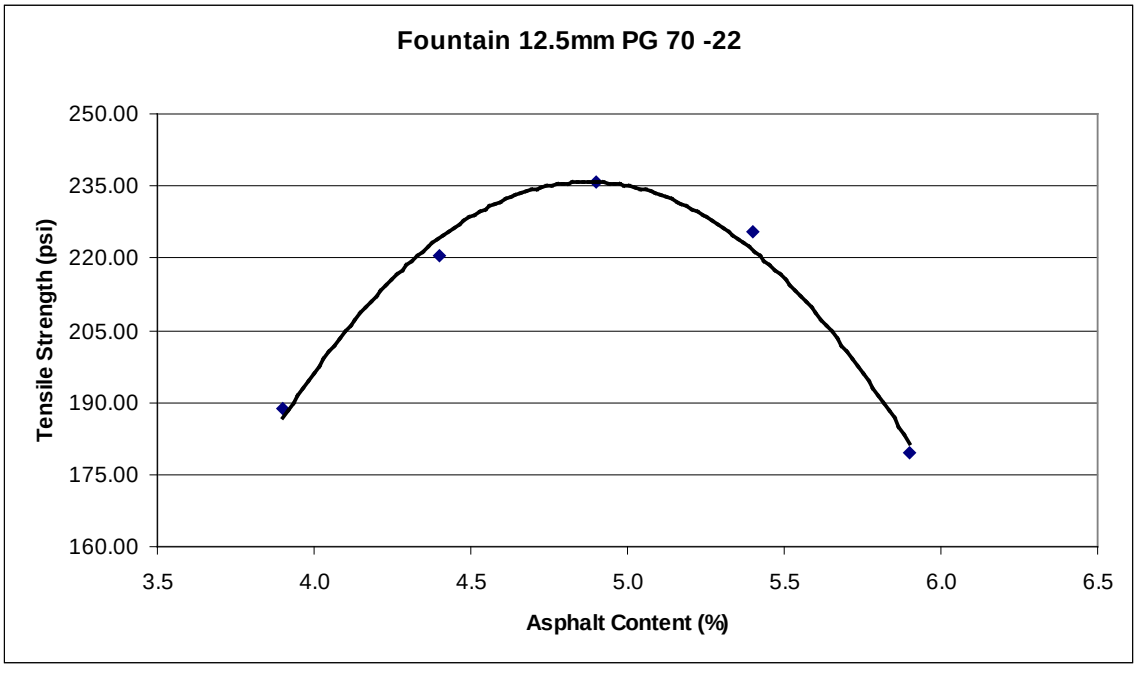

Figure 3.7 Parabolic Relation of ITS and Asphalt Content for Fountain S – 12.5 C Mix.

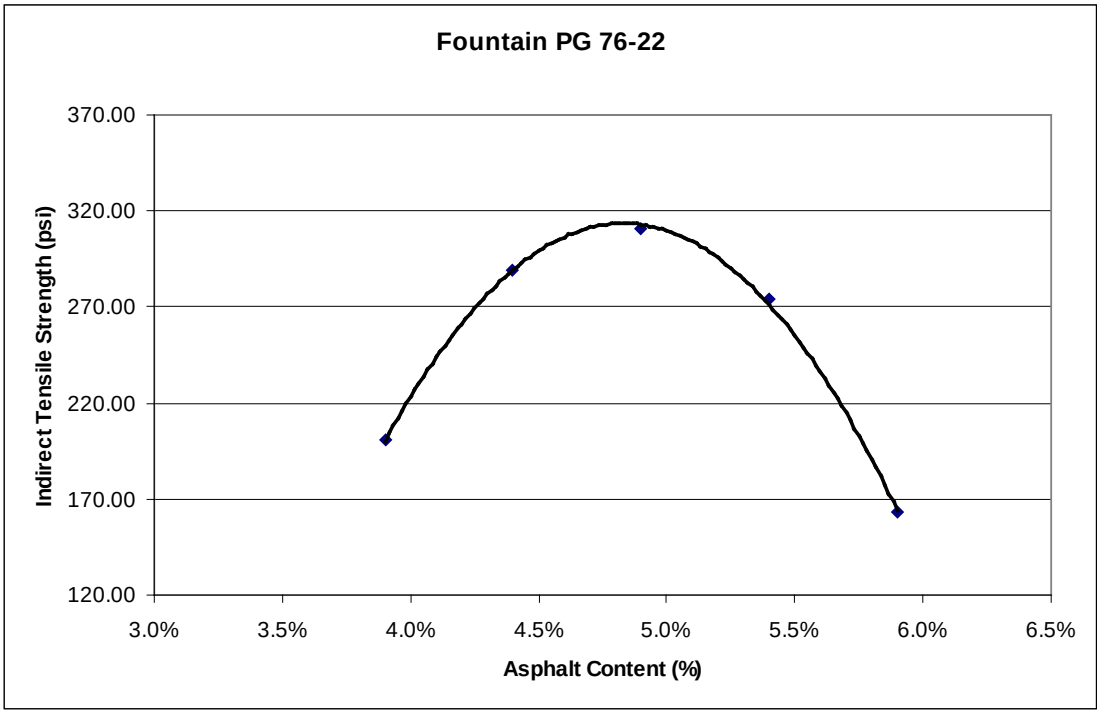

Figure 3.8 Parabolic Relation of ITS and Asphalt Content for Fountain S – 12.5 D Mix.

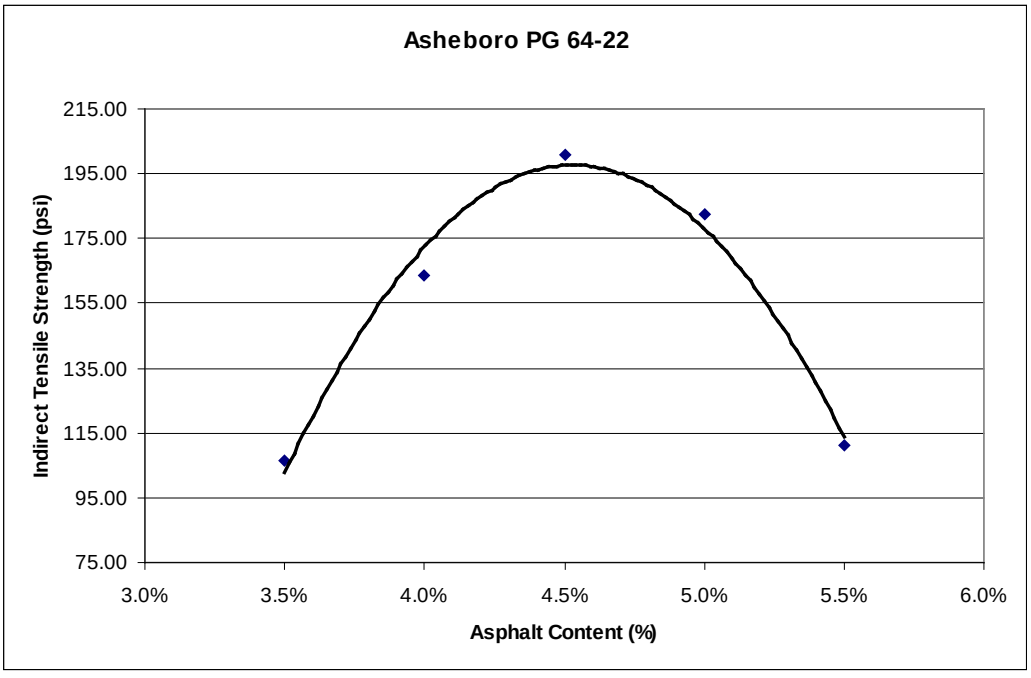

Figure 3.9 Parabolic Relation of ITS and Asphalt Content for Asheboro S – 12.5 B Mix.

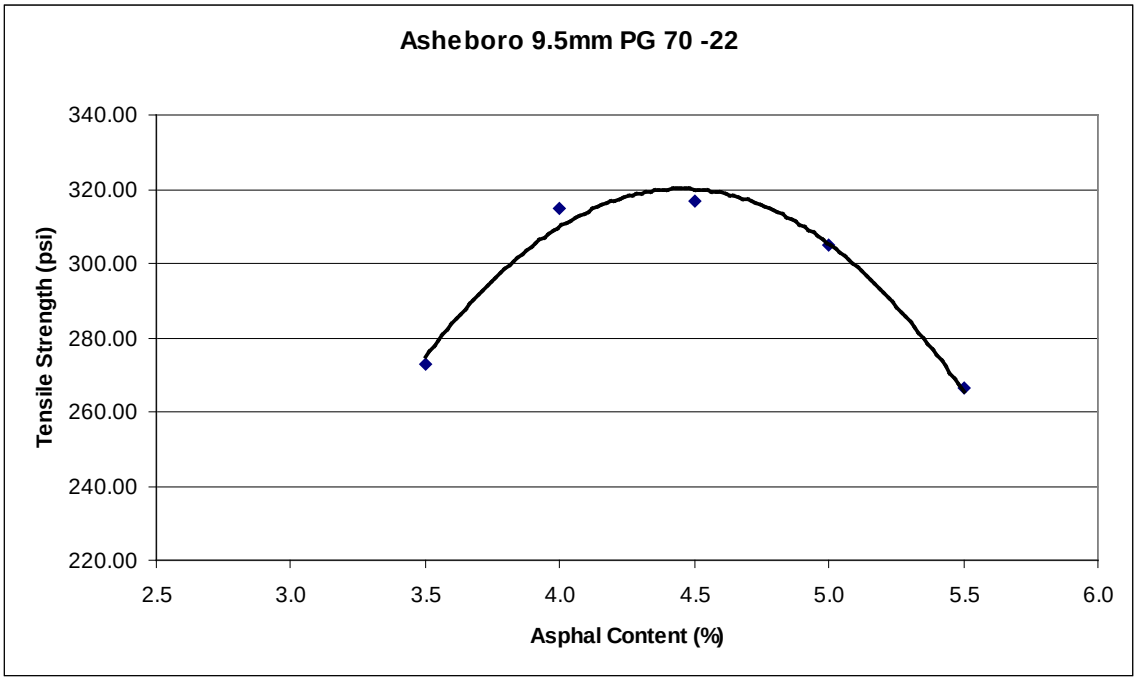

Figure 3.10 Parabolic Relation of ITS and Asphalt Content for Asheboro S – 9.5 C Mix.

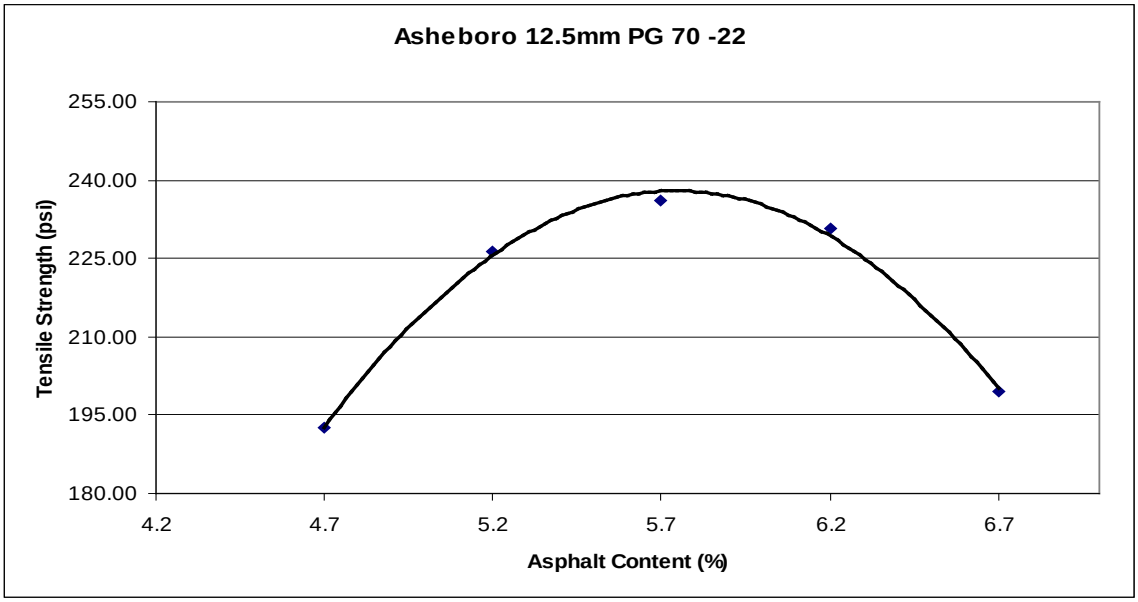

Figure 3.11 Parabolic Relation of ITS and Asphalt Content for Asheboro S – 12.5 C Mix.

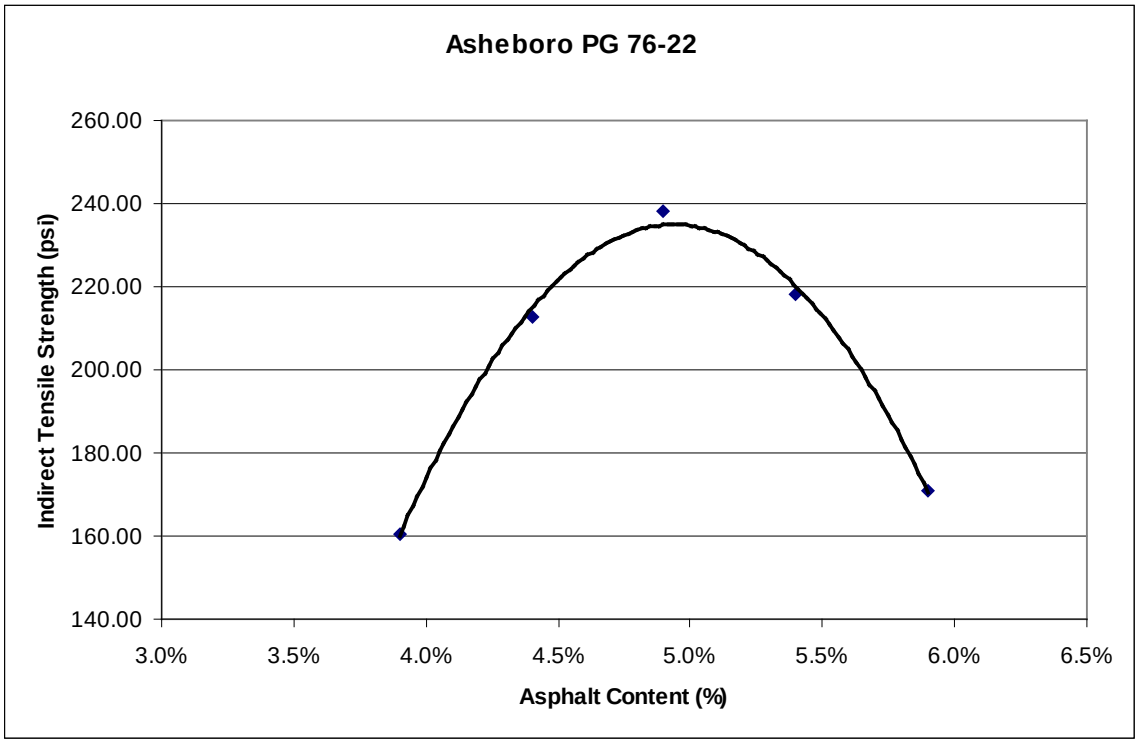

Figure 3.12 Parabolic Relation of ITS and Asphalt Content for Asheboro S – 12.5 D Mix.

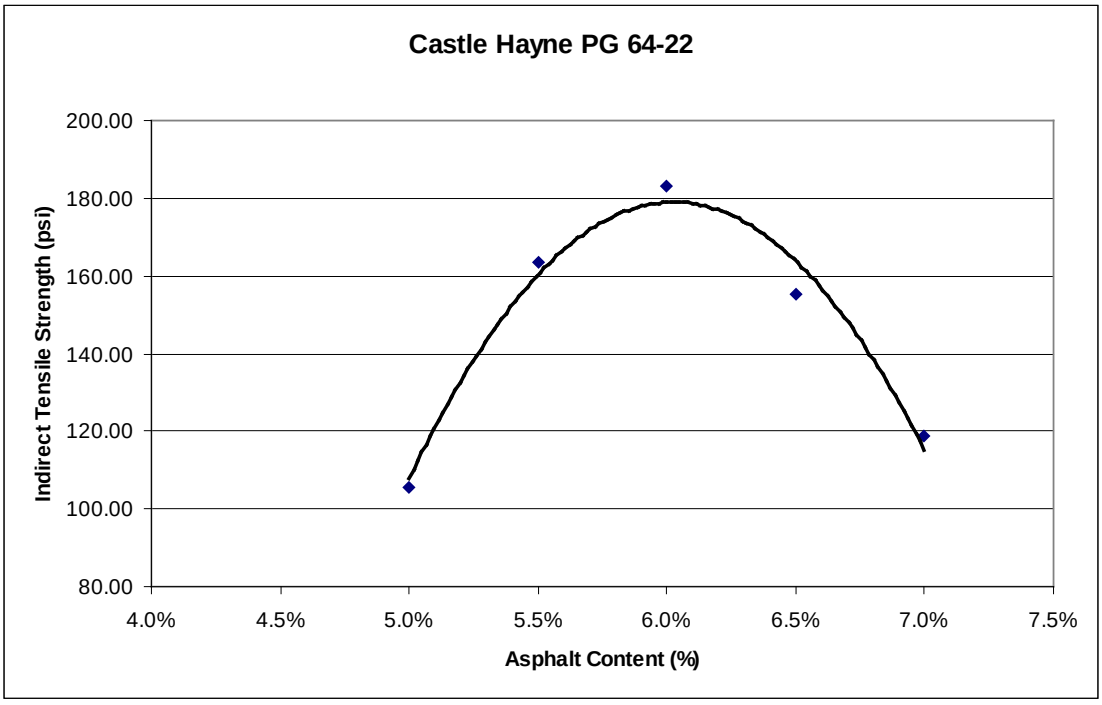

Figure 3.13 Parabolic Relation of ITS and Asphalt Content for Castle Hayne S – 12.5 B Mix.

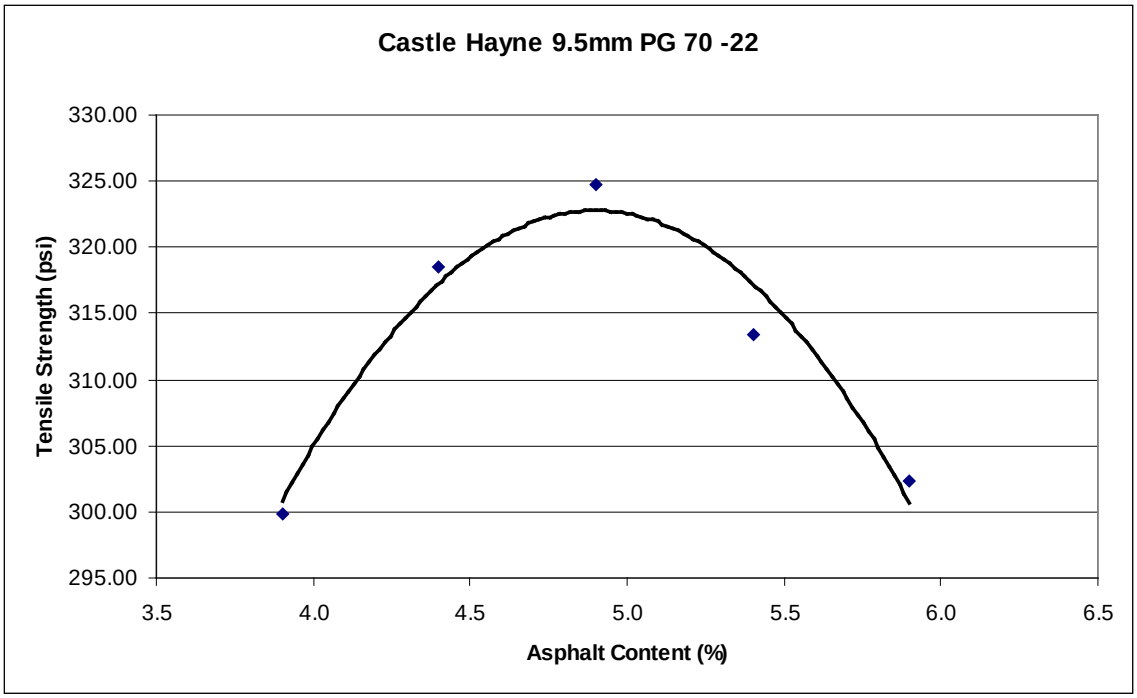

Figure 3.14 Parabolic Relation of ITS and Asphalt Content for Castle Hayne S – 9.5 C Mix.

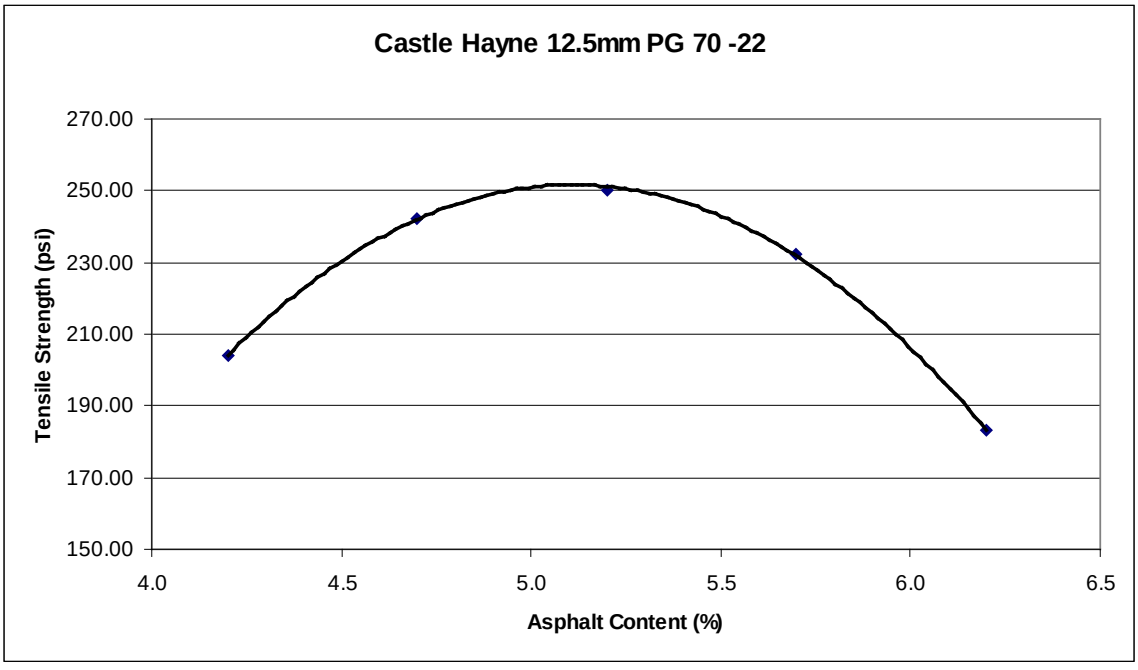

Figure 3.15 Parabolic Relation of ITS and Asphalt Content for Castle Hayne S – 12.5 C Mix.

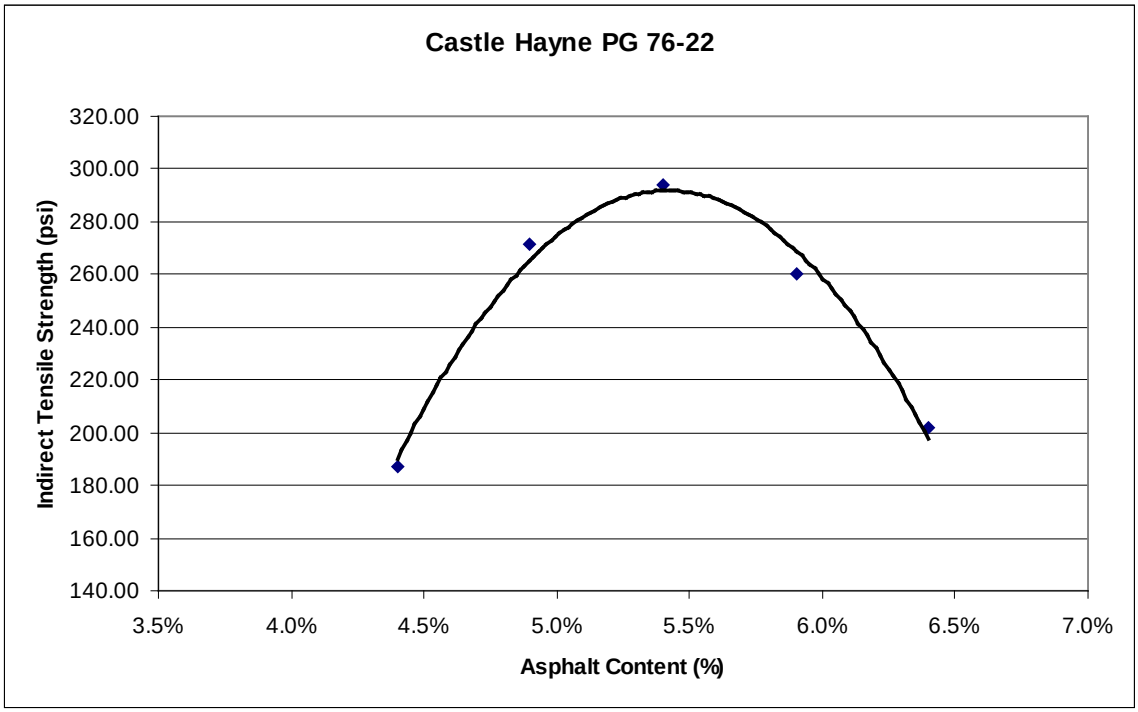

Figure 3.16 Parabolic Relation of ITS and Asphalt Content for Castle Hayne S – 12.5 D Mix.

Using the parabolic relationship seen in Figures 3.4 to 3.15 above, the maximum ITS and corresponding asphalt content can be estimated and compared to the SuperPave™ mix design asphalt content. Table 3.19 compares the asphalt content suggested by the maximum ITS and the asphalt content from the SuperPave™ mix design process.

Table 3.21 ITS vs SuperPave™ Asphalt Contents

Aggregate	Mix Type	SuperPave™ Asphalt Content	Max ITS Asphalt Content	Percent Difference
Fountain	S – 12.5 B	4.9%	4.8%	-2.1%
Fountain	S – 12.5 C	4.9%	4.9%	0%
Fountain	S – 9.5 C	5.1%	5.1%	0%
Fountain	S – 12.5 D	4.9%	4.8%	-2.0%
Asheboro	S – 12.5 B	4.5%	4.5%	0%
Asheboro	S – 12.5 C	5.7%	5.8%	1.75%
Asheboro	S – 9.5 C	4.5%	4.4%	-2.2%
Asheboro	S – 12.5 D	4.9%	5.0%	2.0%
Castle Hayne	S – 12.5 B	6.0%	6.1%	1.7%
Castle Hayne	S – 12.5 C	5.2%	5.1%	-1.9%
Castle Hayne	S – 9.5 C	4.9%	4.9%	0%
Castle Hayne	S – 12.5 D	5.4%	5.4%	0%

Using ITS to confirm the design asphalt content for a mix design is highly accurate (within about ±2%) and as such is an excellent yet simple “proof test” for the volumetric mix design. Because variability may be higher for certain mixes, a higher percentage difference may occur in practice. Nonetheless, this test acts as a proof test in that it suggests asphalt contents that are consistently very near to volumetrically selected asphalt contents.

CHAPTER 4

4. EVALUATION OF MOISTURE SENSITIVITY USING INDIRECT TENSILE STRENGTH TEST

4.1. Introduction

Evaluation of a mixture's moisture sensitivity is currently the final step in the Superpave™ volumetric mix design process. The Superpave™ mix design system has adopted AASHTO T-283 (Resistance of Compacted Bituminous Mixtures to Moisture Induced Damage) as the basis for assessing moisture susceptibility in a proposed mix. This chapter describes indirect tensile strength results of asphalt concrete mixtures from three aggregate sources (Castle Hayne, Fountain and Asheboro) with two gradations. Specimens were tested for unconditioned, half conditioned and fully conditioned states. To determine the effectiveness of the anti-strip agents in preventing moisture damage, indirect tensile strengths were also determined for specimens containing additive such as hydrated lime and liquid anti-stripping agent and results are discussed in the following sections.

4.2. Moisture Sensitivity Testing

Indirect Tensile Strength testing was performed on the specimens in accordance with AASHTO T-283. Specimens were prepared with 6 inch diameter and a height of 4 inch with 7±1 % air-voids level. The freeze/thaw cycle, which is optional in T-283, was not used in this project. Detailed mixture information of each aggregate source and gradation are provided in Chapter 3. Details regarding hydrated lime and liquid anti-stripping agent addition are also furnished in the previous chapter. Three specimens were tested each for

unconditioned, half conditioned and fully conditioned states, respectively. For half conditioned and full conditioned states, three specimens were saturated and then conditioned in a water bath at 140^{o} F (60°C) for 12 and 24 hours respectively. After conditioning, the indirect tensile strengths for the conditioned and unconditioned samples were measured at 77° F.

Factors such as exposure duration, temperature and amount of moisture influence the amount of stripping (moisture damage) that takes place. Under AASHTO T-283, where the temperature and duration is fixed, two variables dictate the amount of moisture present. The first is air voids, which determines how much total volume is available in the sample for water to occupy. The second variable is the degree of saturation; this is the percentage of air voids filled with water. Specimen air voids were selected as 7% and the degree of saturation was confined to the narrow range of 69%-75% to minimize variability in the test data based on previous research [23].

4.3. Consideration of Test Variables

To better control the amount of air voids in the test specimens, the Superpave^{TM} gyratory compactor was used to compact the test samples. The Superpave gyratory compactor can monitor the sample height throughout the compaction process and from the recorded sample height and known diameter, the theoretical mixture volume was calculated. The estimated bulk density (G_{mb}) was then determined from these values. This estimate assumes the specimen to be a smooth walled cylinder. However, due to surface voids the estimated density is different from the actual G_{mb} measured. After compaction, the bulk

density was determined by ASTM D-2726 (Standard Method for Bulk Specific Gravity and Density of Compacted Bituminous Mixtures using Saturated Surface-Dry Specimens). The actual density was then compared to the calculated density to obtain a correction factor (CF). The correction factor was then calculated using Equation 1.

$$CF = \text{Actual Density} / \text{Calculated Density} \quad (1)$$

This correction factor was then applied to the compaction of test specimens in the following manner. Prior to compaction, a bulk density was calculated for a desired level of air voids. This calculated density was then multiplied by the correction factor for the specific mix. Finally, a compaction height was calculated based on the corrected bulk density, the sample mass and the sample diameter. The process resulted in samples that were within 0.5 percent of the desired air void content.

The second test variable addressed was the degree of saturation. The sample set that was to be conditioned prior to testing was first partially saturated with water. This was accomplished by applying a partial vacuum to the sample submerged in water. The degree of saturation is equal to the volume of absorbed water divided by the volume of air voids. Earlier research work (Khosla et. al (2000)) [31] indicates that the volume of absorbed water is a function of the magnitude of the partial vacuum, and the duration of the vacuum is secondary. Prior to saturation, a volume of water was calculated, from the known air voids, which would achieve the desired degree of saturation. After saturation, the saturated surface dry weight of the specimen was recorded. This weight was then

compared to data for the specimen prior to vacuum saturation to determine a degree of saturation. By controlling the level of vacuum with a valve, the degree of saturation was controlled to within three percent of the target level of 72%.

4.4. Results and Discussion

Moisture may damage asphalt concrete in three ways. The moisture may combine with the asphalt resulting in a loss of cohesion of the asphalt film. The water may also cause failure of the bond at the asphalt aggregate interface. Finally, degradation of the aggregate may result from the moisture in the asphalt concrete. The loss of cohesion and the failure of the asphalt bond with the aggregate are defined as stripping. Stripping in asphalt pavements can lead to premature failure of the pavement system. Indirect Tensile Strength values of an asphalt concrete specimen depends mainly on the type of the aggregate used in making the specimen, the aggregate interlock in the specimen and the cohesion of the binding agent, asphalt. The indirect tensile strengths were measured, the TSR values for each mixture were calculated, and results are discussed in the following sections.

4.4.1. Mixtures Containing No Additive

Indirect tensile strength tests were performed on half conditioned, fully conditioned and unconditioned samples for each of the three aggregates with two different gradations (without any additives) for PG 70-22 and results are shown in Table 4.1. Figure 4.2 shows the comparison of loss in tensile strength values for all the PG 70-22 mixtures. The results for PG 76-22 and PG 64-22 asphalt binder are shown in Table 4.2 and Figure 4.3. From Table 4.1, it can be seen that among the 12.5mm and 9.5 mm unconditioned mixes,

the Castle Hayne mixture sample had the highest indirect tensile strength and Asheboro mix samples had the lowest indirect tensile strength. From Figure 4.2, it can be seen that among the 12.5mm and 9.5mm mixes, conditioned Fountain mixes had the highest decrease in indirect tensile strength values compared to unconditioned Fountain mix samples.

Table 4.1 Indirect Tensile Strength for Mixes Using PG 70-22 and TSR values

Gradation NMSA	Aggregate Source	Tensile Strength (psi)			TSR
		Unconditioned Specimens	Half conditioned Specimens	Full conditioned Specimens	
12.5mm	Fountain	173	144	107	62
	Castle Hayne	185	159	149	81
	Asheboro	113	92	78	69
9.5mm	Fountain	193	153	142	74
	Castle Hayne	195	184	154	79
	Asheboro	125	116	93	74

Table 4.2 Indirect Tensile Strength for S 12.5 D and S – 12.5 C Mixes and TSR Values

Mix Type	Aggregate Source	Tensile Strength (psi)			TSR
		Unconditioned Specimens	Half conditioned Specimens	Full conditioned Specimens	
S – 12.5 D	Fountain	240	218	201	84
	Castle Hayne	223	206	185	83
	Asheboro	238	217	199	84
S – 12.5 B	Fountain	149	131	111	74
	Castle Hayne	283	255	228	81
	Asheboro	211	198	173	82

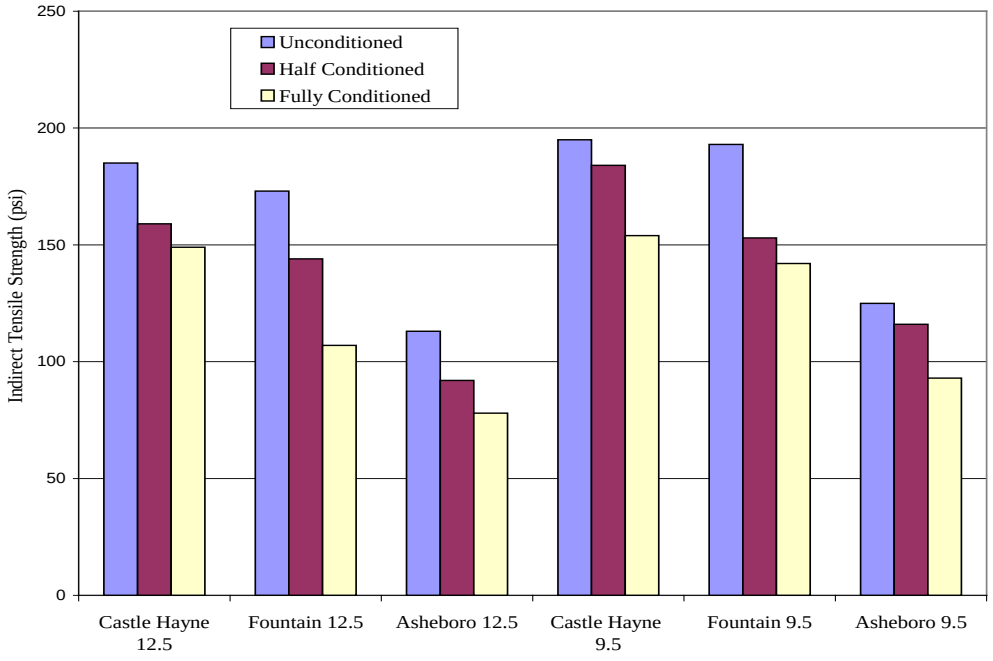

Figure 4.1 Comparison of Loss in Tensile Strength Values for Mixes Using PG 70-22

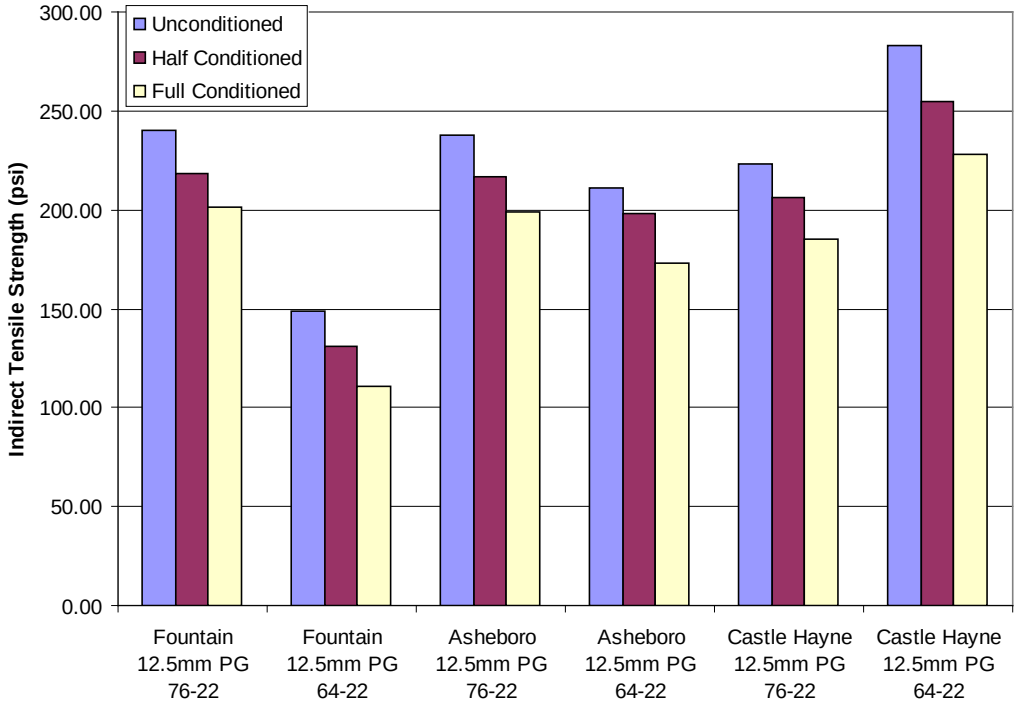

Figure 4.2 Comparison of Loss in Tensile Strength Values for S – 12.5 D and S – 12.5 B Mixes

Castle Hayne mixtures performed generally better than Asheboro and Fountain aggregates, experiencing a lesser decrease in indirect tensile strength after conditioning. This can be explained by Castle Hayne aggregate's limestone origin. The indirect tensile strength results confirm the approximate expectations about the moisture susceptibility of these aggregates. TSR values of all mixes without anti-strip additive are less than 85 percent minimum required by NCDOT, and therefore they fail the TSR test.

Although TSR values indicate that Asheboro aggregate's performance is better than Fountain aggregate, it can also seen from Tables 4.1 and 4.2 that individual tensile strengths of Fountain aggregate in the fully conditioned state are usually higher than Asheboro aggregate. Also in the 9.5mm gradation, indirect tensile strength with Fountain

aggregate is higher than the unconditioned indirect tensile strength of Asheboro aggregate. This indicates that the individual tensile strength should be considered along with TSR value for making decisions on performance of mixtures.

4.4.2. Mixtures Containing Additive

To prevent moisture damage in asphalt pavements, additives are often used to alter the interaction between the asphalt binder and the mineral aggregate. These additives can change the molecular charge of the binder or reduce the viscosity of the asphalt cement. Most asphalt plants are required to use such anti-strip additives to reduce the moisture sensitivity of the asphalt concrete. These additives work with both the aggregates and the binder to increase the adhesion between aggregate and asphalt and reduce the attraction between water and aggregate, which prevents stripping in the asphalt concrete. Indirect tensile strengths discussed earlier were also determined for specimens containing both hydrated lime and liquid anti-stripping agent. The beneficial effects of lime with regards to moisture damage have been known for many years [26, 27 and 28]. However, questions arise as to the proper way of introducing lime into the asphalt mixture. From literature [25, 26], it is observed that the most common method used for incorporating lime is the addition of dry lime to wet aggregates. Based on this experience and upon recommendation from NCDOT personnel, the method of adding dry lime to wet aggregates without marination was adopted for this study. Hydrated lime was added at a level of 1.0 percent by weight of dry aggregates. Alternately, the LOF 6500 anti-strip additive, in the 0.5 percent concentration, was used as liquid anti-stripping agent.

Indirect tensile strength tests were performed on half conditioned, fully conditioned and unconditioned samples for each of the PG 70-22 Fountain aggregate mixes, and results are shown in Table 4.3. The data in Table 4.3 show the reduction in tensile strength for the specimens without additive as compared to the specimens containing additive, thus demonstrating the effectiveness of the additive in preventing moisture damage. Figures 4.4 and 4.5 show a comparison of Indirect Tensile Strength values and percent decrease in Indirect Tensile Strength values (TSR) for the PG 70-22 Fountain 12.5mm mixture with and without additives. From Figure 4.4, it can be seen that the reduction in tensile strength from unconditioned state to conditioned state is less when additives are used. In addition, there is no appreciable reduction in tensile strength from half conditioned state to fully conditioned state when additives were introduced. Without additives, the PG 70-22 Fountain 12.5mm mixture TSR value of 61.8% failed the NCDOT criteria of 85%. When lime was added, the TSR value increased to 90%, and with liquid anti-stripping agent, the TSR value increased to 87.6%. When lime is added to a hot mix, it reacts with aggregate, strengthening the bond between the asphalt and the aggregate. At the same time lime reacts with the aggregate, it also reacts with asphalt. Lime reacts with highly polar molecules that may otherwise react in the mix to form water-soluble soaps, which promote stripping. When those molecules react with lime, they form insoluble salts that no longer attract water [27].

Figures 4.6 and 4.7 show comparison of Indirect Tensile Strength values and TSR values for the PG 70-22 Fountain 9.5mm mixture with and without additives. Unlike the 12.5mm gradation, Figure 4.6 shows that there is a reduction in tensile strength value between half conditioned and fully conditioned state. From Figure 4.7 it can be seen that

when lime is added TSR value increased to 90.6%, and with liquid anti-stripping agent, TSR value increased to 85.7%. Without additives, PG 70-22 Fountain 9.5mm gradation failed to satisfy NCDOT criteria. From the above results, it can be concluded that additives are required for PG 70-22 Fountain aggregate because of its high propensity to strip.

Table 4.3 Indirect Tensile Strength for Fountain Mixes using PG 70-22 and TSR Values

Fountain aggregate Gradation NMSA	Mix type	Tensile Strength (psi)			TSR
		Unconditioned	Half conditioned	Full conditioned	
12.5mm	Without additive	173	144	107	62
	Liquid anti-stripping agent	178	158	156	88
	With Lime	180	163	162	90
9.5mm	Without additive	193	153	142	74
	Liquid anti-stripping agent	196	180	168	86
	With lime	204	191	185	91

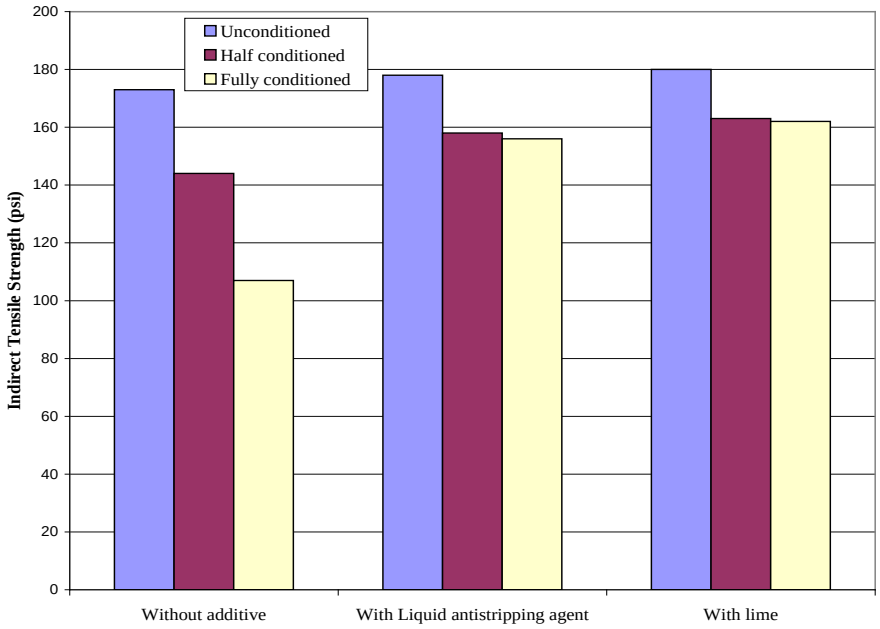

Figure 4.3 Comparison of Indirect Tensile Strength Values for Fountain S – 12.5 C Mixes

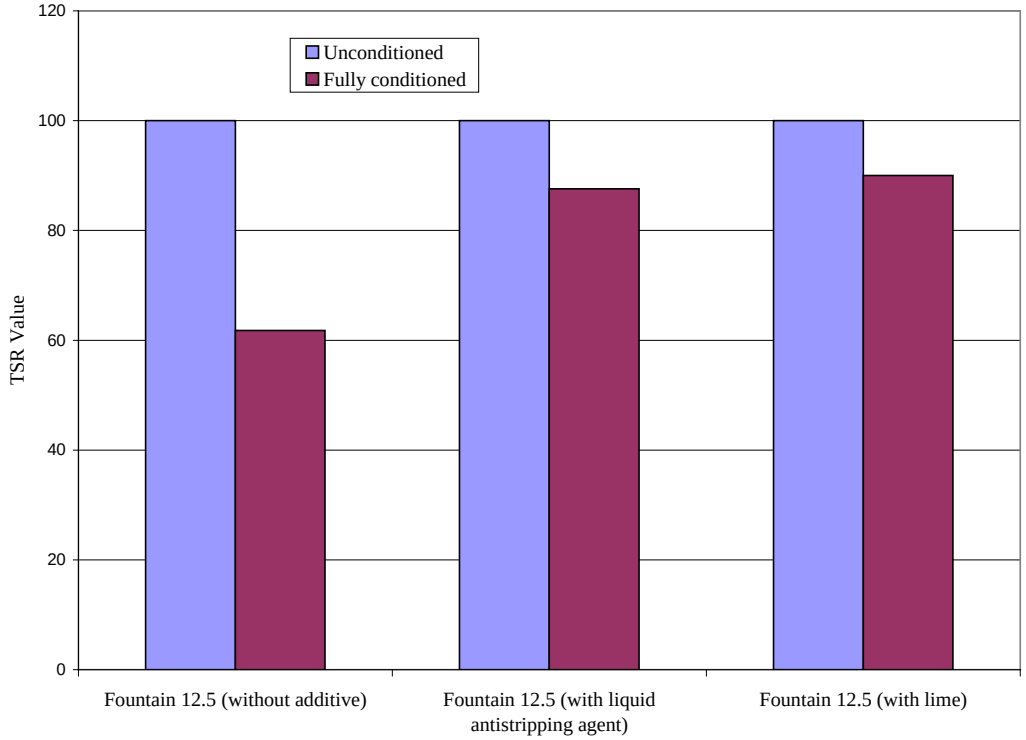

Figure 4.4 Comparison of Tensile Strength Value as % of Unconditioned Tensile strength for Fountain S – 12.5 C Mixes

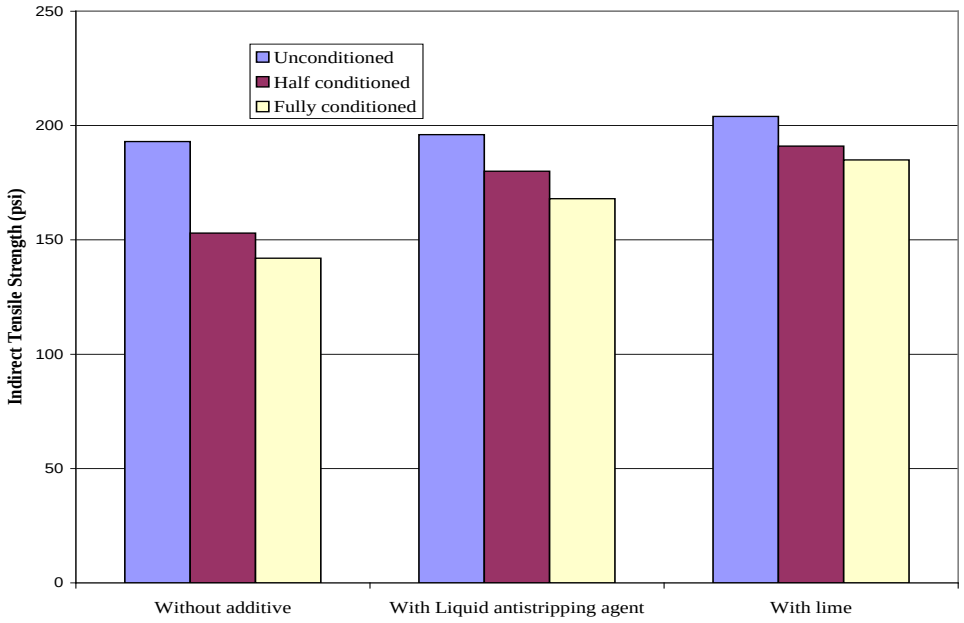

Figure 4.5 Comparison of Indirect Tensile Strength Values for Fountain S - .5 C Mixes

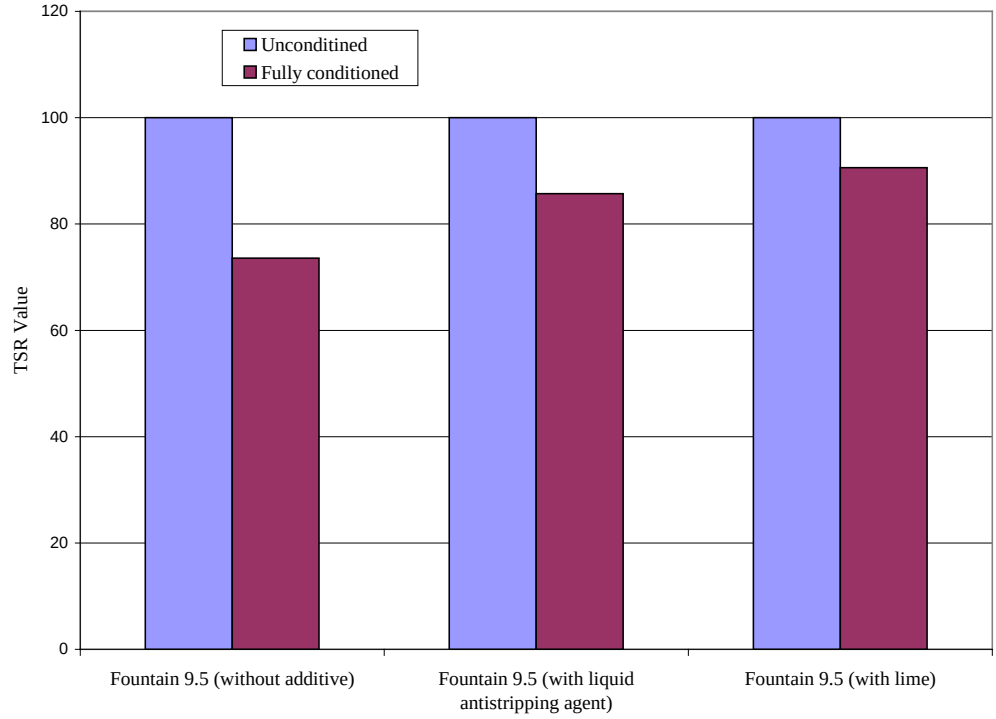

Figure 4.6 Comparison of Tensile Strength Value as % of Unconditioned Tensile Strength for Fountain S – 9.5 C Mixes

From Table 4.3, it can be seen that for the Fountain mixes using PG 70-22, both TSR and individual tensile strength values are higher for mixtures with lime as compared to mixtures with liquid anti-stripping agent.

Indirect tensile strength tests were performed on half conditioned, fully conditioned and unconditioned samples of each of the Asheboro aggregate mixes and Castle Hayne aggregate mixes with PG 70-22, and results are shown in Tables 4.4 and 4.5, respectively. Figures 4.8 and 4.9 show a comparison of Indirect Tensile Strength values and percent decrease in Indirect Tensile Strength values (TSR) for PG 70-22 Asheboro 12.5mm mixture with and without additives (lime and LOF 6500). From Figure 4.8, it can be seen that the reduction in tensile strength from unconditioned state to conditioned state is less when additives are added. Without additives the PG 70-22 Asheboro 12.5mm mixture failed (69%) to satisfy the NCDOT criteria of 85% TSR value. However when lime is added, the TSR value increased to 86%, and with liquid anti-stripping agent the TSR value increased to 86%. Figures 4.10 and 4.11 show comparisons of the Indirect Tensile Strength values and TSR values for the PG 70-22 Asheboro 9.5mm mixture with and without additives. From Figure 4.10, it can be seen that when lime is added, the TSR value increased to 89%, and with liquid anti-stripping agent, TSR value increased to 88%. Without additives, the PG 70-22 Asheboro 9.5mm gradation failed to satisfy NCDOT criteria. From the above results, it can be concluded that additives are required for PG 70-22 Asheboro mixtures.

Table 4.4 Indirect Tensile Strength for Asheboro Aggregate Mixes Using PG 70-22 and TSR Values

Asheboro aggregate Gradation NMSA	Mix type	Tensile Strength (psi)			TSR
		Unconditioned	Half conditioned	Full conditioned	
12.5mm	Without additive	113	92	78	69
	Liquid anti-stripping agent	121	109	104	86
	With Lime	118	106	101	86
9.5mm	Without additive	125	116	93	74
	Liquid anti-stripping agent	127	120	112	88
	With lime	129	124	115	89

From Table 4.4, it can be seen that there is no significant difference between TSR values and individual tensile strength values for Asheboro mixtures containing hydrated lime and liquid antistripping agent. In the case of 9.5mm gradation, the values are slightly higher when lime was added and in the case of 12.5mm gradation, liquid anti-stripping agent showed slightly higher values.

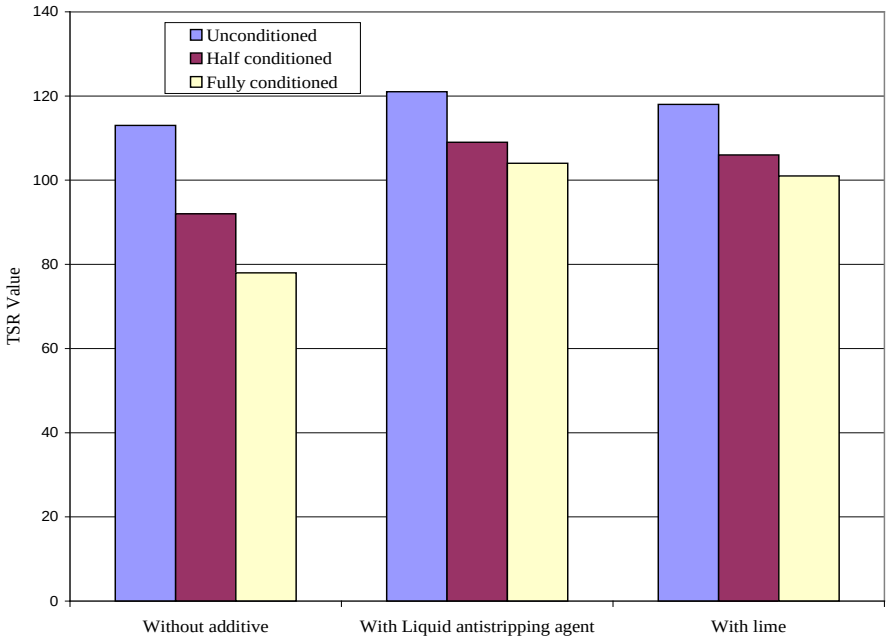

Figure 4.7 Comparison of Indirect Tensile Strength Values for Asheboro S – 12.5 C Mixes

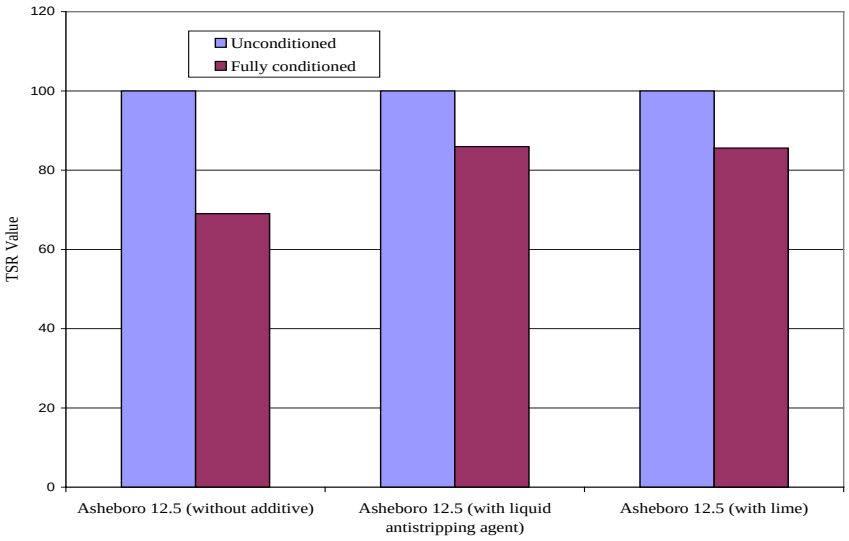

Figure 4.8 Comparison of Tensile Strength Value as % of Unconditioned Tensile Strength for Asheboro S – 12.5 C Mixes

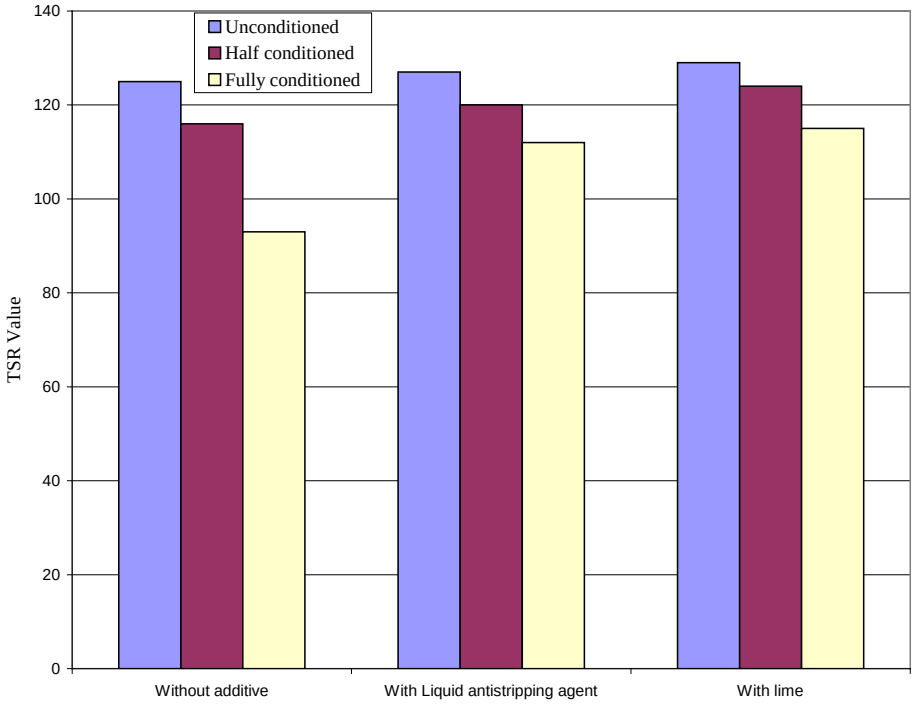

Figure 4.9 Comparison of Indirect Tensile Strength Values for Asheboro S – 9.5 C Mixes

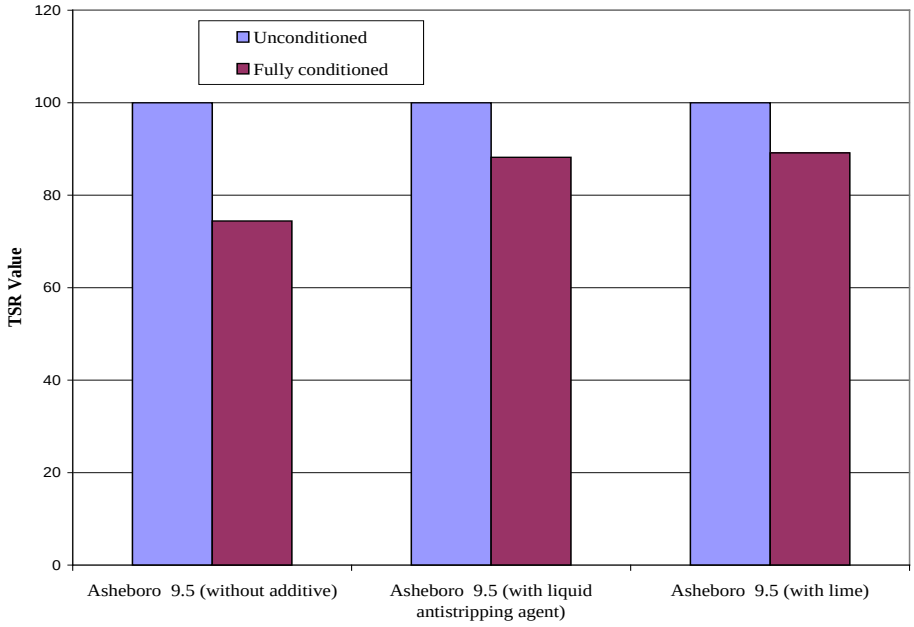

Figure 4.10Comparison of Tensile Strength Value as % of Unconditioned Tensile Strength Value for Asheboro S – 9.5 C Mixes

Table 4.5 Indirect Tensile Strength for Castle Hayne Mixes Using PG 70-22 and TSR Values

Castle Hayne aggregate Gradation NMSA	Mix type	Tensile Strength (psi)			TSR
		Unconditioned	Half conditioned	Full conditioned	
12.5mm	Without additive	185	159	149	81
	Liquid anti-stripping agent	183	169	156	86
	With Lime	209	181	181	87
9.5mm	Without additive	195	184	154	79
	Liquid anti-stripping agent	199	187	181	91
	With lime	201	195	184	92

Figures 4.12 and 4.13 show comparison of Indirect Tensile Strength values and percent decrease in Indirect Tensile Strength values (TSR) for the PG 70-22 Castle Hayne 12.5mm mixture with and without additives. From Figure 4.12, it can be seen that there is no reduction in tensile strength from unconditioned state to conditioned state when lime is added. A similar trend was also found in Fountain aggregate. Even though Castle Hayne 12.5mm mixture performed better without any additives as compared to Asheboro and Fountain aggregate, because of its limestone origin, it failed (81%) to satisfy the NCDOT criteria of 85% TSR value. However, when lime was added, TSR value increased to 87%, and with liquid anti-stripping agent TSR value increased to 86%. Figures 4.14 and 4.15 show a comparison of Indirect Tensile Strength values and TSR values for the PG 70-22 Castle Hayne 9.5mm mixture with and without additives. Figure 4.14 shows that there is a reduction in tensile strength value between half

conditioned and fully conditioned state when additives are added. However, this reduction is not as significant as compared to mixtures with no additives. From Figure 4.15, it can be seen that when lime was added the TSR value increased to 92%, and with liquid anti-stripping agent, TSR value increased to 91%, satisfying NCDOT criteria of 85%.

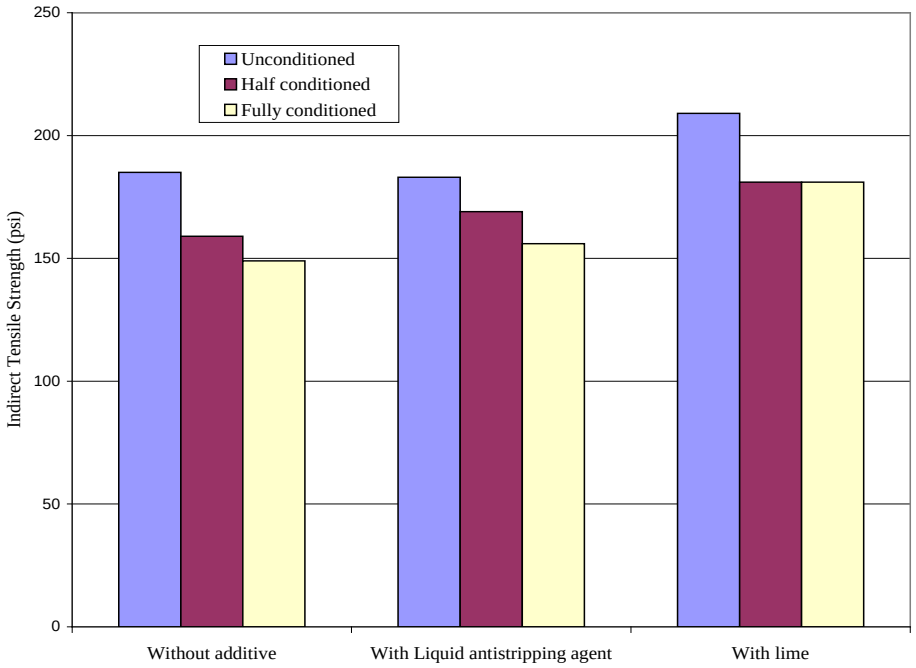

Figure 4.11 Comparison of Indirect Tensile Strength Values for Castle Hayne S – 12.5 C Mixes

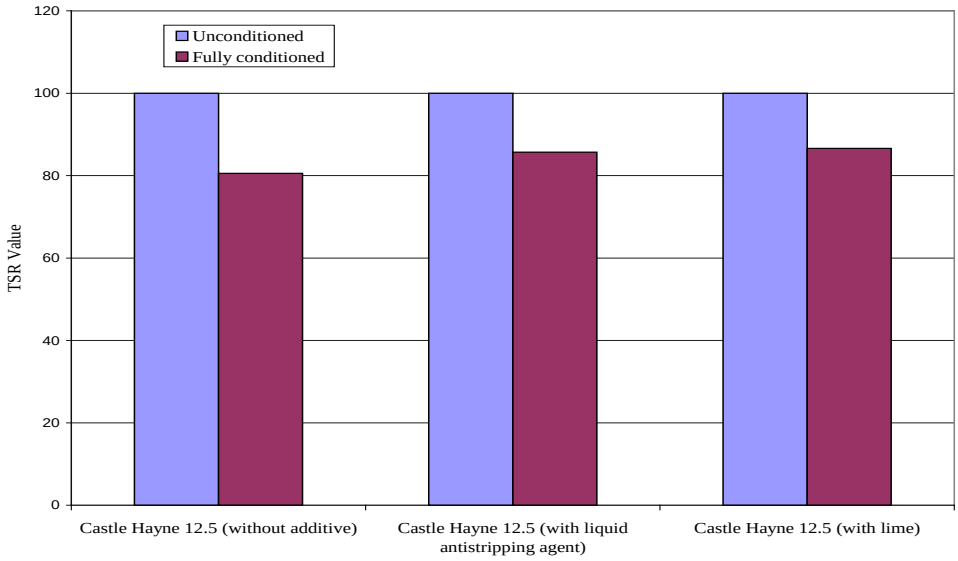

Figure 4.12 Comparison of Tensile Strength as % of Unconditioned Tensile Strength Value for Castle Hayne S – 12.5 C Mixes

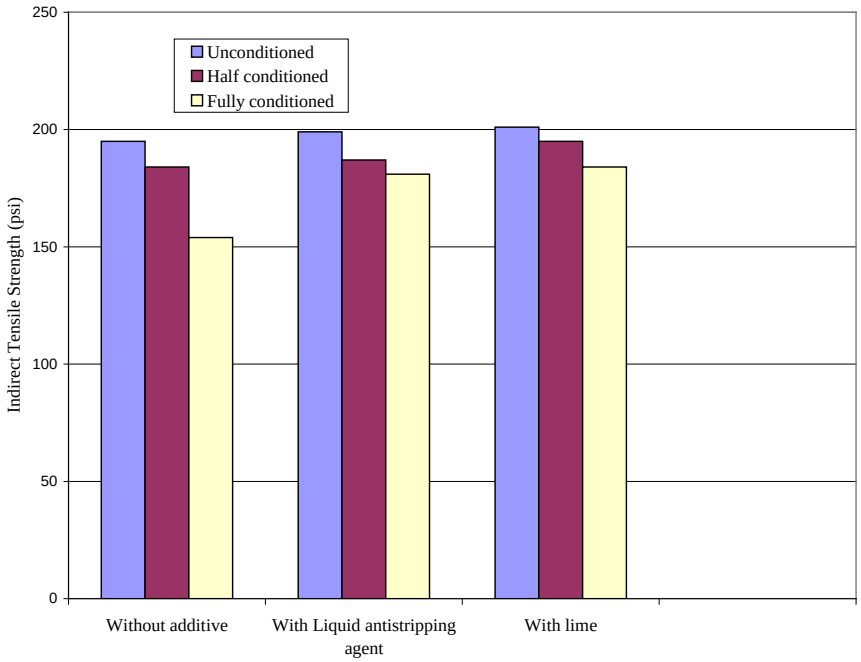

Figure 4.13 Comparison of Indirect Tensile Strength Values for Castle Hayne S – 9.5 C Mixes

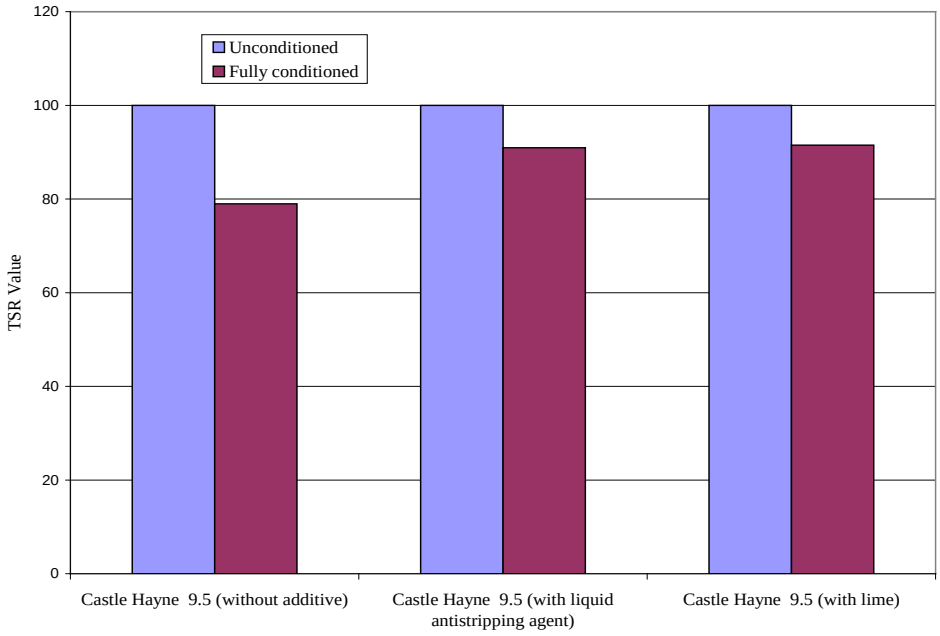

Figure 4.14 Comparison of Tensile Strength Value as % of Unconditioned Tensile Strength Value for Castle Hayne S – 9.5 C Mixes

In both gradations of Castle Hayne aggregate, individual tensile strength of mixtures with hydrated lime is higher than the mixtures containing liquid anti-stripping agent.

Indirect tensile strength tests were performed on half conditioned, fully conditioned and unconditioned samples of each of the aggregate types using PG 76-22 and PG 64-22, and results are shown in Tables 4.6 and 4.7, respectively. Figures 4.16 and 4.17 show a comparison of Indirect Tensile Strength values and percent decrease in Indirect Tensile Strength values (TSR) for all 12.5mm mixes with and without lime additives.

Table 4.6 Indirect Tensile Strength for S 12.5 D Mixes and TSR Values

Aggregate Source	Mix Type	Tensile Strength (psi)			TSR
		Unconditioned	Half Conditioned	Full Conditioned	
Fountain	No Additive	240	218	201	84
	With Lime	279	265	261	93
Asheboro	No Additive	238	217	199	84
	With Lime	293	278	255	87
Castle Hayne	No Additive	223	206	185	83
	With Lime	305	285	258	85

Table 4.7 Indirect Tensile Strength for S – 12.5 B Mixes and TSR Values

Aggregate Source	Mix Type	Tensile Strength (psi)			TSR
		Unconditioned	Half Conditioned	Full Conditioned	
Fountain	No Additive	149	131	111	74
	With Lime	189	174	165	87
Asheboro	No Additive	211	198	173	82
	With Lime	287	259	237	83
Castle Hayne	No Additive	283	255	228	81
	With Lime	296	264	255	86

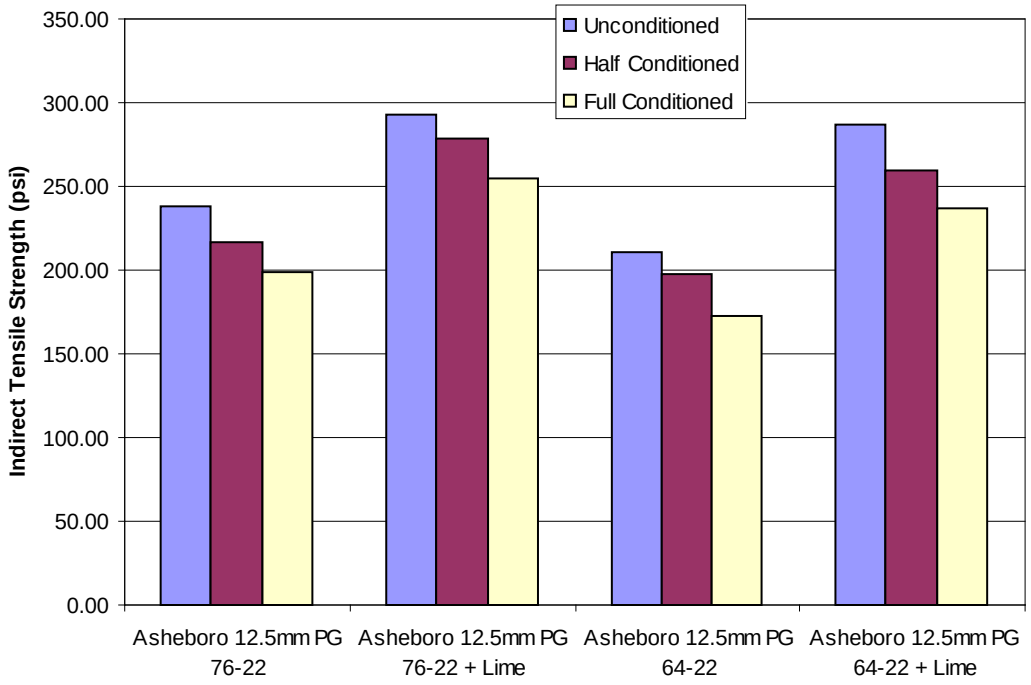

Figure 4.15 Comparison of Indirect Tensile Strength Values for Fountain 12.5mm Mixtures Using PG 76-22 and PG 64-22, with and without Lime

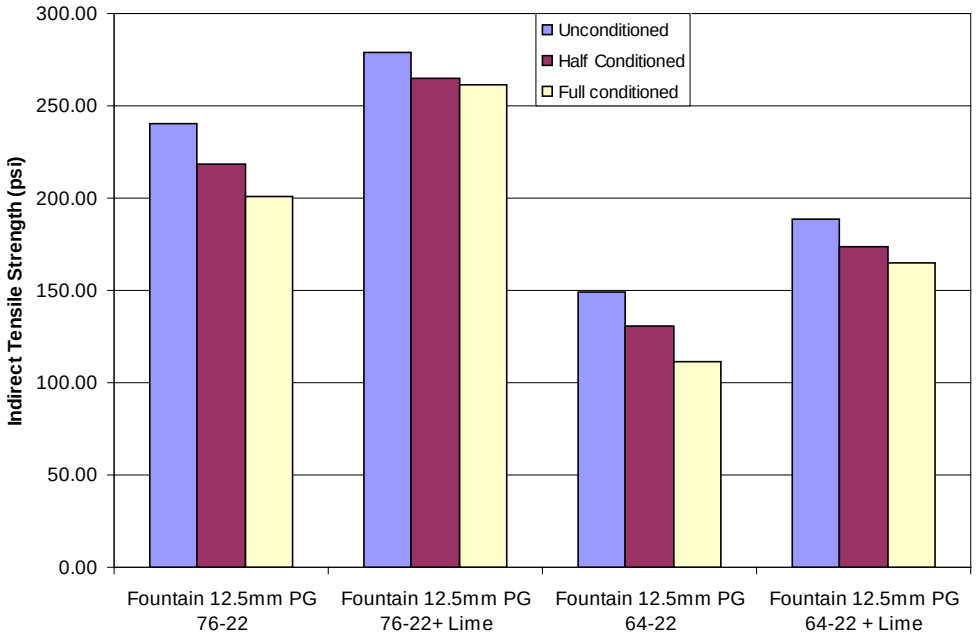

Figure 4.16 Comparison of Indirect Tensile Strength Values for Asheboro 12.5mm Mixtures Using PG 76-22 and PG 64-22, with and without Lime

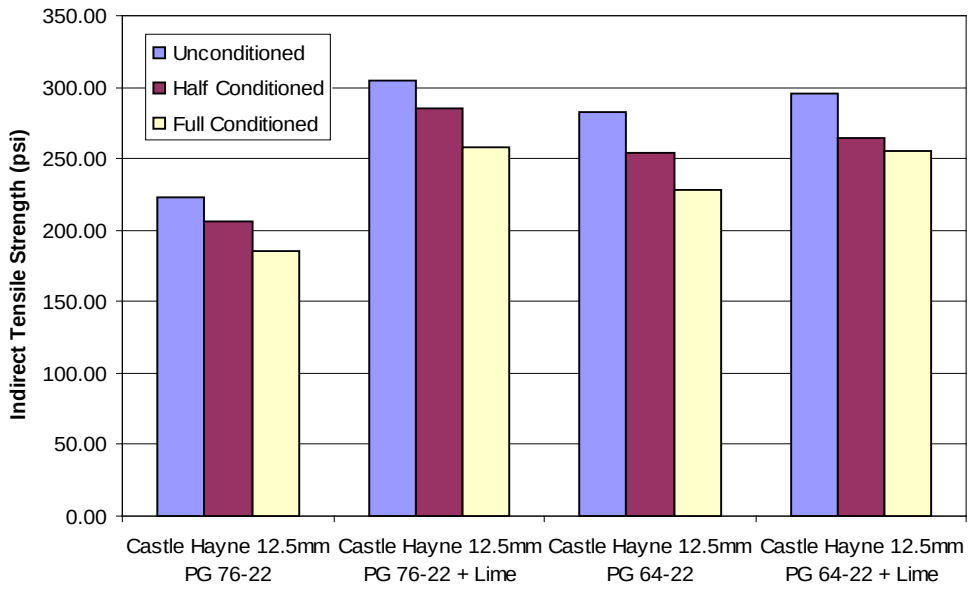

Figure 4.17 Comparison of Indirect Tensile Strength Values for Castle Hayne 12.5mm Mixtures Using PG 76-22 and PG 64-22, with and without Lime

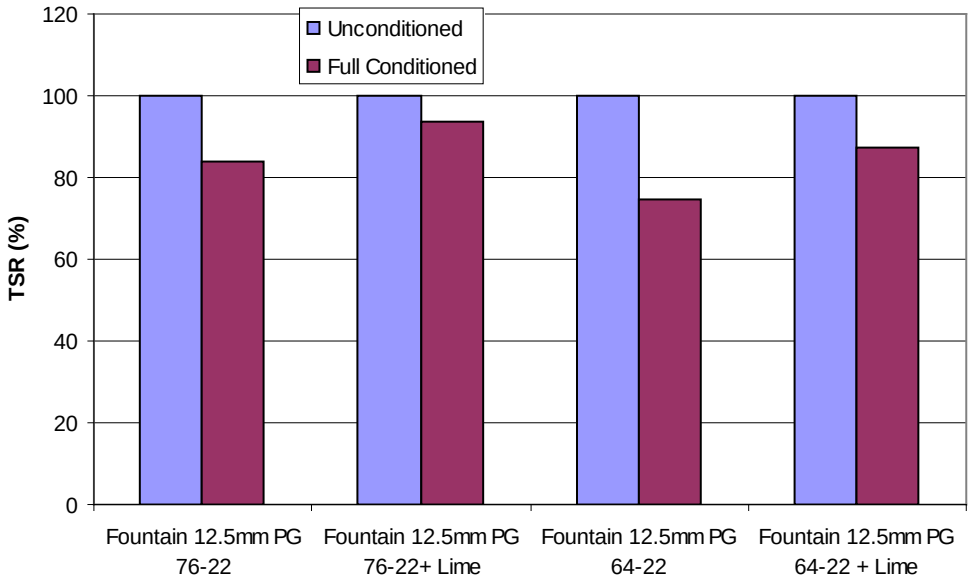

Figure 4.18 Comparison of Tensile Strength Value as % of Unconditioned Tensile Strength Value for Fountain 12.5mm Gradation Mixtures

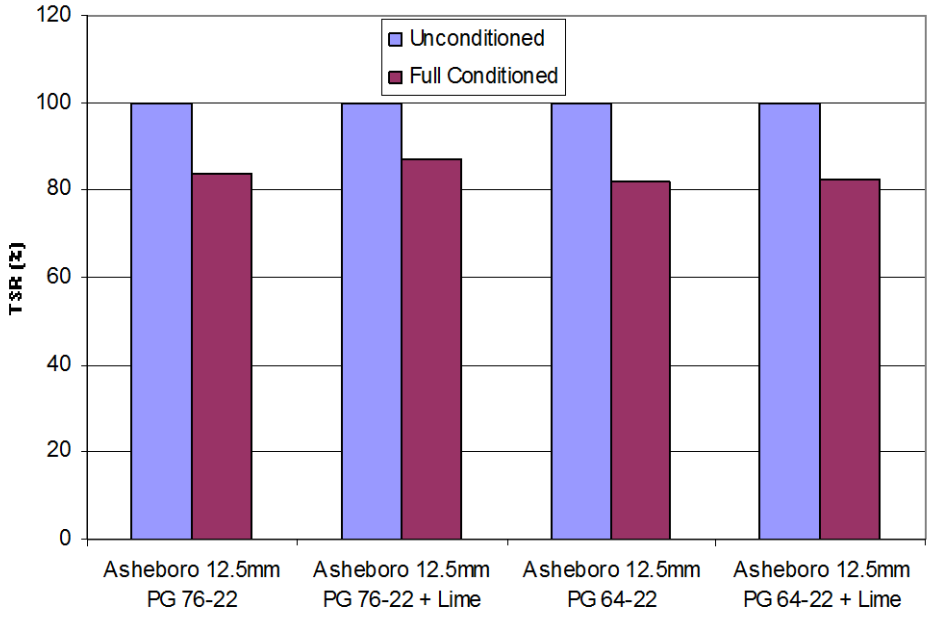

Figure 4.19 Comparison of Tensile Strength Value as % of Unconditioned Tensile Strength Value for Asheboro 12.5mm Gradation Mixtures

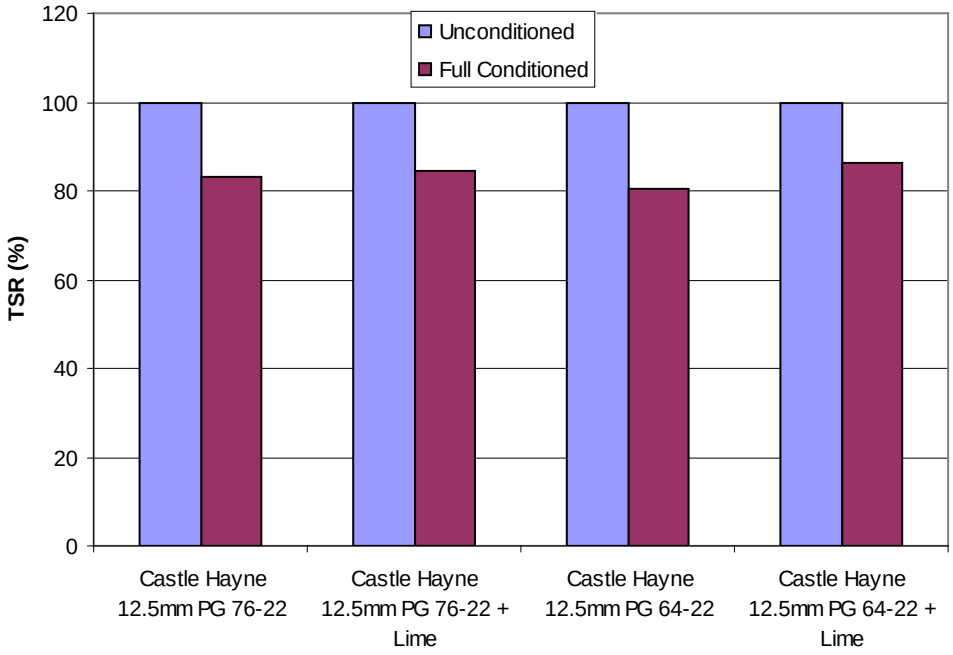

Figure 4.20 Comparison of Tensile Strength Value as % of Unconditioned Tensile Strength Value for Castle Hayne 12.5mm Gradation Mixtures

It can be seen from Figures 4.16 – 4.21 that for all mixes there is an increase in indirect tensile strength when lime is added to the mix. It is also seen that lime is added, the TSR increases, improving the performance of the water damaged samples.

4.5. Statistical Analysis

Statistical analysis was conducted on the S – 12.5 C mixes to determine if there was any difference between the TSR values of lime added mixtures and LOF 6500 anti-strip additive mixtures. The ANOVA results are shown in Table 4.5

Table 4.8 ANOVA Table

Source	df	SS	MS	F-Stat	P-value
Treatments	1	7.26	7.26	1.50	0.24
Error	10	48.24	4.82		
Total	11	55.51			

Since the P-value is higher than 0.05 (α level critical Value) at 95% confidence level, it can be concluded that there is no statistical difference between TSR values between lime added mixtures and LOF 6500 added mixtures. Because of the lack of statistical difference between the additive types in the S – 12.5 C and S – 9.5 C mixes, only lime was used for the S – 12.5 D and S – 12.5 B mixes.

4.6. Summary

The TSR test results show that hydrated lime (by weight of dry aggregates) or liquid anti-stripping agent is necessary for all the aggregate mixture gradations used in this study. Even though there is no statistical difference between TSR values of mixtures with lime

and mixtures with liquid anti-stripping agent, individual tensile strength values are higher for all the mixtures except for Asheboro 12.mm gradation. However, the difference is very small in Asheboro 12.5mm gradation. In addition, earlier research studies show that if the asphalt mixture is held at high temperature for long periods, the effectiveness of liquid anti-stripping agent may be reduced. As indicated in Chapter 2, lime not only reduces moisture susceptibility it also increases stiffness and other characteristics of mixtures. Because of all the above reasons lime was selected as the additive for all mixtures for further performance studies.

CHAPTER 5

5. PERFORMANCE BASED TESTING OF ASPHALT CONCRETE MIXTURES USING SIMPLE SHEAR TESTER

5.1. Introduction

The Shear Frequency Sweep Test conducted with the Simple Shear Tester was developed in the SHRP research program. The test protocol was first introduced as SHRP Designation M-003: "Standard Method of Test for Determining the Shear Stiffness Behavior of Modified and Unmodified Hot Mix Asphalt with Superpave Shear Test Device" (Harrigan, Leahy & Youtcheff, 1994) [32]. Later the test protocol was adopted by the American Association of State Highway and Transportation Officials (AASHTO) as a Provisional Standard: AASHTO Designation: TP7-94 (AASHTO, 1994) [33]. The SST performs shear tests to predict permanent deformation and fatigue cracking. The mixtures were evaluated for their performance with respect to fatigue and rutting distresses. Performance evaluation tests were conducted on both conditioned and unconditioned specimens, (without additive and with hydrated lime as additive) to investigate the effect of moisture damage on fatigue and rutting characteristics of the mixtures. The results are discussed in this chapter.

5.2. Performance Evaluation using the Simple Shear Tester

Shear tests were performed in accordance with AASHTO TP7 Procedures E and F [33]. The tests included Frequency Sweep test at Constant Height (FSCH) and Repeated Shear test at Constant Height (RSCH). These tests were conducted on the conditioned and the unconditioned specimens of all three aggregate sources (Castle Hayne, Fountain and

Asheboro) for both 9.5 mm and 12.5mm gradations using PG 70-22 asphalt binder for phase one. Phase two testing and on conditioned and unconditioned specimens of all three aggregate sources using one 12.5mm gradation and PG 76-22 and PG 64-22 asphalt binder was also conducted. Tests were also performed with the above mixtures using hydrated lime as additive.

5.3. Specimen Preparation

The specimens prepared for FSCH and RSCH tests were 150mm (6-in.) in diameter using Superpave Gyratory Compactor (SGC) and compacted to 7±1% air voids. Specimens were conditioned according to AASHTO T283. The specimens were sawed to a thickness of 50 mm (2-in.). The specific gravities of the specimens were measured. The specimens were then glued between the loading platens using DEVCON^{TM} 5 minute plastic putty and were cured for several hours before testing. The results were based on the average of three specimens.

5.4. Selection of Test Temperature for FSCH and RSCH

In the abridged fatigue analysis (SHRP A-003A) procedure, the pavement temperature is assumed to be 20^{o}C through out the year. The resistance of a mix to fatigue cracking is calculated based on the mix properties evaluated using FSCH at 20^{o}C. The seven-day average high pavement temperature at 50-mm depth from pavement surface at 98% reliability was estimated using SHRPBIND version 2.0 software for Raleigh area (North Carolina State University) and was determined to be 58.5^{o}C.

5.5. Frequency Sweep Test at Constant Height

The testing system consists of an environmental chamber that maintains a constant

temperature and two hydraulic actuators that apply horizontal and vertical loads. A hydraulic pump runs the actuators and the displacement and loading is controlled by computer. For both the FSCH and RSCH tests, the computer applies a standard loading or displacement pattern and the deformations are measured using LVDTs.

The FSTCH test is performed to measure linear visco-elastic properties of asphalt concrete for rutting and fatigue cracking analysis. This test uses a dynamic type of loading and is a strain controlled test with the maximum shear strain limited to ± 0.005 percent (maximum peak to peak of 0.0001 mm/mm). This test is conducted at a constant height requiring the vertical actuator to be controlled by the vertical LVDT. During the test, a horizontal shear strain is applied using a sinusoidal straining pattern. At the same time, the specimen height is kept constant by compressing or pulling the specimen axially based on the closed loop feedback given by the vertical LVDTs attached to the sides of the specimen. The specimen is sheared from the bottom as presented in Figure 5.1 below.

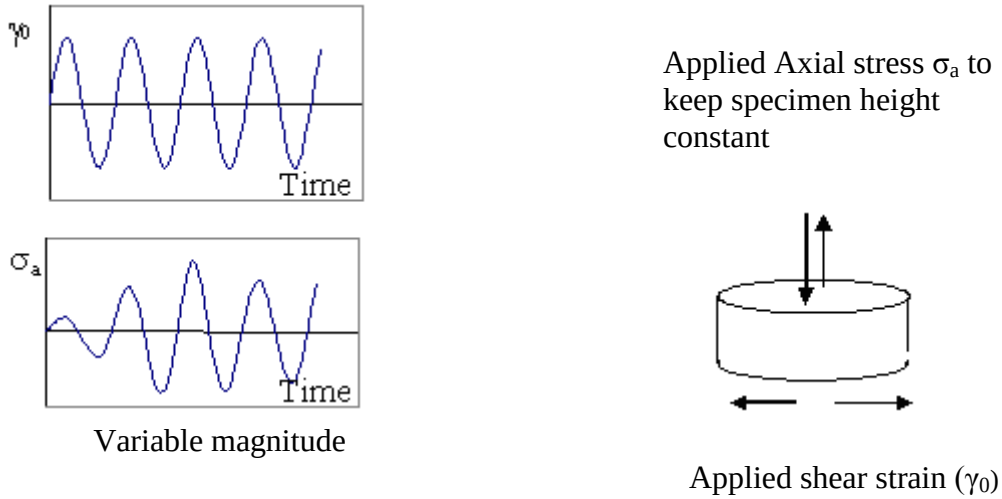

Figure 5.1 Schematic of Shear Frequency Sweep Test

The specimen is preconditioned by applying a sinusoidal horizontal shear strain with amplitude of approximately 0.0001 mm/mm at a frequency of 10 Hz for 100 cycles. After preconditioning the specimen, a series of 10 tests are conducted in descending order of frequency. The frequencies used are 10, 5, 2, 1, 0.5, 0.2, 0.1, 0.05, 0.02 and 0.01 Hz. A specific number of cycles between 4 and 50 are applied. During the test, axial and shear loads and deformations are measured and recorded. The simple shear test device is shown in Figure 5.2 and LVDT arrangements are shown in Figure 5.3.

Figure 5.2 SUPERPAVE Simple Shear Tester (SST)

Three mixtures Castle Hayne, Fountain and Asheboro for both 9.5mm and 12.5mm gradations (unconditioned, half conditioned, and fully conditioned) using PG 70-22, PG 76-22 and PG 64-22 asphalt binder were tested at a temperature of 20^{o}C. Dynamic Shear

Modulus and Phase angle were measured at each frequency for each mixture. The ratio of the stress response of the test specimen to the applied shear strain is used to compute a complex modulus for a given frequency. The delay in the response of the material is measured as phase angle.

Figure 5.3 Simple Shear (FSTCH and RSTCH) Test Specimen

5.6. Frequency Sweep Test at Constant Height Test Results

From the test results, the following graphs of Complex Modulus (Dynamic Shear Modulus) (|G*|) vs. frequency (on log scale) were generated for unconditioned (UC), half conditioned (HC), and fully conditioned (FC) mixtures to evaluate the mix properties.

From the test results, the graphs of complex modulus (Dynamic shear modulus) vs. Frequency (on log scale) as shown in Figures 5.4 to 5.15 were generated for

unconditioned, half conditioned and full conditioned mixtures. The results of Frequency Sweep Tests are tabulated in Tables 5.1-5.12.

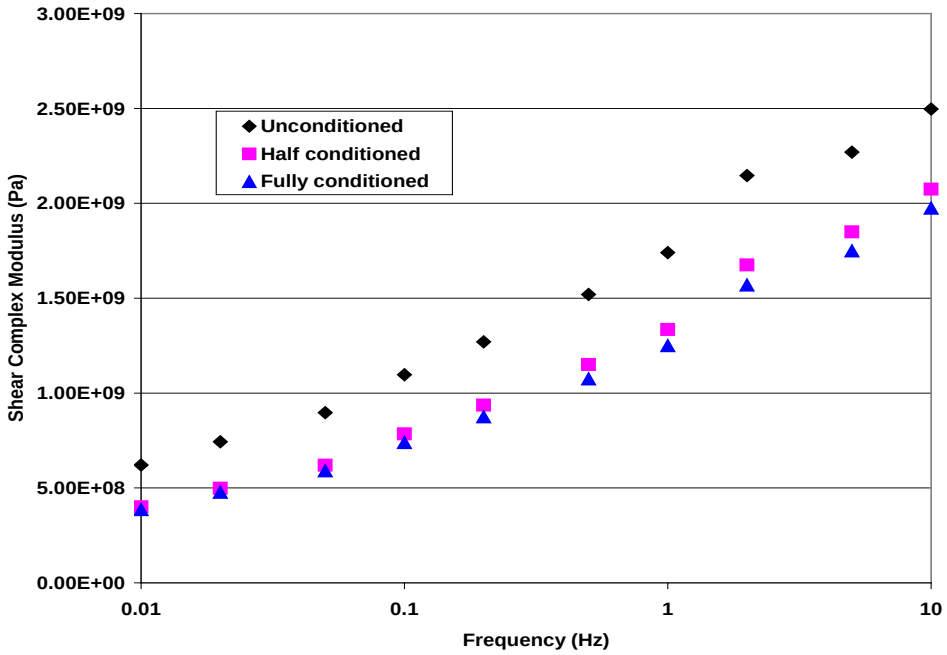

Figure 5.4 Plot of Complex Modulus vs. Frequency for Castle Hayne 12.5mm S – 12.5 C Mix

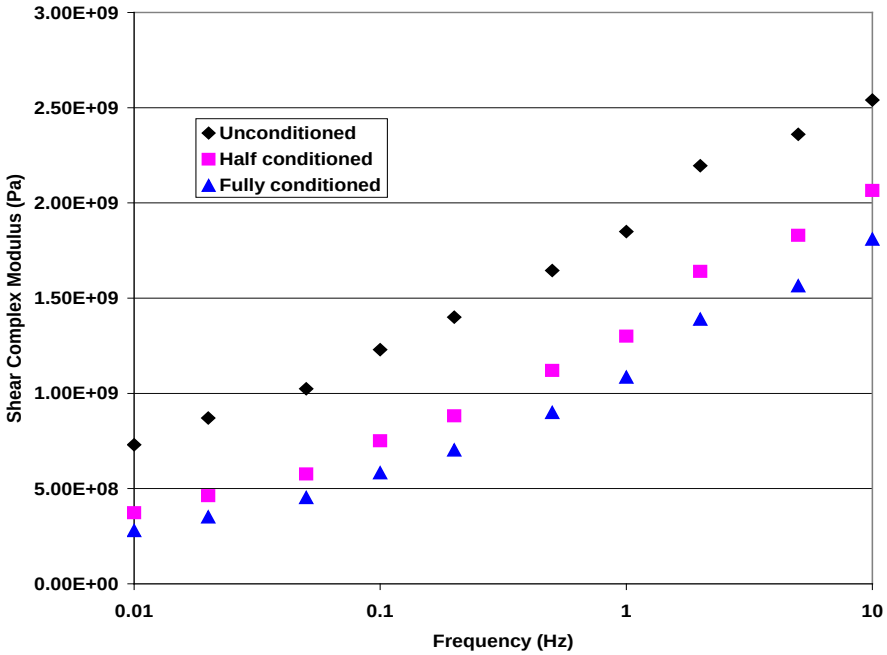

Figure 5.5 Plot of Complex Modulus vs. Frequency for Castle Hayne S – 9.5 C Mix

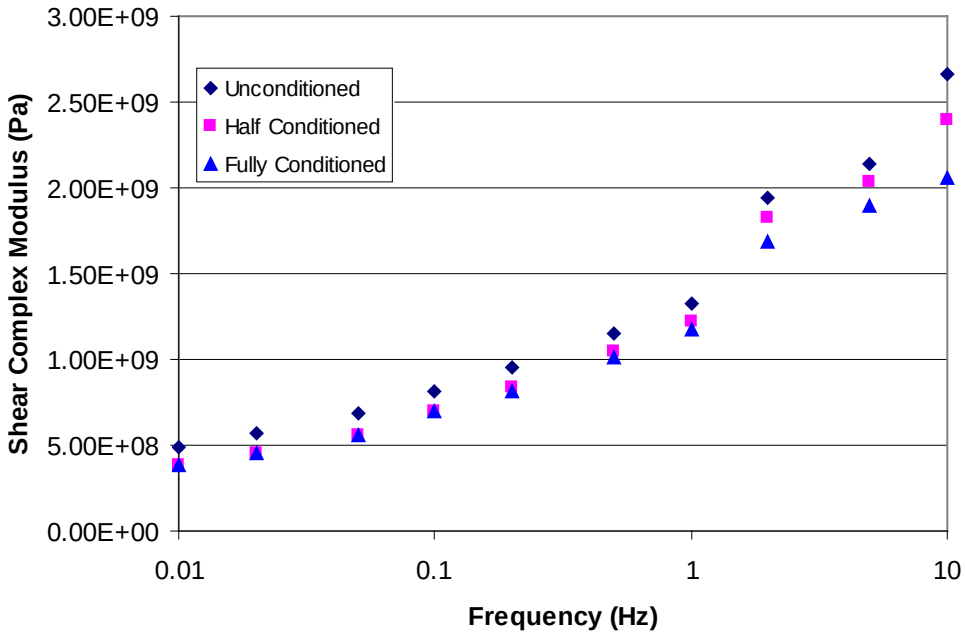

Figure 5.6 Plot of Complex Modulus vs. Frequency for Castle Hayne S – 12.5 D Mix

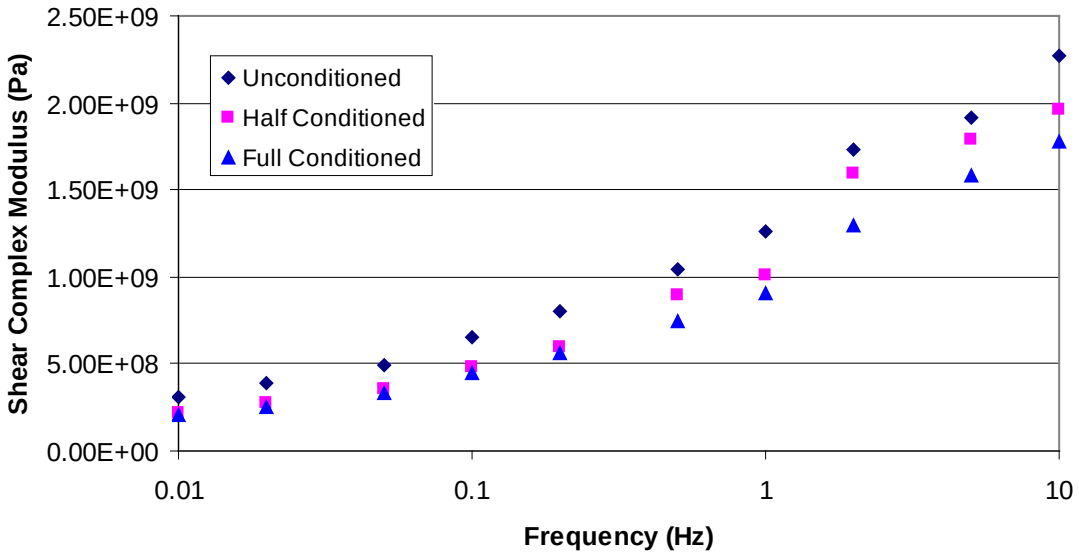

Figure 5.7 Plot of Complex Modulus vs. Frequency for Castle Hayne S – 12.5 B Mix

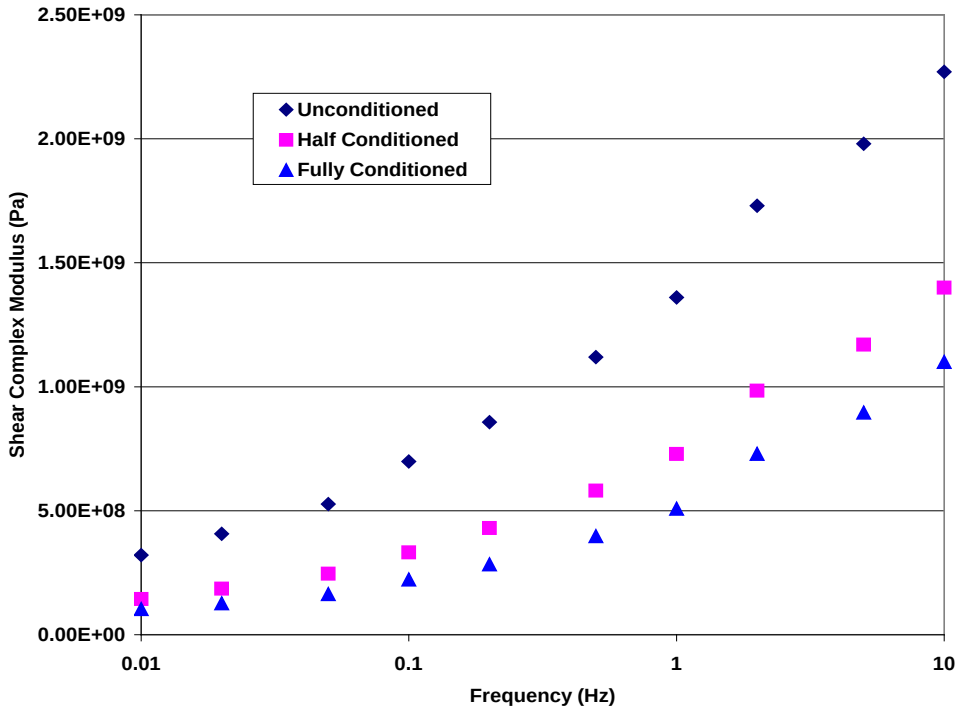

Figure 5.8 Plot of Complex Modulus vs. Frequency for Fountain S – 12.5 C Mix

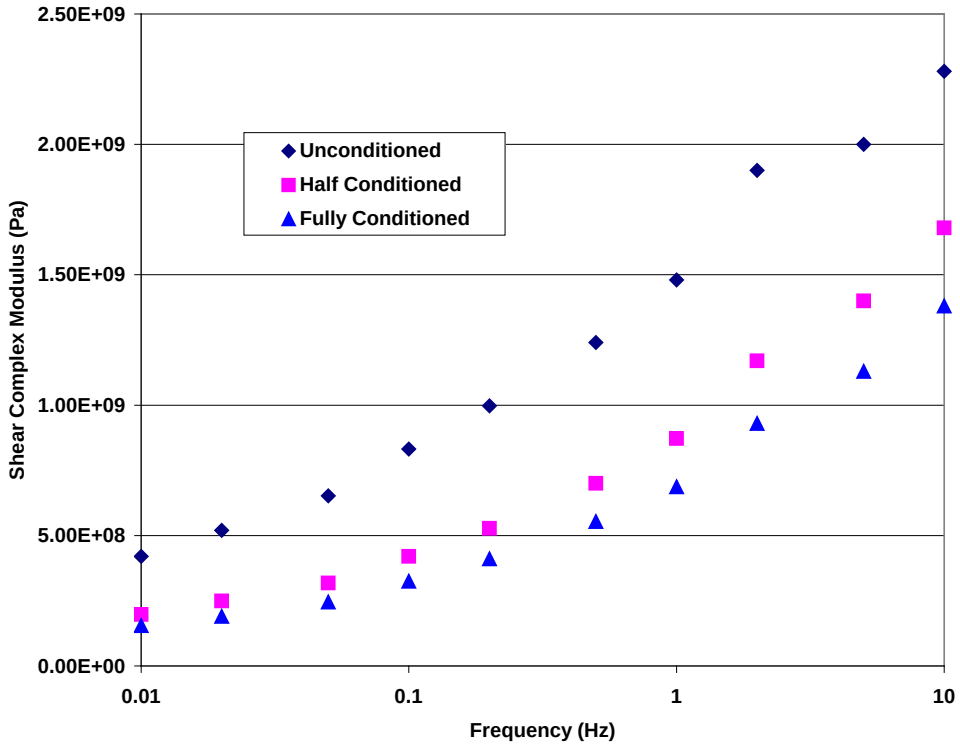

Figure 5.9 Plot of Complex Modulus vs. Frequency for Fountain S – 9.5 C Mix

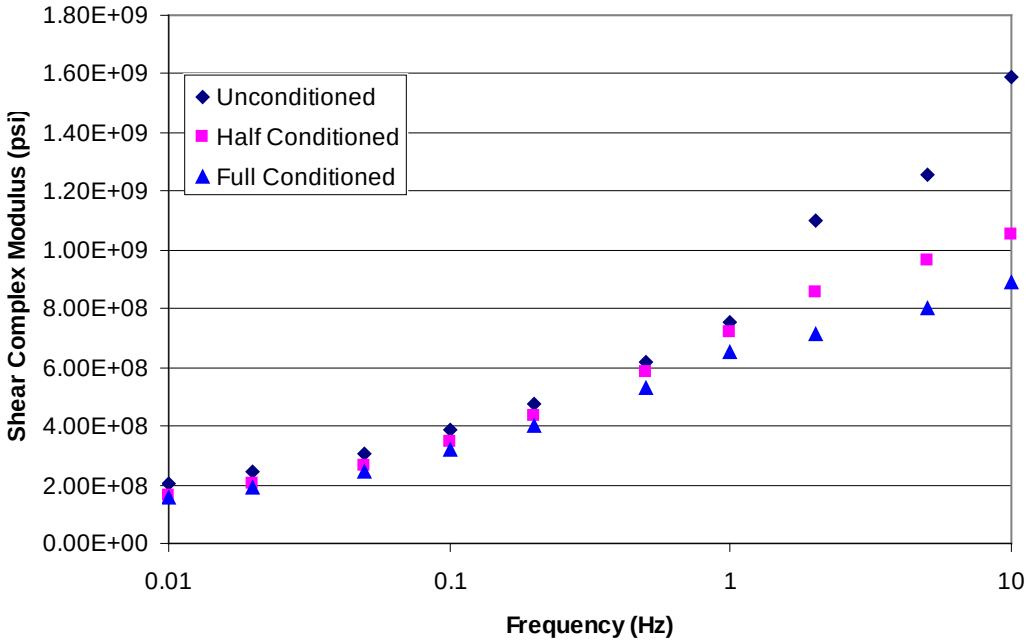

Figure 5.10 Plot of Complex Modulus vs. Frequency for Fountain S – 12.5 D Mix

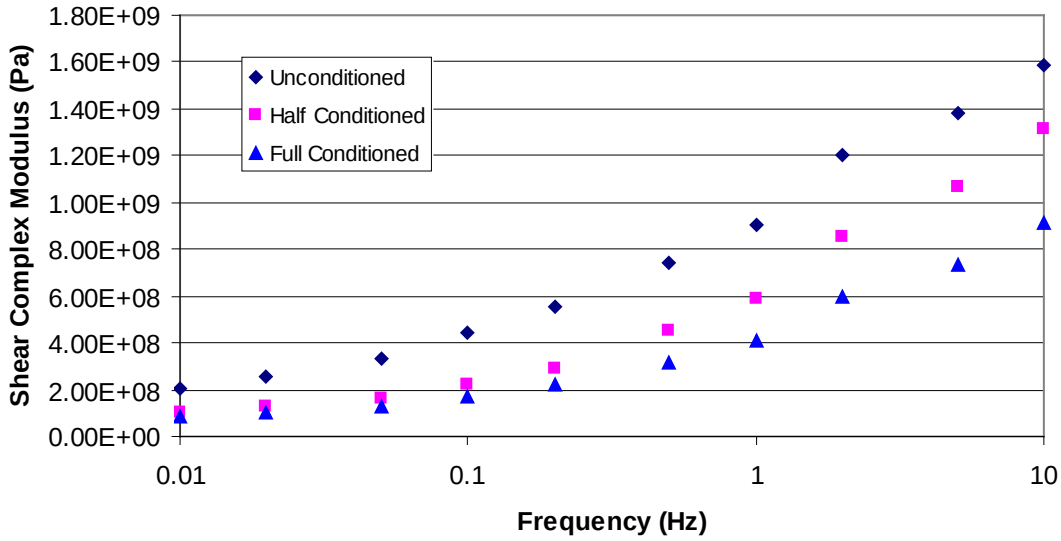

Figure 5.11 Plot of Complex Modulus vs. Frequency for Fountain S – 12.5 B Mix

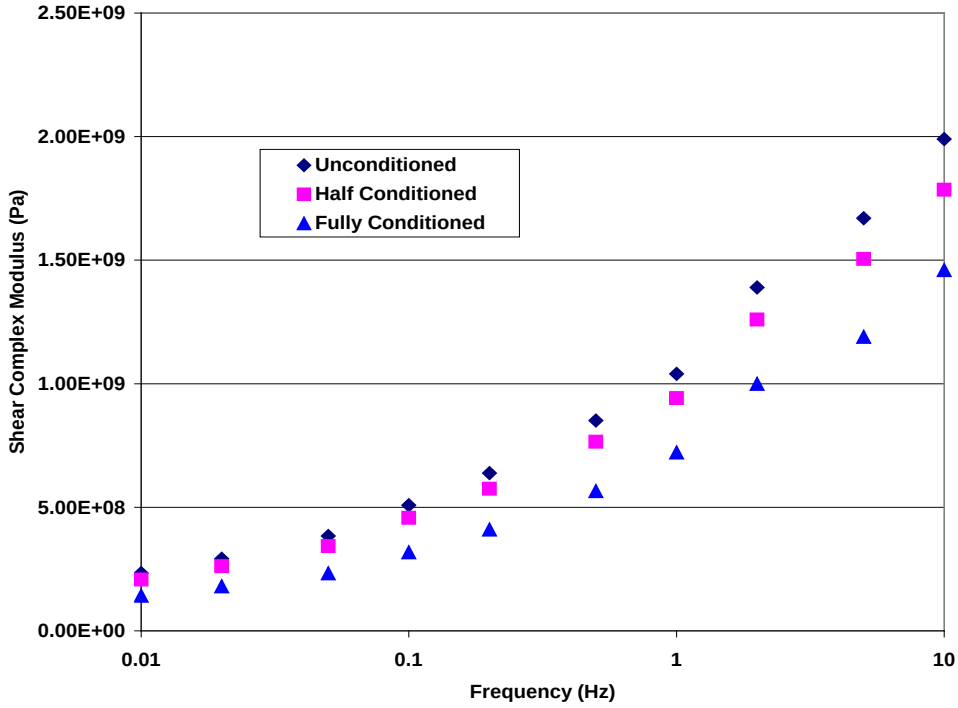

Figure 5.12 Plot of Complex Modulus vs. Frequency for Asheboro S – 12.5 C Mix

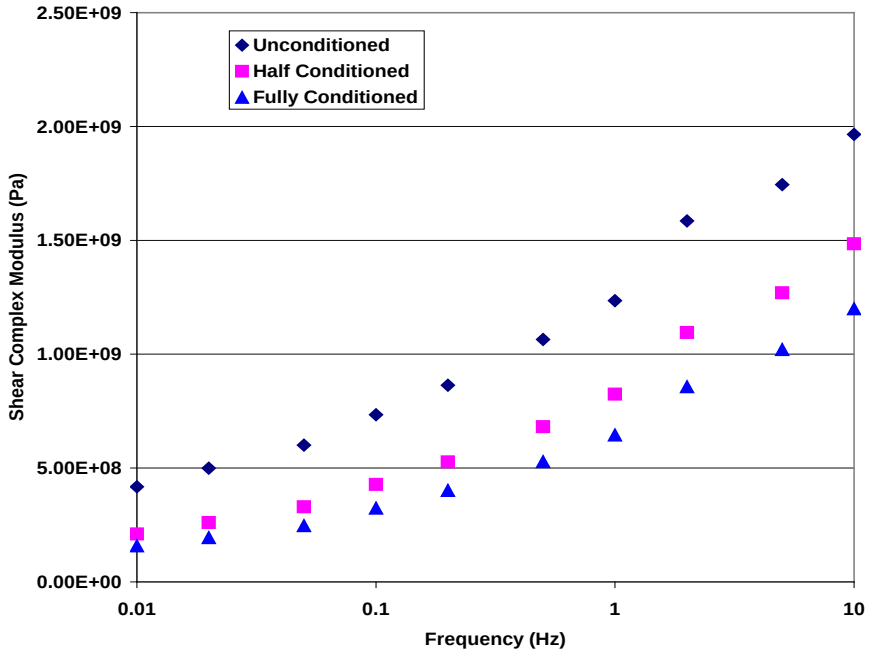

Figure 5.13 Plot of Complex Modulus vs. Frequency for Asheboro S – 9.5 C Mix

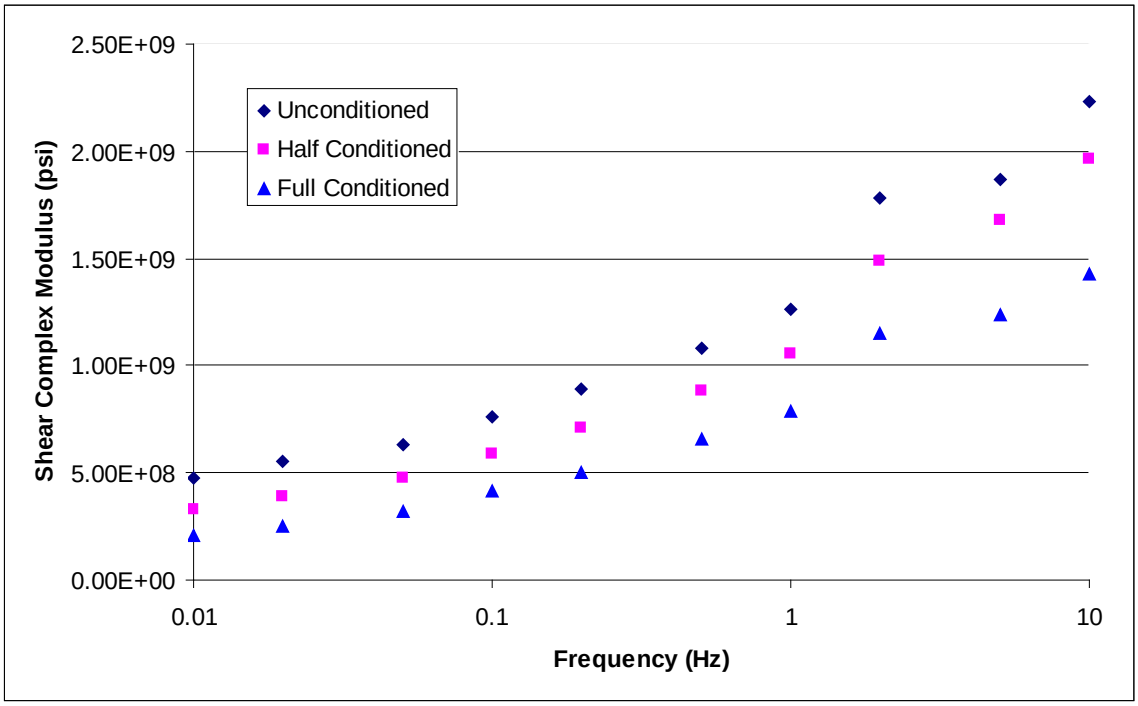

Figure 5.14 Plot of Complex Modulus vs. Frequency for Asheboro S – 12.5 D Mix

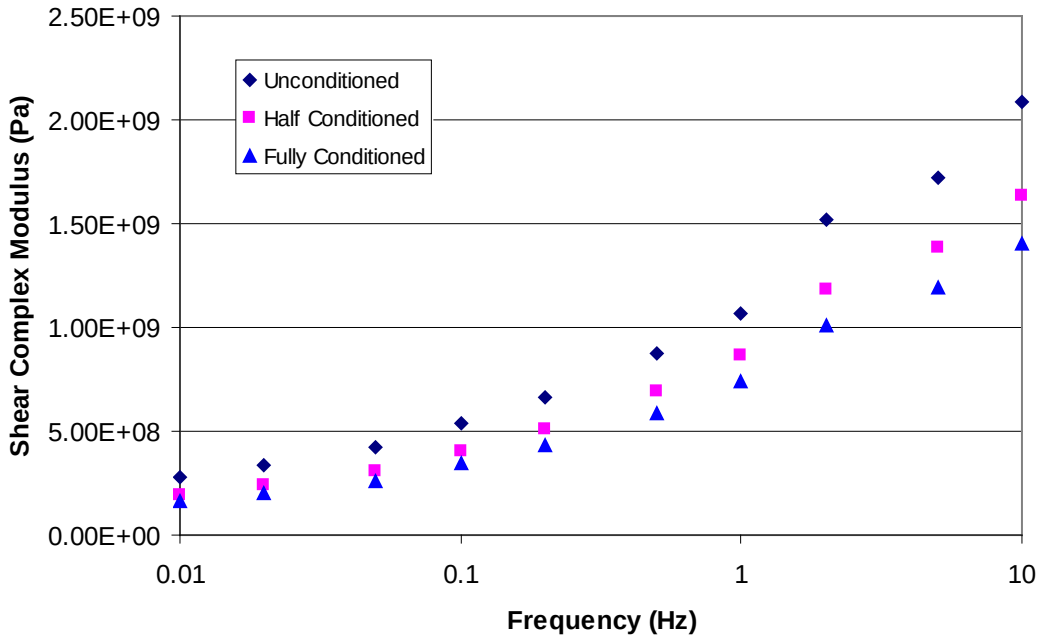

Figure 5.15 Plot of Complex Modulus vs. Frequency for Asheboro S – 12.5 B Mix

From Figures 5.4 - 5.15, it can be seen that as loading frequency increases, the mixture's shear modulus also increases. This behavior was anticipated based on the widely accepted theory of an asphaltic material's visco-elastic response under loading. It can also be seen that the modulus is reduced when the specimen is half conditioned and fully conditioned, which signifies the extent of moisture susceptibility of the aggregates. Tables 5.1 to 5.12 show that as the load frequency increases, the phase angle (time differential between applied load and measured strain response) generally decreases as the elastic component (G') of the mixture stiffness becomes more predominate in the material's load response. Also from the data in these tables, it can further be seen that the phase angles of all mixtures increase when the mixtures are subjected to moisture

damage, indicating loss in elastic component of stiffness. The combination of shear stiffness and phase angles are expected to influence the fatigue life of the mixtures to a large extent. The phase angle represents the relationship between the shear loss and shear storage moduli.

In all gradations of Fountain mixtures, the difference in stiffness value between unconditioned state to the conditioned state is higher compared to Castle Hayne and Asheboro aggregate, which is also observed in tensile strength testing. Research has shown that even though granitic aggregates are stronger, they are more vulnerable to stripping because of high siliceous content. The behavior of mixtures with Fountain aggregate in conditioned state can be explained in terms of its granitic gneiss origin.

In all mixtures, there is a difference in shear modulus between the unconditioned and half conditioned state, signifying that even half conditioned state can induce significant moisture damage in specimens. Castle Hayne aggregate had higher stiffness in unconditioned, half-conditioned and fully conditioned states considering all aggregates, gradations, and asphalt binder grades. Considering all 12.5mm mixtures, fully conditioned state stiffness values of Fountain mixtures are lower than both Castle Hayne and Asheboro mixtures, even though the unconditioned state stiffness values are higher than Asheboro in some cases. This signifies the higher moisture susceptibility of Fountain aggregate. Fountain aggregate shows higher reduction in stiffness value from unconditioned sate to conditioned state in all mixtures.

From Tables 5.1 – 5.12, it can be seen that in lower frequencies the difference in shear moduli and phase angle between half-conditioned and full conditioned is lower, and as

frequency increases, the difference in moduli and phase angle also increases. Also from Tables 5.1 - 5.12, it can be seen that the stiffness values and phase angle values are similar for PG 70-22 12.5mm and 9.5mm gradation at 10Hz in both unconditioned state and half conditioned state, though Castle Hayne 12.5mm gradation had a slightly higher value at the fully conditioned state. However, since the fatigue performance of mixtures does not only depend on stiffness values, it cannot be concluded that performance of both the mixtures will be the same. But in the case of Asheboro aggregate, even though the stiffness value in unconditioned states are almost the same between 9.5mm and 12.5mm gradations, the 12.5mm gradation had a higher stiffness value in both half conditioned state and fully conditioned state. In Fountain aggregate, the same trend is observed in unconditioned state, but a reverse trend is observed in conditioned state. Therefore, it can be concluded that behavior of mixes in conditioned state is mainly dependent on the aggregate type.

Table 5.1 Results of Frequency Sweep Tests (Castle Hayne S – 12.5 C Mix)

Frequency (Hz)	Average G* (Pa) /Phase Angle (Deg)		
	Castle Hayne 12.5 Unconditioned	Castle Hayne 12.5 Half conditioned	Castle Hayne 12.5 Full conditioned
0.01	6.21E+08/30.51	4.01E+08/35.45	3.86E+08/35.19
0.02	7.44E+08/29.29	4.98E+08/33.95	4.78E+08/33.42
0.05	8.97E+08/26.16	6.20E+08/30.83	5.91E+08/30.41
0.1	1.10E+09/25.11	7.85E+08/29.29	7.40E+08/28.99
0.2	1.27E+09/22.92	9.37E+08/27.13	8.76E+08/26.98
0.5	1.52E+09/20.07	1.15E+09/24.41	1.08 E+09/24.74
1	1.74E+09/19.10	1.34E+09/22.20	1.25 E+09/23.14
2	2.15E+09/16.83	1.68E+09/20.80	1.57 E+09/23.21
5	2.27E+09/14.58	1.85E+09/17.61	1.75 E+09/19.28
10	2.50E+09/14.35	2.08E+09/17.48	1.98 E+09/18.97

Table 5.2 Results of Frequency Sweep Tests (Castle Hayne S – 9.5 C Mix)

Frequency (Hz)	Average G* (Pa) /Phase Angle (Deg)		
	Castle Hayne 9.5 Unconditioned	Castle Hayne 9.5 Half conditioned	Castle Hayne 9.5 Full conditioned
0.01	7.31E+08/28.32	3.73E+08/35.41	2.80E+08/37.06
0.02	8.71E+08/27.39	4.63E+08/34.31	3.52E+08/36.80
0.05	1.02E+09/23.24	5.77E+08/31.37	4.54E+08/34.46
0.1	1.23 E+09/22.30	7.51E+08/30.2	5.84E+08/32.47
0.2	1.4 E+09/20.33	8.82E+08/28.34	7.03E+08/29.74
0.5	1.65 E+09/18.01	1.12 E+09/25.30	9.00E+08/27.91
1	1.85 E+09/16.26	1.30 E+09/23.12	1.09E+09/25.95
2	2.2 E+09/15.90	1.64 E+09/21.18	1.39E+09/23.55
5	2.36 E+09/12.84	1.83 E+09/18.05	1.57E+09/20.37
10	2.54 E+09/12.69	2.07 E+09/16.71	1.81E+09/19.29

Table 5.3 Results of Frequency Sweep Tests (Castle Hayne S – 12.5 D Mix)

Frequency (Hz)	Average G* (Pa) /Phase Angle (Deg)		
	Castle Hayne 12.5 Unconditioned	Castle Hayne 12.5 Half conditioned	Castle Hayne 12.5 Full conditioned
0.01	4.94 E+08/41.48	3.86 E+08/45.70	3.85 E+08/47.76
0.02	5.73 E+08/41.53	4.59 E+08/44.64	4.55 E+08/47.82
0.05	6.81 E+08/40.13	5.60 E+08/43.66	5.58 E+08/46.70
0.1	8.15 E+08/39.19	6.99 E+08/42.22	6.94 E+08/45.23
0.2	9.54 E+08/38.04	8.34 E+08/40.27	8.18 E+08/43.70
0.5	1.16 E+09/35.65	1.04 E+09/37.64	1.01 E+09/40.36
1	1.33 E+09/34.06	1.22 E+09/36.00	1.17 E+09/39.49
2	1.94 E+09/43.62	1.83 E+09/43.03	1.68 E+09/48.12
5	2.14 E+09/31.34	2.04 E+09/31.85	1.89 E+09/36.43
10	2.66 E+09/34.24	2.39 E+09/34.46	2.06 E+09/37.92

Table 5.4 Results of Frequency Sweep Tests (Castle Hayne S – 12.5 B Mix)

Frequency (Hz)	Average G* (Pa) /Phase Angle (Deg)		
	Castle Hayne 12.5 Unconditioned	Castle Hayne 12.5 Half conditioned	Castle Hayne 12.5 Full conditioned
0.01	3.11 E+08/43.83	2.16 E+08/43.98	2.01 E+08/44.99
0.02	3.88 E+08/43.31	2.73 E+08/43.77	2.55 E+08/44.66
0.05	4.96 E+08/41.30	3.57 E+08/41.67	3.35 E+08/42.07
0.1	6.54 E+08/40.38	4.78 E+08/40.53	4.46 E+08/41.97
0.2	8.03 E+08/38.08	6.56 E+08/39.67	5.58 E+08/40.13
0.5	1.04 E+09/34.80	8.93 E+08/36.61	7.41 E+08/38.00
1	1.26 E+09/32.60	1.01 E+08/33.95	9.03 E+08/36.37
2	1.73 E+09/37.81	1.59 E+09/38.65	1.30 E+09/40.75
5	1.92 E+09/25.99	1.79 E+09/27.72	1.58 E+09/29.97
10	2.28 E+09/26.46	1.96 E+09/27.54	1.78 E+09/29.61

Table 5.5 Results of Frequency Sweep Tests (Fountain S – 12.5 C Mix)

Frequency (Hz)	Average G* (Pa) /Phase Angle (Deg)		
	Fountain 12.5 Half conditioned	Fountain 12.5 Half conditioned	Fountain 12.5 Full conditioned
0.01	3.21 E+08/38.35	1.44E+08/40.40	1.03E+08/37.69
0.02	4.07E+08/36.51	1.86E+08/40.74	1.27E+08/39.54
0.05	5.27E+08/34.19	2.46E+08/39.84	1.64E+08/40.45
0.1	6.99E+08 /33.13	3.22E+08/39.11	2.23E+08/41.22
0.2	8.57E+08/30.72	4.30E+08/37.69	2.84E+08/40.84
0.5	1.12E+09/27.06	5.81E+08/35.26	3.98E+08/39.27
1	1.36E+09/24.72	7.29E+08/33.22	5.08E+08/39.20
2	1.73E+09/21.06	9.84E+08/31.27	7.30E+08/36.88
5	1.98E+09/18.51	1.17E+09/27.01	8.96E+08/32.73
10	2.27E+09/17.83	1.40E+09/24.73	1.10E+09/30.39

Table 5.6 Results of Frequency Sweep Tests (Fountain S – 9.5 C Mix)

Frequency (Hz)	Average G* (Pa) /Phase Angle (Deg)		
	Fountain 9.5 Unconditioned	Fountain 9.5 Half conditioned	Fountain 9.5 Full conditioned
0.01	4.20E+08/35.94	1.98E+08/37.24	1.55E+08/37.52
0.02	5.20E+08/35.10	2.49E+08/37.46	1.90E+08/37.80
0.05	6.52E+08/32.29	3.18E+08/36.86	2.45E+08/37.38
0.1	8.32E+08/31.16	4.20E+08/36.61	3.25E+08/37.64
0.2	9.97E+08/28.92	5.28E+08/35.95	4.11E+08/37.01
0.5	1.24E+08/25.75	7.00E+08/33.29	5.54E+08/35.19
1	1.48E+09/23.66	8.72E+08/32.13	6.87E+08/34.47
2	1.90E+09/23.04	1.17E+09/30.84	9.30E+08/32.64
5	2.00E+09/17.81	1.40E+09/26.20	1.13E+09/28.92
10	2.28E+09/17.04	1.68E+09/24.03	1.38E+09/27.24

Table 5.7 Results of Frequency Sweep Tests (Fountain S – 12.5 D Mix)

Frequency (Hz)	Average G* (Pa) /Phase Angle (Deg)		
	Fountain 12.5 Unconditioned	Fountain 12.5 Half conditioned	Fountain 12.5 Full conditioned
0.01	2.04 E+08/41.84	1.65 E+08/46.12	1.54 E+08/48.81
0.02	2.44 E+08/41.19	2.05 E+08/45.46	1.90 E+08/48.58
0.05	3.04 E+08/41.03	2.67 E+08/45.27	2.43 E+08/48.09
0.1	3.84 E+08/40.84	3.48 E+08/45.18	3.19 E+08/47.84
0.2	4.76 E+08/40.53	4.38 E+08/44.79	3.98 E+08/46.89
0.5	6.19 E+08/40.03	5.83 E+08/44.28	5.29 E+08/46.15
1	7.52 E+08/39.61	7.22 E+08/43.71	6.52 E+08/45.47
2	1.10 E+09/43.45	8.57 E+08/43.54	7.13 E+08/44.28
5	1.26 E+09/34.82	9.63 E+08/38.71	8.03 E+08/43.53
10	1.59 E+09/33.24	1.05 E+09/38.80	8.89 E+08/43.92

Table 5.8 Results of Frequency Sweep Tests (Fountain S – 12.5 B Mix)

Frequency (Hz)	Average G* (Pa) /Phase Angle (Deg)		
	Fountain 12.5 Unconditioned	Fountain 12.5 Half conditioned	Fountain 12.5 Full conditioned
0.01	1.26 E+08/44.90	1.06 E+08/46.08	8.28 E+07/47.59
0.02	1.58 E+08/46.37	1.28 E+08/47.07	1.00 E+08/49.32
0.05	2.13 E+08/47.04	1.63 E+08/48.00	1.29 E+08/51.93
0.1	2.95 E+08/46.26	2.24 E+08/47.43	1.71 E+08/51.23
0.2	3.87 E+08/45.24	2.89 E+08/46.86	2.21 E+08/50.67
0.5	5.47 E+08/43.38	4.52 E+08/45.83	3.13 E+08/49.12
1	6.99 E+08/42.96	5.86 E+08/44.29	4.06 E+08/49.18
2	1.08 E+09/47.24	8.52 E+08/45.06	5.95 E+08/50.49
5	1.28 E+09/42.31	1.06 E+09/43.61	7.32 E+08/45.50
10	1.73 E+09/39.85	1.32 E+09/41.98	9.12 E+08/43.73

Table 5.9 Results of Frequency Sweep Tests (Asheboro S – 12.5 C Mix)

Frequency (Hz)	Average G* (Pa) /Phase Angle (Deg)		
	Asheboro 12.5 Unconditioned	Asheboro 12.5 Half conditioned	Asheboro 12.5 Full conditioned
0.01	2.34E+08/39.50	2.08E+08/40.60	1.42E+08/39.9
0.02	2.92E+08/39.71	2.62E+08/40.20	1.8E+08/40.27
0.05	3.84E+08/38.46	3.43E+08/38.77	2.33E+08/40.14
0.1	5.08E+08/37.84	4.58E+08/38.16	3.18E+08/39.75
0.2	6.38E+08/36.58	5.75E+08/37.02	4.1E+08/38.98
0.5	8.51E+08/34.08	7.66E+08/34.17	5.66E+08/36.58
1	1.04E+09/31.95	9.42E+08/32.30	7.22E+08/34.71
2	1.39E+09/29.30	1.26E+09/30.60	1E+09/32.45
5	1.67E+09/25.01	1.51E+09/26.02	1.19E+09/27.97
10	1.99E+09/23.39	1.79E+09/24.595	1.46E+09/25.79

Table 5.10 Results of Frequency Sweep Tests (Asheboro S – 9.5 C Mix)

Frequency (Hz)	Average G* (Pa) /Phase Angle (Deg)		
	Asheboro 9.5 Unconditioned	Asheboro 9.5 Half conditioned	Asheboro 9.5 Full conditioned
0.01	4.18E+08/31.83	2.11E+08/37.31	1.59E+08/36.93
0.02	4.99E+08/30.83	2.61E+08/36.99	1.95E+08/37.22
0.05	6.01E+08/29.38	3.3E+08/35.00	2.48E+08/35.57
0.1	7.35E+08/28.66	4.28E+08/34.63	3.25E+08/35.62
0.2	8.64E+08/26.92	5.27E+08/33.28	4.02E+08/34.35
0.5	1.07E+09/24.97	6.82E+08/30.74	5.29E+08/32.70
1	1.24E+09/23.38	8.25E+08/29.21	6.46E+08/31.47
2	1.59E+09/21.38	1.10E+09/26.98	8.58E+08/28.45
5	1.75E+09/18.73	1.27E+09/23.54	1.02E+09/24.93
10	1.97E+09/18.27	1.49E+09/21.86	1.20E+09/23.17

Table 5.11 Results of Frequency Sweep Tests (Asheboro S – 12.5 D Mix)

Frequency (Hz)	Average G* (Pa) /Phase Angle (Deg)		
	Asheboro 12.5 Unconditioned	Asheboro 12.5 Half conditioned	Asheboro 12.5 Full conditioned
0.01	4.78 E+08/40.26	3.32 E+08/41.96	2.04 E+08/43.79
0.02	5.50 E+08/38.71	3.92 E+08/41.95	2.54 E+08/45.93
0.05	6.30 E+08/38.18	4.76 E+08/40.42	3.20 E+08/43.98
0.1	7.64 E+08/37.64	5.92 E+08/40.47	4.15 E+08/43.70
0.2	8.92 E+08/36.17	7.05 E+08/39.32	5.02 E+08/42.51
0.5	1.08 E+09/34.38	8.86 E+08/37.85	6.54 E+08/40.30
1	1.26 E+09/33.32	1.05 E+09/36.18	8.49 E+08/38.33
2	1.78 E+09/38.16	1.49 E+09/39.83	1.25 E+09/41.39
5	1.87 E+09/29.76	1.68 E+09/31.64	1.44 E+09/33.62
10	2.23 E+09/28.30	1.96 E+09/30.87	1.73 E+09/32.31

Table 5.12 Results of Frequency Sweep Tests (Asheboro S – 12.5 B Mix)

Frequency (Hz)	Average G* (Pa) /Phase Angle (Deg)		
	Asheboro 12.5 Unconditioned	Asheboro 12.5 Half conditioned	Asheboro 12.5 Full conditioned
0.01	2.78 E+08/41.11	1.96 E+08/44.77	1.64 E+08/48.76
0.02	3.35 E+08/41.55	2.41 E+08/45.34	2.02 E+08/49.33
0.05	4.21 E+08/41.07	3.11 E+08/45.56	2.62 E+08/49.48
0.1	5.43 E+08/40.92	4.08 E+08/45.36	3.46 E+08/49.26
0.2	6.68 E+08/39.77	5.13 E+08/44.41	4.36 E+08/48.41
0.5	8.75 E+08/37.33	6.94 E+08/41.63	5.91 E+08/46.00
1	1.07 E+09/35.46	8.63 E+08/39.03	7.37 E+08/43.75
2	1.52 E+09/38.72	1.18 E+09/36.10	1.01 E+09/40.91
5	1.72 E+09/29.96	1.39 E+09/31.39	1.19 E+09/36.21
10	2.09 E+09/29.22	1.63 E+09/30.64	1.40 E+09/34.02

Figure 5.16 shows percentage loss in shear modulus for mixtures using PG 70-22 from the unconditioned state to conditioned states. Figures 5.17 and 5.18 show percentage loss in shear modulus for PG 76-22 and PG 64-22 mixtures. Fountain mix had the highest percentage decrease in shear modulus value (comparing the conditioned and unconditioned samples) compared to Castle Hayne and Asheboro aggregates, which is consistent with previous classification as having a high propensity to strip.

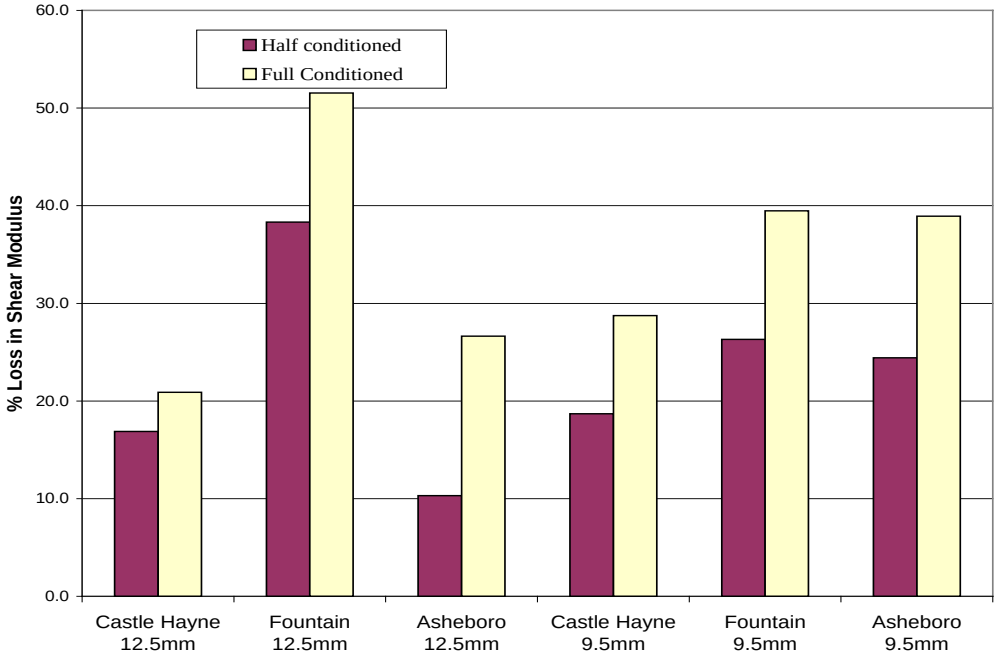

Figure 5.16 Comparison of percentage Loss in Shear Modulus Values for PG 70-22 Mixtures at 10Hz

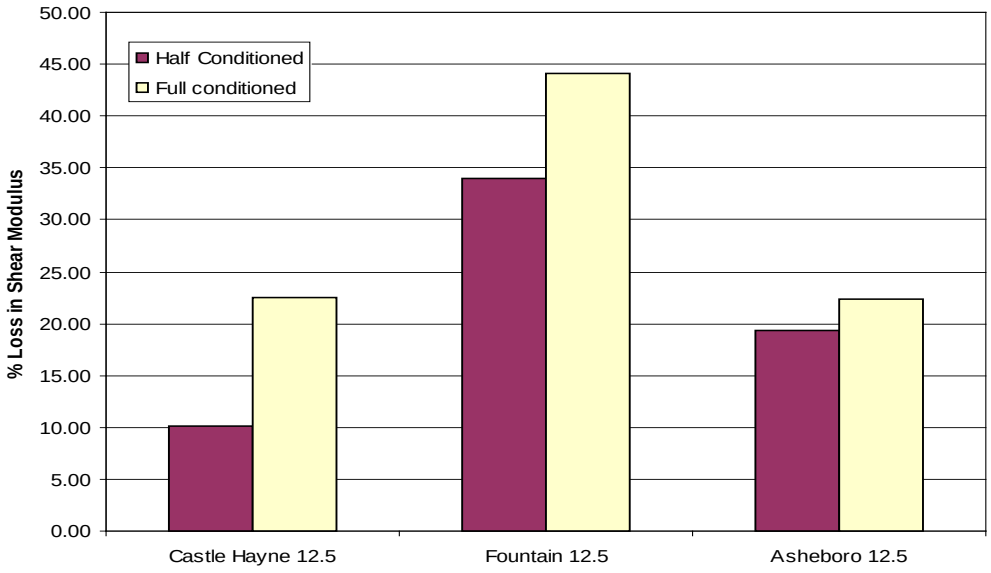

Figure 5.17 Comparison of percentage Loss in Shear Modulus Values for PG 76-22 Mixtures at 10Hz

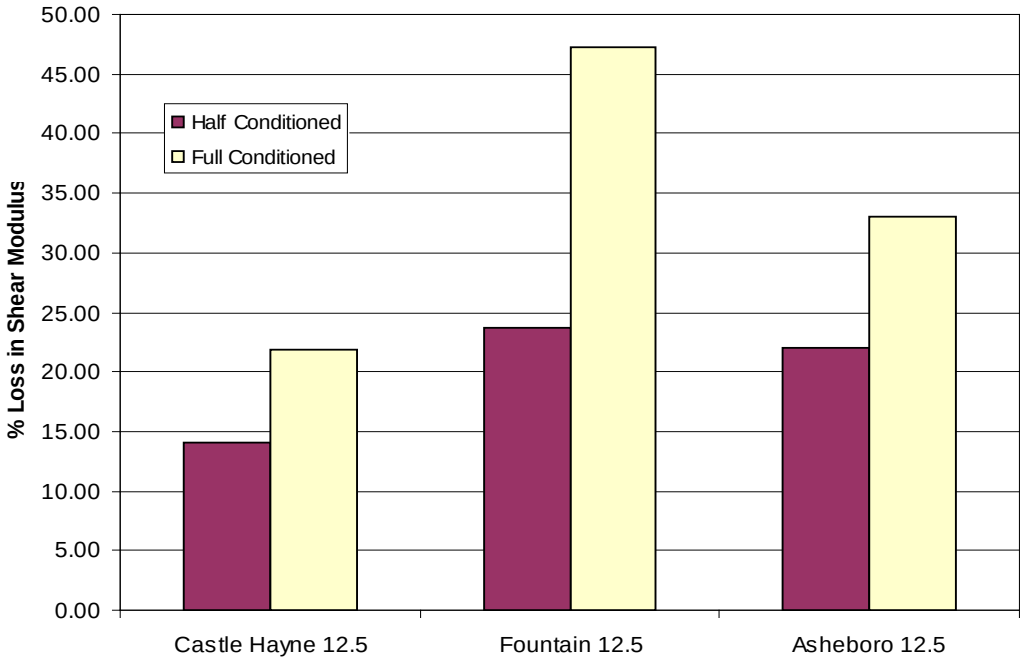

Figure 5.18 Comparison of percentage Loss in Shear Modulus Values for PG 64-22 Mixtures at 10Hz

When the specimens are subjected to moisture damage, the stiffness of the Fountain mixture (12.5mm gradation, PG 70-22 asphalt binder) was reduced by almost 39% for half conditioned mixtures and 50% for fully conditioned mixtures compared to the unconditioned state. But with Castle Hayne mixture (12.5mm gradation, PG 70-22 asphalt binder), shear modulus was reduced by 18% for half conditioned mixtures and 20% for fully conditioned mixtures compared to the unconditioned state. The performance of Asheboro when subjected to moisture damage is in-between Castle aggregate and Fountain aggregate, which is also consistent with both TSR results and previous classifications. Similar trends were observed for mixtures with PG 76-22 and PG 64-22 asphalt binder, signifying that water-damaged performance is primarily a function of aggregate type.

5.7. Shear Test Results of Mixtures Containing Lime

5.7.1. Frequency Sweep Test at Constant Height

The 9.5mm and 12.5mm gradation mixes with Castle Hayne, Fountain, and Asheboro aggregate (unconditioned, half conditioned and full conditioned) with lime as additive were tested at a temperature of 20^{o}C. Dynamic shear moduli and phase angles were measured at each frequency for each of these mixtures. From the test results, the graphs of complex modulus (Dynamic shear modulus) vs. Frequency (on log scale), as shown in Figures 5.19 to 5.30, are generated for unconditioned, half conditioned and fully conditioned mixtures. The results of Frequency Sweep Tests are tabulated in Tables 5.13-5.24. Figures 5.19 to 5.30 show that as loading frequency increases, the mixture shear

modulus increases, as commonly found. In addition, from these figures, it can be seen that modulus values decrease by a small amount when specimens are half conditioned and fully conditioned, which is not as significant as when mixtures were tested without addition of lime. The ability of lime to decrease moisture susceptibility of the aggregates is again, as expected, significant.

Tables 5.13 to 5.24 show that as the loading frequency increases, the phase angle generally decreases as the elastic component (G') of the mixture's stiffness becomes more predominant in the material's response. In addition, from the data in these tables it is evident that phase angles of all the mixtures increased when the mixtures are subjected to moisture damage, indicating a loss in elastic component of stiffness in mixtures containing lime. However, the difference is small as compared to mixtures without addition of lime.

Figures 5.19 - 5.22 show that with Fountain aggregate, there is a relatively small difference in shear moduli at 10Hz between the half conditioned and fully conditioned mixtures compared to Figure 5.16, which shows that there was a considerable reduction in stiffness without an addition of lime. For Fountain 12.5mm gradation using PG 70-22 asphalt binder, the reduction in moduli is only 2.6% from unconditioned state to half conditioned state and 3.04% from unconditioned to fully conditioned state as compared to 39% and 50% respectively for similar Fountain mixtures without lime. This indicates that lime is very effective in reducing the moisture susceptibility of Fountain aggregate. In the case of Fountain 9.5mm gradation, the reduction in moduli from unconditioned state to fully conditioned state is only 8.5% as compared to 27% reduction without lime addition.

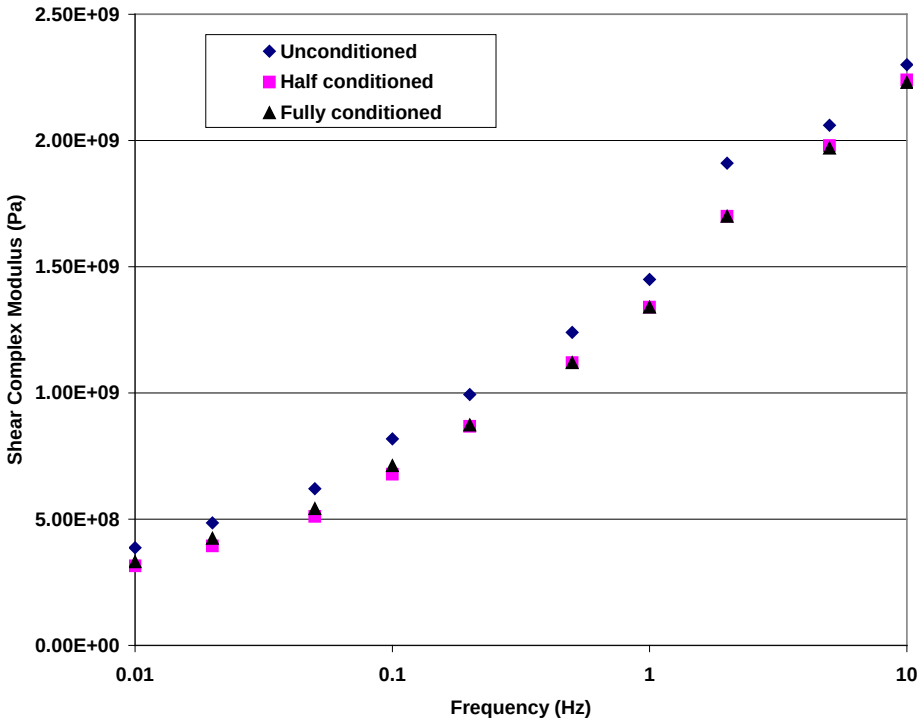

Figure 5.19 Plot of Complex Modulus vs. Frequency for Fountain S – 12.5 C Mix (With Lime)

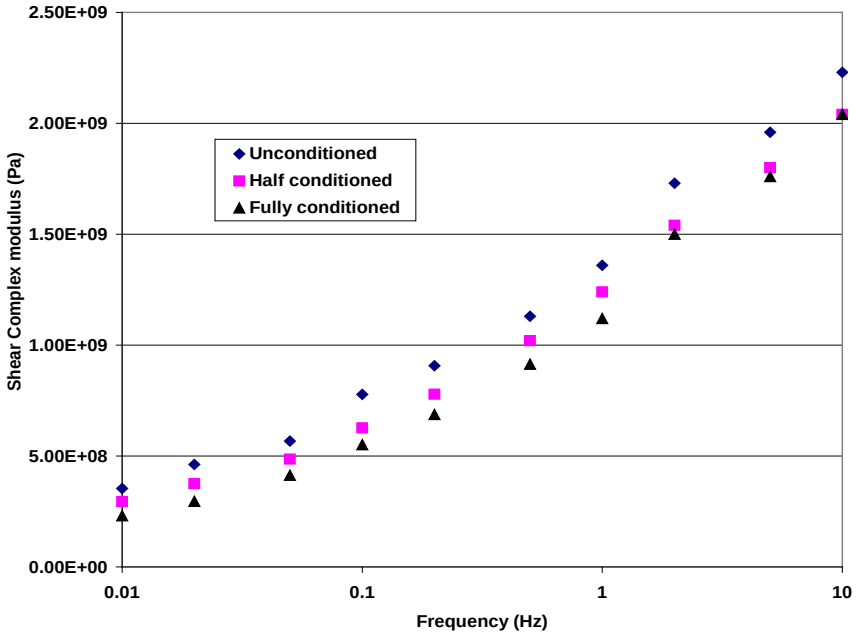

Figure 5.20 Plot of Complex Modulus vs. Frequency for Fountain S – 9.5 C Mix (With Lime)

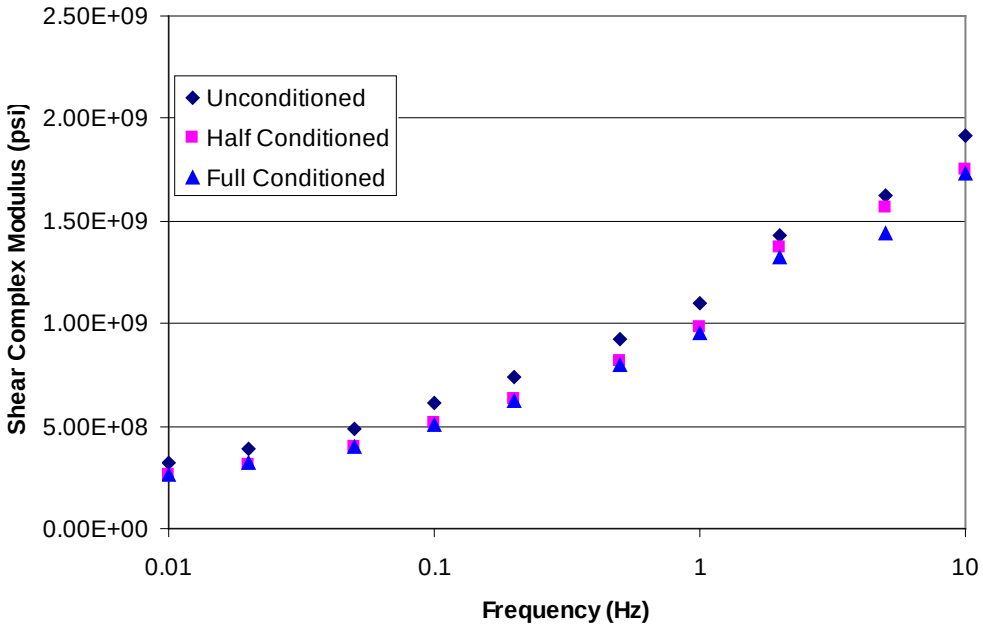

Figure 5.21 Plot of Complex Modulus vs. Frequency for Fountain S – 12.5 D Mix (With Lime)

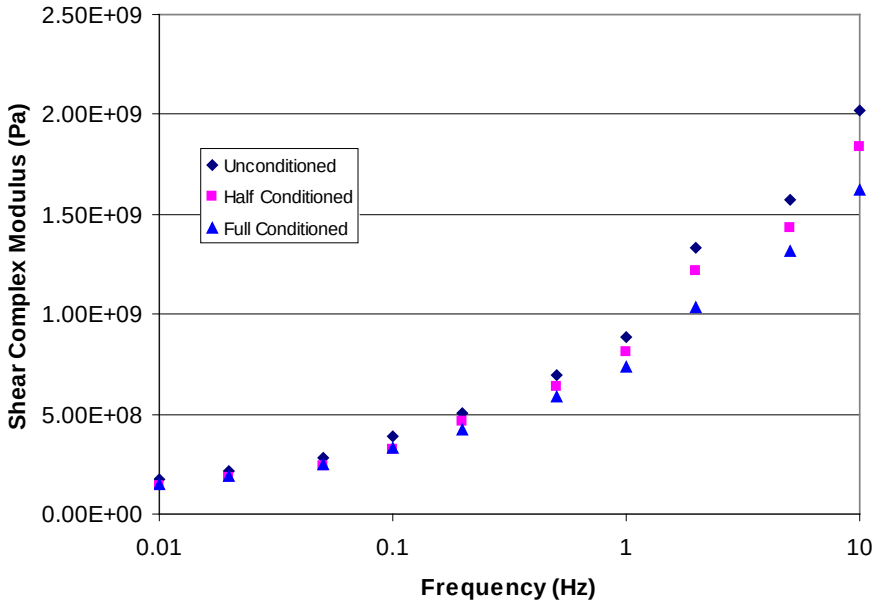

Figure 5.22 Plot of Complex Modulus vs. Frequency for Fountain S – 12.5 B Mix (With Lime)

From Figure 5.23, it can be seen that in the Castle Hayne S – 12.5 C mix, the reduction in shear moduli at 10 Hz is 3.4% from unconditioned state to fully conditioned state and 9.12% from unconditioned state to fully conditioned state. The corresponding reductions in shear moduli for same mixture without additives were 18% and 21%, respectively. Figure 5.24 and Table 5.18 show frequency sweep test results for Castle Hayne 9.5mm gradation mixtures with lime. It can be seen that the reduction in shear moduli from unconditioned state to half conditioned and fully conditioned state at 10Hz are 15% and 16%, respectively. For mixtures of above gradation without lime addition, the corresponding values were 19% and 30%, respectively. Considering all 9.5mm mixtures, Castle Hayne had highest shear moduli in both unconditioned state and fully conditioned state.

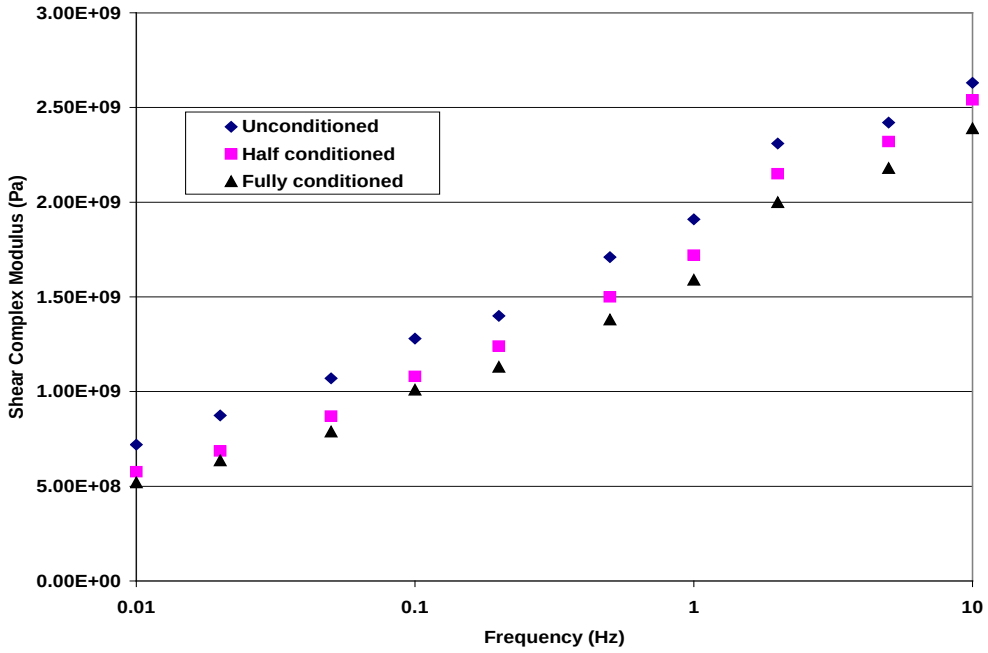

Figure 5.23 Plot of Complex Modulus vs. Frequency for Castle Hayne S – 12.5 C Mix (With Lime)

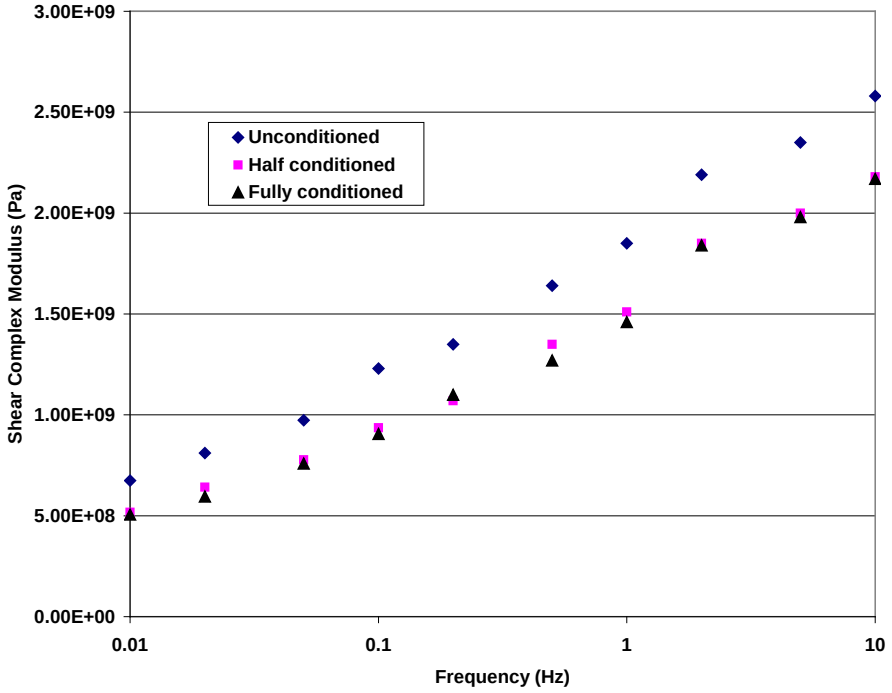

Figure 5.24 Plot of Complex Modulus vs. Frequency for Castle Hayne S – 9.5 C Mix (With Lime)

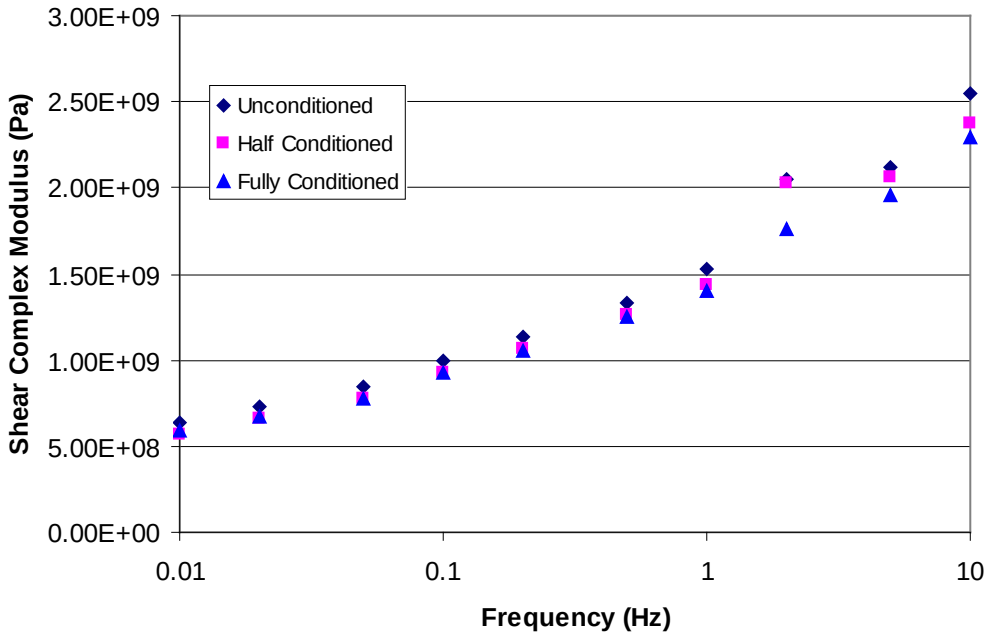

Figure 5.25 Plot of Complex Modulus vs. Frequency for Castle Hayne S – 12.5 D Mix (With Lime)

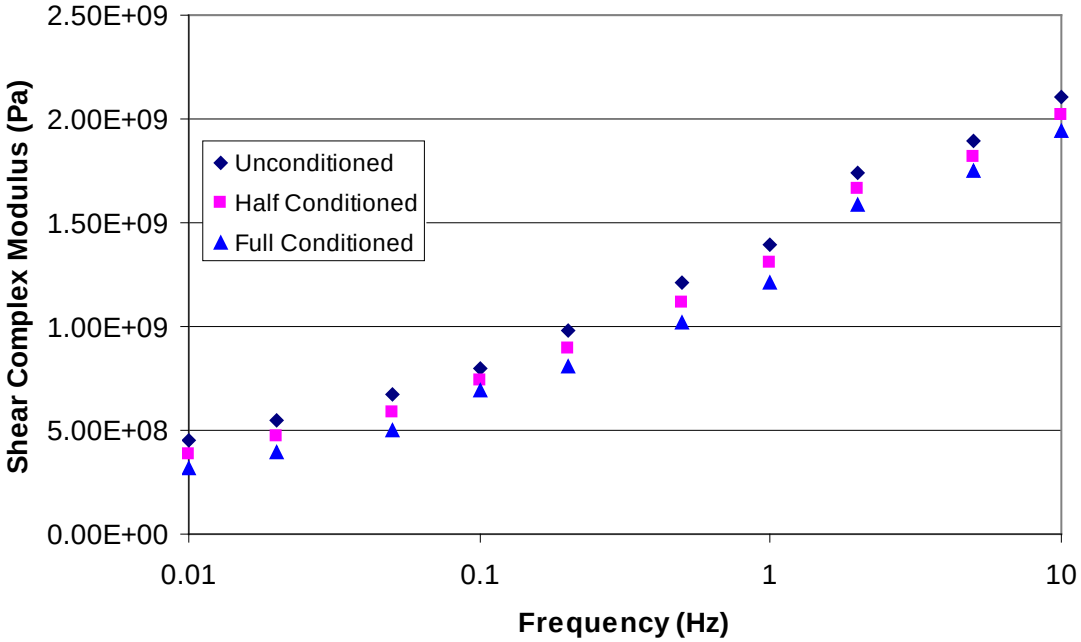

Figure 5.26 Plot of Complex Modulus vs. Frequency for Castle Hayne S – 12.5 B Mix (With Lime)

Figures 5.27 - 5.30 show frequency sweep test results for Asheboro aggregate. From Figure 5.27, it can be seen that there is no appreciable difference in shear moduli values of 12.5mm mixtures at 10Hz for both conditioned and unconditioned states. There is only 2% and 5% reduction of shear moduli from unconditioned state to half conditioned and fully conditioned mixtures, respectively. In Asheboro 9.5mm gradation mixtures, there is only 4.76% reduction in shear moduli at 10Hz from Unconditioned to half conditioned specimens, while this difference is 8% for specimens from unconditioned state to fully conditioned. However, for mixtures without hydrated lime, a 40% reduction of shear moduli from unconditioned state to fully conditioned state was observed. Phase two results are similar, showing significant reductions in loss for mixtures with lime added.

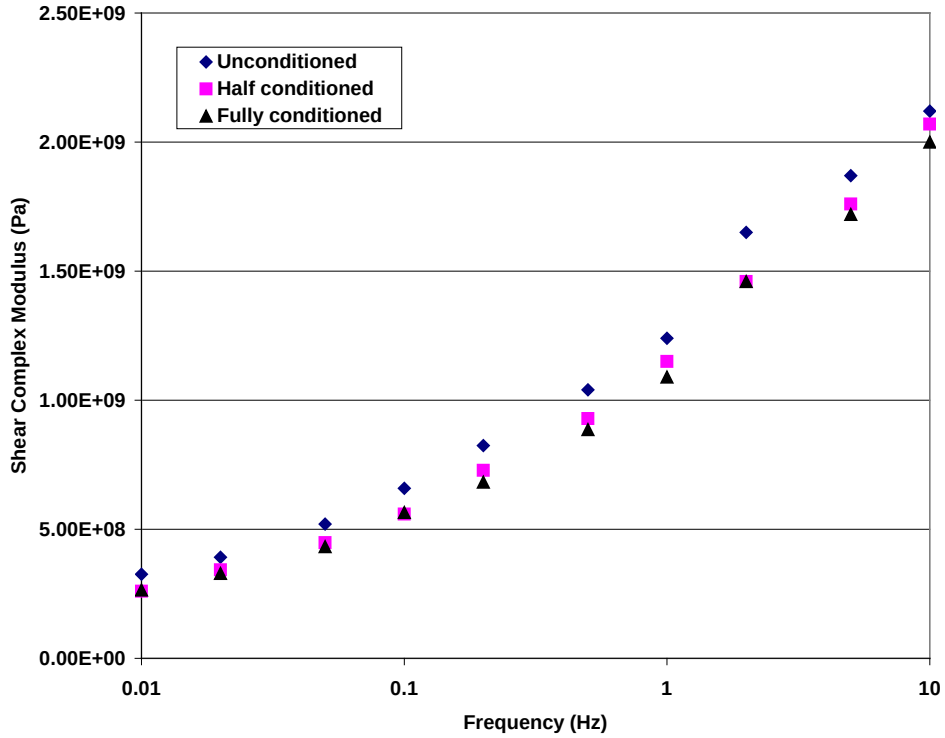

Figure 5.27 Plot of Complex Modulus vs. Frequency for Asheboro S – 12.5 C Mix (With Lime)

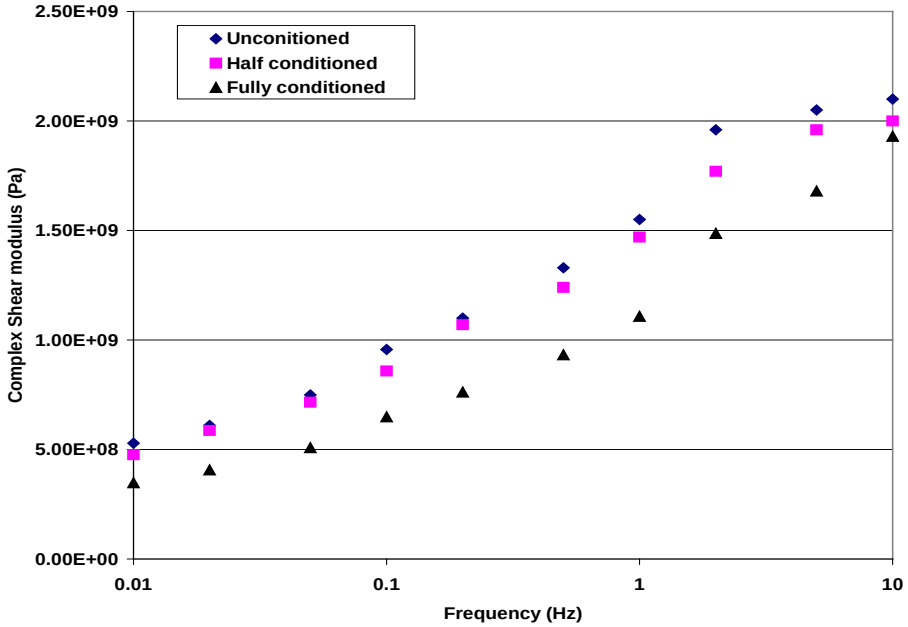

Figure 5.28 Plot of Complex Modulus vs. Frequency for Asheboro S – 9.5 C Mix (With Lime)

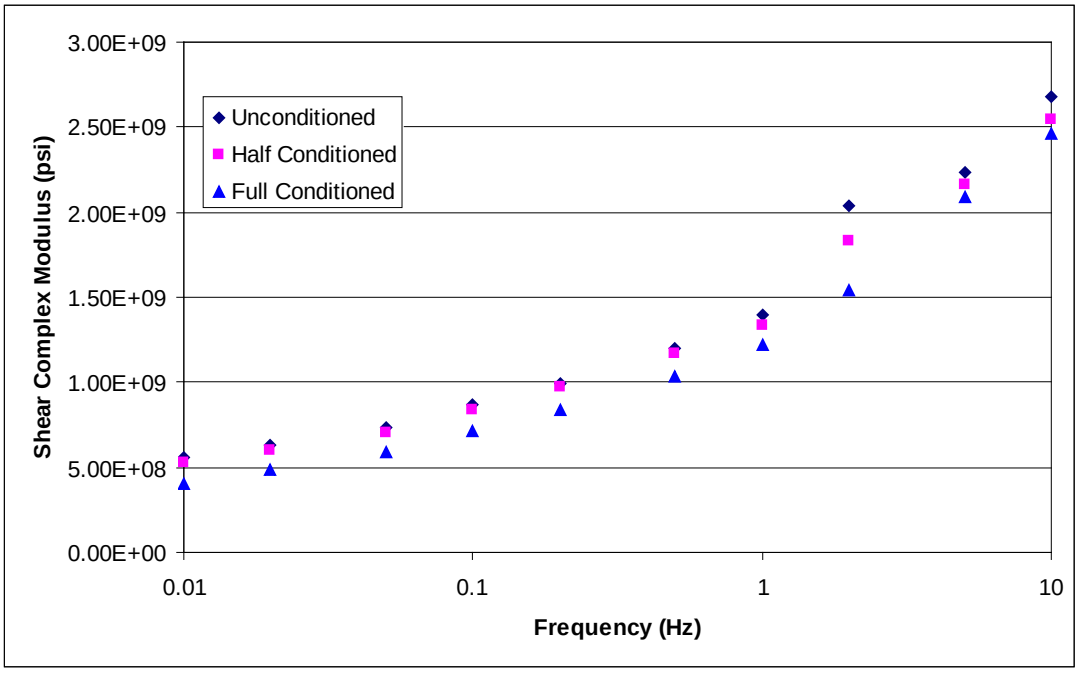

Figure 5.29 Plot of Complex Modulus vs. Frequency for Asheboro S – 12.5 D Mix (With Lime)

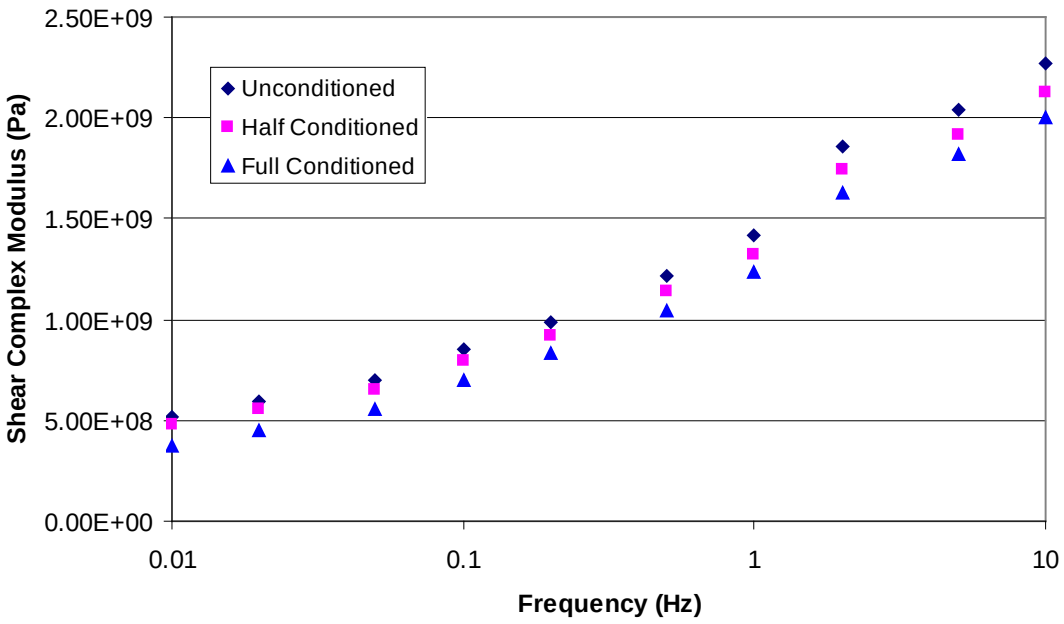

Figure 5.30 Plot of Complex Modulus vs. Frequency for Asheboro S – 12.5 B Mix (With Lime)

Table 5.13 Results of Frequency Sweep Tests (Fountain S – 12.5 C Mix with Lime)

Frequency (Hz)	Average G* (Pa) /Phase Angle (Deg)		
	Fountain 12.5mm Unconditioned	Fountain 12.5mm Half conditioned	Fountain 12.5mm Fully conditioned
0.01	3.87E+08/36.80	3.15E+08/39.23	3.31E+08/37.72
0.02	4.85E+08/34.06	3.94E+08/38.81	4.24E+08/37.58
0.05	6.21E+08/30.65	5.11E+08/33.42	5.42E+08/34.80
0.1	8.18E+08/33.87	6.78E+08/37.58	7.12E+08/33.76
0.2	9.94E+08/29.67	8.68E+08/32.71	8.73E+08/31.64
0.5	1.24E+09/25.83	1.12E+09/28.97	1.12E+09/28.54
1	1.45E+09/23.86	1.34E+09/26.43	1.34E+09/26.29
2	1.91E+09/22.29	1.70E+09/24.40	1.70E+09/24.23
5	2.06E+09/18.31	1.98E+09/20.88	1.97E+09/20.75
10	2.30E+09/17.30	2.24E+09/19.81	2.23E+09/20.15

Table 5.14 Results of Frequency Sweep Tests (Fountain S – 9.5 C Mix with Lime)

Frequency (Hz)	Average G* (Pa) /Phase Angle (Deg)		
	Fountain 9.5mm Unconditioned	Fountain 9.5mm Half conditioned	Fountain 9.5mm Fully conditioned
0.01	3.54E+08/36.41	2.95E+08/39.41	2.31E+08/40.62
0.02	4.62E+08/34.25	3.75E+08/37.56	2.96E+08/40.58
0.05	5.67E+08/35.72	4.86E+08/36.29	4.13E+08/38.84
0.1	7.78E+08/31.48	6.27E+08/33.47	5.51E+08/36.06
0.2	9.07E+08/29.75	7.79E+08/31.75	6.87E+08/35.77
0.5	1.13E+09/27.30	1.02E+09/29.51	9.14E+08/33.47
1	1.36E+09/25.16	1.24E+09/26.88	1.12E+09/31.43
2	1.73E+09/22.06	1.54E+09/23.94	1.50E+09/30.81
5	1.96E+09/19.38	1.80E+09/20.02	1.76E+09/24.09
10	2.23E+09/18.25	2.04E+09/19.46	2.04E+09/23.07

Table 5.15 Results of Frequency Sweep Tests (Fountain S – 12.5 D Mix with Lime)

Frequency (Hz)	Average G* (Pa) /Phase Angle (Deg)		
	Fountain 12.5mm Unconditioned	Fountain 12.5mm Half conditioned	Fountain 12.5mm Fully conditioned
0.01	3.18 E+08/41.43	2.59 E+08/42.87	2.59 E+08/43.74
0.02	3.91 E+08/42.25	3.13 E+08/43.28	3.18 E+08/43.98
0.05	4.82 E+08/41.16	3.99 E+08/42.75	4.00 E+08/43.52
0.1	6.15 E+08/40.87	5.17 E+08/41.98	5.10 E+08/42.79
0.2	7.37 E+08/39.95	6.29 E+08/40.64	6.22 E+08/41.89
0.5	9.26 E+08/37.55	8.16 E+08/38.21	7.99 E+08/40.22
1	1.10 E+09/35.70	9.84 E+08/36.55	9.54 E+08/36.98
2	1.43 E+09/39.93	1.37 E+09/41.33	1.33 E+09/42.61
5	1.63 E+09/30.67	1.57 E+09/31.56	1.44 E+09/32.52
10	1.92 E+09/30.72	1.75 E+09/31.09	1.74 E+09/32.23

Table 5.16 Results of Frequency Sweep Tests (Fountain S – 12.5 B Mix with Lime)

Frequency (Hz)	Average G* (Pa) /Phase Angle (Deg)		
	Fountain 12.5mm Unconditioned	Fountain 12.5mm Half conditioned	Fountain 12.5mm Fully conditioned
0.01	1.72 E+08/43.03	1.42 E+08/43.84	1.53 E+08/44.22
0.02	2.16 E+08/43.33	1.79 E+08/44.09	1.88 E+08/45.04
0.05	2.84 E+08/42.73	2.36 E+08/43.87	2.47 E+08/43.96
0.1	3.91 E+08/40.21	3.24 E+08/42.73	3.32 E+08/43.38
0.2	5.06 E+08/40.15	4.63 E+08/41.67	4.26 E+08/42.54
0.5	6.94 E+08/38.94	6.35 E+08/40.06	5.87 E+08/40.97
1	8.83 E+08/38.78	8.07 E+08/39.22	7.40 E+08/40.24
2	1.34 E+09/40.75	1.22 E+09/42.85	1.03 E+09/43.78
5	1.57 E+09/32.96	1.43 E+09/33.29	1.32 E+09/33.99
10	2.02 E+09/31.22	1.83 E+09/32.65	1.62 E+09/33.02

Table 5.17 Results of Frequency Sweep Tests (Castle Hayne S – 12.5 C Mix with Lime)

Frequency (Hz)	Average G* (Pa) /Phase Angle (Deg)		
	Castle Hayne 12.5 Unconditioned	Castle Hayne 12.5 Half conditioned	Castle Hayne 12.5 Fully conditioned
0.01	7.20E+08/29.98	5.77E+08/33.31	5.20E+08/38.62
0.02	8.74E+08/26.89	6.86E+08/34.04	6.36E+08/33.86
0.05	1.07E+09/24.98	8.70E+08/27.88	7.89E+08/31.45
0.1	1.28E+09/20.61	1.08E+09/25.87	1.01E+09/28.56
0.2	1.40E+09/21.81	1.24E+09/23.62	1.13E+09/26.32
0.5	1.71E+09/19.01	1.50E+09/22.32	1.38E+09/24.23
1	1.91E+09/17.57	1.72E+09/20.32	1.59E+09/22.58
2	2.31E+09/19.14	2.15E+09/21.48	2.00E+09/25.08
5	2.42E+09/14.91	2.32E+09/16.76	2.18E+09/18.93
10	2.63E+09/14.79	2.54E+09/17.57	2.39E+09/19.45

Table 5.18 Results of Frequency Sweep Tests (Castle Hayne S – 9.5 C Mix with Lime)

Frequency (Hz)	Average G* (Pa) /Phase Angle (Deg)		
	Castle Hayne 9.5mm Unconditioned	Castle Hayne 9.5mm Half conditioned	Castle Hayne 9.5mm Fully conditioned
0.01	6.74E+08/30.31	5.17E+08/32.42	5.06E+08/33.18
0.02	8.11E+08/28.38	6.42E+08/31.87	5.95E+08/30.98
0.05	9.73E+08/25.88	7.77E+08/26.73	7.59E+08/28.64
0.1	1.23E+09/22.99	9.36E+08/27.14	9.06E+08/26.60
0.2	1.35E+09/20.74	1.07E+09/24.43	1.10E+09/24.41
0.5	1.64E+09/18.7	1.35E+09/20.81	1.27E+09/23.25
1	1.85E+09/16.41	1.51E+09/19.05	1.46E+09/21.41
2	2.19E+09/16.19	1.85E+09/17.62	1.84E+09/22.83
5	2.35E+09/13.6	2.00E+09/15.43	1.98E+09/18.34
10	2.58E+09/13.56	2.18E+09/14.60	2.17E+09/18.42

Table 5.19 Results of Frequency Sweep Tests (Castle Hayne S – 12.5 D Mix with Lime)

Frequency (Hz)	Average G* (Pa) /Phase Angle (Deg)		
	Castle Hayne 12.5mm Unconditioned	Castle Hayne 12.5mm Half conditioned	Castle Hayne 12.5mm Fully conditioned
0.01	6.39 E+08/33.07	5.63 E+08/39.04	5.88 E+08/40.92
0.02	7.31 E+08/32.50	6.55 E+08/37.98	6.72 E+08/39.93
0.05	8.42 E+08/31.19	7.76 E+08/36.55	7.82 E+08/38.74
0.1	9.93 E+08/30.41	9.26 E+08/35.04	9.24 E+08/38.34
0.2	1.13 E+09/29.29	1.06 E+09/34.13	1.05 E+09/37.69
0.5	1.34 E+09/27.52	1.26 E+09/31.62	1.26 E+09/35.98
1	1.52 E+09/26.57	1.43 E+09/30.37	1.41 E+09/34.47
2	2.05 E+09/32.30	2.02 E+09/36.70	1.76 E+09/36.77
5	2.12 E+09/24.47	2.06 E+09/28.36	1.96 E+09/31.98
10	2.55 E+09/25.41	2.38 E+09/28.10	2.29 E+09/31.24

Table 5.20 Results of Frequency Sweep Tests (Castle Hayne S – 12.5 B Mix with Lime)

Frequency (Hz)	Average G* (Pa) /Phase Angle (Deg)		
	Castle Hayne 12.5mm Unconditioned	Castle Hayne 12.5mm Half conditioned	Castle Hayne 12.5mm Fully conditioned
0.01	4.51 E+08/33.63	3.87 E+08/34.71	3.22 E+08/35.78
0.02	5.46 E+08/33.20	4.71 E+08/33.79	3.96 E+08/35.38
0.05	6.72 E+08/32.32	5.87 E+08/32.09	5.02 E+08/32.86
0.1	7.93 E+08/31.02	7.44 E+08/32.02	6.94 E+08/32.41
0.2	9.76 E+08/30.36	8.90 E+08/31.15	8.03 E+08/31.93
0.5	1.21 E+09/29.80	1.12 E+09/30.42	1.02 E+09/31.03
1	1.40 E+09/28.62	1.30 E+09/29.32	1.21 E+09/30.03
2	1.74 E+09/30.75	1.66 E+09/29.85	1.59 E+09/31.95
5	1.89 E+09/27.52	1.82 E+09/28.45	1.75 E+09/30.08
10	2.11 E+09/25.79	2.02 E+09/26.28	1.94 E+09/28.96

Table 5.21 Results of Frequency Sweep Tests (Asheboro S – 12.5 C Mix with Lime)

Frequency (Hz)	Average G* (Pa) /Phase Angle (Deg)		
	Asheboro 12.5mm Unconditioned	Asheboro 12.5mm Half conditioned	Asheboro 12.5mm Fully conditioned
0.01	3.26E+08/36.54	2.60E+08/38.49	2.65E+08/37.69
0.02	3.92E+08/36.74	3.43E+08/38.88	3.29E+08/35.66
0.05	5.20E+08/35.10	4.48E+08/36.04	4.33E+08/36.36
0.1	6.59E+08/34.75	5.59E+08/37.75	5.65E+08/33.49
0.2	8.24E+08/32.11	7.28E+08/34.31	6.83E+08/33.47
0.5	1.04E+09/28.62	9.29E+08/31.71	8.86E+08/32.16
1	1.24E+09/26.81	1.15E+09/29.33	1.09E+09/29.99
2	1.65E+09/23.79	1.46E+09/24.41	1.46E+09/26.43
5	1.87E+09/20.75	1.76E+09/22.73	1.72E+09/23.40
10	2.12E+09/19.14	2.07E+09/21.14	2.00E+09/22.08

Table 5.22 Results of Frequency Sweep Tests (Asheboro S – 9.5 C Mix with Lime)

Frequency (Hz)	Average G* (Pa) /Phase Angle (Deg)		
	Asheboro 9.5mm Unconditioned	Asheboro 9.5mm Half conditioned	Asheboro 9.5mm Full conditioned
0.01	5.29E+08/28.40	4.76E+08/31.83	3.48E+08/34.40
0.02	6.10E+08/26.43	5.87E+08/34.08	4.07E+08/35.80
0.05	7.49E+08/26.17	7.16E+08/34.09	5.09E+08/34.12
0.1	9.57E+08/26.42	8.58E+08/27.72	6.49E+08/34.31
0.2	1.10E+09/24.19	1.07E+09/30.34	7.62E+08/31.61
0.5	1.33E+09/21.84	1.24E+09/27.74	9.33E+08/31.60
1	1.55E+09/19.84	1.47E+09/25.97	1.11E+09/30.67
2	2.00E+09/22.06	1.86E+09/27.51	1.49E+09/31.08
5	2.05E+09/17.22	1.96E+09/20.88	1.68E+09/25.59
10	2.10E+09/17.88	2.00E+09/21.71	1.93E+09/24.71

Table 5.23 Results of Frequency Sweep Tests (Asheboro S – 12.5 D Mix with Lime)

Frequency (Hz)	Average G* (Pa) /Phase Angle (Deg)		
	Asheboro 12.5mm Unconditioned	Asheboro 12.5mm Half conditioned	Asheboro 12.5mm Fully conditioned
0.01	5.58 E+08/34.69	5.28 E+08/35.49	4.08 E+08/37.04
0.02	6.35 E+08/33.86	6.03 E+08/34.63	4.83 E+08/35.12
0.05	7.34 E+08/32.00	7.08 E+08/32.96	5.85 E+08/34.35
0.1	8.66 E+08/31.39	8.43 E+08/32.29	7.18 E+08/34.96
0.2	9.97 E+08/29.63	9.75 E+08/30.75	8.43 E+08/33.56
0.5	1.20 E+09/27.99	1.17 E+09/29.06	1.04 E+09/31.69
1	1.40 E+09/26.85	1.34 E+09/27.37	1.22 E+09/30.20
2	2.04 E+09/30.40	1.83 E+09/31.44	1.54 E+09/32.81
5	2.23 E+09/23.80	2.16 E+09/25.10	2.09 E+09/29.16
10	2.68 E+09/22.94	2.54 E+09/25.66	2.46 E+09/28.47

Table 5.24 Results of Frequency Sweep Tests (Asheboro S – 12.5 B Mix with Lime)

Frequency (Hz)	Average G* (Pa) /Phase Angle (Deg)		
	Asheboro 12.5mm Unconditioned	Asheboro 12.5mm Half conditioned	Asheboro 12.5mm Fully conditioned
0.01	5.12 E+08/37.08	4.76 E+08/38.58	3.75 E+08/39.75
0.02	5.92 E+08/36.99	5.51 E+08/37.51	4.52 E+08/39.33
0.05	7.04 E+08/35.02	6.55 E+08/36.61	5.55 E+08/38.96
0.1	8.49 E+08/34.62	7.92 E+08/36.23	6.95 E+08/38.52
0.2	9.90 E+08/33.70	9.24 E+08/35.37	8.31 E+08/37.95
0.5	1.22 E+09/31.99	1.14 E+09/33.73	1.05 E+09/36.61
1	1.41 E+09/30.58	1.32 E+09/32.40	1.24 E+09/34.74
2	1.86 E+09/29.57	1.74 E+09/33.35	1.63 E+09/35.43
5	2.04 E+09/27.84	1.91 E+09/30.83	1.82 E+09/31.88
10	2.27 E+09/25.43	2.12 E+09/28.45	2.00 E+09/30.26

Figure 5.31 shows percentage loss in shear modulus for phase one mixtures from the unconditioned state to conditioned states. Figures 5.32 and 5.33 show percentage loss in

shear modulus for phase two mixtures. The percentage in shear modulus loss for all mixtures with lime is significantly less than mixtures without lime. This signifies that addition of lime can overcome the stripping propensity of various aggregate types and increase stiffness of asphalt pavements.

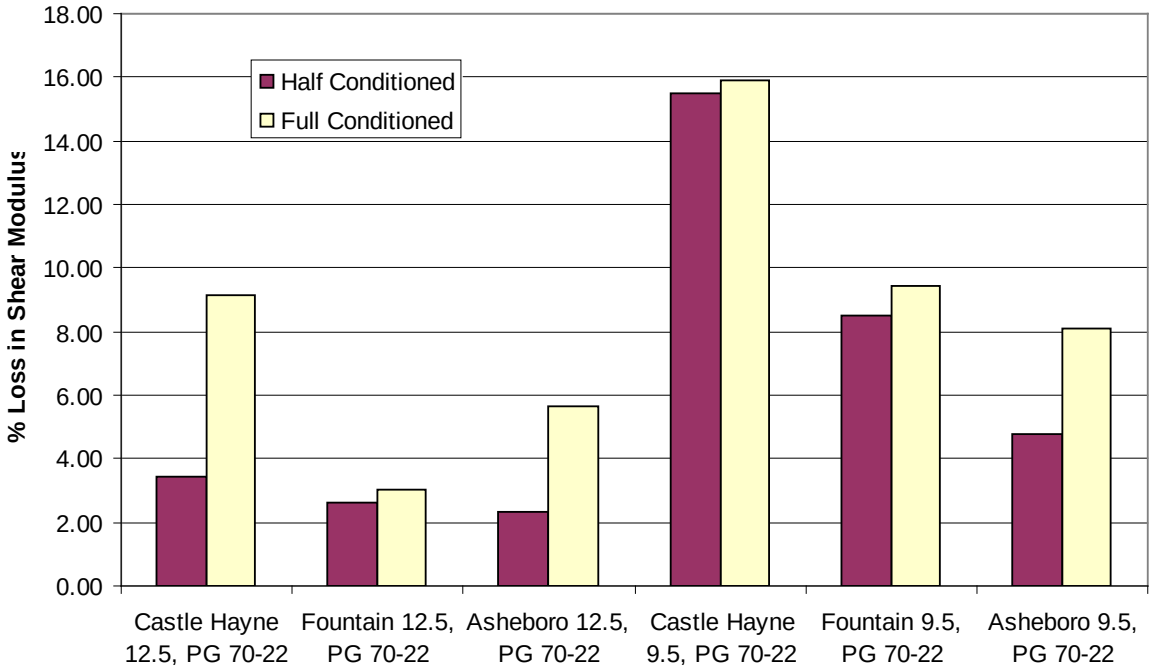

Figure 5.31 Comparison of percentage Loss in Shear Modulus Values for Mixtures Using PG 70-22 at 10Hz

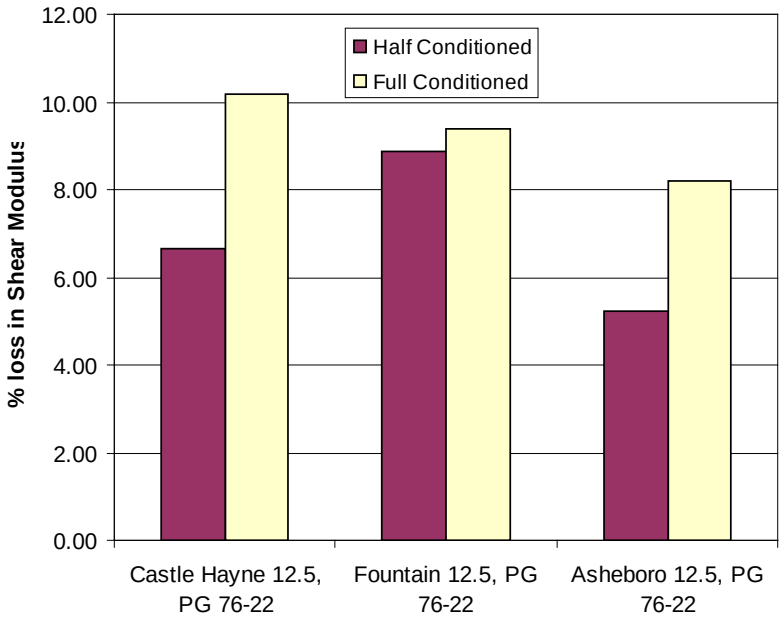

Figure 5.32 Comparison of percentage Loss in Shear Modulus Values for S – 12.5 D Mixes at 10Hz

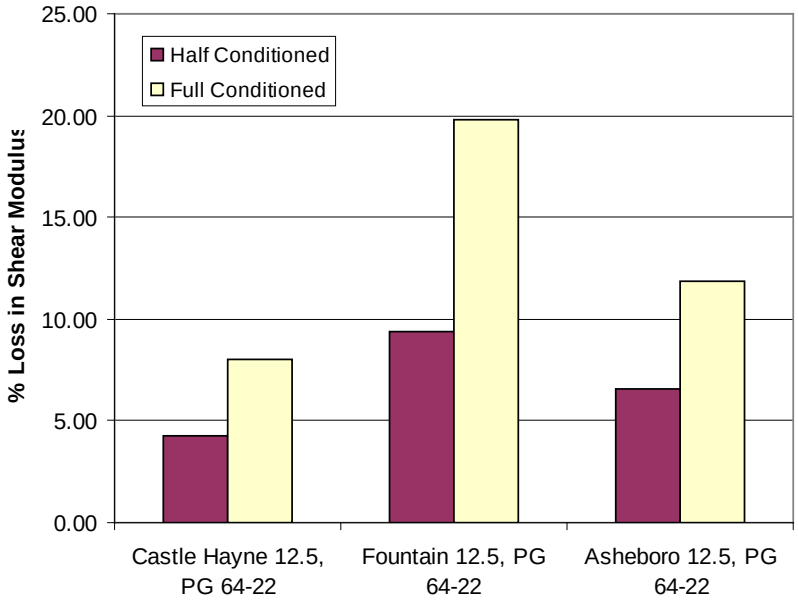

Figure 5.33 Comparison of percentage Loss in Shear Modulus Values for S – 12.5 B Mixes at 10Hz

5.8. Repeated Shear Test at Constant Height

This test was performed to estimate the rutting potential of a mixture. The visco-elastic properties of an asphalt mixture at high temperatures are related to its permanent deformation characteristics. The accumulation of plastic shear strain in a mixture under repeated loading can give some indication about the mixture's resistance to permanent deformation. The repeated shear testing at constant height was selected to evaluate the accumulated shear strain and permanent deformation characteristics of the mixture.

The RSCH test is a stress-controlled test with the feedback to the vertical load actuator from the magnitude of the shear load. The test is conducted at constant height, requiring the vertical actuator to be controlled by the vertical LVDT. The horizontal actuator under control by the shear load cell applies haversine loads. The horizontal LVDT measures the difference in horizontal displacement between two points on the specimen separated by 37.5mm, thus away from the end effects and away from the deformation of the glue. It preconditions the specimen by applying a haversine load corresponding to a 7-kPa shear stress for 100 cycles. The 0.7-second load cycle consists of a 0.1-second shear load followed by 0.6-second rest period. After preconditioning the specimen, it applies a 68 ± 5 kPa haversine shear pulse for 5,000 cycles or until 5% shear strain is reached. This corresponds to a frequency of approximately 1.43 Hz. During the test, axial and shear loads and deformations are measured and recorded. This test was conducted according to AASHTO TP-7 Procedure F. The tests were conducted at their respective seven-day average high pavement temperature (58.5^{o}C) at 50-mm depth from the pavement surface.

5.8.1. Repeated Shear at Constant Height Results

This test was performed to estimate the rutting potential of a mixture. The repeated shear test at constant height (RSCH) was selected to evaluate the accumulated shear strain and permanent deformation characteristics of the mixtures. The results of the RSCH tests are shown in Figures 5.46 - 5.57. The shear strain at the end of 5000 cycles is provided for each mixture in Tables 5.25 and 5.26. From Figures 5.46 - 5.57, as expected, the shear strains of conditioned specimens are higher than the shear strains of unconditioned specimens. Considering both gradations**,** Castle Hayne mixture has the lowest shear strain among all the mixtures in unconditioned state. Among 12.5mm & 9.5mm mixtures, conditioned Fountain mix samples had the highest percentage increase in shear strain when compared to its unconditioned Fountain mix samples. Conditioned Castle Hayne mix had the lowest percentage increase in shear strain when compared to the unconditioned Castle Hayne mix. From 5.34 to 5.45, it can be seen that increase in shear strain is rapid in first 1000 cycles and then it takes place gradually. Also from Figures 5.17 to 5.22, it can be seen that except for Castle Hayne 9.5mm gradation mixture, all other mixtures show large difference in shear stains between half conditioned state and fully conditioned state. The most likely explanation for the non conformity in the Castle Hayne S – 9.5 C mix is that the finer gradation of the 9.5mm mix is more easily compromised by water damage to begin with, but with further damage the limestone origins of Castle Hayne aggregate become a greater factor and mitigate the damage. With all aggregates, there exists a large difference in shear strains between unconditioned state to fully conditioned state.

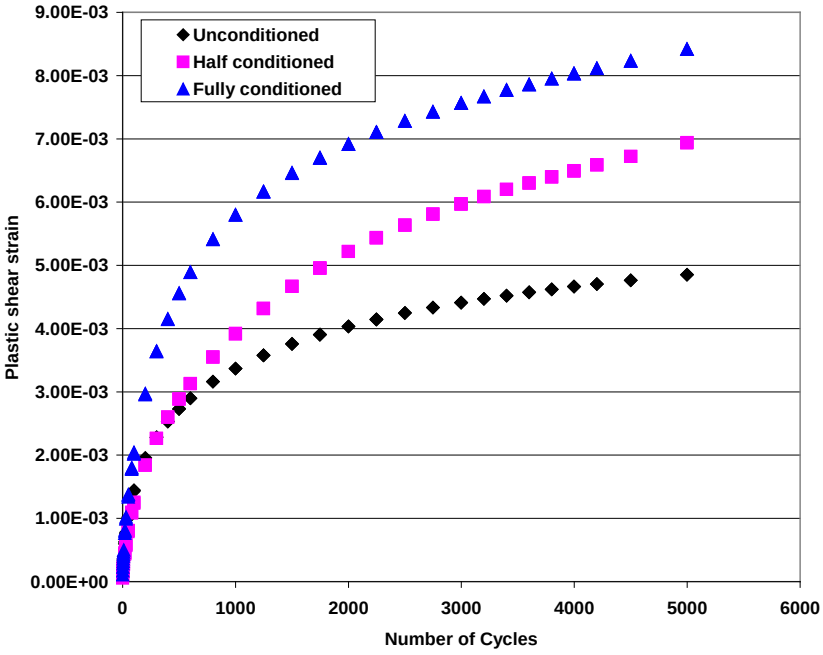

Figure 5.34 Relationship showing shear strain vs. number of cycles (Castle Hayne S – 12.5 C Mix)

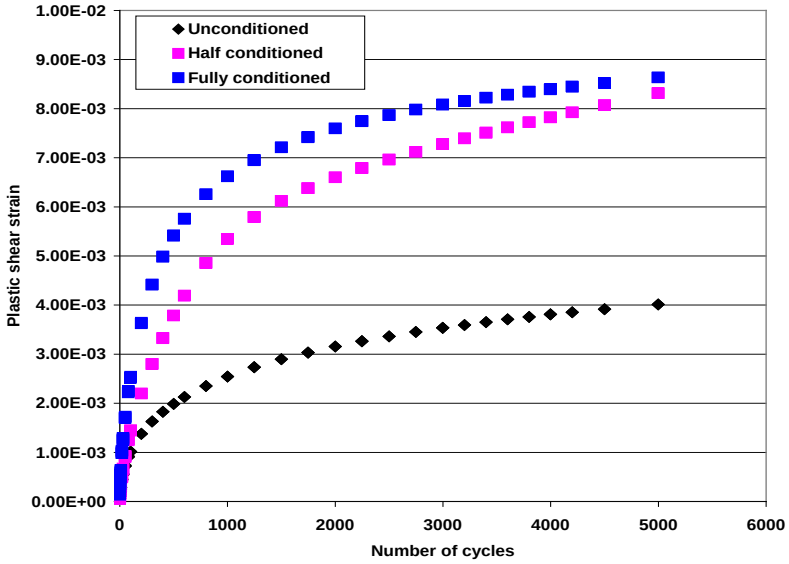

Figure 5.35 Relationship showing shear strain vs. number of cycles (Castle Hayne S – 9.5 C Mix).

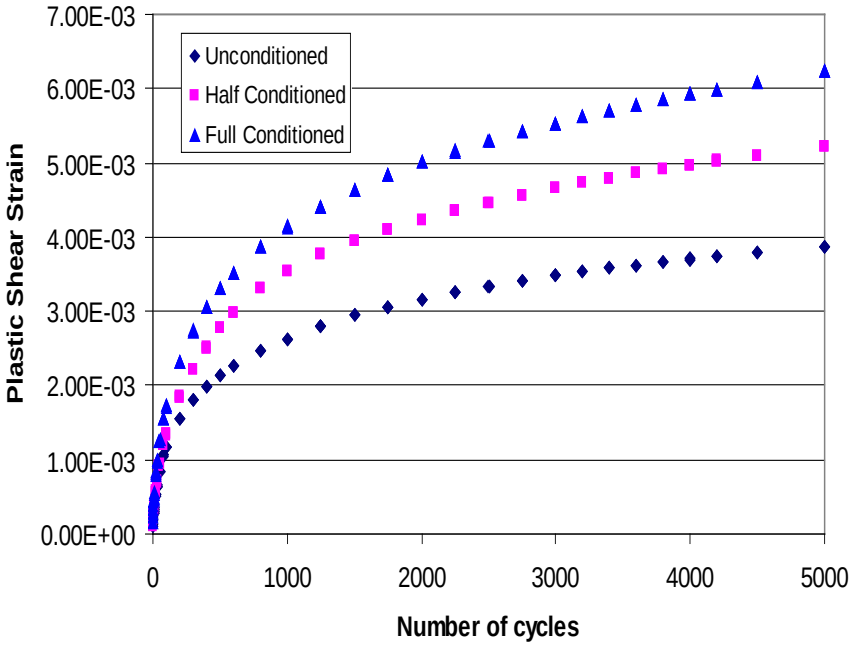

Figure 5.36 Relationship showing shear strain vs. number of cycles (Castle Hayne S – 12.5 D Mix)

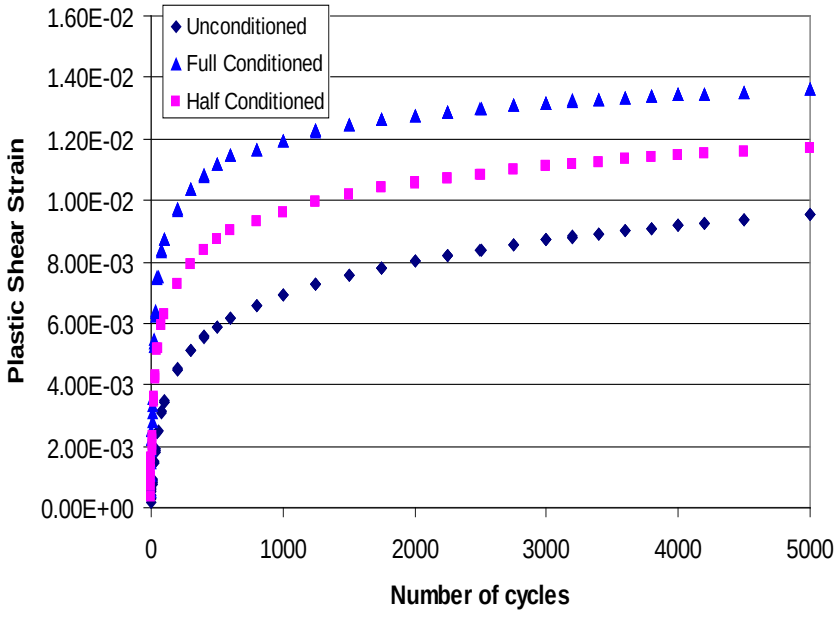

Figure 5.37 Relationship showing shear strain vs. number of cycles (Castle Hayne S – 12.5 B Mix).

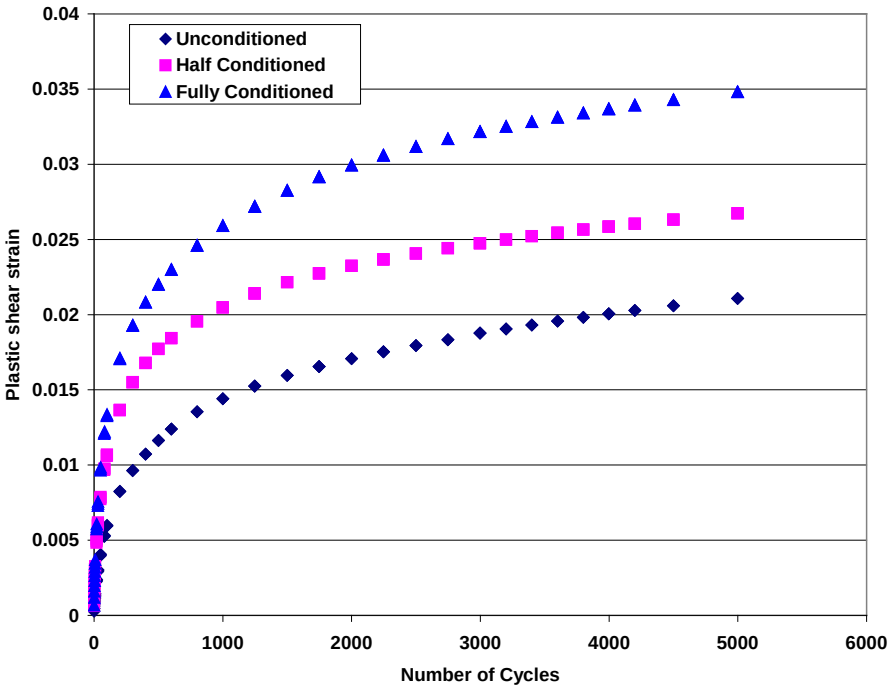

Figure 5.38 Relationship showing shear strain vs. number of cycles (Asheboro S – 12.5 C Mix).

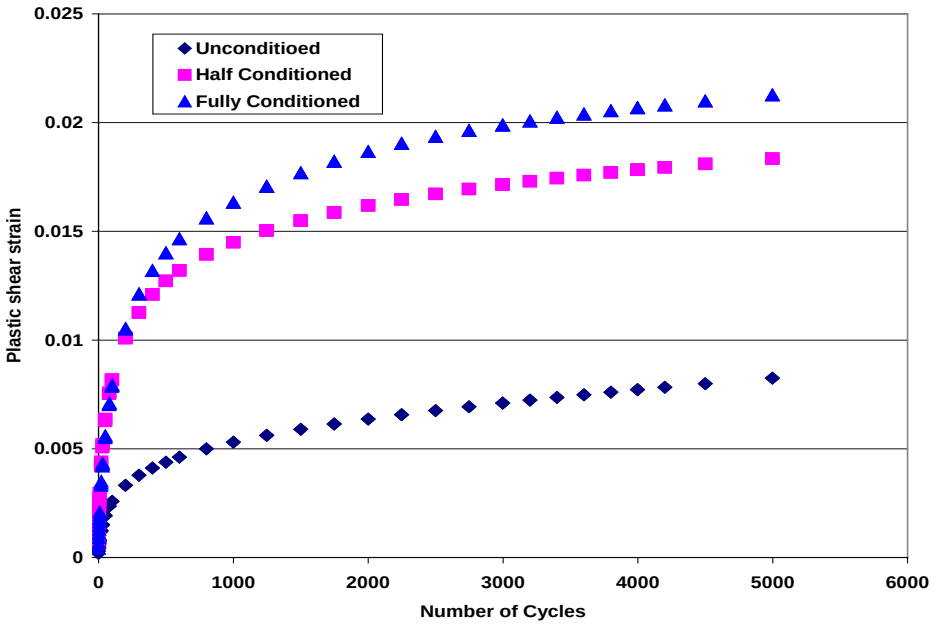

Figure 5.39 Relationship showing shear strain vs number of cycles (Asheboro S – 9.5 C Mix).

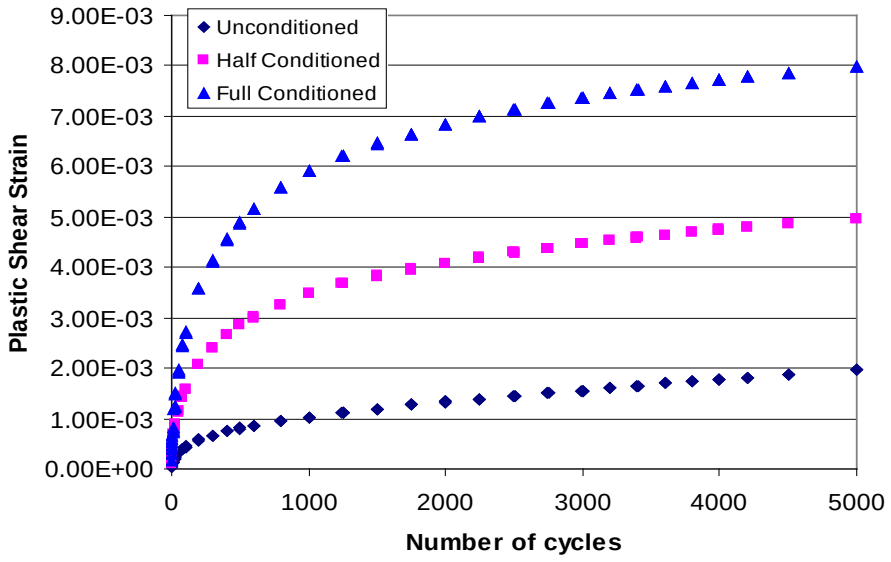

Figure 5.40 Relationship showing shear strain vs. number of cycles (Asheboro S – 12.5 D Mix)

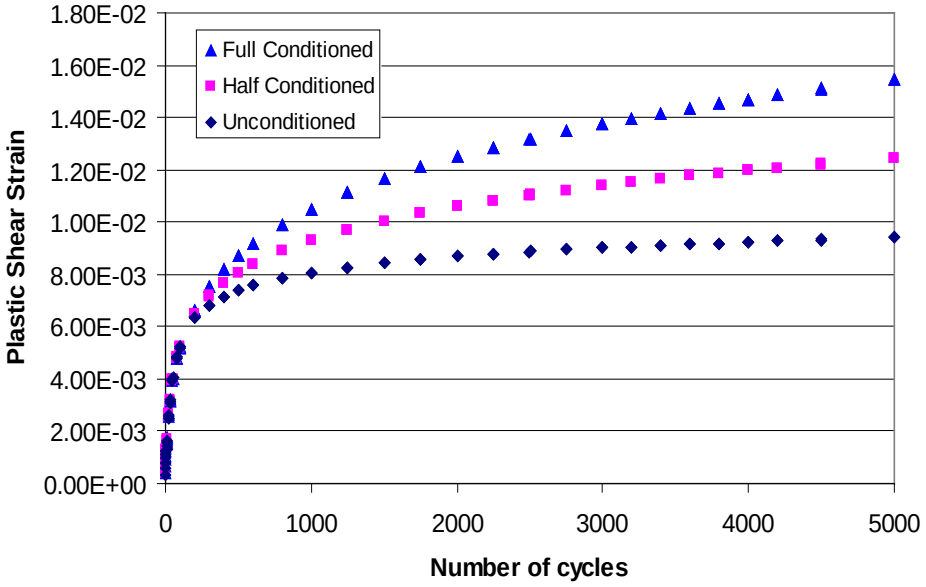

Figure 5.41 Relationship showing shear strain vs. number of cycles (Asheboro S – 12.5 B Mix).

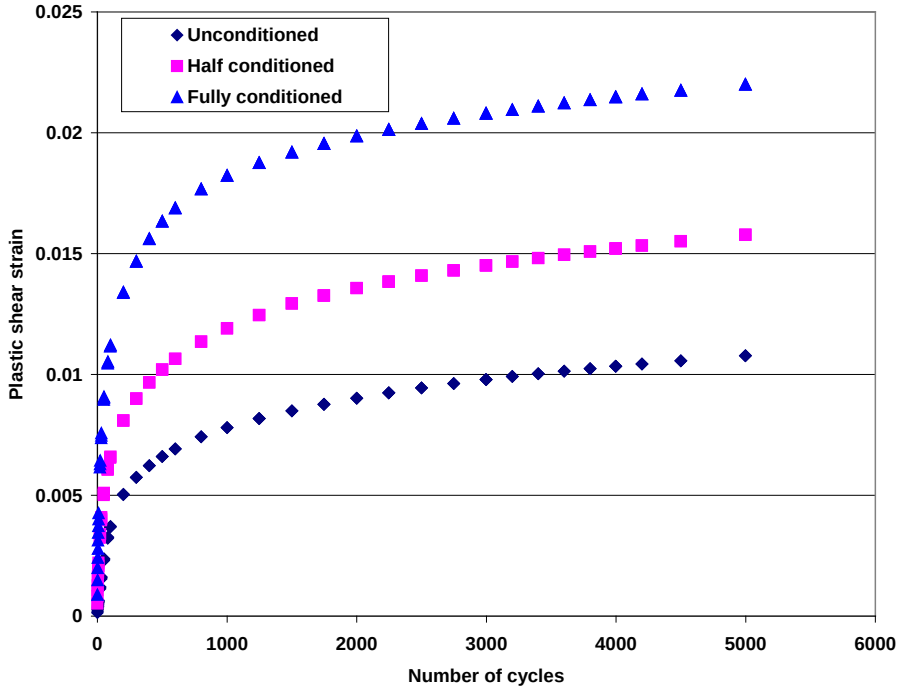

Figure 5.42 Relationship showing shear strain vs. number of cycles (Fountain S – 12.5 C Mix)

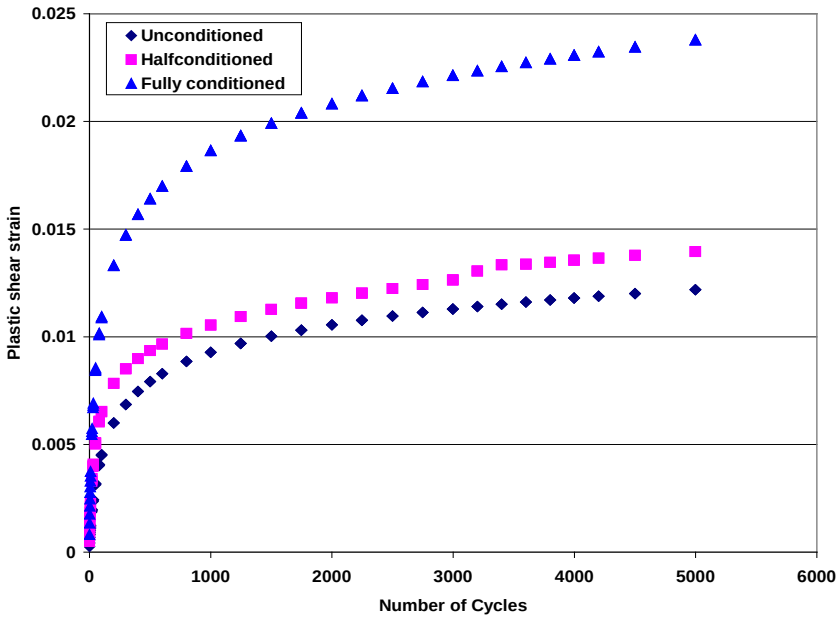

Figure 5.43 Relationship showing shear strain vs. number of cycles (Fountain S – 9.5 C Mix)

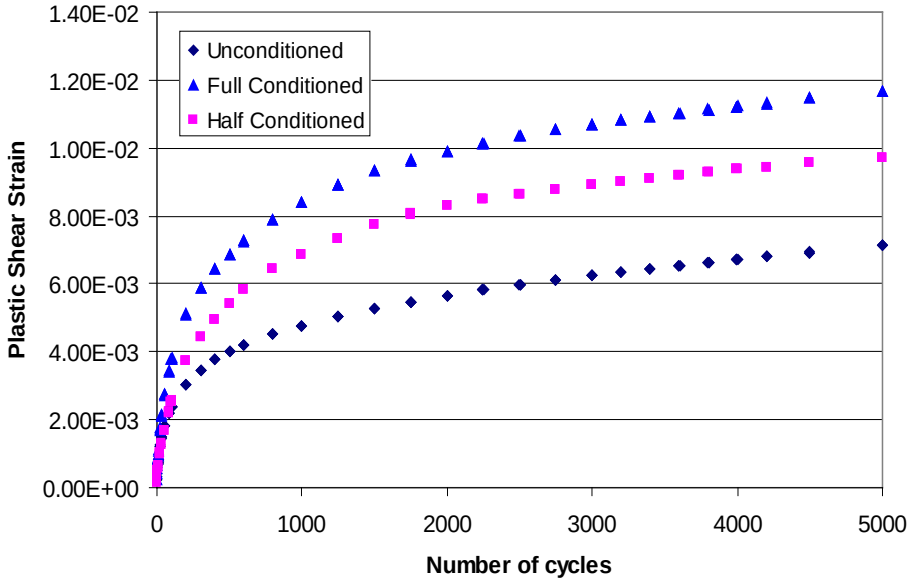

Figure 5.44 Relationship showing shear strain vs. number of cycles (Fountain S – 12.5 D Mix)

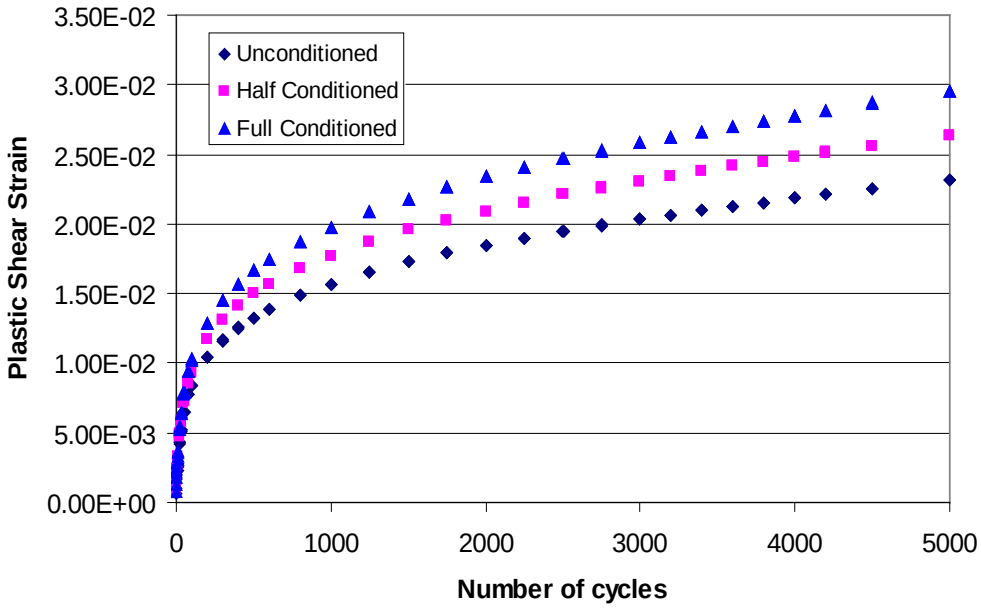

Figure 5.45 Relationship showing shear strain vs. number of cycles (Fountain S – 12.5 B Mix).

Table 5.25 Summary of RSCH Results Part 1 (Without Additives)

Source/Gradation		Shear strain
Castle Hayne 12.5mm PG 70-22	Unconditioned sample	0.0048
	Half conditioned	0.0069
	Fully conditioned	0.0084
Castle Hayne 9.5mm PG 70-22	Unconditioned sample	0.0040
	Half conditioned	0.0083
	Fully conditioned	0.0086
Fountain 12.5 mm PG 70-22	Unconditioned sample	0.0107
	Half conditioned	0.0157
	Fully conditioned	0.0220
Fountain 9.5mm PG 70-22	Unconditioned sample	0.0121
	Half conditioned	0.0139
	Fully conditioned	0.0237
Asheboro 12.5mm PG 70-22	Unconditioned sample	0.0210
	Half conditioned	0.0267
	Fully conditioned	0.0348
Asheboro 9.5mm PG 70-22	Unconditioned sample	0.0082
	Half conditioned	0.0183
	Fully conditioned	0.0212

Table 5.26 Summary of RSCH Results Part 2 (Without Additives)

Source/Gradation		Shear strain
Castle Hayne 12.5mm PG 76-22	Unconditioned sample	0.0039
	Half conditioned	0.0052
	Fully conditioned	0.0062
Castle Hayne 12.5mm PG 64-22	Unconditioned sample	0.0096
	Half conditioned	0.0117
	Fully conditioned	0.0136
Fountain 12.5 mm PG 76-22	Unconditioned sample	0.0071
	Half conditioned	0.0097
	Fully conditioned	0.0117
Fountain 12.5mm PG 64-22	Unconditioned sample	0.0231
	Half conditioned	0.0264
	Fully conditioned	0.0300
Asheboro 12.5mm PG 76-22	Unconditioned sample	0.0020
	Half conditioned	0.0050
	Fully conditioned	0.0080
Asheboro 12.5mm PG 64-22	Unconditioned sample	0.0094
	Half conditioned	0.0124
	Fully conditioned	0.0154

5.8.2. Analysis of RSCH Test Results (With Lime Additive)

RSCH test was also performed to estimate the rutting potential of mixtures containing hydrated lime. The results of the RSCH tests are shown in Figures 5.46 to 5.57. The shear strain at the end of 5000 cycles is provided for each mixture in Tables 5.27 and 5.28. In this case, it is observed that shear strains of conditioned specimens are higher compared to unconditioned specimens. However, the difference is not as much as in specimens without lime additive. It can be seen that in Figures 5.46 to 5.49, in the case of Castle Hayne aggregate, the magnitude of shear strain values are very low compared to Asheboro and Fountain aggregate. Also, the slope for Castle Hayne mixtures is generally less than those of Asheboro and Fountain mixtures, indicating that Castle Hayne mixtures perform better in rutting.

Considering Table 5.27 and 5.28, it can be seen that shear strains for conditioned samples reduced considerably when lime was added as an anti-stripping agent. In some instances, the addition of lime caused an increase in shear strain for unconditioned samples. But even in cases where the unconditioned shear strain was higher in mixtures with lime as compared to mixtures without lime, the shear strain after conditioning showed significant decreases when comparing mixtures without lime to mixtures containing lime. This phenomenon indicates that the true benefits of lime are seldom seen until moisture damage occurs. The dispersion of the tiny hydrated lime particles throughout the mix makes it stiffer and tougher, thus reducing the likelihood of breaking the bond between the asphalt cement and the aggregate in presence of moisture. Rutting is permanent deformation of the asphalt, caused when the elasticity of the material is exceeded.

Hydrated lime significantly improves the performance of asphalt in this respect. Unlike most mineral fillers, lime is chemically active rather than inert. It reacts with the bitumen, removing undesirable components at the same time that its tiny particles disperse throughout the mix, making it more resistant to rutting. The filler effect of the lime in the asphalt reduces the potential of the asphalt to deform at high

temperatures, especially during its early life when it is most susceptible to rutting. The hydrated lime filler actually stiffens the asphalt film and reinforces it. Furthermore, the lime makes the HMA less sensitive to moisture effects by improving the aggregate-asphalt bond. This synergistically improves rut resistance. In addition to these benefits, adding hydrated lime to marginal aggregates that have plastic fines can improve the aggregate through the mechanisms of cation exchange, flocculation/agglomeration, and pozzolanic reactions. These reactions result in a change in the characteristics of the fines so that they are no longer plastic but act as agglomerates held together by a “pozzolanic cement” [27]. This process makes the aggregate fines much less susceptible to moisture by reducing their ability to attract and hold water.

From 5.55, it can be seen that in the Asheboro 9.5mm mixture, there was a high percent increase of shear strain from unconditioned state to fully conditioned state. Therefore, there is a need to study whether higher dosages of lime can further reduce plastic shear strain or to determine the optimum dose for various gradations and aggregate types.

Aggregate gradation affects HMA mix rutting potential. However, while considering 12.5mm and 9.5mm gradation, there is no definite trend in the behavior of plastic shear

strain values for mixtures containing hydrated lime and mixtures without any additive. This is because not only gradation and type of aggregate affect plastic shear strain, but HMA volumetric properties also influence rutting performance. Voids in mineral aggregate (VMA) and voids filled with asphalt (VFA) are two properties related to rutting. A single gradation was used for mixtures containing PG 76-22 and PG 64-22 asphalt binders and therefore these results are more directly comparable, due to mitigation of differences in some of the other factors contributing to rutting.

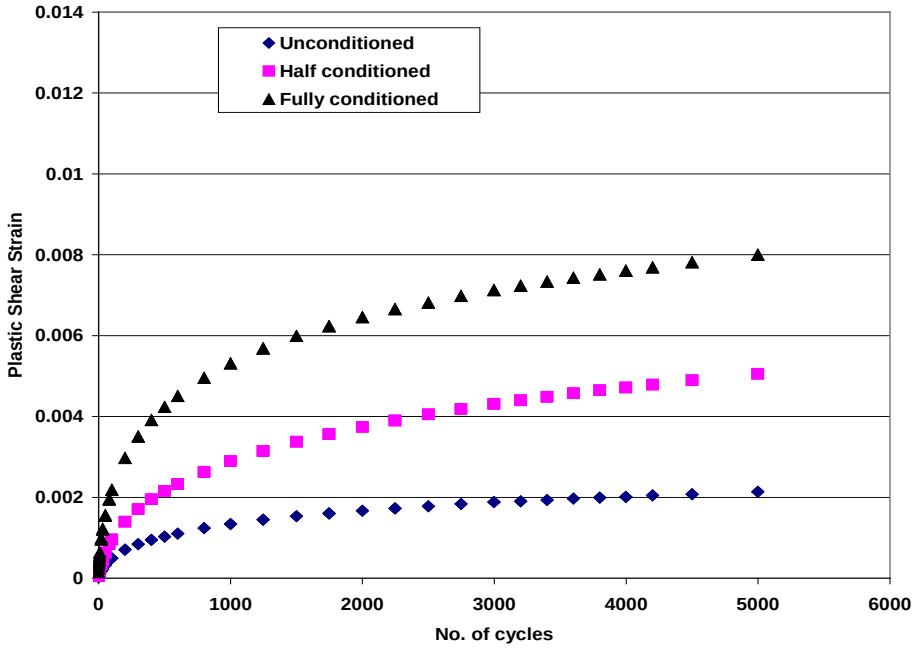

Figure 5.46 Relationship Showing Shear Strain vs Number of Cycles (Castle Hayne S – 12.5 C Mix with Lime)

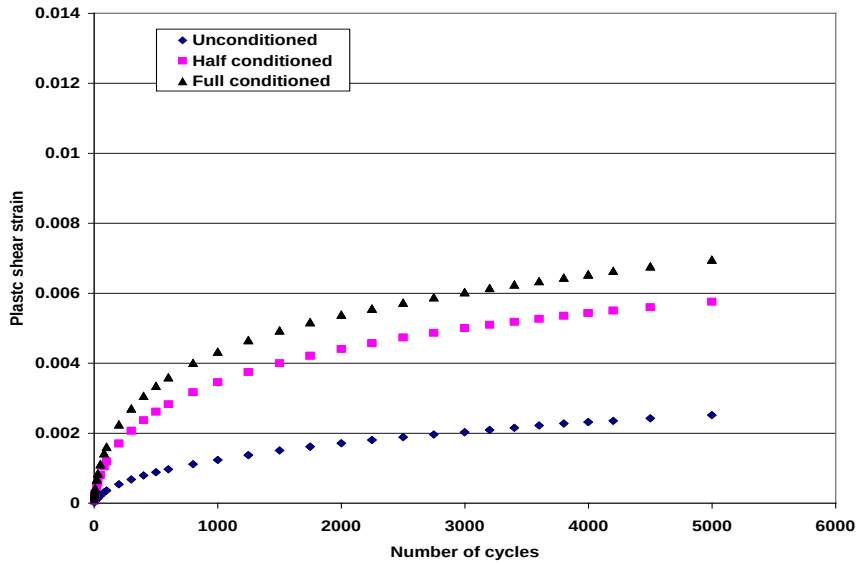

Figure 5.47 Relationship Showing Shear Strain vs Number of Cycles (Castle Hayne S – 9.5 C Mix with Lime)

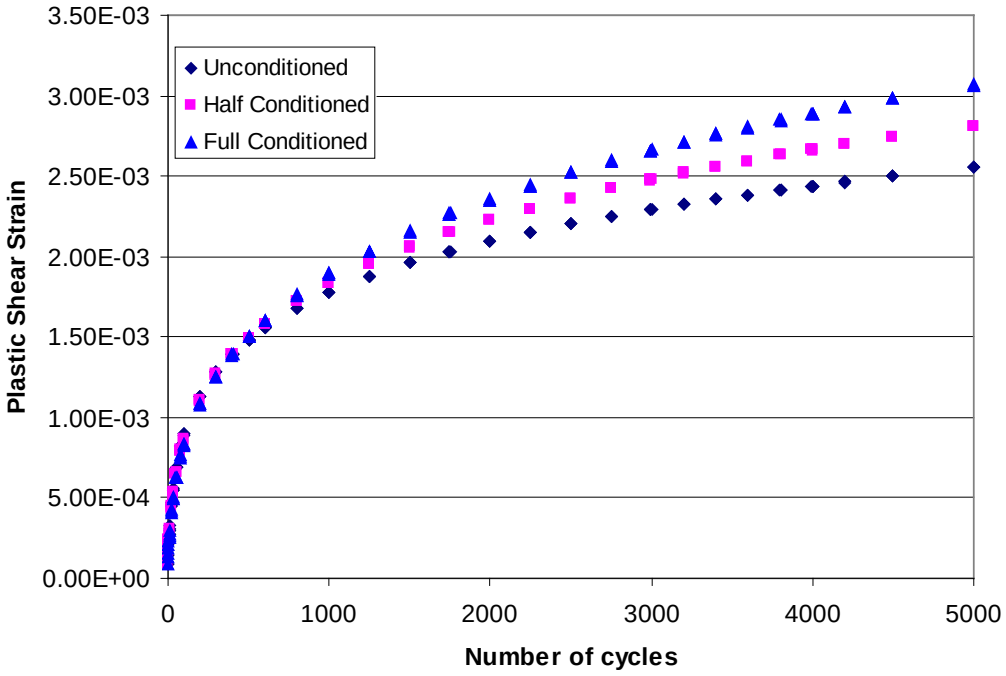

Figure 5.48 Relationship Showing Shear Strain vs Number of Cycles (Castle Hayne S – 12.5 D Mix with Lime)

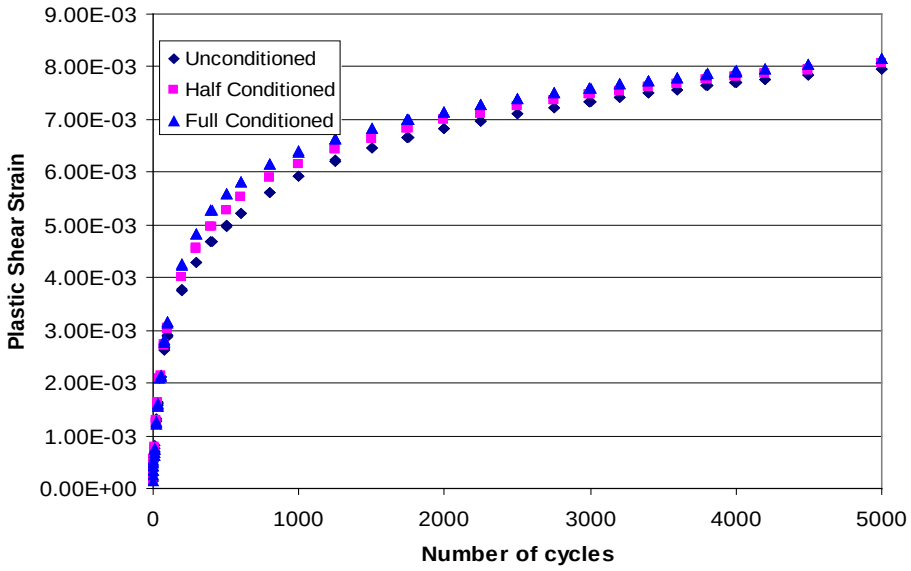

Figure 5.49 Relationship Showing Shear Strain vs Number of Cycles (Castle Hayne S – 12.5 B Mix with Lime)

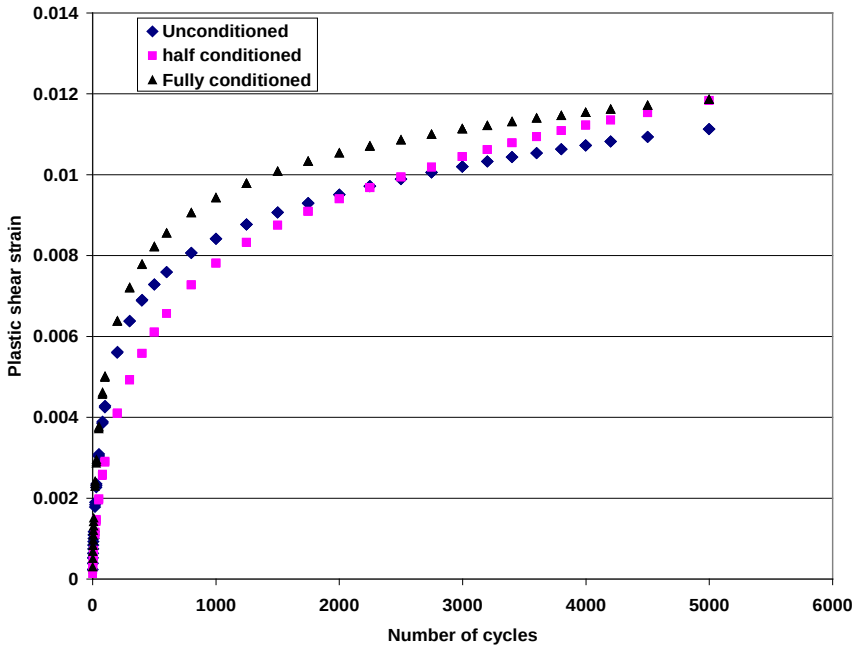

Figure 5.50 Relationship Showing Shear Strain vs Number of Cycles (Fountain S – 12.5 C Mix with Lime)

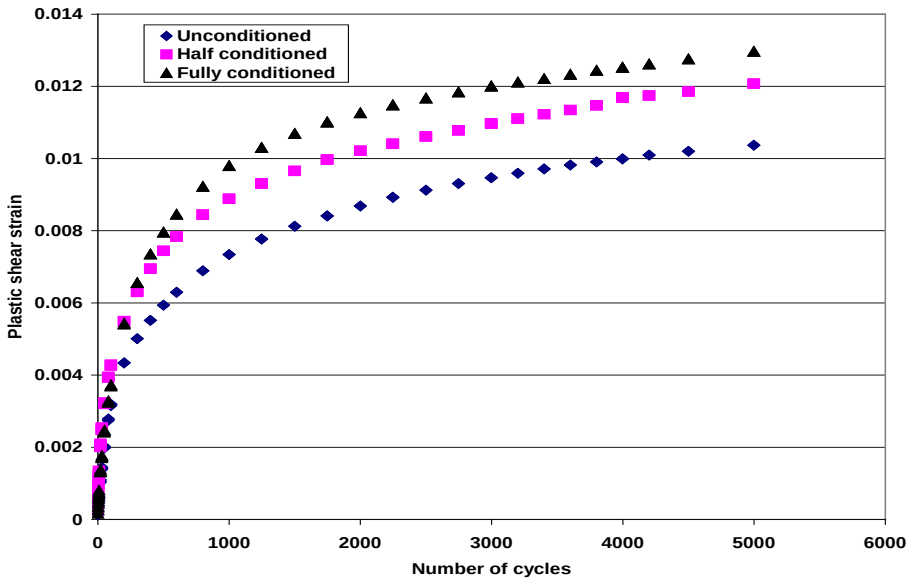

Figure 5.51 Relationship Showing Shear Strain vs Number of Cycles (Fountain S – 9.5 C Mix with Lime)

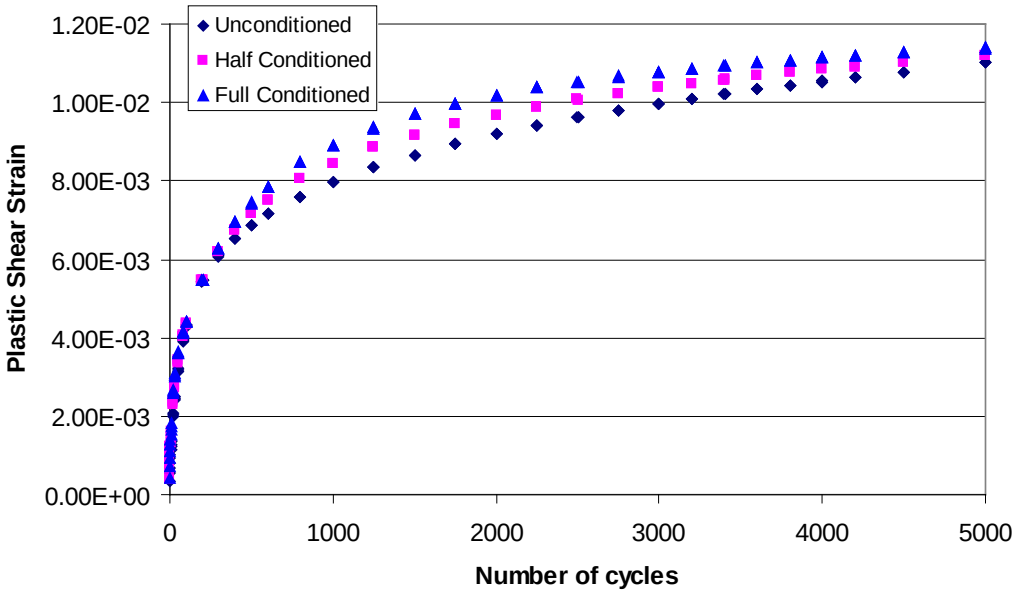

Figure 5.52 Relationship Showing Shear Strain vs Number of Cycles (Fountain S – 12.5 D Mix with Lime)

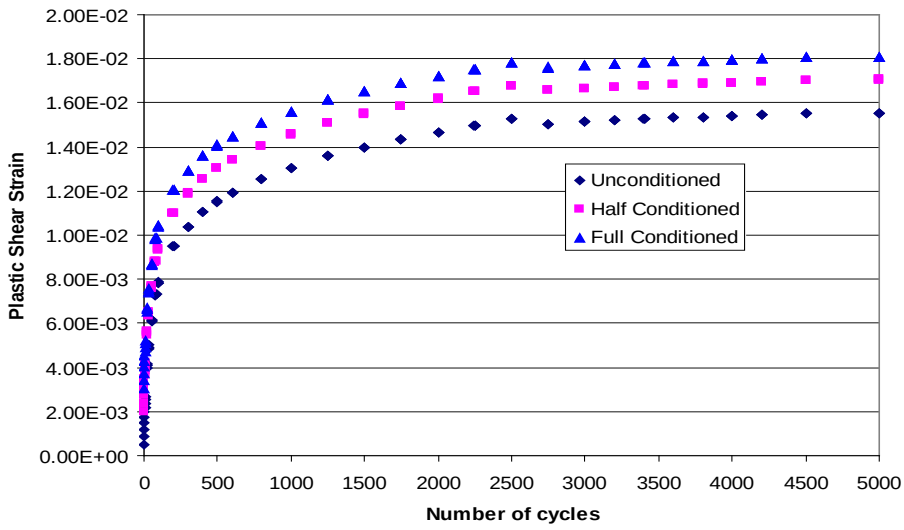

Figure 5.53 Relationship Showing Shear Strain vs Number of Cycles (Fountain S – 12.5 B Mix with Lime)

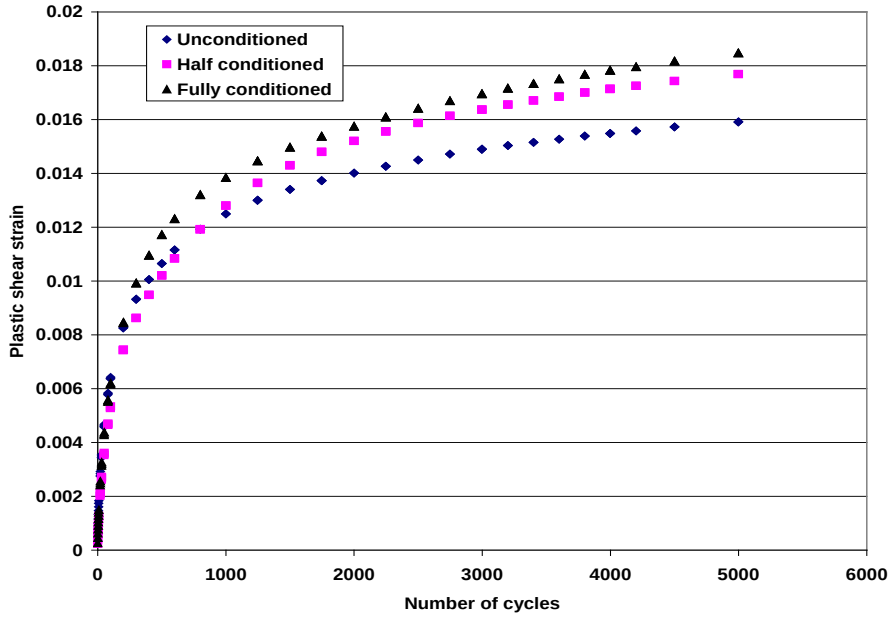

Figure 5.54 Relationship Showing Shear Strain vs Number of Cycles (Asheboro S – 12.5 C Mix with Lime)

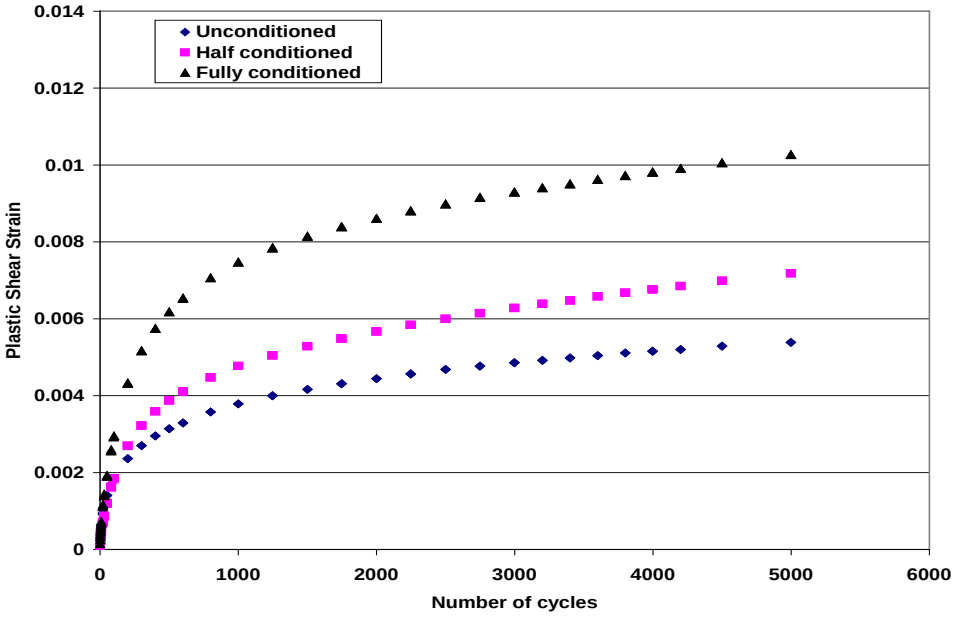

Figure 5.55 Relationship Showing Shear Strain vs Number of Cycles (Asheboro S – 9.5 C Mix with Lime)

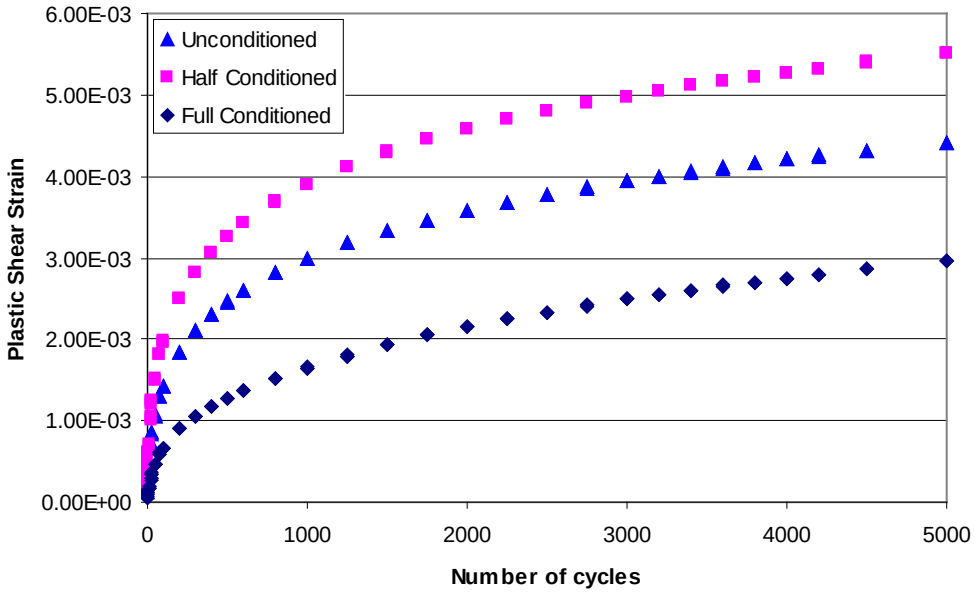

Figure 5.56 Relationship Showing Shear Strain vs Number of Cycles (Asheboro S – 12.5 D Mix with Lime)

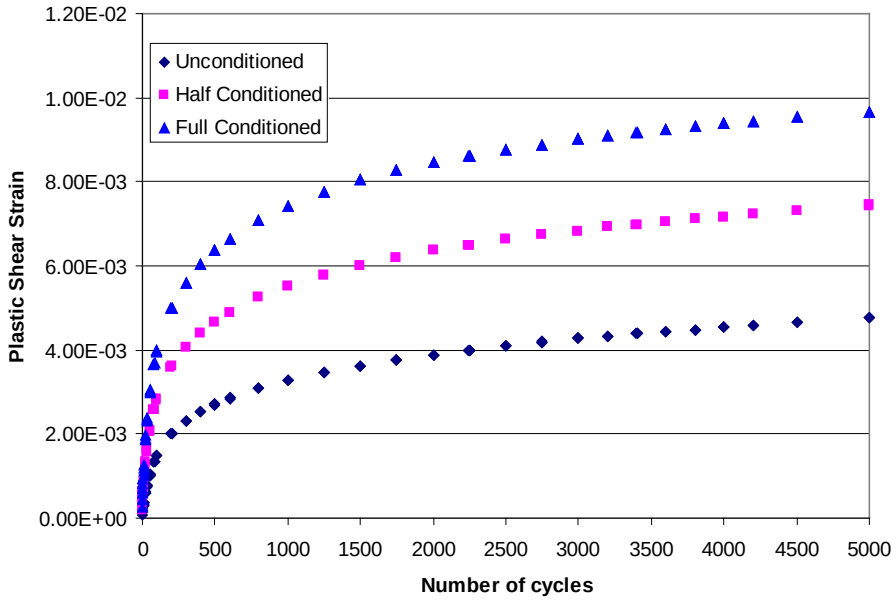

Figure 5.57 Relationship Showing Shear Strain vs Number of Cycles (Ahseboro S – 12.5 D Mix with Lime)

Table 5.27 Summary of RSCH Results Part 1 (With Lime Additive)

Source/Gradation		Shear strain
Castle Hayne 12.5 mm PG 70-22	Unconditioned sample	0.00214
	Half conditioned	0.00505
	Fully conditioned	0.00800
Castle Hayne 9.5mm PG 70-22	Unconditioned sample	0.00252
	Half conditioned	0.00575
	Fully conditioned	0.00695
Fountain 12.5mm PG 70-22	Unconditioned sample	0.01113
	Half conditioned	0.01184
	Fully conditioned	0.01186
Fountain 9.5mm PG 70-22	Unconditioned sample	0.01037
	Half conditioned	0.01207
	Fully conditioned	0.01296
Asheboro 12.5mm PG 70-22	Unconditioned sample	0.01592
	Half conditioned	0.01769
	Fully conditioned	0.01846
Asheboro 9.5mm PG 70-22	Unconditioned sample	0.00539
	Half conditioned	0.00718
	Fully conditioned	0.01026

Table 5.28 Summary of RSCH Results Part 2 (With Lime Additive)

Source/Gradation		Shear strain
Castle Hayne 12.5 mm PG 76-22	Unconditioned sample	0.0026
	Half conditioned	0.0028
	Fully conditioned	0.0031
Castle Hayne 12.5mm PG 64-22	Unconditioned sample	0.0080
	Half conditioned	0.0081
	Fully conditioned	0.0082
Fountain 12.5mm PG 76-22	Unconditioned sample	0.0110
	Half conditioned	0.0112
	Fully conditioned	0.0114
Fountain 12.5mm PG 64-22	Unconditioned sample	0.0155
	Half conditioned	0.0170
	Fully conditioned	0.0181
Asheboro 12.5mm PG 76-22	Unconditioned sample	0.0030
	Half conditioned	0.0044
	Fully conditioned	0.0055
Asheboro 12.5mm PG 64-22	Unconditioned sample	0.0048
	Half conditioned	0.0074
	Fully conditioned	0.0097

5.9. Summary

From the shear test results, it can be concluded that lime is very effective in improving the properties of asphalt concrete mixtures. In addition, it can be seen from the test results that simple shear test is very effective in differentiating the performance of mixtures against moisture damage.

CHAPTER 6

6. PERFORMANCE EVALUATION OF ASPHALT CONCRETE MIXTURES USING DYNAMIC MODULUS TESTING

6.1. Introduction

Dynamic modulus |E*| has been widely used as a stiffness parameter for asphalt mixtures employed in mechanistic-empirical structural pavement design procedures. The dynamic modulus has also been selected to characterize the asphalt mixtures in the new AASHTO "2002 Guide for the Design of Pavement Structures". For linear viscoelastic materials such as HMA mixes, the stress-to-strain relationship under a continuous sinusoidal loading is defined by its complex dynamic modulus (E*). This complex number relates stress to strain for linear viscoelastic materials subjected to continuously applied sinusoidal loading in the frequency domain. The complex modulus is defined as the ratio of the amplitude of the sinusoidal stress (at any given time, t, and angular load frequency, ω), $\sigma = \sigma_0 \sin(\omega t)$ and the amplitude of the sinusoidal strain $\varepsilon = \varepsilon_0 \sin(\omega t - \varphi)$, at the same time and frequency, that results in a steady state response. Mathematically, the "dynamic modulus" is defined as the absolute value of the complex modulus, i.e. $|E^*| = \sigma_0/\varepsilon_0$. Stiffness data of an HMA mix as obtained from the |E*| test provide very important information about the linear viscoelastic behavior of that particular mix over a wide range of temperature and loading frequency. Dynamic Modulus tests were conducted on both conditioned and unconditioned specimens, without any additive and with hydrated lime as additive to investigate the effect of moisture damage on mixtures.

6.2. Complex Modulus

Complex mathematics gives a convenient tool to analyze the visco-elastic behavior of the asphalt mixtures and binders in cyclic loading. The sinusoidal one-dimensional loading can be represented by a complex form:

$$\sigma^* = \sigma_0 e^{i\omega t} \tag{6-1}$$

and the resulting strain

$$\varepsilon^* = \varepsilon_0 e^{i(\omega t - \varphi)} \tag{6-2}$$

The axial complex modulus $E^*(i\omega)$ is defined as the complex quantity

$$\frac{\sigma^*}{\varepsilon^*} = E^*(i\omega) = \left(\frac{\sigma_0}{\varepsilon_0}\right) e^{i\varphi} = E_1 + iE_2 \tag{6-3}$$

in which σ_0 is the stress amplitude, ε_0 is strain amplitude and ω is angular velocity, which is related to the frequency by:

$$\omega = 2\pi f \tag{6-4}$$

In the complex plane, the real part of the complex modulus $E^*(i\omega)$ is called the storage or elastic modulus E_1 while the imaginary part is the loss or viscous modulus E_2, shown in Figure 6.1. For elastic materials $\varphi = 0$, and for viscous materials $\varphi = 90°$. The alternative nomenclature is to call storage modulus as E' and loss modulus as E".

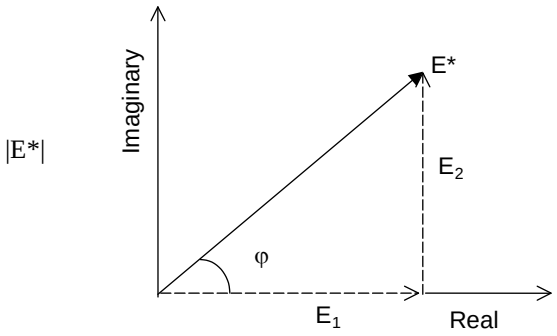

Figure 6.1 Complex plane

If a linearly visco-elastic material is subjected to a uniaxial compressive, tensile or shear loading $\sigma = \sigma_0 \sin \omega t$, the resulting steady state strain $\varepsilon = \varepsilon_0 \sin(\omega t - \varphi)$ will be out of phase with the stress by the lag angle φ, as shown in Figure 6.2.

The ratios of stress and stain amplitudes σ_0/ε_0 define the dynamic (or cyclic) modulus $|E^*(\omega)|$, shown in Equation 6.5:

$$\left|E^*(\omega)\right| = \sqrt{E_1^{\ 2} + E_2^{\ 2}} = \frac{\sigma_0}{\varepsilon_0} \tag{6-5}$$

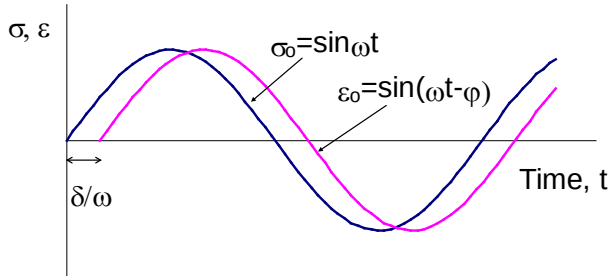

Figure 6.2 Sinusoidal stress and strain in cyclic loading.

Where E_1 and E_2 can be expressed as function of phase lag or lag angle:

$$E_1 = \frac{\sigma_0 \cos\varphi}{\varepsilon_0} \quad \text{and} \quad E_2 = \frac{\sigma_0 \sin\varphi}{\varepsilon_0} \tag{6-6}$$

The loss tangent defines the ratio of lost and stored energy in a cyclic deformation:

$$\tan\varphi = \frac{E_2}{E_1} \tag{6-7}$$

6.3. Compressive Dynamic Modulus Test

For viscoelastic materials, such as asphalt concrete, the complex modulus (E*) is often used to represent the stiffness of the material. The complex modulus has an elastic or storage component and a loss component. The storage (elastic) component is related to the material's ability to store energy whereas the loss component is responsible for the damping and energy loss in the system. Just like the overall modulus, the storage modulus (E') and the loss modulus (E") change with temperature and rate of loading. For purely elastic materials, there is no damping loss and thus the elastic component is equal to the overall modulus. The loading pattern for Complex modulus is shown in Figure 6.3

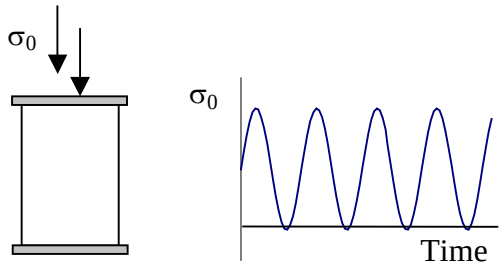

Figure 6.3 Loading pattern for compressive dynamic modulus testing.

Complex modulus is related to loss and storage moduli via Eq. 6.8.

$$E^* = E' + iE'' \tag{6.8}$$

Where E' = storage modulus;

E” = loss modulus; and

$i = (-1)^n$

The magnitude of E*, so-called dynamic modulus, is represented by |E*| and can be obtained from: $E^* = (E'^2 + E''^2)^{1/2}$ (6.9)

The phase angle, φ, is defined as:

$$\tan \varphi = E''/ E' \quad (6.10)$$

Dynamic modulus and phase angle are determined from uniaxial compression test using a sinusoidal loading history. In uniaxial compression, axial stress (σ) is determined from:

$$\sigma = P/A \quad (6.11)$$

Where P = load; and

A = cross-sectional area.

$\varepsilon = \Delta/GL$

Where Δ = change in displacement; and GL = gauge length.

The dynamic modulus is determined from:

$|E^*| = \sigma_0/ \varepsilon_0$

(6.12)

Where σ_0 = the stress amplitude; and

ε_0 = the strain amplitude.

The phase angle is determined from:

$\varphi = 2\pi f \Delta t$ (6.13)

Where f = loading frequency in Hz; and

Δt = time delay between the stress and strain cycles.

6.4. Specimen Fabrication and Instrumentation

Dynamic Modulus tests were conducted on the conditioned and the unconditioned specimens of three different mixtures (Castle Hayne, Fountain and Asheboro) for both 9.5 mm and 12.5mm gradations using only PG 70-22 asphalt binder. The mixtures were compacted into gyratory plugs of 150 mm in diameter by 178 mm in height. Later, specimens were cut and cored to cylindrical specimens with dimensions of 100 mm in diameter and 150 mm in height. Both ends were cut to ensure a more consistent air void distribution along the height of the test specimens. Tests were also conducted with the above mixtures using hydrated lime as an additive. The mass of hot mix added used to make the gyratory plugs was adjusted so that the air void content in the final test specimens would fall within 7% ± 0.5%. Two replicates of each specimen were tested.

Testing was performed using a closed-loop servo-hydraulic machine, manufactured by Material Testing Service (MTS) as shown in Fig 6.4. This machine is capable of applying loads, up to 20 kips, over a wide range of frequencies (25 to 0.01 Hz). A temperature chamber, cooled by liquid nitrogen, was used to control the test temperatures. The system was capable of applying temperatures between -10°C and 55°C, which were the lowest and highest temperatures respectively. Dummy specimens with thermocouples embedded in the middle of the specimen were used to monitor the temperature to which the specimens were subjected. The measurement control system was completely computer controlled. This system was capable of acquiring signals from up to 16 channels

simultaneously. Of these 16 channels, only 6 were used in the testing described herein. One channel was dedicated to the load cell on the machine, one to the actuator LVDT (linear variable differential transducer), and four vertical LVDT's to the specimen.

Figure 6.4 Material Testing System

Data acquisition was controlled through a 16-bit board manufactured by National Instruments. In addition, LabView software produced by National Instruments was used to interface with the board. Several programs were developed, using this software, to control data acquisition. In this research, sinusoidal loading was exclusively used and data was collected at 100 points per cycle. For all testing for the present study, a 5 kip load cell was utilized, as the maximum applied load was about 4 kip. Vertical deformations were measured using LVDTs. Four spring type LVDTs measured deformations at 90° radial intervals. Targets were glued to the specimen face and the

LVDTs were mounted to the targets. The LVDTs were mounted to measure the deformation in the middle two-thirds of the specimen (100 mm). For consistency in measurements, a gluing device was used to maintain consistent spacing between the LVDT targets. Figure 6.5 shows general schematic of dynamic modulus test.

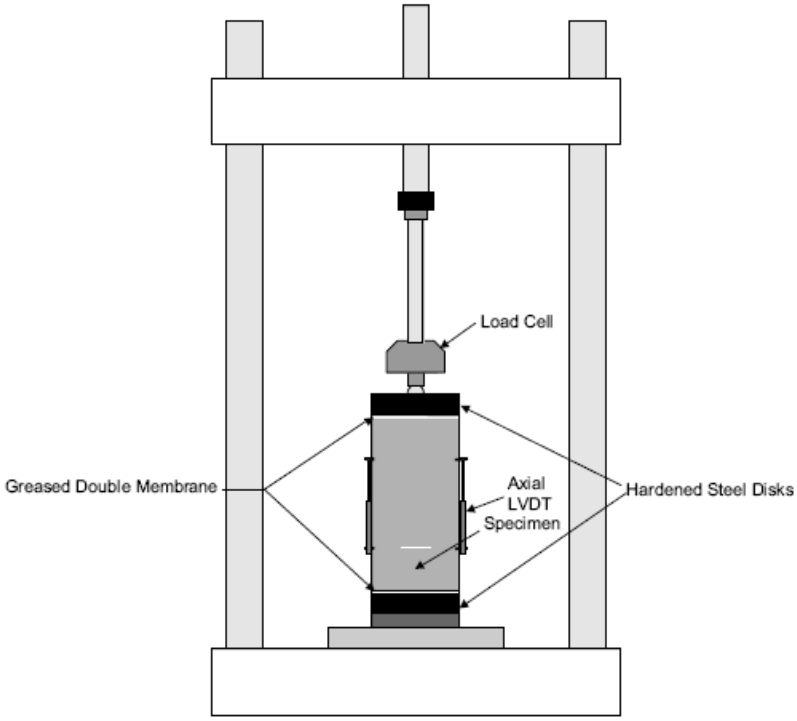

Figure 6.5 General schematic of Dynamic Modulus Test [35]

6.5. Test Description

The complex modulus test is performed in a stress-controlled manner and is designed to measure the viscoelastic response of asphalt concrete. In order to measure this response, the stress applied to the specimen must not exceed linear viscoelastic limit or the specimen must not reach a damaged state. For the present study, 75 microstrain was used as the limit of viscoelastic behavior. Since the material is temperature and frequency

dependent, load level was adjusted at each combination of frequency and temperature to ensure that the strain did not exceed 75με. Testing was performed by applying sinusoidal loadings at different frequencies and temperatures. Each specimen was subjected to testing frequencies of 25, 10, 5, 1, 0.5, 0.1, 0.05, and 0.01 Hz. In addition, prior to applying the first frequency at each temperature, a preconditioning cycle was applied. The preconditioning cycles were applied at 25 Hz and one-half the normal load applied at 25 Hz. In addition, the mixtures were subjected to a temperature sweep. At each temperature, loads were applied at the above mentioned frequencies. Temperature sweep was done at -10°, 10°, 35° and 54°C. Following each loading frequency a five-minute rest period was allowed before the next frequency was applied. Details on the testing sequence can be found in Table 6.1.

Table 6.1 Specimen Loading Information

Frequency (Hz)	Number of Loading
25-Preconditioning	200
25	200
10	200
5	100
1	20
0.5	15
0.1	15
0.05	10
0.01	8

6.6. Master Curve Construction

The underlying principle behind the development of the dynamic modulus master curve and the testing procedure is time-temperature superposition. According to this principle, the dynamic modulus is solely dependent on the reduced frequency, which is a function of temperature and frequency. Therefore, the effect on the dynamic modulus of altering

the temperature can be reproduced by testing at different frequencies. In the dynamic modulus test, a single specimen is used for all testing temperatures and all frequencies. Although the dynamic modulus test is supposed to be nondestructive, the stress-controlled mode used in the compression dynamic modulus test causes an increase in the mean strain as the test proceeds. Therefore, the testing method needs to be designed so that the testing at the temperature and frequency used in the early sequence in the temperature-frequency sweep has the least effect on the subsequent testing temperatures and frequencies. This consideration is reflected in AASHTO's protocol for dynamic modulus testing [35], TP62-03, by beginning the test at the lowest temperature and proceeding to the highest temperature. In addition, at a given temperature, testing begins at the highest frequency and goes to the lowest frequency. This sequence is intuitive because asphalt concrete becomes stiffer at low temperatures and high frequencies.

To construct a master curve, the dynamic moduli versus frequency curves at various temperatures (Figure 6.6) are horizontally shifted along the frequency axis in a semi-log scale to form a single curve (Figure 6.7) at a predetermined reference temperature. Figure 6.8 shows master curve formation in log-log scale. The reference temperature selected in this research was 10°C. The first step involved in the determination of shift factors was to determine what frequency temperature combinations yielded the same moduli values. Since the horizontal shift was performed in a logarithmic scale, the shift factor was determined by calculating the ratio of the frequency at the reference temperature to the frequency at the temperature in question. After the horizontal shift, the frequency at the reference temperature is called reduced frequency. In order to accomplish this shift, a

difference of squares technique was used in order to minimize the error between the sigmoidal fitting function and the shifted data. The sigmoidal function is the fit recommended in AASHTO TP-62 and the form that provided the best fit across the entire reduced frequency spectrum. This functional form is presented in Eq. 6.14. The coefficients (a, b, d, and e) presented in Eq. 6.14 and the shift factors for each temperature other than the reference temperature were simultaneously determined.

$$\log|E^*| = a + \frac{b}{1 + \frac{1}{\exp^{d+e(\log f_R)}}} \qquad (6.14)$$

The mastercurve was constructed using the averaged dynamic modulus values from the two replicates tested for each mixture. “AMyMOD” Software was used to analyse the dynamic modulus test data. “AMyMOD” software was developed by Proff. Richard Kim’s research group at North Carolina State University. The software would read in the raw data and detect the last five cycles of data for each temperature and frequency combination as per AASHTO TP-62. The last five cycles of data were analyzed and fitted according to the following functional form:

$$f(t) = a + bt + c\cos(\omega t + \varphi) \qquad (6.15)$$

Where *f(t)* is load or deformation time history; *a*, *b*, and *c* are regression coefficients;

φ is the phase angle; and ω is the angular frequency. Coefficient *c* represents the amplitude of the sinusoidal waveform, and the dynamic modulus is then calculated from the ratio of these coefficients from load and deformation histories

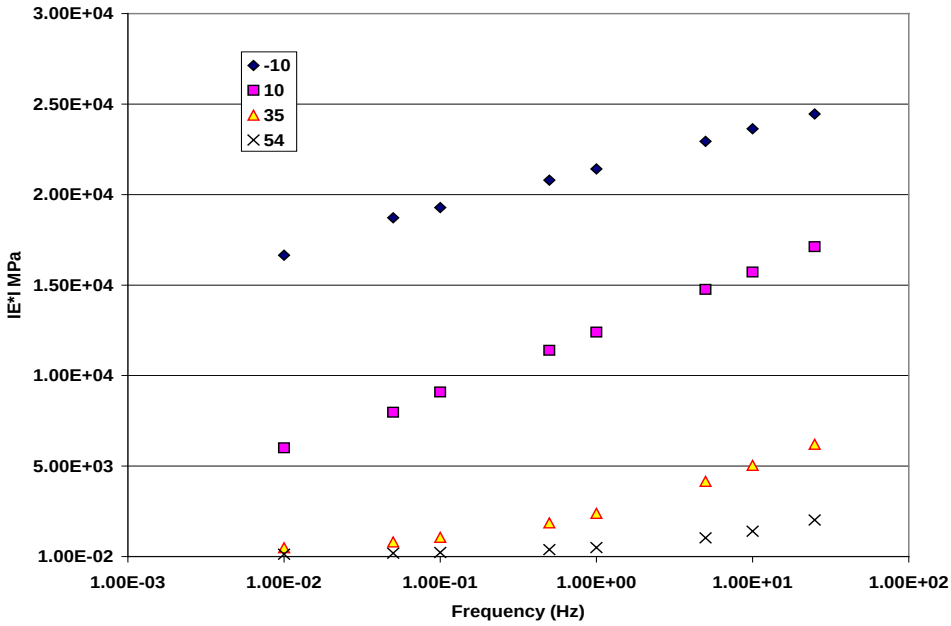

Figure 6.6 Mastercurve development before shifting

(Castle Hayne S – 12.5 C Mix - Unconditioned (without Additive))

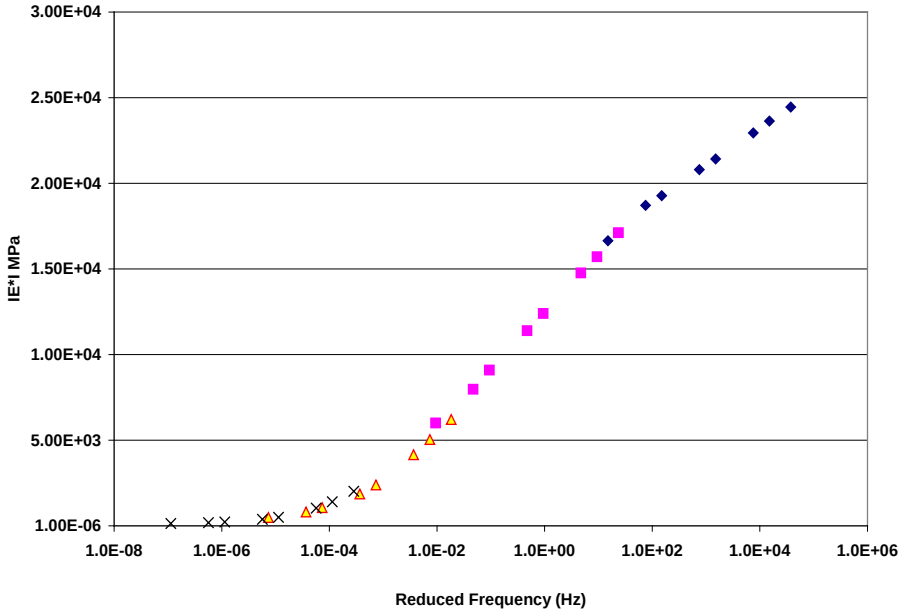

Figure 6.7 Mastercurve development after shifting in semi-log space (Castle Hayne S – 12.5 C Mix - Unconditioned (without Additive))

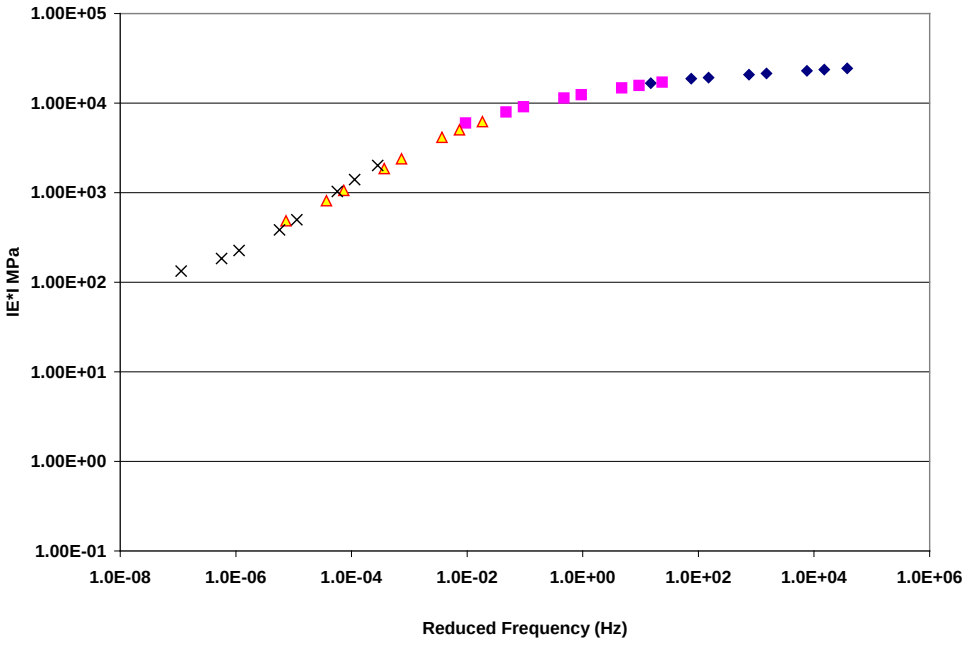

Figure 6.8 Mastercurve development after shifting in log-log space (Castle Hayne S – 12.5 C Mix - Unconditioned (without Additive))

6.7. Test Results and Discussion

The mastercurves for Castle Hayne S – 12.5 C Mix without additive (for unconditioned, half conditioned and fully conditioned specimens) are shown in Figures 6.9 and 6.10. Figure 6.9 shows mastercurve in semi-log scale and 6.10 shows mastercurve in log-log scale. Figure 6.9 shows that at higher reduced frequency (lower temperature), there is no significant difference in dynamic modulus values. In addition, as frequency reduces, the fully conditioned specimens have lower dynamic modulus compared to unconditioned specimens. However, there is no difference in moduli value between unconditioned and half conditioned stages. Figure 6.9 little difference in the modulus values at lower reduced frequencies. From Figure 6.10 (log-log scale), it is evident that as frequency decreases (in other words as temperature increases), there is a smaller difference between unconditioned specimens and fully conditioned specimens.

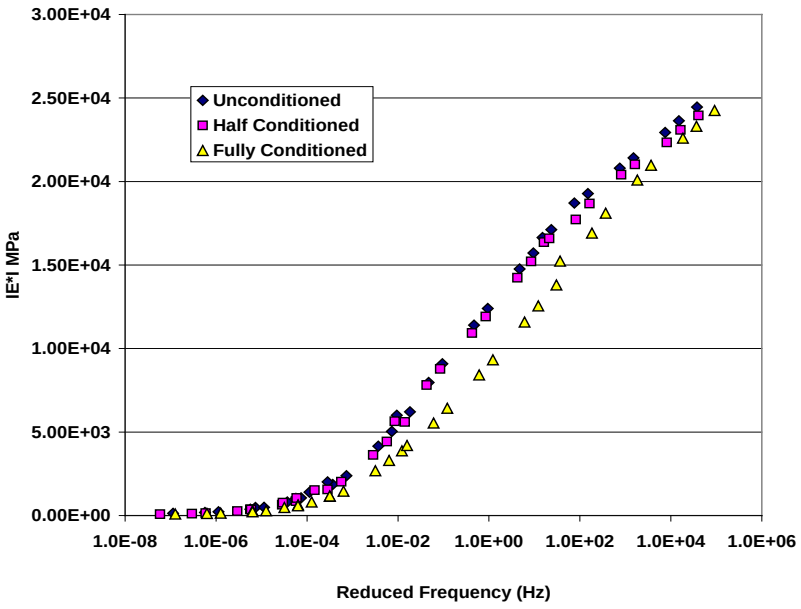

Figure 6.9 Mastercurve for Castle Hayne S – 12.5 C Mix without Additive (In Semi-Log Space)

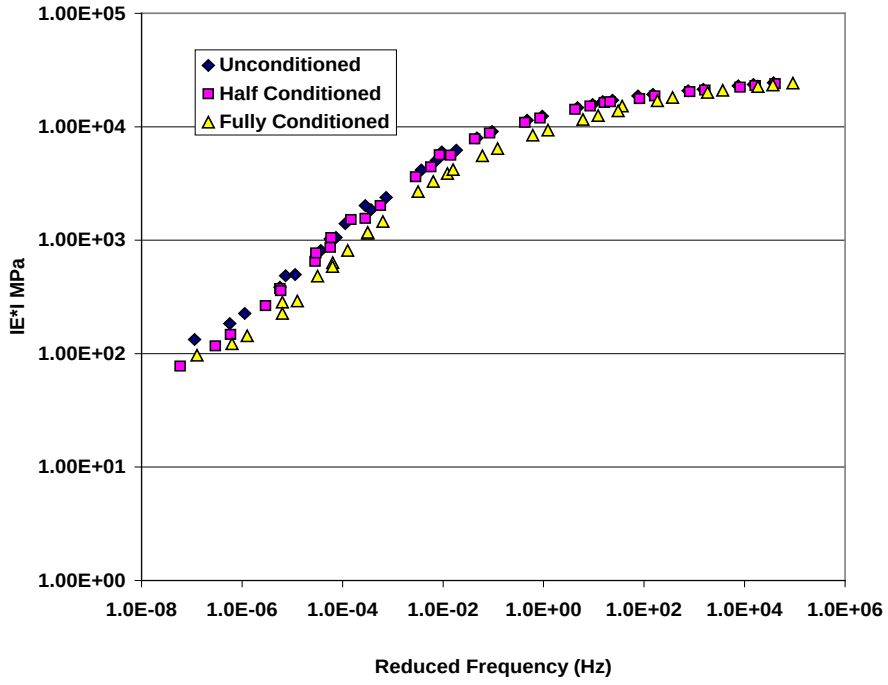

Figure 6.10 Mastercurve for Castle Hayne S – 12.5 C Mixture without Additive (Log-Log Space)

Since distress problems related to asphalt concrete mixtures are not severe at low temperature, it was decided to plot mastercurve in log-log scale for the remaining mixtures. This will help to understand the behavior of mixtures against conditioning at relatively medium and high temperatures. The mastercurve formation for 9.5mm gradation Castle Hayne mixture is shown in Figure 6.11. It can be seen from this figure that there is a difference in |E *| value between unconditioned state and conditioned state. However, there is no difference in |E *| value between half conditioned and fully conditioned stage.

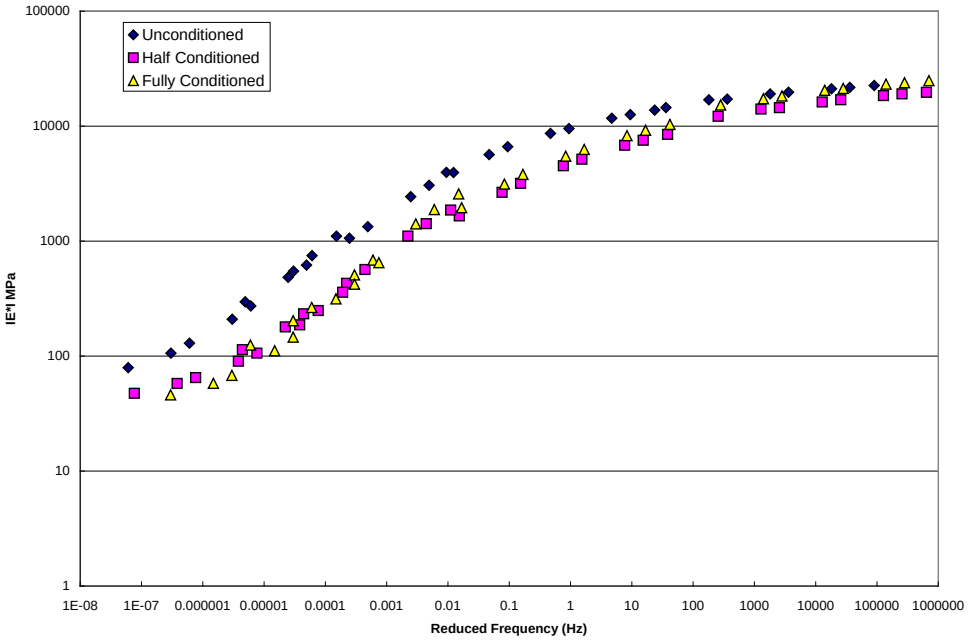

Figure 6.11 Mastercurve for Castle Hayne S – 9.5 C Mixture without Additive (Log-Log Space)

Figure 6.12 and 6.13 shows mastercurves for Fountain 12.5mm and 9.5mm gradation mixtures, respectively. It can be seen from Figure 6.12 that there is an appreciable difference in |E *| value between unconditioned and fully conditioned state. Comparing Figures 6.12 and 6.13, the difference in |E *| values is lower between unconditioned state and conditioned state in the case of Fountain 9.5mm gradation mixture.

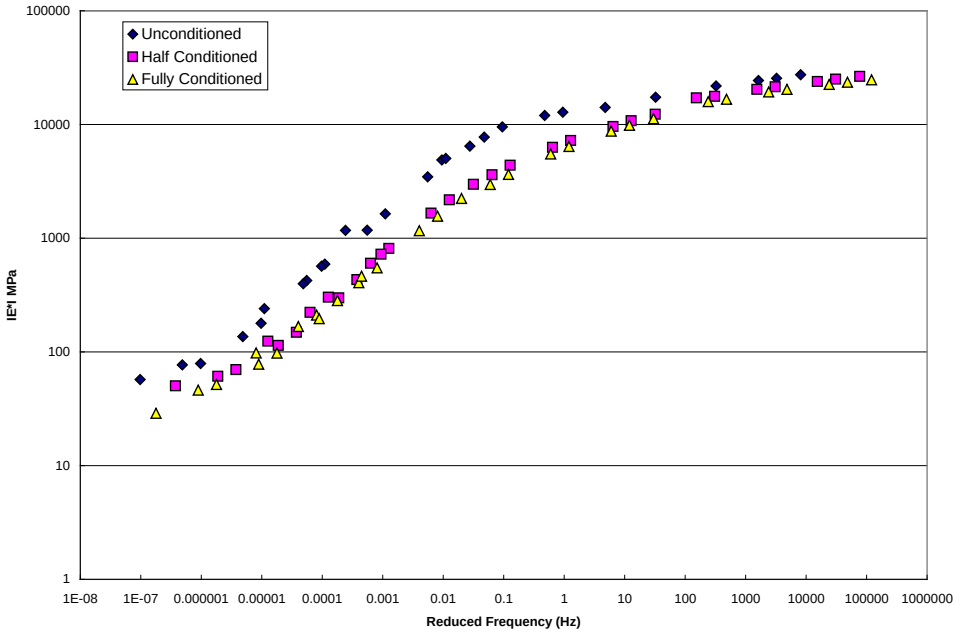

Figure 6.12 Mastercurve for Fountain S – 12.5 C Mixture without Additive (Log-Log Space)

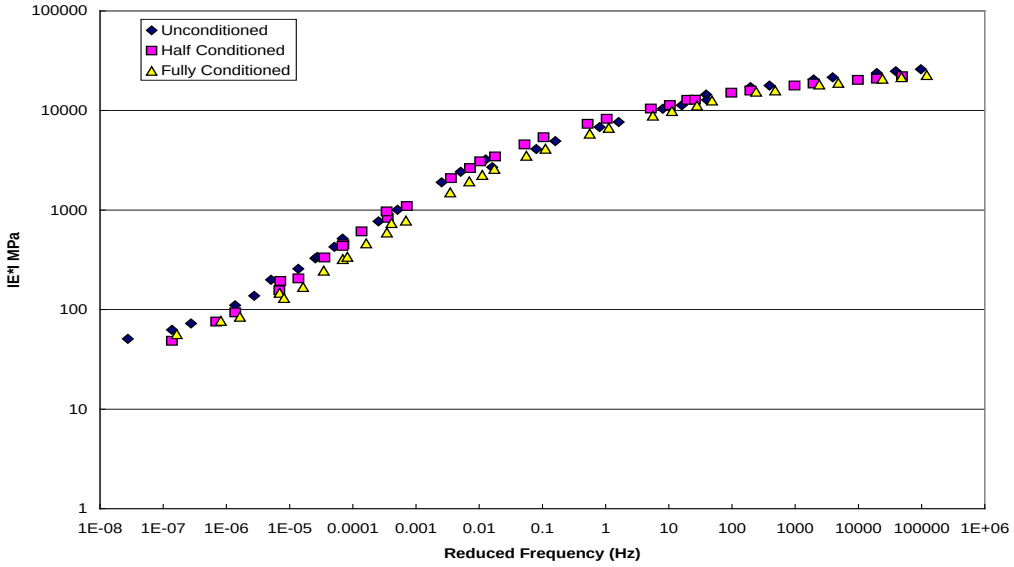

Figure 6.13 Mastercurve for Fountain S – 9.5 C Mixture without Additive (Log-Log Space)

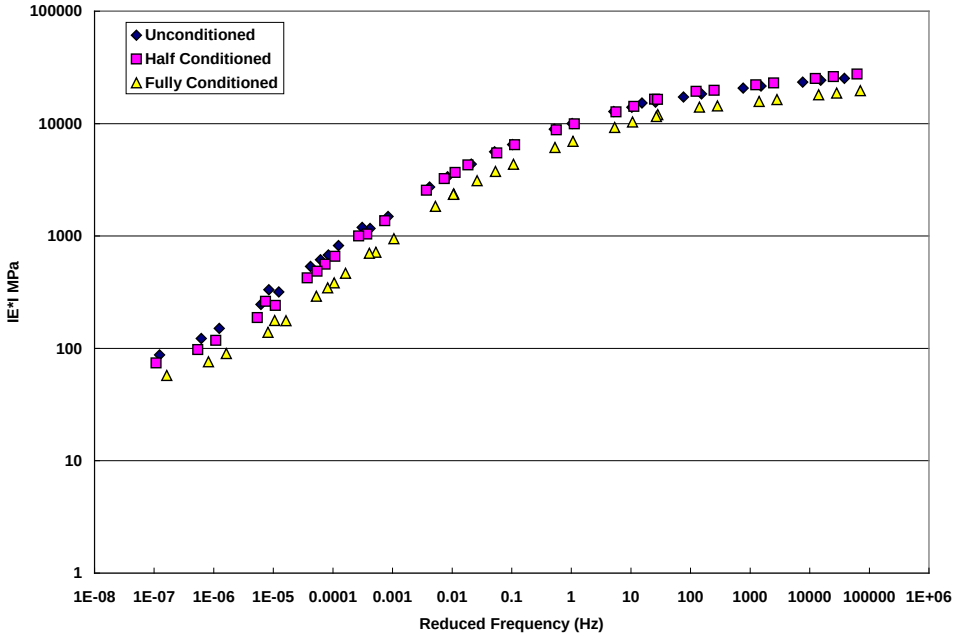

Figure 6.14 Mastercurve for Asheboro S – 12.5 C Mixture without Additive (Log-Log Space)

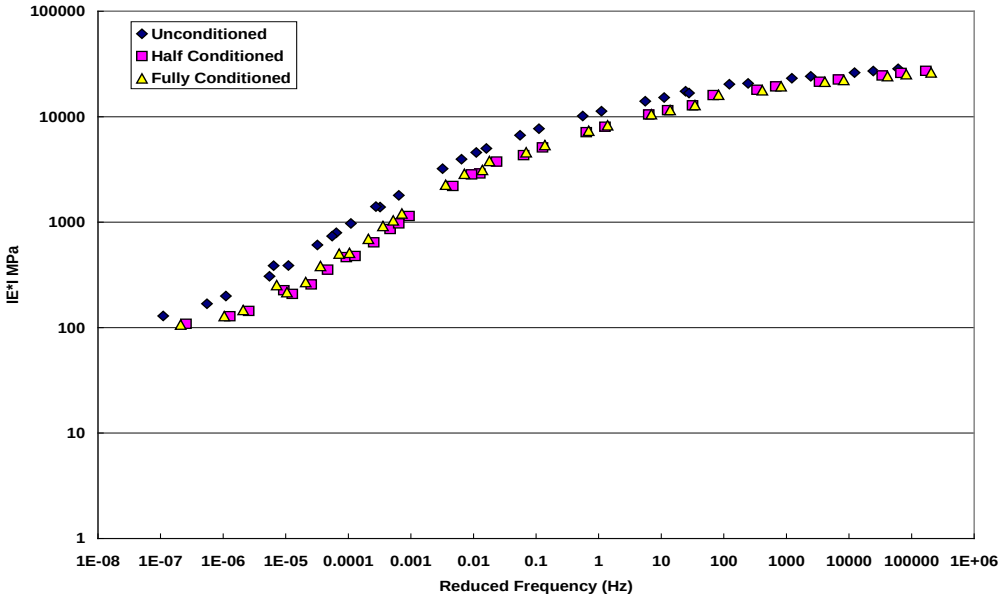

Figure 6.15 Mastercurve for Asheboro S – 9.5 C Mixture without Additive (Log-Log Space)

Figures 6.14 and 6.15 show mastercurves for Asheboro 12.5mm and 9.5mm gradation mixtures (without additives). The Reduction in difference in |E *| value is less in both cases while comparing conditioned and unconditioned states. In general the mixture behavior with moisture conditioning is different fro dynamic modulus as compared to shear test results. It can be seen from the master curves that the aggregate source and gradation did not seem to impact the modulus values in conditioned states. Differences in behavior observed between the two tests may be due to the difference in loading condition and specimen size. In dynamic modulus testing, 100mm diameter specimen with 150mm height were used, whereas in shear testing, 150mm diameter specimen with 50mm height was used. The Superpave volumetric mixture design procedure focuses on average percent air voids for specifying and designing AC mixtures. In both tests, specimen air voids was selected as 7%. Since specimen size is smaller in shear testing, the air void distribution is uniform within the specimen as compared to dynamic modulus testing. Specimens with the same average percent air voids may have a different distribution of air voids and intuitively are expected to respond differently under different loading conditions. Literature and experience have shown that specimens compacted using gyratory compactors tend to have non-uniform air void distribution along the height [38, 39]. The reason for air-void gradients can be explained by the distribution of forces during compaction, which decrease with depth. Masad, et al [38], studied the air void distribution in Superpave Gyratory compactor (SGC) compacted specimens using X-ray tomography (Figure 6.16). The middle of the SGC specimen was compacted more than the top and the bottom. Gyratory specimens are subjected to a high axial compressive

stress, a side-to-side shear stress, and a torsional shear stress. Under high axial compressive stresses and many gyrations, it is expected that the interior of the specimen will become better compacted. Also, in dynamic modulus testing the stain levels are very low which would affect the aggregate structure.

Figure 6.17 to 6.22 show mastercurves of Castle Hayne, Fountain and Asheboro aggregate mixtures with lime, added as an additive. From the figures, it can be seen that there is no significant difference in dynamic modulus values between conditioned and unconditioned state, which is consistent with the ability of lime to mitigate the moisture susceptibility.

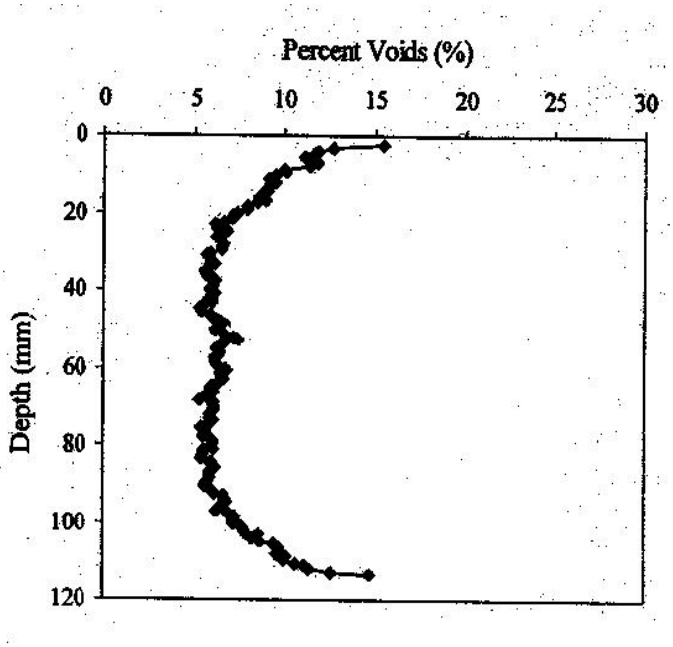

Figure 6.16 Void Distributions in a SGC Specimen [38]

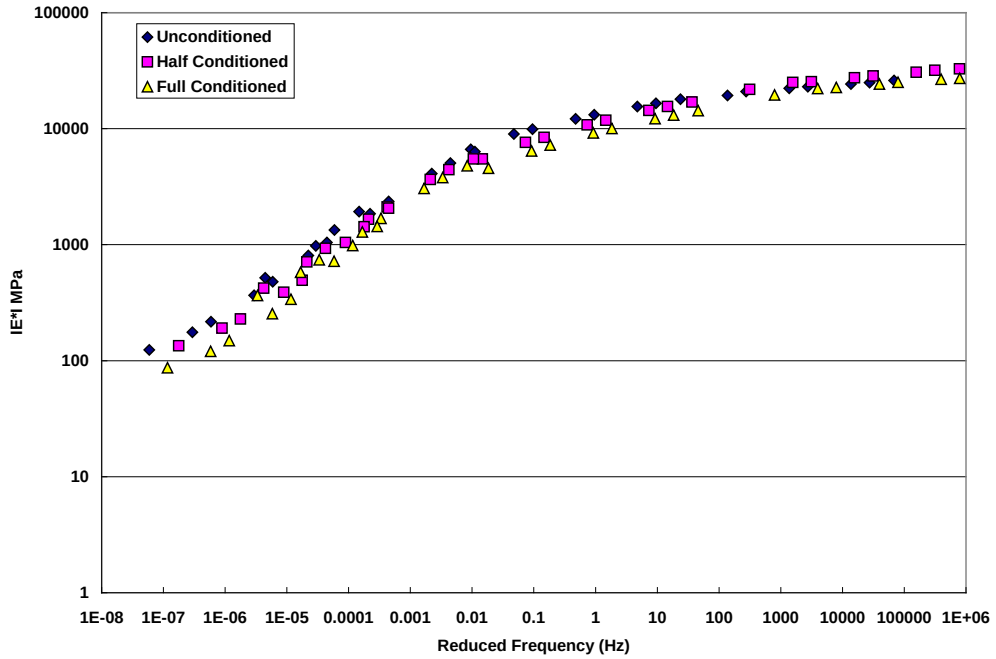

Figure 6.17 Mastercurve for Castle Hayne S – 12.5 C Mixture with Lime Additive (Log-Log Space)

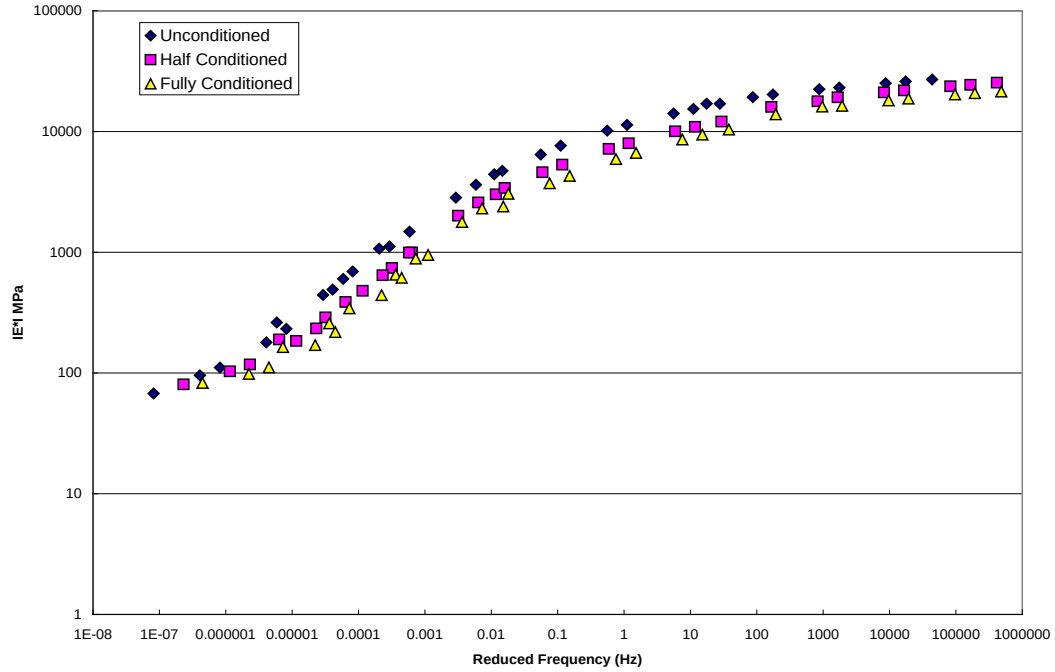

Figure 6.18 Mastercurve for Castle Hayne S – 9.5 C Mixture with Lime Additive (Log-Log Space)

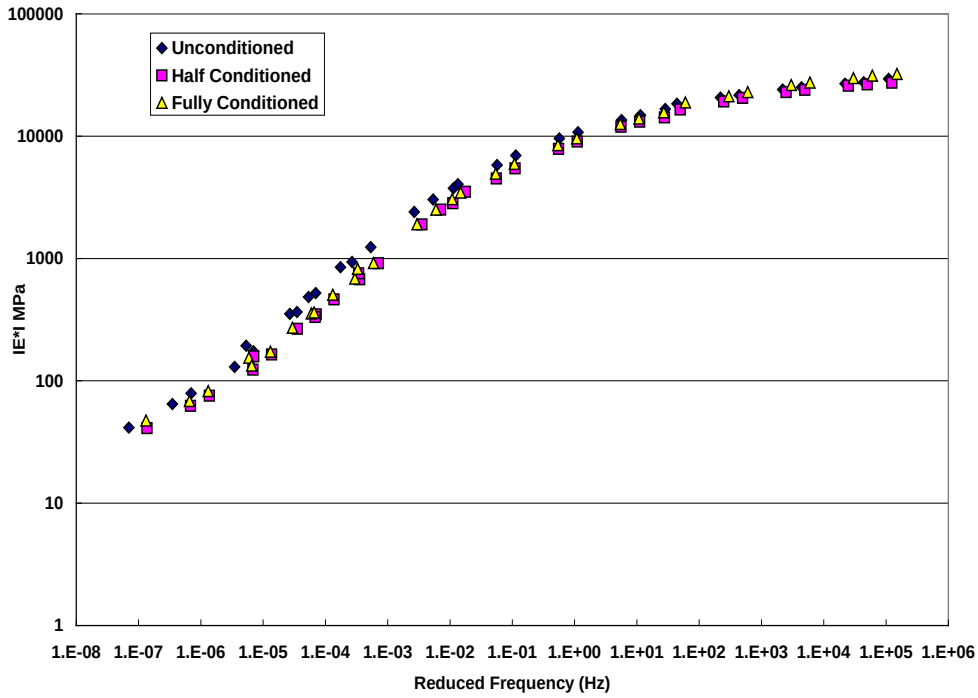

Figure 6.19 Mastercurve for Fountain S – 12.5 C Mixture with Lime Additive (Log-Log Space)

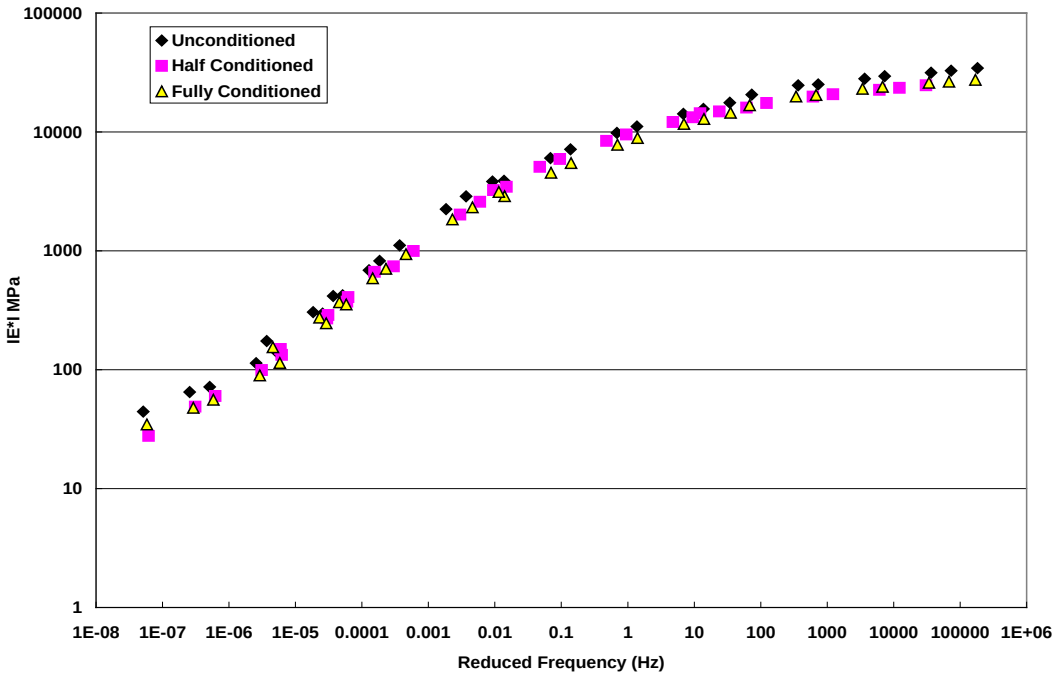

Figure 6.20 Mastercurve for Fountain S – 9.5 C Mixture with Lime Additive (Log-Log Space)

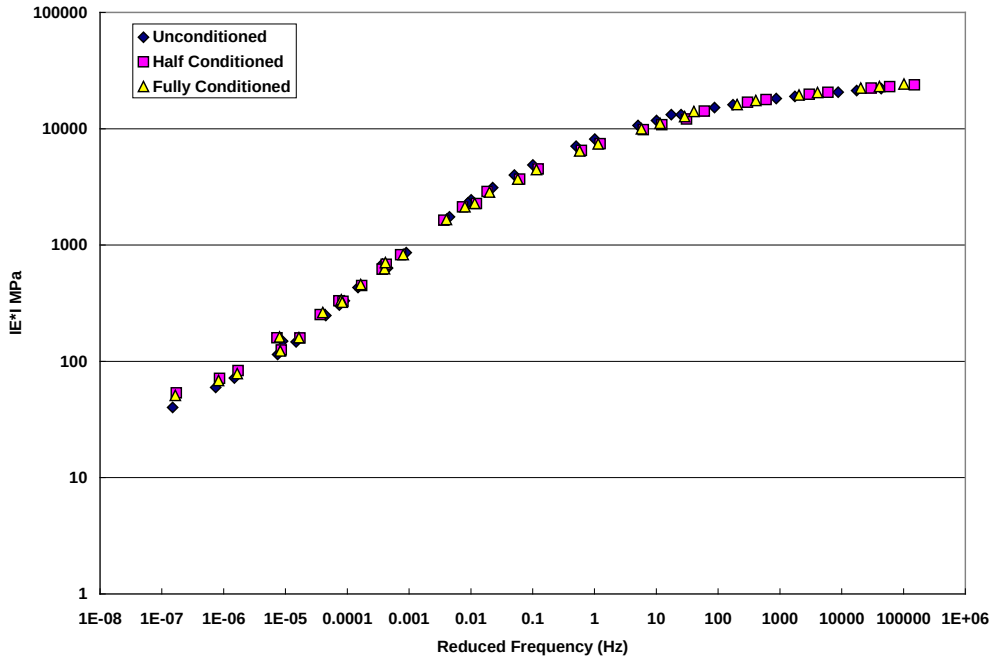

Figure 6.21 Mastercurve for Asheboro S – 12.5 C Mixture with Lime Additive (Log-Log Space)

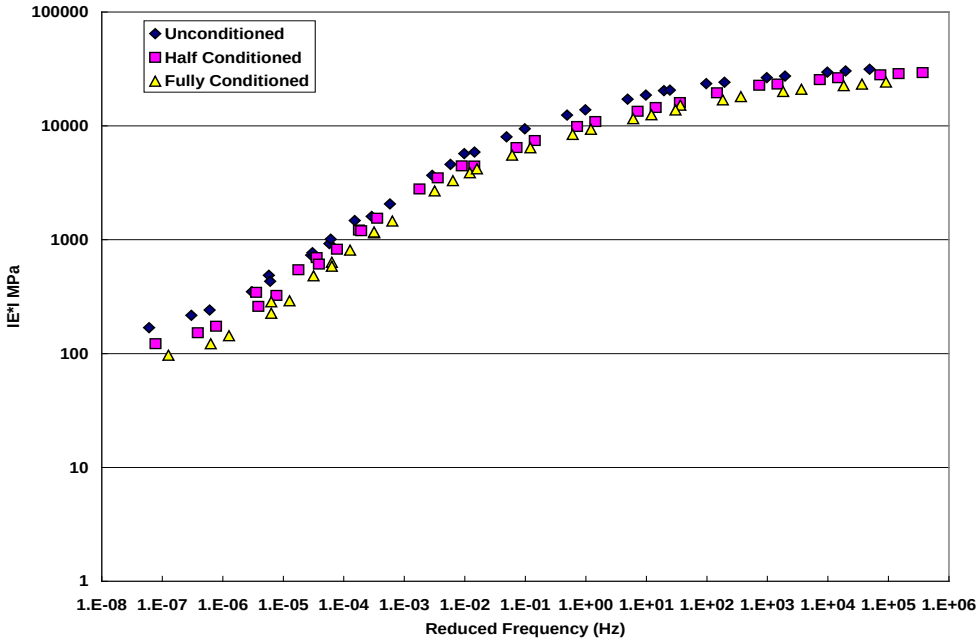

Figure 6.22 Mastercurve for Asheboro S – 9.5 C Mixture with Lime Additive (Log-Log Space)

6.8. Predicting Dynamic Moduli from Sigmoidal Fit

This section presents the procedure to calculate dynamic modulus for all mixtures tested in this project between -10°C and 54°C. The following steps are used to calculate the dynamic modulus at any temperature and frequency. Table 6.2 and 6.3 provides a list of coefficients determined from testing for each of the mixtures. These coefficients define the shape of the sigmoidal curve and determine the shape of the shift factor versus temperature relationship. The procedure is as follows: (i) Identify the mixture where |E*| needs to be calculated (ii) Determine the frequency (f) in Hz and temperature in degrees Celsius at which |E*| is to be computed (iii) Determine the shift factor coefficients from Table 6.2 and 6.3 (iv) Substitute coefficients into the following equation, where *T* is the temperature and *aT* is the shift factor:

$$Log(a_T) = \alpha_1 T^2 + \alpha_2 T + \alpha_3$$

(v) Compute the shift factor (vi) Compute the reduced frequency ($f_R = f \times a_T$) (vii) Determine the sigmoidal function regression coefficients a, b, d, and e from Table 6.4 (viii) Substitute the regression coefficients and f_R into the sigmoidal function Eq. (6.14) to determine the dynamic modulus in MPa. |E*| values were calculated for mixtures without additive and mixtures having lime using the above method and are tabulated in Table 6.4. |E*| values were calculated for 10Hz frequency and 20^0C temperature was selected.

Table 6.2 Coefficients to Predict |E*| at any Temperature and Frequency (For Mixtures without Additives)

Mixture Type		Shift function coefficients			Sigmoidal coefficients			
		α_1	α_2	α_3	a	b	d	e
Castle Hayne 12.5mm	UC	6.91E-04	-1.56E-01	1.48E+00	1.41E+00	2.98E+00	2.30E+00	5.09E-01
	HC	6.42E-04	-0.15756	1.428948	1.01E+00	3.37011	2.378029	0.484894
	FC	0.000949	-0.17395	1.728231	1.331359	3.055338	1.923901	0.483977
Castle Hayne 9.5mm	UC	7.67E-04	-1.66E-01	1.62E+00	1.12E+00	3.25E+00	2.02E+00	4.53E-01
	HC	0.001534	-0.20628	2.18495	0.937661	3.462634	1.609187	0.465453
	FC	1.25E-03	-0.19951	2.108398	1.23E+00	3.063422	1.494979	0.477856
Fountain 12.5mm	UC	2.08E-04	-0.127	1.22	1.39	2.99	2.44	0.652
	HC	9.00E-04	-0.15852	1.617875	1.16E+00	3.267331	1.61783	0.52679
	FC	0.000885	-0.16654	1.744046	0.932825	3.489294	1.56508	0.486664
Fountain 9.5mm	UC	5.23E-04	-1.61E-01	1.79E+00	9.53E-01	3.51E+00	1.69E+00	4.30E-01
	HC	8.26E-04	-1.64E-01	1.57E+00	8.42E-01	3.53E+00	1.96E+00	4.61E-01
	FC	9.65E-04	-1.72E-01	1.75E+00	1.04E+00	3.34E+00	1.66E+00	4.61E-01
Asheboro 12.5mm	UC	7.39E-04	-1.55E-01	1.55E+00	1.06E+00	3.31E+00	1.86E+00	5.13E-01
	HC	0.000843	-0.16437	1.707941	1.097527	3.31632	1.672974	0.478748
	FC	7.68E-04	-0.1561	1.553797	1.27E+00	3.034483	1.802248	0.519196
Asheboro 9.5mm	UC	8.05E-04	-1.64E-01	1.61E+00	1.51E+00	2.95E+00	1.88E+00	4.79E-01
	HC	1.04E-03	-0.17271	1.787167	1.56E+00	2.858241	1.601219	0.515512
	FC	0.001224	-0.18705	1.922502	1.489616	2.926254	1.661832	0.492549

Table 6.3 Coefficients to Predict |E*| at Any Temperature and Frequency (For Lime Added Mixtures)

Mixture Type		Shift function coefficients			Sigmoidal coefficients			
		α_1	α_2	α_3	a	b	d	e
Castle Hayne 12.5mm	UC	7.13E-04	-1.61E-01	1.52E+00	1.33E+00	3.08E+00	2.36E+00	4.89E-01
	HC	0.001458	-0.20362	2.056819	1.02028	3.496331	2.001163	0.418577
	FC	1.65E-03	-0.22339	2.371466	8.19E-01	3.628921	2.035545	0.415698
Castle Hayne 9.5mm	UC	6.23E-04	-1.56E-01	1.55E+00	1.23E+00	3.20E+00	2.07E+00	5.10E-01
	HC	1.27E-03	-0.19097	2.009596	1.31E+00	3.074038	1.777245	0.503486
	FC	0.00149	-0.19726	2.004306	1.384811	2.92328	1.722477	0.534662
Fountain 12.5mm	UC	7.50E-04	-1.64E-01	1.63E+00	8.59E-01	3.62E+00	2.00E+00	4.69E-01
	HC	0.001027	-0.17512	1.628895	0.966945	3.560898	1.760814	0.468157
	FC	9.15E-04	-0.16903	1.651017	9.59E-01	3.501457	1.818276	0.483745
Fountain 9.5mm	UC	8.94E-04	-0.17637	1.667486	1.04E+00	3.49889	1.87649	0.478674
	HC	5.53E-04	-1.51E-01	1.42E+00	6.87E-01	3.74E+00	2.03E+00	4.73E-01
	FC	0.000876	-0.1767	1.802455	0.83061	3.637275	1.831858	0.458413
Asheboro 12.5mm	UC	6.34E-04	-1.53E-01	1.53E+00	1.20E+00	3.25E+00	1.85E+00	4.51E-01
	HC	0.000773	-0.16036	1.583159	1.243212	3.214146	1.857762	0.482238
	FC	1.00E-03	-0.1748	1.792547	1.18E+00	3.220589	1.676045	0.492229
Asheboro 9.5mm	UC	6.83E-04	-1.58E-01	1.50E+00	1.81E+00	2.70E+00	1.91E+00	5.12E-01
	HC	1.11E-03	-0.18907	1.985784	1.49E+00	2.987159	1.813453	0.463574
	FC	0.000949	-0.17395	1.728231	1.331359	3.055338	1.923901	0.483977

Table 6.4 |E*| values at 20^0C (10Hz frequency)

Mixture Type		|E*| MPa (without additive)	|E*| MPa(with lime)
Castle Hayne 12.5mm	UC	1.17E+04	1.23E+04
	HC	1.07E+04	1.07E+04
	FC	8.55E+03	9.05E+03
Castle Hayne 9.5mm	UC	8.42E+03	1.04E+04
	HC	5.57E+03	7.56E+03
	FC	4.40E+03	6.18E+03
Fountain 12.5mm	UC	9.54E+03	1.27E+04
	HC	6.91E+03	7.97E+03
	FC	5.76E+03	7.81E+03
Fountain 9.5mm	UC	7.43E+03	9.30E+03
	HC	7.32E+03	8.25E+03
	FC	6.03E+03	7.68E+03
Asheboro 12.5mm	UC	7.44E+03	9.19E+03
	HC	6.86E+03	9.09E+03
	FC	6.64E+03	6.70E+03
Asheboro 9.5mm	UC	1.02E+04	1.25E+04
	HC	7.67E+03	9.91E+03
	FC	7.62E+03	8.55E+03

CHAPTER 7

7. PERFORMANCE ANALYSIS OF MIXTURES

The resulting parameters of shear tests and dynamic modulus tests are the material responses that can be used to predict the pavement's performance under service for distresses such as fatigue cracking and rutting. Fatigue and Rutting analysis are performed using surrogate models developed by SHRP 003-A project and distress models of Asphalt Institute. Fatigue analysis of the SHRP model considers material properties as well as pavement structural layer thickness whereas rutting analysis considers only the material properties.

7.1. Fatigue Analysis

Fatigue or load associated cracking was identified in the Strategic Highway Research Program (SHRP) as one of the primary distress mechanisms affecting the long-term performance of asphalt pavements. The other two major distress conditions are permanent deformation (rutting) and low temperature cracking. Fatigue cracking generally starts as a series of short longitudinal cracks in areas subjected to repeated wheel loadings. With additional traffic, the numbers of cracks increase and interconnect into a typical "alligator" crack pattern. In an asphalt pavement structure under load, the highest tensile stresses normally occur on the underside of the asphalt layer. Fatigue cracks initiate in these high tensile stress zones and then gradually propagate through the asphalt layer of the pavement. One way to reduce the potential for fatigue cracking is to make the asphalt pavement thicker to reduce the magnitude of the tensile stresses.

However, it costs money to build pavements thicker. Hence, the challenge becomes how to build more cost effective pavements that are fatigue resistant. The stiffness of an asphalt mix plays a major role in the fatigue resistance of an asphalt pavement. Just as with increasing pavement thickness, a higher mix stiffness reduces the tensile stresses at the bottom of the asphalt treated layer and the likelihood of crack initiation. One mix characteristic that has a notable effect on the fatigue resistance of dense graded asphalt pavement structures, regardless of pavement thickness, is air void content. In an asphalt mix, air voids act as stress concentration points and are the likely place where cracks begin.

7.2. SUPERPAVE Fatigue Model Analysis

The abridged fatigue analysis system from SHRP 003-A predicts the resistance of mix to fatigue distress for a pavement structure under a given traffic load. The resistance of a mix to fatigue cracking depends on the material properties such as initial flexural loss stiffness and voids filled with asphalt (VFA) and the pavement structural property, horizontal tensile strain at the bottom of the asphalt concrete layer. The abridged procedure requires an estimate of the flexural stiffness modulus of the asphalt aggregate mix at 20^{o}C. The flexural stiffness can be estimated from the shear stiffness of the mixture as measured from the FSCH tests at 10 Hz at 20^{o}C. This estimate is used in the multilayer elastic analysis to determine the critical level of strain to which the mix is subjected under the standard traffic load.

Multi-layer elastic analysis is used to determine the design strain, the maximum principal tensile strain at the bottom of the asphalt concrete layer, under the standard AASHTO

axle load of 18 kips. A pavement structure was assumed to conduct this analysis. The pavement structure and loading are given in Figure 7.1. The assumed pavement structure consists of an asphalt concrete layer, an aggregate base course, and a subbase resting on the subgrade. The asphalt concrete layer is 4 inches thick and the two layers beneath have a thickness of 8 inches each. The Poisson ratios and moduli of the layers are shown in Figure 7.1. A standard 18-kip single axle load with dual tires inflated to 100 psi was used for the analysis. The horizontal tensile strains at the bottom of AC layer are estimated at outer edge, overall center, inner edge, and tire center of dual tires using *KENPAVE* software for multilayer elastic analysis of pavement sections. The critical tensile strain is used as the design strain in this analysis.

The flexural properties of the mix are estimated using the following regression equations [36].

$$S_o = 8.56 * (G_o)^{0.913} \qquad (R^2 = 0.712) \qquad (7.1)$$

$$S_o" = 81.125 * (G_o")^{0.725} \qquad (R^2 = 0.512) \qquad (7.2)$$

Where

S_o = initial flexural stiffness at 50^{th} loading cycle is psi

G_o = shear stiffness at 10 Hz in psi

S_o" = initial flexural loss stiffness at 50^{th} loading cycle is psi

G_o" = shear loss stiffness at 10 Hz in psi

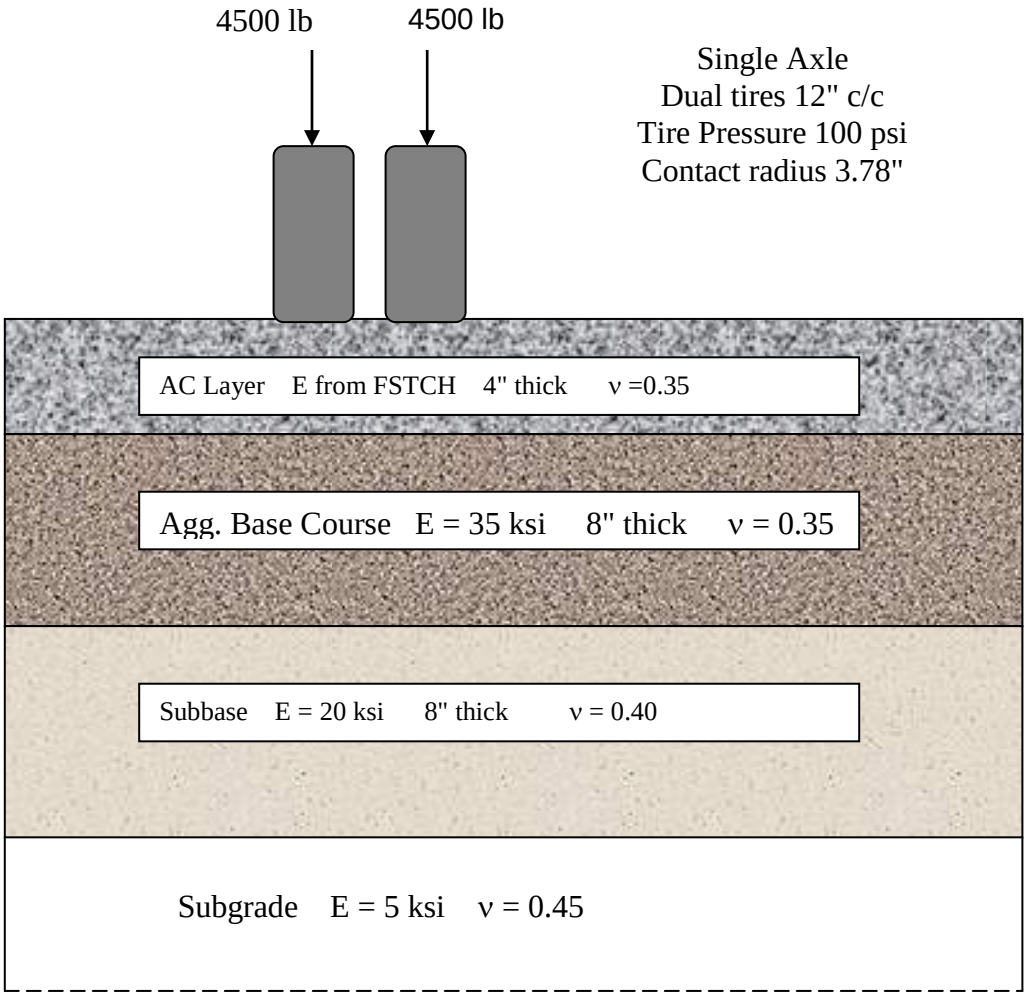

Figure 7.1 Typical Pavement Structure and Loading

The fatigue resistance of a mix is then estimated from the following strain-dependent surrogate model.

$$N_{supply} = 2.738E5 * e^{0.077VFA} * \varepsilon_0^{-3.624} * S_0'^{-2.72} \qquad (7.3)$$

Where

Nsupply = estimated fatigue life of the given pavement section in ESALs

VFA = voids filled with asphalt

ε_0 = critical tensile strain at the bottom of AC layer

The coefficient of determination for the surrogate model for fatigue analysis is 0.79 with a coefficient of variation of 90 percent. The estimation of fatigue life for mixtures is discussed in the following sections.

7.2.1. Fatigue Analysis of Mixtures

The fatigue life of mixtures were estimated using the abridged fatigue analysis system for unconditioned (UC), half conditioned (HC) and fully conditioned (FC) specimens of Castle Hayne, Fountain and Asheboro aggregate mixtures. First, the flexural stiffness modulus values of the mixtures were estimated using the shear stiffness and phase angles at 10 Hz measured in the FSCH tests. The flexural and shear modulus values of all mixtures are summarized in Tables 7.1 and 7.2 for mixtures without additive.

The Nsupply values were estimated by considering the flexural loss modulus, voids filled with asphalt (VFA) (in this case, the specimen VFA is considered) and critical tensile strain at the bottom of asphalt concrete layer, as shown in Tables 7.3 and 7.4. The results clearly indicate that the mixtures in the unconditioned state have higher fatigue life than the mixtures of conditioned state. The fatigue life of the mixtures varies between aggregate sources and asphalt binder grades, but there is a constant trend of decreased fatigue life with conditioning.

The flexural and shear modulus values of all mixtures with lime additive are summarized in Tables 7.5 and 7.6 and Nsupply values are summarized in Tables 7.7 and 7.8. Comparing Tables 7.3 and 7.4 to Tables 7.7 and 7.8 respectively, it can be seen that Nsupply of conditioned samples increased significantly for lime mixtures compared to

mixtures without additive. The percentage increase in fatigue life varied from 2% to 20% for fully conditioned samples. This increase varied across aggregate types and asphalt binder grades, with the highest increase coming from the most water-susceptible aggregates and the lowest increase coming from the lease water-susceptible aggregates. This phenomenon is expected because the primary action of lime is to decrease water susceptibility and this action will be most significant with a highly water-susceptible aggregate. Magnitudes aside, the trend of increased fatigue life with lime additive was constant. Because of the high variability in fatigue life increase across aggregate types, additional studies should be conducted to determine whether or not an interaction exists between lime dosage and either asphalt grade or aggregate type.

Table 7.1 Fatigue Life (Nsupply) Analysis for Mixtures Using PG 70-22 without any Additives (4" thick AC layer)

Mix	Asphalt Binder Grade	|G*| pa	Phase Angle	So	So"
Fountain 12.5-UC	PG 70-22	2.27E+09	17.83	9.33E+05	3.44 E+05
Fountain 12.5-HC	PG 70-22	1.40E+09	24.73	6.00E+05	3.03 E+05
Fountain 12.5-FC	PG 70-22	1.10E+09	30.39	4.81E+05	2.92 E+05
Fountain 9.5-UC	PG 70-22	2.28E+09	17.04	9.37E+05	3.34 E+05
Fountain 9.5-HC	PG 70-22	1.68E+09	24.03	7.09E+05	3.40 E+05
Fountain 9.5-FC	PG 70-22	1.38E+09	27.24	5.92E+05	3.21 E+05
Asheboro 12.5-UC	PG 70-22	1.99E+09	23.39	8.27E+05	3.77 E+05
Asheboro 12.5-HC	PG 70-22	1.79E+09	24.59	7.49E+05	3.61 E+05
Asheboro 12.5-FC	PG 70-22	1.46E+09	25.79	6.23E+05	3.22 E+05
Asheboro 9.5-UC	PG 70-22	1.97E+09	18.27	8.18E+05	3.15 E+05
Asheboro 9.5-HC	PG 70-22	1.49E+09	21.86	6.35E+05	2.92 E+05
Asheboro 9.5-FC	PG 70-22	1.20E+09	23.17	5.21E+05	2.59 E+05
Castle Hayne 12.5-UC	PG 70-22	2.50E+09	14.4	10.19 E+05	3.16 E+05
Castle Hayne 12.5-HC	PG 70-22	2.08E+09	17.5	8.61 E+05	3.18 E+05
Castle Hayne 12.5-FC	PG 70-22	1.98E+09	19	8.23 E+05	3.25E+05
Castle Hayne 9.5-UC	PG 70-22	2.54E+09	12.69	10.34 E+05	2.93E+05
Castle Hayne 9.5-HC	PG 70-22	2.07E+09	16.71	8.57 E+05	3.07 E+05
Castle Hayne 9.5-FC	PG 70-22	1.81E+09	19.29	7.58 E+05	3.08 E+05

Table 7.2 Summary of Estimated Material Properties for Mixtures Using PG 76-22 and PG 64-22 without any Additives (4" thick AC layer)

Mix	Asphalt Binder Grade	|G*| pa	Phase Angle	So	So"
Fountain 12.5-UC	PG 76-22	1.59E+09	33.24	6.74E+05	4.05E+05
Fountain 12.5-HC	PG 76-22	1.05E+09	38.80	4.62E+05	3.30E+05
Fountain 12.5-FC	PG 76-22	8.89E+08	43.92	3.96E+05	3.15E+05
Fountain 12.5-UC	PG 64-22	1.73E+09	39.85	7.28E+05	4.83E+05
Fountain 12.5-HC	PG 64-22	1.32E+09	41.98	5.68E+05	4.09E+05
Fountain 12.5-FC	PG 64-22	9.12E+08	43.73	4.05E+05	3.21E+05
Asheboro 12.5-UC	PG 76-22	2.23E+09	28.30	9.18E+05	4.66E+05
Asheboro 12.5-HC	PG 76-22	1.96E+09	30.87	8.16E+05	4.50E+05
Asheboro 12.5-FC	PG 76-22	1.73E+09	32.31	7.28E+05	4.23E+05
Asheboro 12.5-UC	PG 64-22	2.09E+09	29.22	8.66E+05	4.54E+05
Asheboro 12.5-HC	PG 64-22	1.63E+09	30.64	6.90E+05	3.92E+05
Asheboro 12.5-FC	PG 64-22	1.40E+09	34.02	6.00E+05	3.75E+05
Castle Hayne 12.5-UC	PG 76-22	2.66E+09	34.24	10.79E+05	6.00E+05
Castle Hayne 12.5-HC	PG 76-22	2.39E+09	34.46	9.78E+05	5.57E+05
Castle Hayne 12.5-FC	PG 76-22	2.06E+09	37.92	8.54E+05	5.31E+05
Castle Hayne 12.5-UC	PG 64-22	2.28E+09	26.46	9.37E+05	4.53E+05
Castle Hayne 12.5-HC	PG 64-22	1.96E+09	27.54	8.16E+05	4.17E+05
Castle Hayne 12.5-FC	PG 64-22	1.78E+09	29.61	7.47E+05	4.08E+05

Table 7.3 Fatigue Life (Nsupply) Analysis for Mixtures Using PG 70-22 without any Additives (4” thick AC layer)

Mix	Asphalt Binder Grade	So"	VFA	Strain	Nsupply
Fountain 12.5-UC	PG 70-22	3.44 E+05	62	1.90E-04	9.13E+05
Fountain 12.5-HC	PG 70-22	3.30 E+05	62	2.38E-04	5.41E+05
Fountain 12.5-FC	PG 70-22	2.92 E+05	62	2.63E-04	4.29E+05
Fountain 9.5-UC	PG 70-22	3.34 E+05	60	1.89E-04	8.13E+05
Fountain 9.5-HC	PG 70-22	3.40 E+05	60	2.19E-04	4.59E+05
Fountain 9.5-FC	PG 70-22	3.21 E+05	60	2.39E-04	3.90E+05
Asheboro 12.5-UC	PG 70-22	3.77 E+05	57	2.02E-04	3.72E+05
Asheboro 12.5-HC	PG 70-22	3.61 E+05	57	2.13E-04	3.45E+05
Asheboro 12.5-FC	PG 70-22	3.22 E+05	57	2.33E-04	3.25E+05
Asheboro 9.5-UC	PG 70-22	3.15 E+05	56	2.04E-04	5.69E+05
Asheboro 9.5-HC	PG 70-22	2.92 E+05	56	2.31E-04	4.38E+05
Asheboro 9.5-FC	PG 70-22	2.59 E+05	56	2.54E-04	3.73E+05
Castle Hayne 12.5-UC	PG 70-22	3.16 E+05	60	1.81E-04	1.11E+06
Castle Hayne 12.5-HC	PG 70-22	3.18 E+05	60	1.98E-04	7.90E+05
Castle Hayne 12.5-FC	PG 70-22	3.25E+05	60	2.03E-04	6.85E+05
Castle Hayne 9.5-UC	PG 70-22	2.93E+05	53	1.80E-04	8.57E+05
Castle Hayne 9.5-HC	PG 70-22	3.07 E+05	53	1.99E-04	5.25E+05
Castle Hayne 9.5-FC	PG 70-22	3.08 E+05	53	2.12E-04	4.81E+05

Table 7.4 Fatigue Life (Nsupply) Analysis for Mixtures Using PG 76-22 and PG 64-22 without any Additives (4" thick AC layer)

Mix	Asphalt Binder Grade	So"	VFA	Strain	Nsupply
Fountain 12.5-UC	PG 76-22	4.05E+05	73	2.27E-04	6.62E+05
Fountain 12.5-HC	PG 76-22	3.30E+05	73	2.71E-04	6.04E+05
Fountain 12.5-FC	PG 76-22	3.15E+05	73	2.89E-04	5.41E+05
Fountain 12.5-UC	PG 64-22	4.83E+05	74	2.18E-04	5.98E+05
Fountain 12.5-HC	PG 64-22	4.09E+05	74	2.46E-04	5.33E+05
Fountain 12.5-FC	PG 64-22	3.21E+05	74	2.87E-04	5.28E+05
Asheboro 12.5-UC	PG 76-22	4.66E+05	71	1.93E-04	6.96E+05
Asheboro 12.5-HC	PG 76-22	4.50E+05	71	2.06E-04	6.13E+05
Asheboro 12.5-FC	PG 76-22	4.23E+05	71	2.18E-04	5.85E+05
Asheboro 12.5-UC	PG 64-22	4.54E+05	73	2.00E-04	8.02E+05
Asheboro 12.5-HC	PG 64-22	3.92E+05	73	2.24E-04	7.88E+05
Asheboro 12.5-FC	PG 64-22	3.75E+05	73	2.40E-04	6.91E+05
Castle Hayne 12.5-UC	PG 76-22	6.00E+05	72	1.77E-04	5.37E+05
Castle Hayne 12.5-HC	PG 76-22	5.57E+05	72	1.87E-04	5.40E+05
Castle Hayne 12.5-FC	PG 76-22	5.31E+05	72	2.01E-04	4.73E+05
Castle Hayne 12.5-UC	PG 64-22	4.53E+05	76	1.91E-04	1.15E+06
Castle Hayne 12.5-HC	PG 64-22	4.17E+05	76	2.06E-04	1.11E+06
Castle Hayne 12.5-FC	PG 64-22	4.08E+05	76	2.15E-04	9.97E+05

Table 7.5 Summary of Estimated Material Properties for Mixtures Using PG 70-22 with Lime (4" thick AC Layer)

Mix	Asphalt Binder Grade	|G*| pa	Phase Angle	So	So"
Fountain 12.5-UC	PG 70-22	2.30E+09	17.3	9.44E+05	3.4 E+05
Fountain 12.5-HC	PG 70-22	2.24E+09	19.81	9.22E+05	3.66E+05
Fountain 12.5-FC	PG 70-22	2.23E+09	20.15	9.18E+05	3.69E+05
Fountain 9.5-UC	PG 70-22	2.23E+09	18.25	9.18E+05	3.45 E+05
Fountain 9.5-HC	PG 70-22	2.04E+09	19.46	8.46E+05	3.38E+05
Fountain 9.5-FC	PG 70-22	2.04E+09	23.07	8.46E+05	3.80E+05
Asheboro 12.5-UC	PG 70-22	2.12E+09	19.14	8.76E+05	3.44E+05
Asheboro 12.5-HC	PG 76-22	2.07E+09	21.14	8.57E+05	3.62E+05
Asheboro 12.5-FC	PG 70-22	2.00E+09	22.08	8.31E+05	3.64E+05
Asheboro 9.5-UC	PG 70-22	2.10E+09	17.88	8.69E+05	3.25E+05
Asheboro 9.5-HC	PG 70-22	2.00E+09	21.71	8.31E+05	3.59E+05
Asheboro 9.5-FC	PG 70-22	1.93E+09	24.71	8.04E+05	3.83 E+05
Castle Hayne 12.5-UC	PG 70-22	2.63E+09	14.8	10.67E+05	3.35E+05
Castle Hayne 12.5-HC	PG 70-22	2.54E+09	17.6	10.34E+05	3.69E+05
Castle Hayne 12.5-FC	PG 70-22	2.39E+09	19.5	9.78 E+05	3.79E+05
Castle Hayne 9.5-UC	PG 70-22	2.58E+09	13.56	10.49 E+05	3.11E+05
Castle Hayne 9.5-HC	PG 70-22	2.18E+09	14.6	8.99E+05	2.90E+05
Castle Hayne 9.5-FC	PG 70-22	2.17E+09	18.42	8.95 E+05	3.40E+05

Table 7.6 Summary of Estimated Material Properties for Mixtures Using PG 76-22 and PG 64-22 with Lime (4” thick AC Layer)

Mix	Asphalt Binder Grade	|G*| pa	Phase Angle	So	So"
Fountain 12.5-UC	PG 76-22	1.92E+09	30.72	8.01E+05	4.42E+05
Fountain 12.5-HC	PG 76-22	1.75E+09	31.09	7.36E+05	4.16E+05
Fountain 12.5-FC	PG 76-22	1.74E+09	32.23	5.69E+05	4.24E+05
Fountain 12.5-UC	PG 64-22	2.02E+09	31.22	7.28E+05	4.63E+05
Fountain 12.5-HC	PG 64-22	1.83E+09	32.65	5.69E+05	4.44E+05
Fountain 12.5-FC	PG 64-22	1.62E+09	33.02	4.06E+05	4.09E+05
Asheboro 12.5-UC	PG 76-22	2.68E+09	22.94	10.86E+05	4.62E+05
Asheboro 12.5-HC	PG 76-22	2.54E+09	25.66	10.34E+05	4.50E+05
Asheboro 12.5-FC	PG 76-22	2.46E+09	28.47	10.04E+05	4.23E+05
Asheboro 12.5-UC	PG 64-22	2.27E+09	25.43	9.33E+05	4.54E+05
Asheboro 12.5-HC	PG 64-22	2.12E+09	28.45	8.77E+05	3.92E+05
Asheboro 12.5-FC	PG 64-22	2.00E+09	30.26	8.31E+05	3.75E+05
Castle Hayne 12.5-UC	PG 76-22	2.55E+09	25.41	10.79E+05	4.78E+05
Castle Hayne 12.5-HC	PG 76-22	2.38E+09	28.10	9.75E+05	4.87E+05
Castle Hayne 12.5-FC	PG 76-22	2.29E+09	31.24	9.41E+05	5.07E+05
Castle Hayne 12.5-UC	PG 64-22	2.11E+09	25.79	8.73E+05	4.21E+05
Castle Hayne 12.5-HC	PG 64-22	2.02E+09	26.28	8.39E+05	4.13E+05
Castle Hayne 12.5-FC	PG 64-22	1.94E+09	28.96	8.09E+05	4.28E+05

Table 7.7 Fatigue Life Analysis for Mixtures Using PG 70-22 with Lime (Nsupply)

Mix	Asphalt Binder Grade	So"	VFA	Strain	Nsupply
Fountain 12.5-UC	PG 70-22	3.4 E+05	62	1.89E-04	9.66E+05
Fountain 12.5-HC	PG 70-22	3.66E+05	62	1.91E-04	7.50E+05
Fountain 12.5-FC	PG 70-22	3.69E+05	62	1.91E-04	7.27E+05
Fountain 9.5-UC	PG 70-22	3.45 E+05	60	1.91E-04	8.37E+05
Fountain 9.5-HC	PG 70-22	3.38E+05	60	2.00E-04	6.47E+05
Fountain 9.5-FC	PG 70-22	3.80E+05	60	2.00E-04	5.48E+05
Asheboro 12.5-UC	PG 70-22	3.44E+05	57	1.96E-04	5.33E+05
Asheboro 12.5-HC	PG 70-22	3.62E+05	57	1.99E-04	4.41E+05
Asheboro 12.5-FC	PG 70-22	3.64E+05	57	2.02E-04	3.94E+05
Asheboro 9.5-UC	PG 70-22	3.25E+05	56	1.97E-04	5.84E+05
Asheboro 9.5-HC	PG 70-22	3.59E+05	56	2.02E-04	4.07E+05
Asheboro 9.5-FC	PG 70-22	3.83 E+05	56	2.05E-04	2.81E+05
Castle Hayne 12.5-UC	PG 70-22	3.35E+05	60	1.76E-04	1.04E+06
Castle Hayne 12.5-HC	PG 70-22	3.69E+05	60	1.80E-04	7.53E+05
Castle Hayne 12.5-FC	PG 70-22	3.79E+05	60	1.85E-04	6.27E+05
Castle Hayne 9.5-UC	PG 70-22	3.11E+05	53	1.78E-04	1.24E+06
Castle Hayne 9.5-HC	PG 70-22	2.90E+05	53	1.94E-04	1.10E+06
Castle Hayne 9.5-FC	PG 70-22	3.40E+05	53	1.94E-04	7.08E+05

Table 7.8 Fatigue Life Analysis for Mixtures Using PG 76-22 and PG 64-22 with Lime (Nsupply)

Mix	Asphalt Binder Grade	So"	VFA	Strain	Nsupply
Fountain 12.5-UC	PG 76-22	4.42E+05	73	2.08E-04	7.23E+05
Fountain 12.5-HC	PG 76-22	4.16E+05	73	2.17E-04	7.20E+05
Fountain 12.5-FC	PG 76-22	4.24E+05	73	2.18E-04	6.80E+05
Fountain 12.5-UC	PG 64-22	4.63E+05	74	2.03E-04	7.70E+05
Fountain 12.5-HC	PG 64-22	4.44E+05	74	2.13E-04	7.29E+05
Fountain 12.5-FC	PG 64-22	4.09E+05	74	2.25E-04	7.42E+05
Asheboro 12.5-UC	PG 76-22	4.62E+05	71	1.76E-04	9.93E+05
Asheboro 12.5-HC	PG 76-22	4.50E+05	71	1.81E-04	8.14E+05
Asheboro 12.5-FC	PG 76-22	4.23E+05	71	1.84E-04	6.77E+05
Asheboro 12.5-UC	PG 64-22	4.54E+05	73	1.91E-04	1.03E+06
Asheboro 12.5-HC	PG 64-22	3.92E+05	73	1.98E-04	8.39E+05
Asheboro 12.5-FC	PG 64-22	3.75E+05	73	2.04E-04	7.61E+05
Castle Hayne 12.5-UC	PG 76-22	4.78E+05	72	1.81E-04	9.22E+05
Castle Hayne 12.5-HC	PG 76-22	4.87E+05	72	1.87E-04	7.76E+05
Castle Hayne 12.5-FC	PG 76-22	5.07E+05	72	1.91E-04	6.47E+05
Castle Hayne 12.5-UC	PG 64-22	4.21E+05	76	1.99E-04	1.23E+06
Castle Hayne 12.5-HC	PG 64-22	4.13E+05	76	2.03E-04	1.20E+06
Castle Hayne 12.5-FC	PG 64-22	4.28E+05	76	2.07E-04	1.01E+06

Figure 7.2 is a scatter plot for all mixtures showing indirect tensile strength of mixtures and their corresponding field fatigue life values. Field fatigue life values were obtained by multiplying Nsupply values by a shift factor of 10 (assuming 10% cracking in the wheel path) [36]. It can be seen that as indirect tensile strength increases fatigue life also increases. The linear regression relationship between Indirect Tensile Strength (ITS) and fatigue life is shown in Fig 7.3. Regression model and ANOVA table for linear regression are shown in Tables 7.4 and 7.5, respectively. From Table 7.4, it can be seen that this relationship has an R^2 value of 0.65. Moreover, from Table 7.5 it can be seen that p-value of this regression model is very much less than 0.05 (α level critical value), indicating that at 5% significance level it can be concluded that there exists a strong relation between indirect tensile strength value and fatigue life of mixtures.

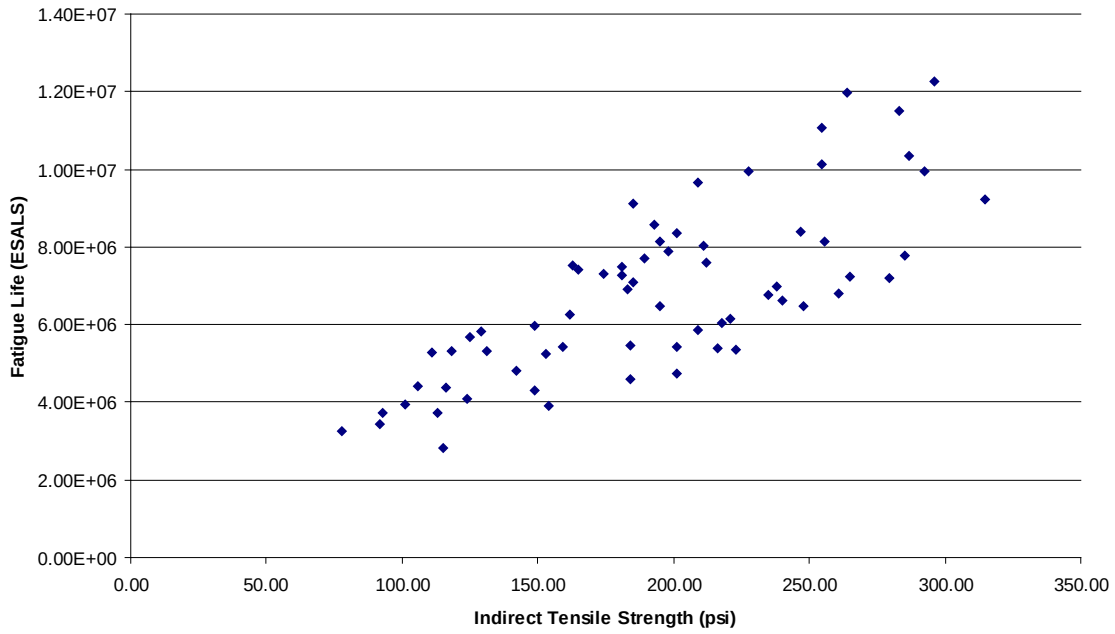

Figure 7.2 Scatter Plot of Individual Tensile Strength (ITS) vs. Fatigue Life for all Mixes

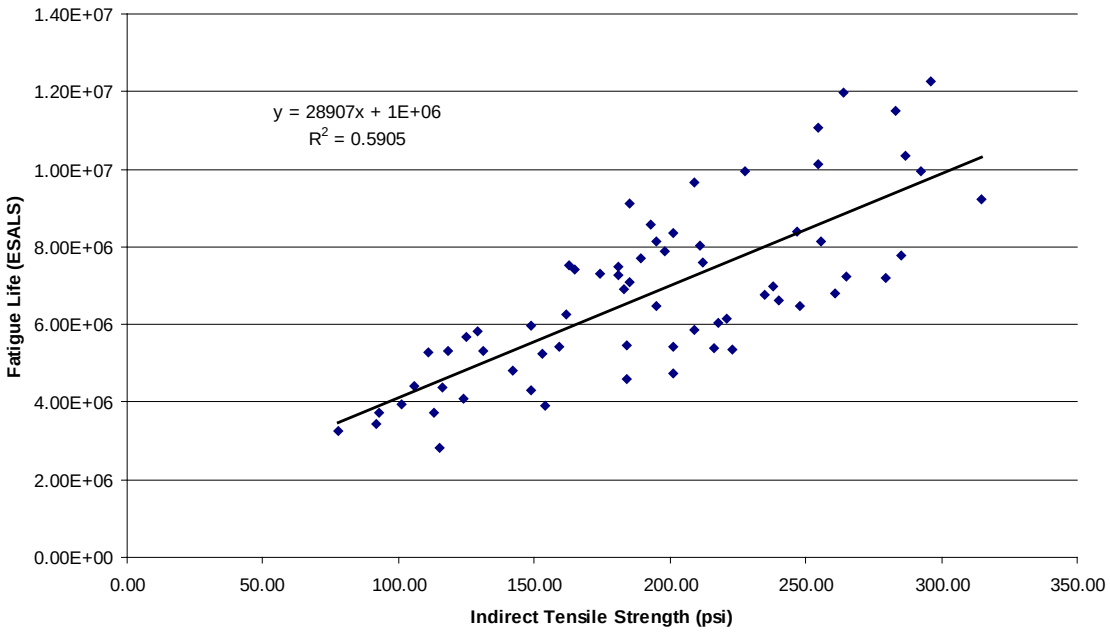

Figure 7.3 Linear Regression Relationship between ITS and Fatigue Life for all Mixes

Table 7.9 Parameter Estimates of Simple Linear Regression

(Fatigue Life Analysis)

Fatigue life = 1.206E+06 + 28906 * ITS

R (correlation coefficient) = 0.768

R-sq = 0.59

Parameter	Estimate	Std. Err.	DF	T-Stat	P-Value
Intercept	1206275	606599	1	1.99	0.0510
Slope	28906	3011.81	1	9.60	<0.0001

Table 7.10 Analysis of Variance Table for Regression Model (Fatigue Life Analysis)

Source	DF	SS	MS	F-stat	P-value
Model	1	1.870	1.870	92.11	<0.0001
Error	64	1.299	2.031		
Total	65	3.170			

From Figures 7.4 – 7.6, it can be seen that that there exists a strong exponential relationship between indirect tensile strength (ITS) and fatigue life for individual mix types (S – 12.5 C, S – 12.5 D, etc.). The R^2 values for the exponential model are 0.69, 0.82 and 0.91 for PG 70-22, PG 76-22 and PG 64-22 respectively. The R^2 values represent the proportion of the total variability in the data that is explained by the model in question. As such, the above listed R^2 values represent increases of 0.05, 0.06 and 0.03, respectively (or 5%, 6% and 3%), which is a significant enough increase to justify the exponential model over the linear model. The R^2 value for the entire data set increases to 0.62 from 0.59 when the exponential model is used. This increased R^2 value signifies that the exponential regression relationship is better fit than linear regression model, and because the exponential regression was a significant improvement over the linear model for individual asphalt grades, the exponential model was selected as the model of choice. Although correlations between ITS and fatigue life are stronger when specimens are separated by mix type, the final design chart contains all mixtures in order to better show general trends. Such strong correlations could be misinterpreted and result in too much

reliance upon the fatigue life estimate, rather than using the estimate as intended, to get a general idea of the projected fatigue life of a mixture.

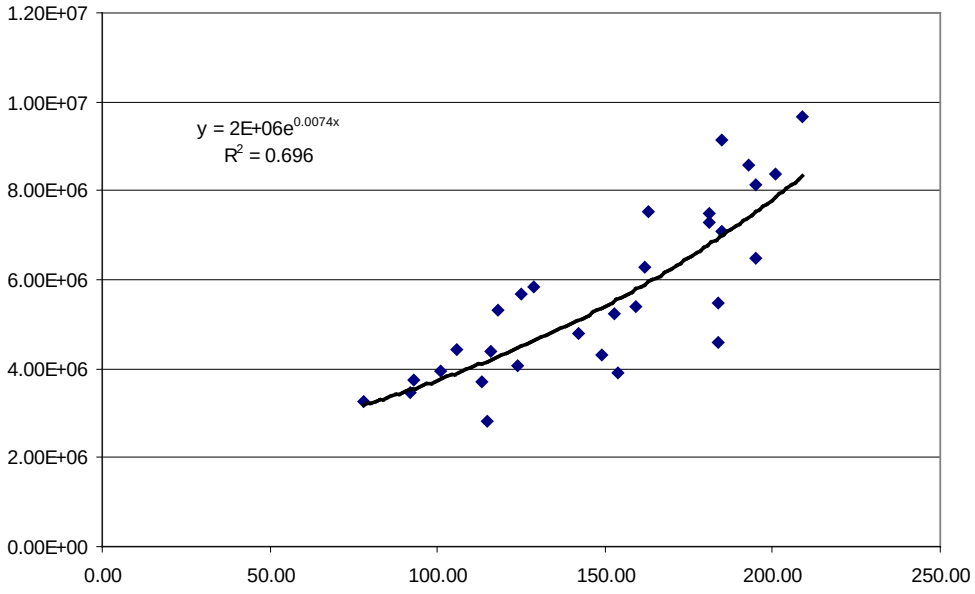

Figure 7.4 Plot of Individual Tensile strength vs. Fatigue Life for Mixes Using PG 70-22

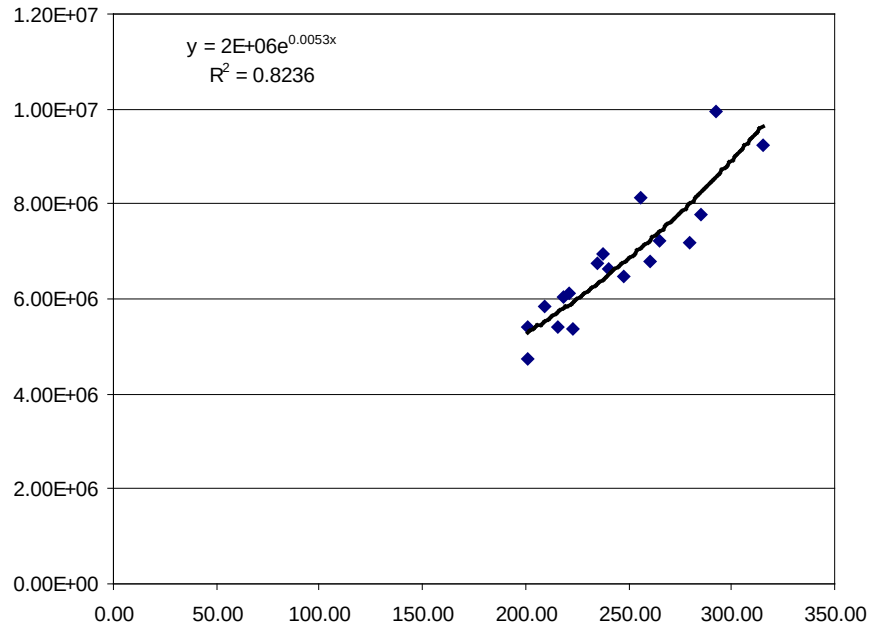

Figure 7.5 Plot of Individual Tensile strength vs. Fatigue Life for Mixes Using PG 76-22

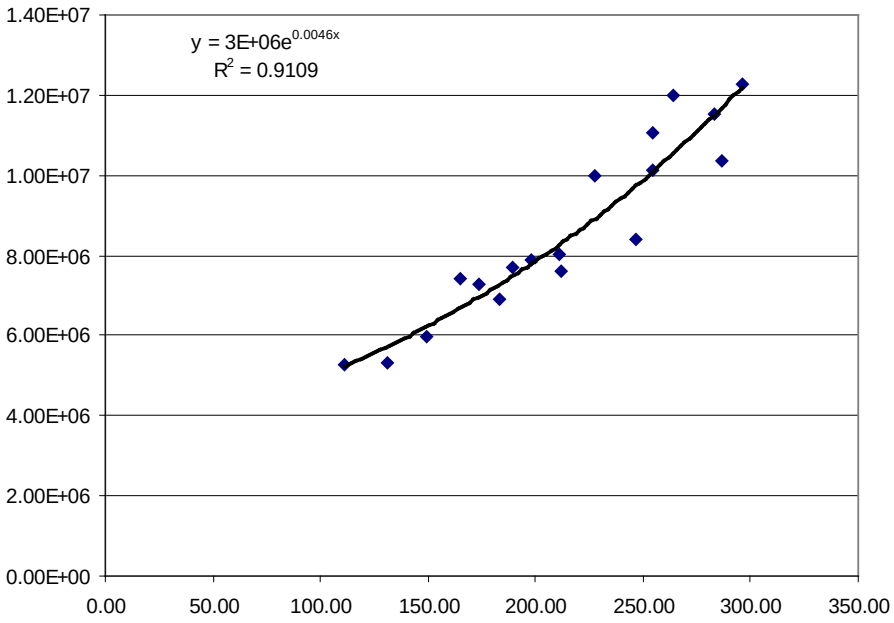

Figure 7.6 Plot of Individual Tensile strength vs. Fatigue Life for Mixes Using PG 64-22

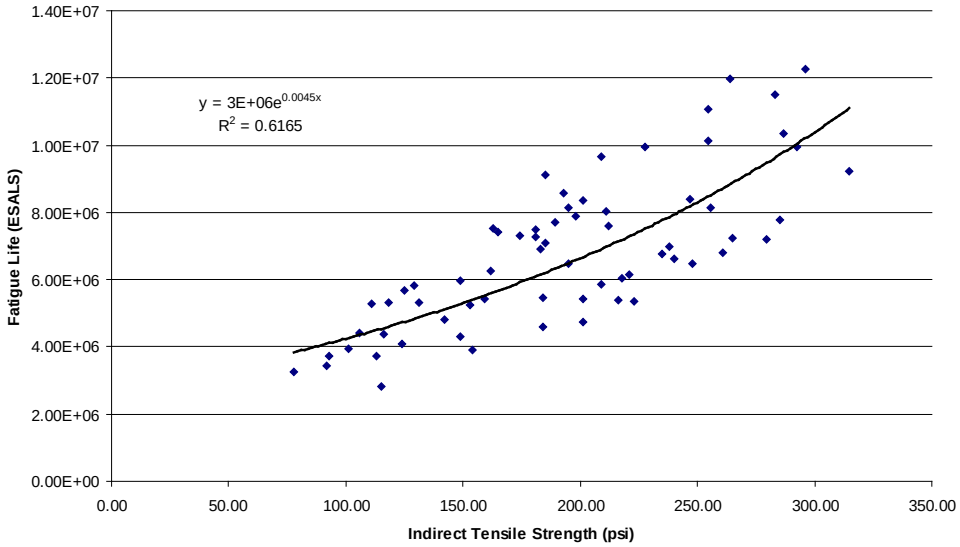

Figure 7.7 Exponential Relationship of ITS to Fatigue Life for all Mixes using 4" Surface Course

The overall exponential model is given by the equation

$$\text{Fatigue life} = 3\ E{+}06\ e^{0.0045\ ITS} \qquad (R^2=0.62)$$

The estimated fatigue life depends on the thickness of the asphaltic surface of the pavements, and on the thickness and modulus of the underlying layers. As this study involves only the mixtures used for surface courses of asphaltic pavements, the thickness and modulus of underlying layers were assumed to be reasonably constant values for the purpose of estimating their fatigue performance. A plot of the fatigue life and the corresponding Indirect Tensile Strength values of the pavements for the asphalt pavements of surface course thicknesses of 3", 5''and 6'' are plotted in Figures 7.8, 7.9

and 7.10, respectively. The exponential regression equation and corresponding R^2 values are shown in the graphs themselves. Figure 7.11 shows combined plot of fatigue life and the corresponding Indirect Tensile Strength values for pavements surface course thicknesses of 3", 4", 5" and 6".

This plot can be used as a design chart, i.e., for different surface course thickness in between the above thickness values can be found by suitable interpolation. From Figure 7.11, it can be seen that for a given individual tensile strength value, fatigue life increases as surface course thickness increases. This is because of the reduction in horizontal tensile strain value underneath the surface course as thickness increases.

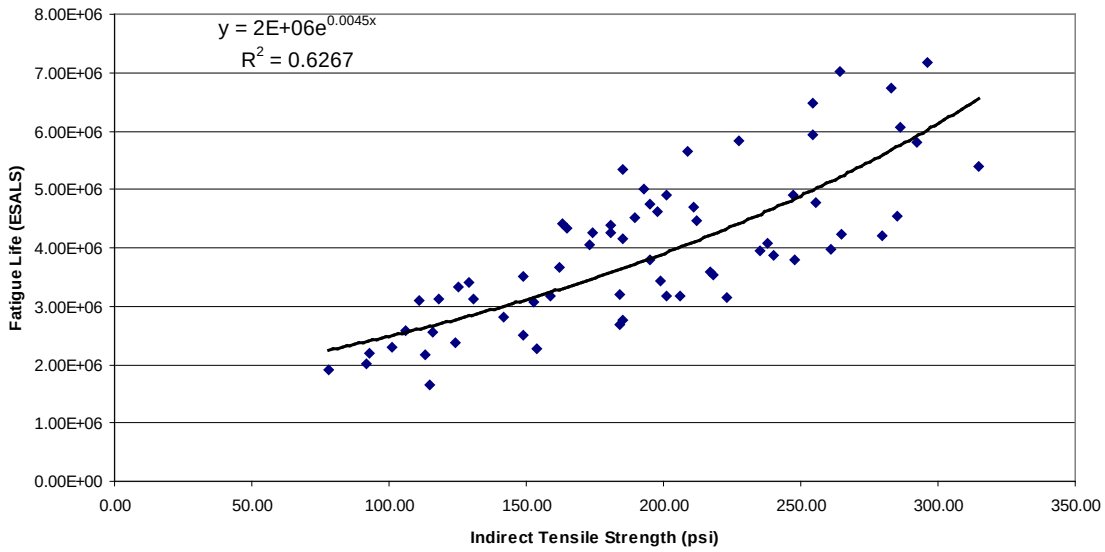

Figure 7.8 Plot of Individual Tensile strength vs. Fatigue life (For 3" Thick Asphalt Layer)

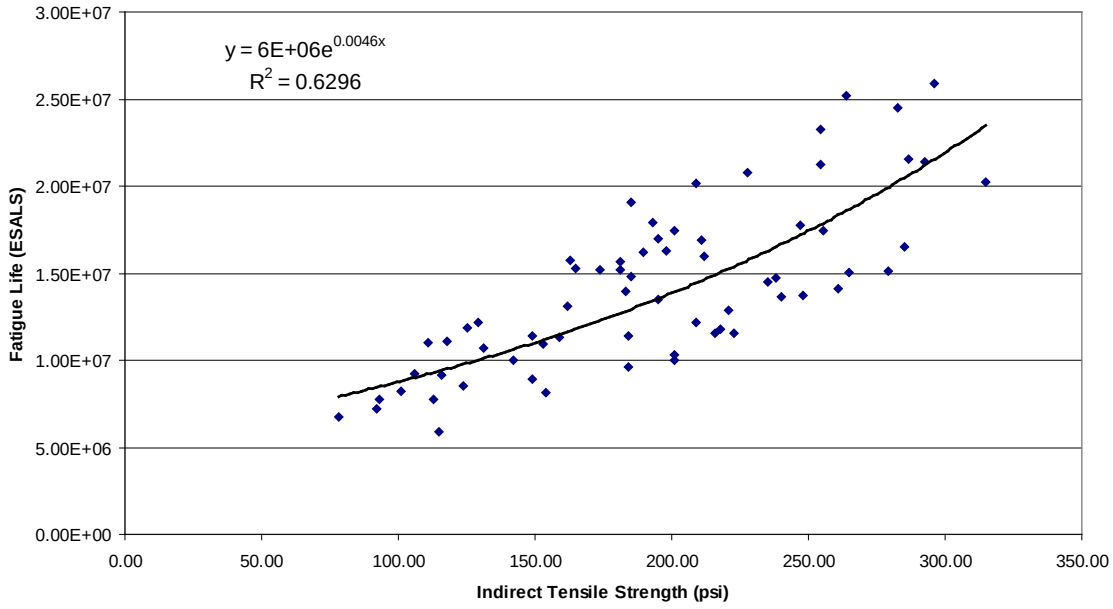

Figure 7.9 Plot of Individual Tensile strength vs. Fatigue life (For 5" Thick Asphalt Layer)

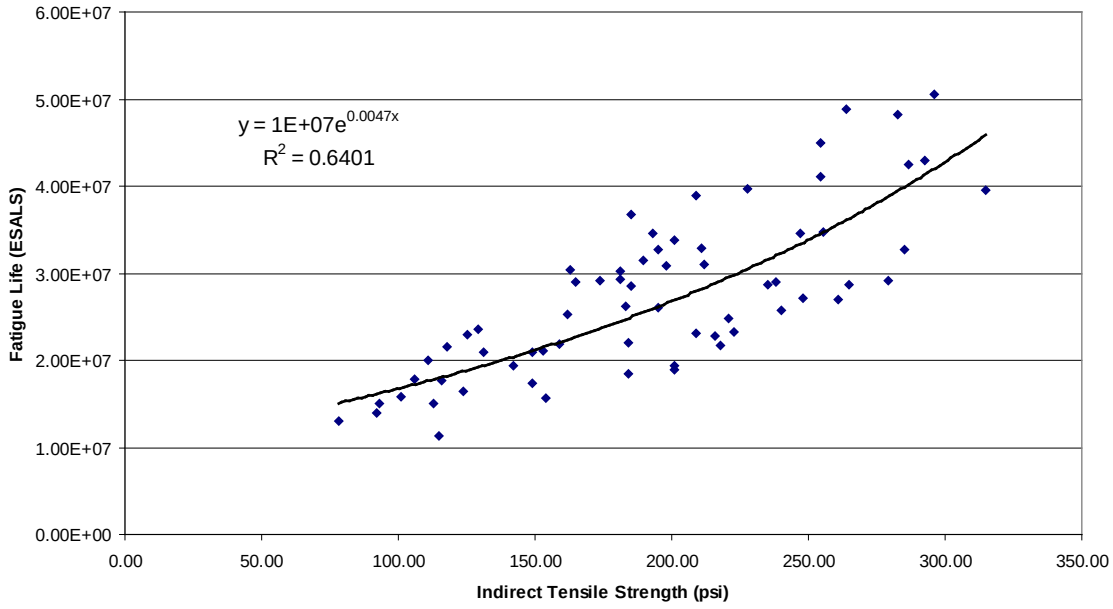

Figure 7.10 Plot of Individual Tensile strength vs. Fatigue life (For 6" Thick Asphalt Layer)

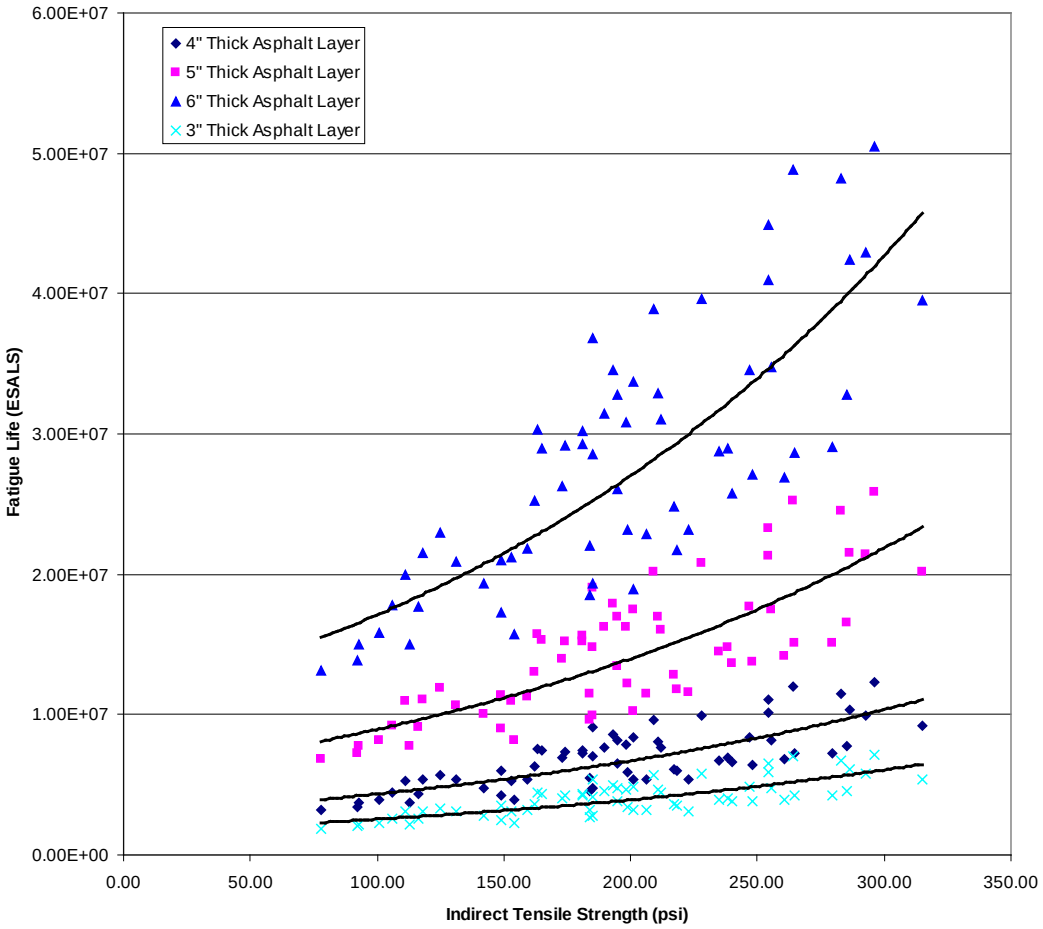

Figure 7.11 Combined Plot of Individual Tensile strength vs. Fatigue life (for 3", 4", 5" and 6" Thick Asphalt Layer)

Figure 7.11 above shows the combined results for all mixtures assuming the typical base courses shown in Figure 7.1 and using 3", 4", 5" and 6" surface course of asphalt concrete. The lines included represent the exponential curves given in Figures 7.7 to 7.10. It is important to note that all fatigue life values are very conservative in that they are all calculated using a specimen whose air voids are 7% of the total mix. Typically, field values are near 4% air voids, resulting in a much stiffer mixture which is more

resistant to fatigue cracking. This study used 7% air voids in order to enable usage of water damaged specimens similar to the specimens used to calculate Tensile Strength Ratio (TSR). In practice, specimens would be fabricated for TSR, ITS values would be recorded and using a conditioned and unconditioned ITS value, Figure 7.11 would be used to produce a range of fatigue life estimates. Because all estimates would be determined using 7% air void specimens, all estimates would be conservative values and field values - unless the drastic conditions used to estimate the fatigue life were present in the field - would be higher, resulting in better fatigue performance than estimated.

7.2.2. Asphalt Institute Model

The number of cycles to failure under fatigue cracking can also be estimated using Asphalt Institute model. Dynamic modulus of the asphalt layer was determined at 20^0C and a frequency of 10Hz. The allowable number of load repetitions is related to the tensile strain at the bottom of the asphalt later, as indicated in the following equation.

$$N_f = 0.00432*C * \varepsilon_t^{-3.291} * E_1^{-0.854} \quad (7\text{-}4)$$

Where,

$C = 10^M$

$M = 4.84 [V_b/(V_a+V_b)-0.69]$

V_b =effective binder content

V_a = air voids (%)

N_f = allowable number of load repetitions to prevent fatigue cracking (20% of area of crack)

ε_t = tensile strain at the bottom of asphalt later

E_1 = Dynamic modulus of asphalt layer (psi)

Fatigue life is calculated using dynamic modulus values given in Table 6.4 (Chapter 6). Critical strain is calculated using KENPAVE software and by assuming pavement structure as shown in Figure 7.1. Figure 7.12 shows relationship between indirect tensile strength and fatigue life of mixtures using AI method. It can be seen from the figure that relationship is not strong since the R^2 value of regression is very low. Therefore, further analysis using AI method was not conducted.

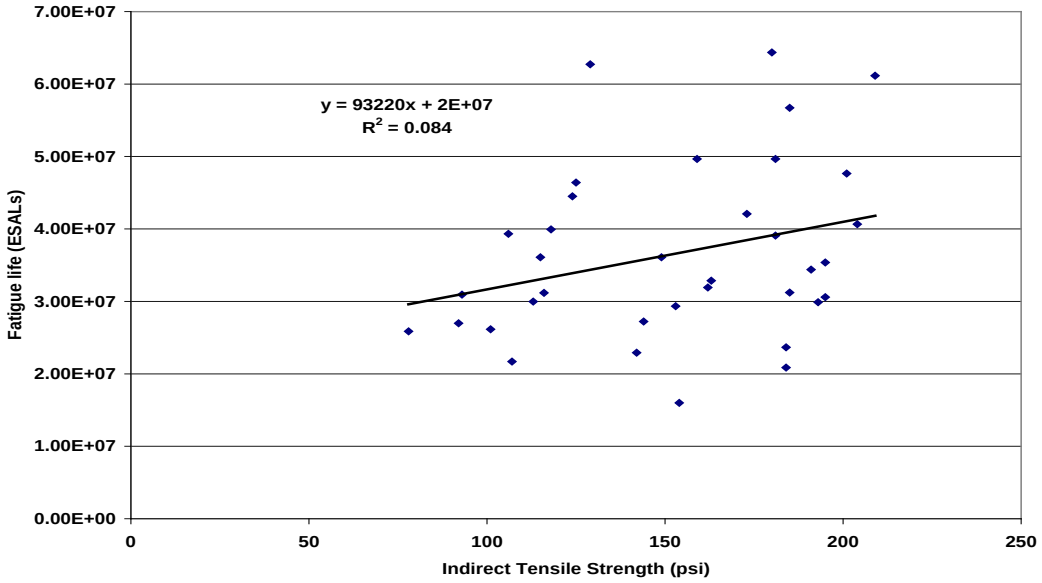

Figure 7.12 Linear Regression Relation between ITS and Fatigue Life

7.3. Rutting of Asphalt Mixtures

Rutting is the formation of twin longitudinal depressions in the wheel paths due to a progressive accumulation of permanent deformation in one or more of the pavement layers. The rate and magnitude of rutting depend on external and internal factors. External factors include load and volume of truck traffic, tire pressure, temperature and

construction practices. Internal factors include properties of the binder, the aggregate and mix properties, and the thickness of the pavement layers. Rutting in hot-mix asphalt concrete can occur from two types of mechanical response: viscous flow and plastic deformation. Plastic deformation occurs as aggregate particles move slightly relative to one another, which is accompanied by viscous flow in the asphalt cement binding these particles together. These processes, though conceptually simple, are very difficult to analyze quantitatively.

7.4. SUPERPAVE Rutting Model Analysis

The permanent deformation system of SHRP A-003A estimates rut depth from the maximum permanent shear strain obtained from RSCH test using the following relation.

Rut depth (in.) = 11 * Maximum permanent shear strain

If rutting in millimeters is desired, the coefficient of the above equation is about 275. The above relationship was obtained for a tire pressure of 100psi and asphalt layer thickness of 15 inches. Studies performed for a similar pavement structure at 200psi and 500psi suggest that this relationship is independent of the tire pressure. However, the same is not true in the case of pavement thickness. The coefficient is expected to decrease with a decrease in asphalt layer thickness [36, 37].

The conversion of the number of RSCH test cycles to ESALs is determined by the following equation:

log (cycles) = -4.36 + 1.24 log (ESALs) [36}

Where,

Cycles = number of cycles obtained from the RSCH test

ESALs = equivalent 18-kip single axle load

According to the above relationship, 5000 cycles of the RSCH test correspond to 3.156 million ESALs. Tables 5.25 - 5.28 give the summary of repeated shear strain values of mixtures with and without additive. If shear strains were to be multiplied by the factor 11 as per SHARP model [37] for estimating the rut depth, the same trend of the shear strains would be observed. The scatter plot between indirect tensile strength (ITS) and plastic shear strain is shown in Figure 7.13.

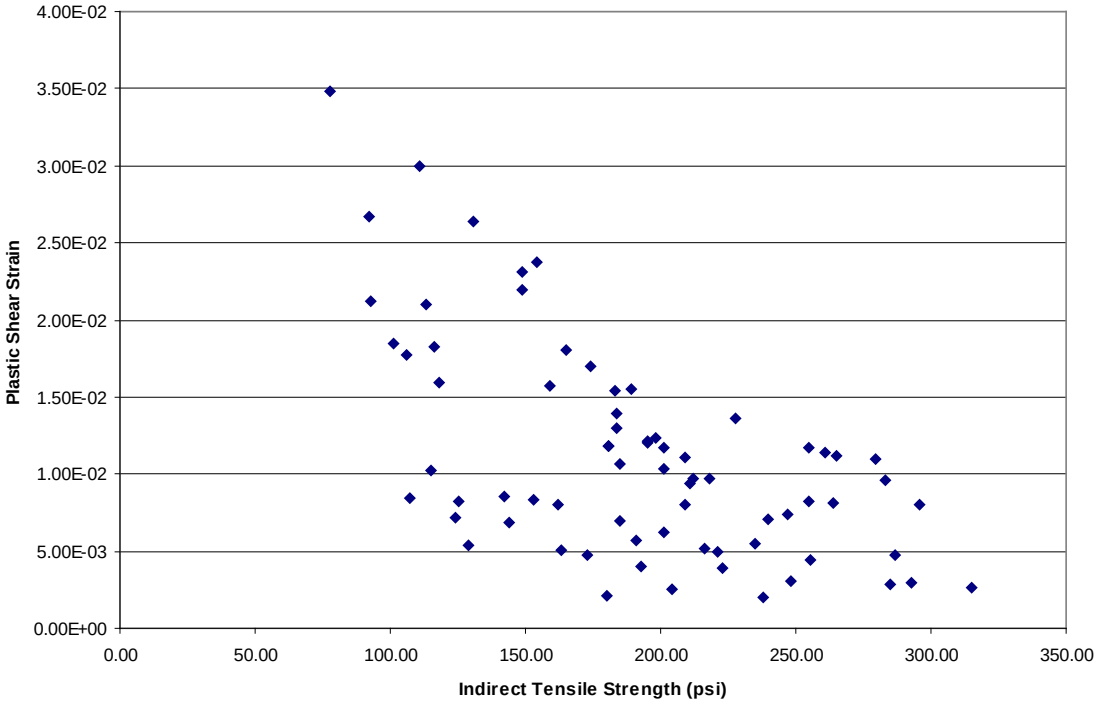

Figure 7.13 Scatter Plot of Plastic Shear Strain vs ITS

Figure 7.14 shows the linear regression relationship between indirect tensile strength and plastic shear strain. The parameter estimates and ANOVA results of regression are shown in Table 7.7 and 7.8. From Table 7.8, by referring to p-value, it can be concluded that at 5% significance level there exists a strong relation between indirect tensile strength and plastic shear strain. From Figure 7.15, it can be seen that there exists a strong logarithmic regression relationship between indirect tensile strength and plastic shear strain of a mixture. The R^2 value of this relationship is 0.58, which signifies that logarithmic regression relationship is stronger than linear regression model, which has an R^2 value of only 0.53.

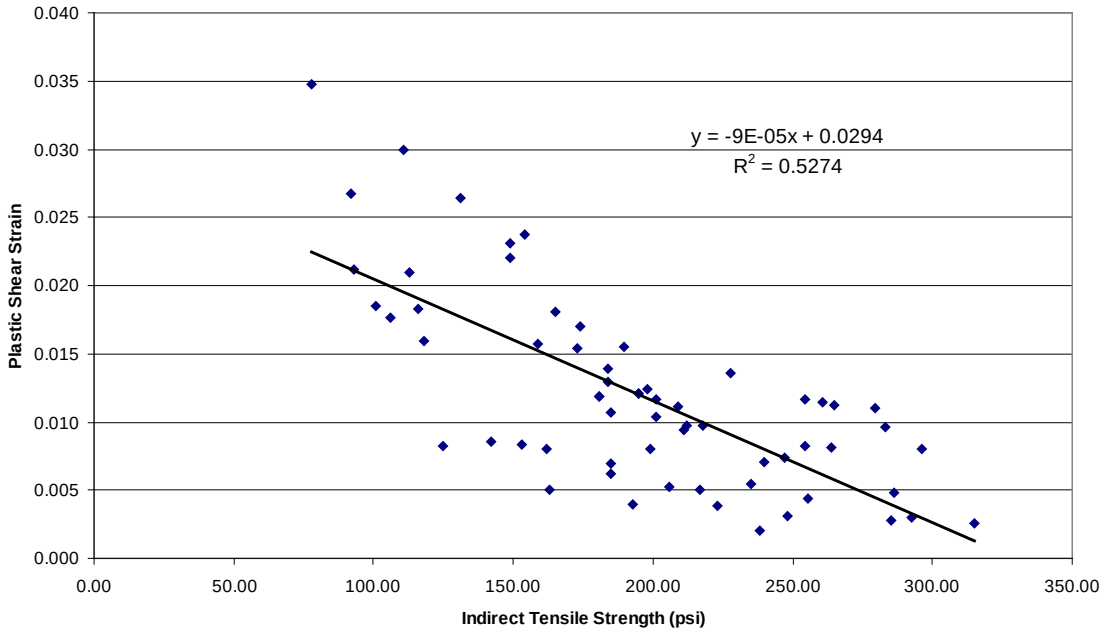

Figure 7.14 Linear Regression Relation between ITS and Plastic Shear Strain

7.4.1. Simple Linear Regression

Shear strain = 0.02941 – 9.084E-05 * ITS

R-sq = 0.53

Table 7.11 Parameter estimates (Rutting Model Analysis)

Parameter	Estimate	Std. Err.	DF	T-Stat	P-Value
Intercept	0.02941	0.02717	1	12.11	<0.0001
Slope	-9.084E-5	1.114E-5	1	-7.17	<0.0001

Table 7.12 Analysis of variance table for regression model (Rutting Model Analysis)

Source	DF	SS	MS	F-stat	P-value
Model	1	0.00143	0.00143	51.41	<0.0001
Error	64	0.00178	2.778E-05		
Total	65	0.00321			

The logarithmic regression relationship between indirect tensile strength (ITS) and plastic shear strain appears to best describe the data ($R^2 = 0.58$) and so the rutting model will be based on the following logarithmic relationship

Plastic shear strain (y) = -0.0167 Ln(ITS) + 0.0991

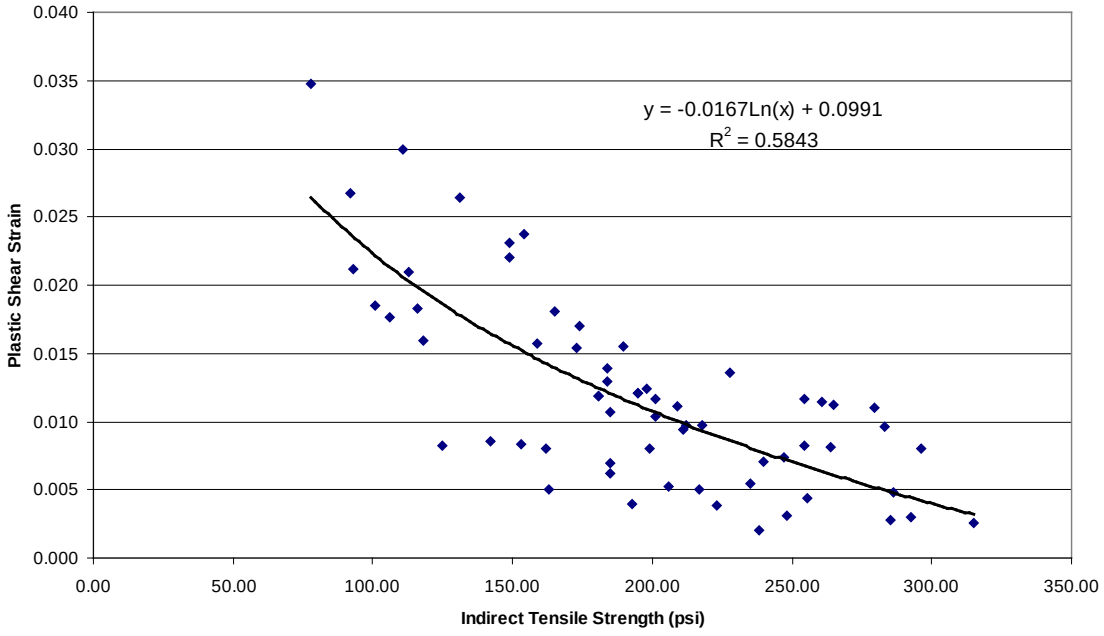

Figure 7.15 Regression Relation between ITS and Plastic Shear Strain

7.5 Evaluation of Tensile strength as design tool for Superpave mixtures

The Tensile Strength Ratio (TSR) value is a very good indicator of moisture susceptibility of the mix. A mix with a high TSR value, because of its low moisture susceptibility is considered to have better rutting and fatigue performance than the mix with a low TSR value. Tables 7.13 and 7.14 show a comparison of TSR, indirect tensile strength, fatigue life and plastic shear strain values of unconditioned and fully conditioned specimens. Considering Fountain and Asheboro aggregates for use in the Superpave volumetric design, a PG 70-22 mixture using Asheboro aggregate would be preferred for its higher TSR values as compared to Fountain mixtures. However, it should be noted from Tables 7.13 and 7.14 that Fountain mixtures have higher tensile strength than Asheboro mixtures before and after conditioning. In addition, Tables 7.13 and 7.14 show that conditioned Fountain mixtures had higher fatigue life than conditioned Asheboro mixtures. In the case of the Asheboro 12.5mm mix, using PG 76-22, the TSR actually decreases by 1% with the addition of lime, but fatigue life increases by 16% and rutting decreases by 33% at fully conditioned state. Therefore, the data suggest that Indirect Tensile Strength values as well as TSR should be taken into consideration for selecting an aggregate source for the design of mixtures.

Figures 7.10 and 7.14 suggest that there exists a strong correlation between indirect tensile strength of a mixture and its fatigue life and plastic shear strain. In this context, it can be concluded that individual tensile strength value can be used as an evaluation tool for Superpave mixtures in the Superpave mix design stage. Following the flowchart (Figure 7.15) shows how tensile strength can be used as a design tool in the Superpave mix design. The exponential relationship (Fig 7.10) was developed between fatigue life

and Indirect Tensile Strength as this relationship had the highest R^2 value. It is evident from Figure 7.10 that with the increased Indirect Tensile Strength values for a mixture comes increased fatigue life. In addition, there exists a minimum indirect tensile strength value for each desired fatigue life. In the mix design stage, this value can be found from Figure 7.10 or using the exponential relationship developed. This minimum indirect tensile strength value ($\sigma_{t\ min}$) should be compared with the conditioned tensile strength value. If the conditioned tensile strength of the mixture is greater than ($\sigma_{t\ min}$) and also if the TSR ratio is greater than 85%, the mix can be finalized. Otherwise, mix modification is needed by using anti-stripping agents or by changing the gradation. As per the SHRP rutting model, the maximum allowable plastic shear strain is 0.05 and for satisfactory performance, 0.03 is the critical value. As per Fig. 7.14, plastic shear strain increases with a decrease in tensile strength. Therefore, a tensile strength value for which plastic shear strain value is limited to 0.03 can be calculated using the logarithmic relationship established in Fig 7.14. In this study, the critical tensile strength value for a plastic shear strain of 0.03 was about 75 psi from the regression relationship established in Figure 7.14. Therefore, all the mixtures should have a minimum indirect tensile strength value of 75 psi.

Table 7.13 Comparison of Fatigue Life & Rut Depth for 12.5mm Mixtures (Without Additive)

Mix Type	TSR	ITS(psi)	Fatigue Life (ESALs)	Plastic shear strain
Fountain 12.5mm PG 70-22	61	173 (UC)	9.13E+05	0.010
		107 (FC)	4.29E+05	0.022
Asheboro 12.5mm PG 70-22	69	113 (UC)	3.72E+05	0.021
		78 (FC)	3.25E+05	0.034
Castle Hayne 12.5mm PG 70-22	80	185 (UC)	1.11E+06	0.004
		149 (FC)	6.85 E+05	0.008
Fountain 12.5mm PG 76-22	84	240 (UC)	6.62E+05	0.007
		201 (FC)	5.41E+05	0.012
Fountain 12.5mm PG 64-22	74	149 (UC)	5.98E+05	0.023
		111 (FC)	5.28E+05	0.030
Asheboro 12.5mm PG 64-22	88	238 (UC)	6.96E+05	0.002
		209 (FC)	5.85E+05	0.008
Asheboro 12.5mm PG 64-22	82	211 (UC)	8.02E+05	0.009
		173 (FC)	6.91E+05	0.015
Castle Hayne 12.5mm PG 64-22	83	223 (UC)	5.37E+05	0.004
		185 (FC)	4.73E+05	0.006
Castle Hayne 12.5mm PG 64-22	81	283 (UC)	1.15E+06	0.010
		228 (FC)	9.97E+05	0.014

Table 7.14 Comparison of Fatigue Life & Rut Depth for 9.5mm Mixtures (Without Additive)

Mix Type	TSR	ITS(psi)	Fatigue Life (ESALs)	Plastic shear strain
Fountain 9.5mm	73	193 (UC)	8.13E+05	0.012
		142 (FC)	3.90E+05	0.023
Asheboro 9.5mm	74	125 (UC)	5.69E+05	0.008
		93 (FC)	3.73E+05	0.021
Castle Hayne 9.5mm	79	195 (UC)	8.57E+05	0.004
		154 (FC)	4.81E+05	0.008

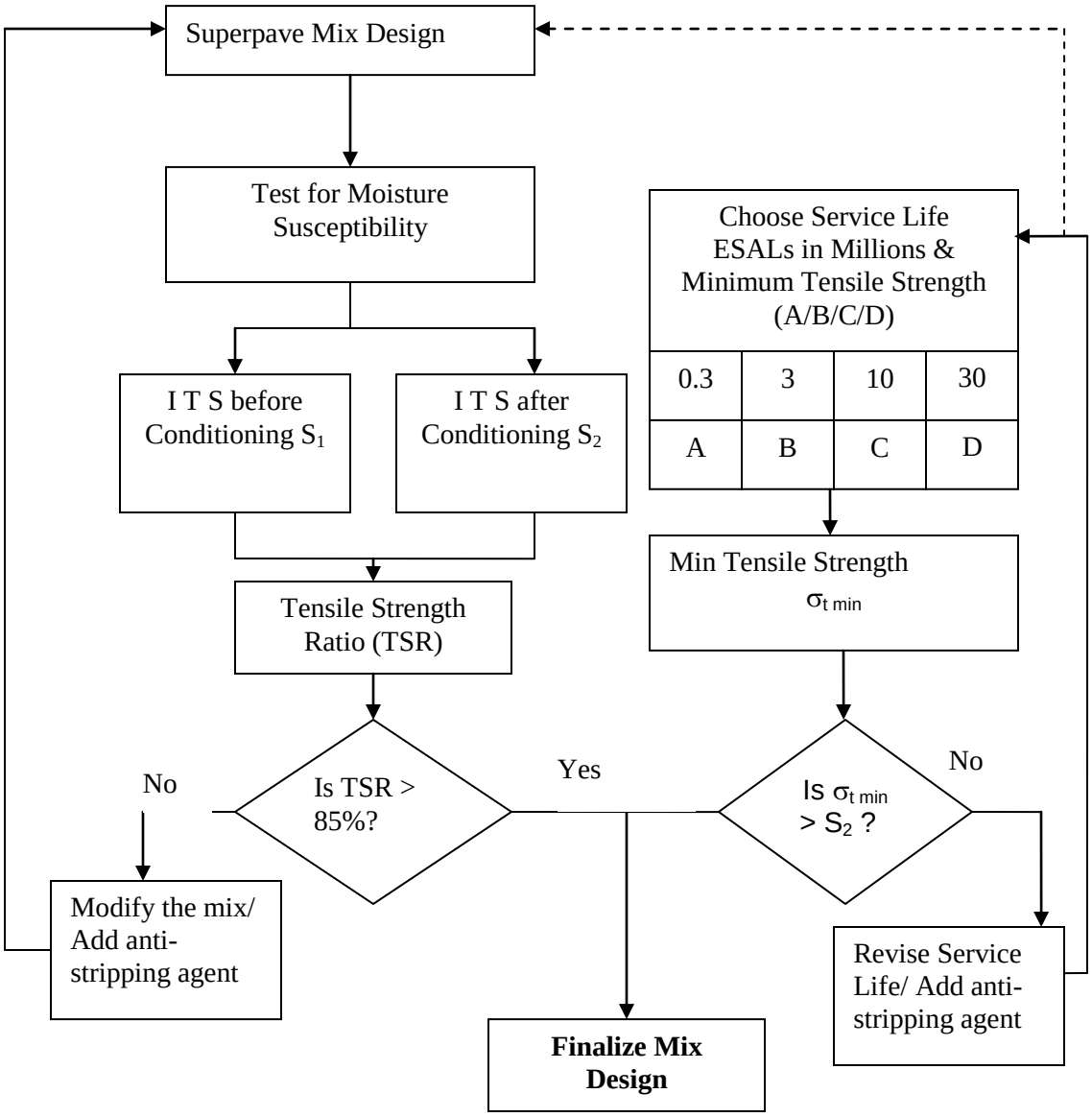

Figure 7.16 Proposed Mix Design Chart for Superpave Volumetric Design

7.5. Example Design

An example design problem using the entire proposed procedure follows.

Design Parameters:

Expected Traffic: 15 Million ESALs

Plastic Strain Limit: 0.03in/in

Aggregate Source: Fountain Quarry

Mix Type: S – 9.5 C

Mix design begins with the normal SuperPave^{TM} volumetric mix design. The complete design can be seen in Chapter 3. As a simple "proof test" for the volumetric mix design, after the volumetric procedure yields a design asphalt content, ITS tests are run as per Section 3.7 to confirm the accuracy of the volumetric design. For the purposes of this example it is assumed that the ITS test results suggest an asphalt content that is very near to the volumetric design asphalt content, thus confirming the volumetric accuracy. Specimens are now prepared at the design asphalt content, but using 7% air voids. One-half of the specimens are conditioned and as per AASHTO T-283 to determine moisture sensitivity. The TSR for this mix comes out to be 74% (Conditioned/Unconditioned = 142psi/193psi), meaning an anti-stripping agent must be used. Specimens are prepared at 7% air voids with lime as an anti-stripping agent and the TSR increases to 90% (Conditioned/Unconditioned = 185psi/204psi). This is where the normal mix design procedure would end, but it is necessary to add one additional step to the design procedure. Using the unconditioned ITS (204psi) in Figures 7.11 and 7.15, it can be seen that in order to resist fatigue cracking for 15 Million ESALs, a top layer of 5"

is required (assuming the typical pavement section in Figure 7.1) and that the plastic strain will be about 0.012in/in, well within design parameters. The reverse calculation of fatigue life given surface course thickness could also be calculated. Assuming a 3" top course it can be seen using the unconditioned and full conditioned ITS values (204psi and 185psi, respectively) in Figure 7.11 that the conservatively estimated fatigue life would be between 5 million and 6 million ESALs. Again, this fatigue life estimate is very conservative in that the estimate is determined using 7% air void specimens and field performance will be based on about 4% air voids. A closer approximation of field fatigue life could be attained by using an ITS conducted at 4% air voids. In this example, the 4% air voids ITS is about 320psi (from Figure 3.6) and the resultant estimate for fatigue life, using Figure 7.11 is 25 million ESALs for a 5" top course and 8 million ESALs for a 3" top course.

The reason for including this final step in the design process is this: if a mix has a TSR of 99%, but the conditioned and unconditioned ITS values are only 99psi and 100psi, respectively, it would require over 6" of asphalt to have the same resistance to fatigue cracking as a 5" thick layer of the example mix (TSR = 90%). Alternately, a mix whose TSR is only 80%, but whose conditioned and unconditioned ITS values are 240psi and 300psi, respectively would only require a 4" thick layer to resist fatigue cracking like the 5" example mix. There is a clear and strong correlation between ITS and fatigue life as predicted by the Superpave Shear Tester, and as such, ITS should be a stronger indication of performance than TSR alone.

CHAPTER 8

8. SUMMARY OF RESULTS AND CONCLUSIONS

Moisture damage of asphalt pavements is a serious problem. Pavements with 8-10% voids allow moisture into the mix but are not open enough for the moisture to readily leave. The presence of moisture tends to reduce the stiffness of the asphalt mix as well as create the opportunity for stripping of the asphalt from the aggregate. This, in combination with repeated wheel loadings, can accelerate pavement deterioration. Strength loss is now evaluated by comparing indirect tensile strengths of an unconditioned control group to those of the conditioned samples. If the average retained strength of the conditioned group is less than eighty-five percent of the control group strength, the mix is determined to be moisture susceptible. This research study shows that total dependency and reliance on the TSR values only can be misleading in many cases. So, the individual values of tensile strength of conditioned and unconditioned specimens in conjunction with TSR values should be examined to assess the effect of water damage on the performance of pavements. This Research study reveals that a minimum tensile strength exists for a given ESAL range, as shown in Figure 7.11. The fatigue life of the mixtures decreases exponentially with decreasing tensile strength. This trend is justified by the loss in stiffness and the initiating of cracks and stripping. So, there exists a minimum tensile strength for a given ESALs level that can be used as a surrogate criterion for fatigue life estimation. This research study also shows that the mixtures with lower tensile strength have higher rut depths, as shown in Figure 7.15. It can be observed that the rut depths of mixtures increase with decreasing tensile strength, which can be attributed to the fact that the aggregate structure is affected due to moisture damage and

subsequent loss in tensile strengths of the mixtures. Thus, by using the recommended criteria as suggested in the flow chart (Figure 7.16), a minimum tensile strength value based on the fatigue and rutting life of a mixture in conjunction with TSR values should be employed in assessing the effect of water damage on the performance of pavements.

Based on the analysis and discussion of the test data, the following specific conclusions can be drawn, which are based on the materials and asphalt mixtures used in this study:

1. Among the 9.5mm unconditioned mixtures, the Castle Hayne mixtures had the highest indirect tensile strength and Asheboro mixtures had the lowest indirect tensile strength values.
2. Among the 12.5mm and 9.5mm mixtures, conditioned Fountain mixtures had the highest decrease in indirect tensile strength values compared to the unconditioned Fountain mixtures.
3. In mixtures containing hydrated lime and liquid antistripping agent, reduction in individual tensile strength value from unconditioned state to conditioned state is not appreciable when compared with mixtures without any additive.
4. Phase angles of all mixtures increase when the mixtures are subjected to moisture damage, indicating loss in elastic component of stiffness.
5. Fatigue life of conditioned mixtures with hydrated lime is higher when compared to conditioned mixtures without the additive, which signifies the ability of hydrated lime to mitigate moisture susceptibility of asphalt concrete mixtures.
6. There is a strong correlation between indirect tensile strength values and the corresponding fatigue life and rutting performance of an asphalt concrete mixture.

7. A mix with an poor TSR and a high indirect tensile strength should have better performance than a mix with lower indirect tensile strength and higher TSR.
8. Because of the strong correlation to fatigue, rutting, and the conclusion above (number 7) greater weight should be given to the indirect tensile strength value than to the TSR value in mixture design.
9. Tensile strength test could be the simple performance or "proof" test sought by engineers and asphalt technicians.
10. Although the correlation between indirect tensile strength and fatigue life was stronger when the data was limited to specific mixtures, the correlation that uses all mixtures is more valuable it understanding the general relationship between indirect tensile strength and fatigue life.
11. When specimens were compacted to Ndes at varying asphalt contents, the maximum indirect tensile strength was attained at asphalt contents very near (within ±0.2% asphalt content) the asphalt content which produced 4% air voids in the mix.
12. Figure 7.11 can be used as a design chart that yields a conservative estimate for fatigue life of asphalt pavements, given indirect tensile strength.

REFERENCES

1. Asphalt Institute. Asphalt Institute Manual Series No. 10 (MS-10), Cause and Prevention of Stripping in Asphalt Pavements. Lexington, KY, 1981.

2. American Association of State Highway and Transportation Officials. Standard Specifications for Transportation Materials and Methods of Sampling and Testing, Nineteenth Edition. Washington, D.C., 1998.

3. Kennedy, T. W. "Prevention of Water Damage in Asphalt Mixtures." ASTM STP 899: Evaluation and Prevention of Water Damage to Asphalt Pavement Materials. American Society for Testing and Materials, Philadelphia, 1985.

4. Terrel, R.L. and Al-Swailmi. Water Sensitivity of Asphalt-Aggregate Mixes: Test Selection. Report No. SHRP A-403. Strategic Highway Research Program, National Research Council, Washington, DC, 1994.

5. Hicks, R.G. " Moisture Damage in Asphalt Concrete." NCHRP Synthesis of Highway Practice 175, Transportation Research Board, Washington, D.C., 1991.

6. Hicks, R.G., Santucci, L., and T. Aschenbrener. "Moisture Sensitivity of Asphalt Pavements." A National Seminar, February 4-6, 2003. California.

7. Lottman, R.P. NCHRP Report 192: Predicting Moisture- Induced Damage to Asphaltic Concrete. TRB, National Research Council, Washington, D.C., 1978.

8. Lottman, R.P. NCHRP Report 246: Predicting Moisture- Induced Damage to Asphaltic Concrete: Field Evaluation. TRB, National Research Council, Washington, D.C., 1982.

9. Tunnicliff, D.G., and R.E.Root. NCHRP Report 274: Use of Antistripping Additives in Asphalt Concrete Mixtures. TRB, National Research Council, Washington, D.C., 1984.

10. Goode, F.F. 1959. Use of Immersion Compression Test in Evaluating and designing Bituminous Paving Mixtures, In ASTM STP 252, pp 113-126.

11. Jimenez, R.A. 1974. Testing for Debonding of Asphalt from Aggregates. In Transportation Research Record 515, TRB, National Research Council, Washington, D.C., pp. 1-17.

12. Kennedy, T. W., F.L. Roberts, and K.W. Lee. 1982. Evaluation of Moisture Susceptibility of Asphalt Mixtures Using the Texas Freeze-Thaw Pedestal Test. Proc., Association of Asphalt Technologists, vol. 51, pp 327-341.

13. Romero, F.L., and K.D. Stuart. 1998. Evaluating Accelerated Rut Testers. Public Roads, Vol. 62, No.1, July-August., pp 50-54.

14. Aschenbrener, T., and G. Currier. 1993. Influence of Testing Variables on the Results from the Hamburg wheel-Tracking device. CDOT-DTD-R-93-22. Colorado Department of Transportation, Denver.

15. Elizabath Rae Hunter. “Evaluating Moisture Susceptibility of Asphalt Mixes.” Thesis., Department of Civil and Architectural Engineering, University of Wyoming, December 2001.

16. Collins, R., D. Watson, and B. Campbell (1995). Development and Use of Georgia Loaded Wheel Tester. Transportation Research Record 1492. Washington D.C.: National Academy Press.

17. Watson, D., A. Johnson, and D. Jared (1997). The Superpave Gradation Restricted Zone and Performance Testing with the Georgia Loaded Tester.

Transportation Research Record 1583. Washington D.C.: National Academy Press.

18. Shami, H., J.Lai, J.D'Angelo, and T.Harman (1997). Development of Temperature- Effect Model for Predicting Rutting of Asphalt Mixtures Using Georgia Loaded Wheel Tester. Transportation Research Record 1590. Washington D.C.: National Academy Press.

19. Anderson, d. and E.Dukatz (1982). The effect of Antistrip Additives on the Properties of Asphalt Cement. Association of Asphalt Paving Technologists, Vol.51, pp 298-317.

20. Tayebali, Fischer W. K., "Effect of Percentage Baghouse Fines on the Amount and Type of Anti-stripping Agent Required to Control Moisture Sensitivity," Department of Civil Engineering, North Carolina State University, Technical Report, (2003).

21. Mohammad, L, C. Abadie, R. Gokmen, and A. Puppala. "Mechanistic Evaluation of hydrated Lime in Hot-Mix Asphalt Mixtures," Transportation Research Record 1723. Washington D.C.: National Academy Press, (2000).

22. Kennedy, T. and J. Anagnos, "A Field Evaluation of Techniques for Treating Asphalt Mixtures with Lime," Report No. FHWA-TX-85-47+253-6, (1984).

23. Birdsall, Brian Gregory. "An Evaluation of Moisture Susceptibility of Asphalt Mixtures". M.S Thesis. North Carolina State University. 1999.

24. Petersen, J.C., H. Plancher, and P.M. Harnsbergen, "Lime Treatment of Asphalt to Reduce Age Hardening and Improve Flow Properties," Proceedings, AAPT, Vol. 56, (1987).

25. www.lime.org, "How to Add Hydrated Lime to Asphalt" (http://www.lime.org/publications.html#asphalt)

26. www.lime.org, “Hydrated Lime - A Solution for High Performance Hot Mix Asphalt” (http://www.lime.org/Asphalt.pdf)

27. Little, Dallas N. & Jon Epps. “The Benefits of Hydrated Lime in Hot Mix Asphalt,” report for National Lime Association, (2001).

28. Hicks, R. Gary & Todd V. Scholz. “Life Cycle Costs for Lime in Hot Mix Asphalt.” Report & Software for National Lime Association, (2001).

29. Mohammad, L, C. Abadie, R. Gokmen, and A. Puppala. “Mechanistic Evaluation of hydrated Lime in Hot-Mix Asphalt Mixtures,” Transportation Research Record 1723. Washington D.C.: National Academy Press, (2000).

30. Lesueur, Didier & Dallas N. Little, “Effect of Hydrated Lime on Rheology, Fracture and Aging of Bitumen,” Transportation Research Report 1661, Transportation Research Board, (1999).

31. Khosla, N. P. , Brian Birdsall, and S. Kawaguchi, “Evaluation of Moisture Susceptibility of Asphalt Mixtures – Conventional and New Methods, “Transportation Research Record No. 1728, 2000, 43-51.

32. Harrigan, E. T., Leahy, R. B., & Youtcheff, J. S. (1994). The Superpave Mix Design Manual Specifications, Test Methods, and Practices”, SHRP-A-379. Strategic Highway Research Program. National Research Council. Washington, DC: National Academy of Science.

33. American Association of State Highway and Transportation Officials, "Standard Test Method for Determining the Permanent Deformation and Fatigue Cracking Characteristics of Hot Mix Asphalt Using a Simple Shear Test Device, "AASHTO designation TP7, (1996).

34. American Association of State Highway and Transportation Officials (AASHTO). (1994). Shear Device, ASHTO Designation: TP-7-94. AASHTO Provisional Standards.

35. AASHTO. Standard Method of Test for Determining Dynamic Modulus of Hot-Mix Asphalt Concrete Mixtures. American Association of State Highway and Transportation Officials, TP 62-03, 2003.

36. Carl. M. Monismith, "Asphalt Concrete: An Extraordinary Material for Engineering Applications", Thirtieth Henry M. Shaw Lecture, North Carolina State University.

37. http://onlinepubs.trb.org/onlinepubs/shrp/SHRP-A-698.pdf

38. Eyad Masad, "Quantifying Laboratory Compaction Effects on the Internal Structure of Asphalt Concrete", Transportation Research Record 1681, TRB, National Research Council, Washington, D.C., July 1999, pp 179-185.

39. Chehab, G., E.N. O'Quinn, and Y.R. Kim. (2000) "Specimen Geometry Study for Direct Tension Test Based on Mechanical Tests and Air Void Variation in Asphalt Concrete Specimens Compacted by Superpave Gyratory Compactor". Transportation Research Record 1723, TRB, National Research Council, Washington, D.C., pp.125-132.